ISBN 978-82-326-6704-8 (printed ver.)
ISBN 978-82-326-5318-8 (electronic ver.)
ISSN 1503-8181 (printed ver.)
ISSN 2703-8084 (electronic ver.)

NTNU
Norwegian University of
Science and Technology

Yiyu Ding
Doctoral thesis

Doctoral theses at NTNU, 2023:34

Yiyu Ding

Trends in Urban Building Stock Energy Use - from Large to Small Scale

Doctoral theses at NTNU, 2023:34
NTNU

NTNU
Norwegian University of
Science and Technology
Thesis for the degree of
Philosophiae Doctor
Faculty of Engineering
Department of Energy and Process Engineering

NTNU
Norwegian University of
Science and Technology

Yiyu Ding

Trends in Urban Building Stock Energy Use - from Large to Small Scale

Thesis for the degree of Philosophiae Doctor

Trondheim, February 2023

Norwegian University of Science and Technology
Faculty of Engineering
Department of Energy and Process Engineering

NTNU
Norwegian University of
Science and Technology

NTNU
Norwegian University of Science and Technology

Thesis for the degree of Philosophiae Doctor

Faculty of Engineering
Department of Energy and Process Engineering

© Yiyu Ding

ISBN 978-82-326-6704-8 (printed ver.)
ISBN 978-82-326-5318-8 (electronic ver.)
ISSN 1503-8181 (printed ver.)
ISSN 2703-8084 (electronic ver.)

Doctoral theses at NTNU, 2023:34

PRINTED IN NORWAY
NO - 1598

NORDIC SWAN ECOLABEL
Printed matter
2041 0731

Printed by Skipnes Kommunikasjon AS

ABSTRACT

In keeping with the commitment of a low-emissions society, energy efficiency strategies for the Norwegian urban building stocks shall make a significant contribution to reducing energy use and greenhouse gas emissions.

In the Nordic climate, a large amount of building energy is used for heating purposes. In countries like Norway, where the energy market is dominated by hydro-power, district heating (DH) systems are expected to serve as an alternative heating method to alleviate the increasing pressure on the grid. Furthermore, in the face of green energy initiatives and the increasing share of energy-efficient buildings, there is a pressing need to transform current DH to low-temperature DH (LTDH) to maintain the economic and environmental competitiveness of DH companies in the heating market. The substantially lowered supply temperature of LTDH has broadened the opportunities and challenges to integrating distributed renewable energy resources, requiring enhancement on intelligent heating load prediction.

In the current research on the energy supply systems and building energy demand, in most cases, measured energy data are employed as a package of information, regardless of energy use patterns associated with building types, while most energy forecasts have not yet conducted in-depth studies on sizing or energy demand requirements for typical building types. There lack of a bridge between demand profiles on building stock functions and urban energy supply systems. In addition to the normal condition, Norway and many countries have carried out confinement regulations to hinder the infection spreading in 2020. The distancing measures and changed work regimes have caused significant impacts on energy demand, so it is important to improve the existing knowledge of building operations during unforeseeable disruptions.

To gain a deeper understanding of the energy use and improve the efficiency of Norwegian urban buildings operation, this thesis focused on identifying representative energy trends regarding load profiles and developing appropriate prediction models for Norwegian urban buildings under normal and special conditions. The thesis started with a future development projection of the environmental impacts comparing the buildings with DH and with only electricity, followed by the approach for typical annual energy profiles. Further, a hybrid heating prediction was proposed for sizing and operation. In the end, the energy demand changes due to the COVID-19 pandemic were studied to examine building operation strategies during special circumstances. Accordingly, four research questions were addressed to fulfill the research goal. In the thesis, the study of building energy use was conducted based on the hourly measured data of kindergartens, schools, nursing homes, and residential buildings. The duration of energy data collection differed by building types and were between two and four years. Since buildings with different floor areas, construction years, and energy labels were involved, to define the representative energy use for

buildings with different characteristics, the energy use was first converted into the average specific energy use, W/m^2. This applied to the most analysis of research examples in the thesis.

Start with Research Question 1: *What are the environmental impacts of heating systems in future building development?* It was answered in a study of 28 DH-supplied kindergartens in Norway, where three cases were found depending on the energy share from DH; i.e. DH high share, DH average share, and DH low share. By following different CO_2 factors of electricity and local DH production, the typical kindergarten with DH high share had almost the lowest CO_2 emission; contrarily, the kindergarten with a lower share of DH or without DH, usually had a wider range of CO_2 emissions due to its dependence of the electricity production mix. Then a projection was made by assuming 14.2% growth rate of kindergartens. The result showed that if more than 50-67% of the new building area connected to DH, a smaller increase of CO_2 emissions from the projected area could be achieved, depending on the CO_2 factors. This proved that buildings with DH were more robust than the ones without DH in terms of CO_2 emissions. This top-down question addressed the identification of typical building types for development planning and the necessity for diversifying local energy supply pathways.

Research Question 2: *What factors shall be considered for building heating and electricity operation and what are the differences between the two delivered energy forms?* It was answered in a study of 40 DH-supplied schools in Norway, using a modified Z-Score to determine working days and holidays, linear regression analysis to predict DH and electricity load profiles, and quality criteria and a cluster method to evaluate the prediction quality. The results showed that the modified Z-Scores might point out the special energy use periods and show the energy demand trend. Operation of the electric appliances might be concluded with reasonably fast responses by following the attendance, while the DH demand mainly followed the outdoor temperature and the daily work schedule, with a slow control response to short holidays, resulting in a waste of some heat energy. The identified specific load profiles may present the current energy use of schools in the Nordic climate. The predicted annual DH demand was 72 kWh/m^2 with a peak load of 48 W/m^2; the predicted annual electricity demand was 57 kWh/m^2 with a peak load of 18 W/m^2. Thus, the buildings with DH may largely reduce the power grid strains.

This long-term prediction also highlighted the importance of accurate heating peak load prediction, especially for the promising LTDH, which was addressed in Research Question 3: *How can the methods for developing and predicting heating load profiles be improved for future daily LTDH operation?* Hereby, a study of 20 DH-supplied nursing homes in Norway proposed a hybrid prediction method, combining long-term DH load prediction by means of linear regression for unit sizing and short-term (day-ahead) load prediction by means of two Artificial Neural Network models, f_{72} and g_{120} (with different input parameters). It was found that including the his-

torical heating loads as the input to the forecasting model improved the prediction quality, especially for the peak load and low-mild heating season, as proved by g_{120} outperforming in the prediction quality evaluation. Meanwhile, to fulfill the different temperature requirements of domestic hot water and space heating, separate energy conversion units shall be implemented on user-side to upgrade the temperature level of LTDH network.

Lastly, the energy impacts due to COVID-19 were addressed in Research Question 4: *What are the energy and economic impacts of the buildings under special circumstances?* Since electric heating still accounts for a high share in the country, a study of educational buildings and residential buildings with electric heating was conducted to investigate the lockdown impacts. The results showed that during the 2020 lockdown period, the electricity demand and load profiles for educational buildings were almost the same as in previous years, while there were apparent changes for the residential buildings. Further, three building operation scenarios were proposed: Scenario 1 considered operation under normal settings, Scenario 2 considered the operation of educational buildings under nighttime and weekend settings, and Scenario 3 considered the operation of residential buildings under work-at-home conditions. The scenario-based analysis showed that the electricity demand might be reduced by one-third in educational buildings, between 2.1-4.1 €/(m^2·yr) might be saved for kindergartens, and 1.4-2.7 €/(m^2·yr) for schools by following Scenario 2. Meanwhile, the electricity density of small apartments varied more significantly than the townhouse. Under Scenario 3, the apartment might spend 2.0-4.1 €/(m^2·yr) more for electricity, while the increased bill for the townhouse may be trivial. Moreover, in a community with various building functions, the composition of each building type adopting different working schemes may influence the unit sizing and utilization rate.

To conclude, the proposed methods may be efficiently applied to other public buildings in a similar climate. This allows public authorities to better understand the energy needs of different building functions, project future demand changes taking into account normal situations and future unforeseeable disruptions, and improve the building energy efficiency.

Keywords: Load profile; Linear regression; Artificial neural network; Low-temperature district heating; Educational buildings; Nursing homes; Residential buildings; COVID-19 lockdown; Scenario-based analysis

SAMMENDRAG

For å bygge et lavutslippssamfunn, skal de norske bybygningsmassene gi et betydelig bidrag til å redusere energibruk og klimagassutslipp med forbedrede energieffektiviseringsstrategier. I det nordiske klimaet brukes en stor mengde bygningsenergi til oppvarming. I land som Norge, hvor energimarkedet domineres av vannkraft, forventes fjernvarmesystemer (FV) å jobbe som en alternativ oppvarmingsmetode for å redusere det økende presset på kraftnettet. Drevet av det grønne skiftet og den økende andelen energieffektive bygninger, er det dessuten et stort behov for å transformere dagens FV til lavtemperatur-FV (LT-FV) slik at FV selskaper opprettholder sine økonomiske og miljømessige konkurranseevnen i varmemarkedet. Den betydelig senkede tilførselstemperaturen til LT-FV har utvidet mulighetene og utfordringene for å integrere distribuerte fornybare energiressurser, og det krever forbedring av intelligent prediksjon av varmebelastninger.

I den nåværende forskningen på energiforsyningssystemene og bygningens energibehov brukes ofte de målte energidataene som en informasjonspakke, uten å ta hensyn til energibruksmønstre knyttet til bygningstyper, mens de fleste energiprognoser ennå ikke har foretatt dybdestudier om dimensjonering eller krav til energibehov for typiske bygningstyper. Det mangler en bro mellom etterspørselsprofiler på bygningsmassefunksjoner og urbane energiforsyningssystemer. I tillegg til normalsituasjon har Norge og mange land gjennomført tiltak og regulering for å hindre smittespredning i 2020. Avstandstiltakene og endret arbeidsregime har påvirket energibehovet i stor grad, så det er jo viktig å forbedre eksisterende kunnskap om bygningsdrift ved uforutsigbare forstyrrelser.

For å få en dypere forståelse av energibruken og effektivisere driften av norske bybygg, har denne avhandlingen jobbet på å identifisere representative energibelastningsprofiler og utvikle hensiktsmessige prediksjonsmodeller for norske bybygg under normale og spesielle situasjoner. Avhandlingen startet med en fremtidig utviklingsprojeksjon av miljøpåvirkningene ved å sammenligne bygningene med FV og kun med elektrisitet, etterfulgt av tilnærmingen for typiske årlige energiprofiler. Videre ble en hybrid oppvarmingsprediksjon foreslått for dimensjonering og dagligdrift. Til slutt ble energibehovsendringene i løpet av nedstengte perioden studert for å undersøke bygningsdriftsstrategier. Fire forskningsspørsmål ble stilt for å oppfylle forskningsmålet.

I avhandlingen ble bygningens energibruk analysert basert på timemålte data fra barnehager, skoler, sykehjem og boligbygg. Varigheten av energidataene var mellom to og fire år. Siden bygninger med ulike gulvarealer, byggeår og energimerker var involvert, for å definere representativ energibruk til bygninger med forskjellige egenskaper, ble energibruken først omregnet til gjennomsnittlig spesifikk energibruk, W/m^2. Dette gjaldt de fleste analyser av forskningseksempler i avhandlingen.

Start med forskningsspørsmål 1: *Hva er miljøpåvirkningene av varmesystemer i fremtidig byggutvikling?* Det ble besvart i en studie av 28 norske barnehager med FV, hvor det ble funnet tre tilfeller avhengig av energiandelen fra FV; dvs. høy andel FV, gjennomsnittlig andel FV og lav andel FV. Ved å følge ulike CO_2-faktorer for elektrisitet og lokal FV-produksjon, hadde den typiske barnehagen med høy andel FV nesten det laveste årlige CO_2-utslipp, hadde barnehagen med lavere andel FV eller uten FV vanligvis et bredere spekter av CO_2-utslipp på grunn av sin avhengighet av elektrisitetsproduksjonen. Deretter ble det gjort en fremskrivning ved å anta 14,2% vekst av barnehager. Resultatet viste at dersom mer enn 50-67% av det nye byggearealet koblet til FV, var det mulig å realisere en mindre økning av CO_2-utslippene fra det prosjekterte området, som var avhengig av CO_2-faktorene. Dette beviste at bygninger med FV var mer robuste enn de uten FV når det gjelder CO_2-utslipp. Dette ovenfra-ned-spørsmålet tok for seg identifiseringen av typisk bygningstype for utviklingsplanlegging og nødvendigheten av å diversifisere lokale energiforsyningsveier.

Forskningsspørsmål 2: *Hvilke faktorer bør vurderes for bygningsvarme og elektrisitetsdrift og hva er forskjellene mellom de to energiformene?* Det ble behandlet i en studie av 40 norske skoler med FV, ved bruk av en modifisert Z-Score metode for å identifisere arbeidsdager og ferie, lineær regresjonsanalyse for å forutsi FV- og elektrisitetsbelastningsprofiler, og kvalitetskriterier og en klyngemetode for å evaluere prediksjonskvaliteten. Resultatene viste at de modifiserte Z-skårene kunne peke ut de spesielle energibruksperiodene og vise trenden i energibehovet. De elektriske apparatene på skolene kunne ha gjort rimelige justeringer ved å overvåke oppmøtet; mens FV-behovet fulgte hovedsakelig utetemperatur og daglig arbeidsplan, med en langsom kontrollrespons på korte ferier, noe som resulterte i sløsing med litt varmeenergi. De identifiserte spesifikke lastprofilene kan presentere dagens energibruk til skoler i det nordiske klimaet. Det estimerte årlige FV-behovet var 72 kWt/m^2 med en topplast på 48 W/m^2; det estimerte årlige elektrisitetsbehovet var 57 kWt/m^2 med en topplast på 18 W/m^2. Derfor kan byggene med FV i stor grad redusere belastningene på strømnettet.

Denne langsiktige prediksjonen fremhevet også viktigheten av nøyaktig prediksjon av varmetopplast, spesielt for den lovende LTFV, som ble behandlet i forskningsspørsmål 3: *Hvordan kan metodene for å utvikle og forutsi varmelastprofiler forbedres for fremtidig daglig LT-FV drift?* En studie av 20 norske sykehjem med FV foreslo en hybrid prediksjonsmetode, som kombinerer langsiktig FV-lastprediksjon ved hjelp av lineær regresjon for enhetsstørrelse og kortsiktig (dag fremover) FV-lastprediksjon ved hjelp av to Kunstig nevrale nettverk-modeller, f_{72} og g_{120} (med ulike inngangsparametere). Det ble funnet at å inkludere de historiske varmelastene som input til prognosemodellen forbedret prediksjonskvaliteten, spesielt for topplast og varm sesong, som bevist ved at g_{120} utkonkurrerte i evalueringen. I tillegg, for å møte de forskjellige temperaturkravene til varmtvann og romoppvarming, skal separate energikonverteringsutstyr implementeres på brukersiden for å oppgradere temperaturnivået til

LT-FV-nettverket.

Den siste oppgaven var energibehovsendringene på grunn av COVID-19-pandemien og det ble handlet i forskningsspørsmål 4: *Hva er de energimessige og økonomiske konsekvensene av bygningene under spesielle situasjoner?* Siden elektrisk oppvarming fortsatt utgjør en høy andel i landet, ble det utført en studie av utdanningsbygg og boligbygg med elektrisk oppvarming for å undersøke virkningene av nedstengning. Sammenligningsresultatene viste at strømbehovet til de undervisningsbyggene var nesten samme som tidligere år, mens det var store endringer for bolighusene under nedstengningene. Videre ble tre bygningsdriftsscenarier foreslått: Scenario 1 vurderte driften under normale situasjoner, Scenario 2 vurderte driften av undervisningsbygg under natt- og helgeinnstillinger, og Scenario 3 vurderte driften av boligbygg under jobb hjemmefra. De scenariebaserte analyseresultatene viste at strømbehovet kunne reduseres med en tredjedel i undervisningsbygg, mellom 2,1-4,1 €/(m^2·år) kunne spares for barnehager, og 1,4-2,7 €/(m^2·år) for skoler ved å følge Scenario 2. Samtidig varierte elektrisitetstettheten til små leiligheter mer betydelig enn rekkehuset. Under Scenario 3 kunne leiligheten bruke 2,0-4,1 €/(m^2·år) mer for strøm, mens den økte regningen for rekkehuset kunne være triviell. Dessuten kan sammensetningen av hver bygningstype ved å ta i bruk ulike arbeidsskjemaer påvirke enhetsstørrelsen og utnyttelsesgraden, i et samfunn med ulike bygningsfunksjoner.

Til slutt kan de foreslåtte metodene effektivt brukes på andre offentlige bygninger i lignende klima. Dette gir offentlige myndigheter en bedre forståelse av energibehovet til ulike bygningsfunksjoner, noe som kan hjelpe myndigheter til å prosjekterer fremtidige behovsendringer med hensyn til normalsituasjon og fremtidige uforutsette forstyrrelser, og forbedrer bygningens energieffektivitet.

Nøkkelord: Lastprofil; Lineær regresjon; Kunstig nevrale nettverk; Lavtemperatur fjernvarme; Utdanningsbygg; Sykehjemsbygg; Boligbygg; Covid-19-nedstengning; Scenariobasert analyse

PREFACE

This thesis is submitted to the Norwegian University of Science and Technology (Norges teknisk-naturvitenskapelige universitet) in partial fulfilment of the requirements for the degree of Doctor of Philosophy (PhD).

The work presented in this thesis was carried out at the Department of Energy and Process Engineering, Faculty of Engineering, Norwegian University of Science and Technology (NTNU), Norway. The doctoral work was conducted under the main supervision from Professor Natasa Nord at the Department of Energy and Process Engineering of NTNU, co-supervision from Professor Helge Brattbø at the Department of Energy and Process Engineering of NTNU, and co-supervision from Associate Professor Shuqin Chen at College of Civil Engineering and Architecture of Zhejiang University, China.

This PhD project is within the framework of the "Methods for Transparent Energy Planning of Urban Building Stocks- ExPOSe-programme" and was funded by the Research Council of Norway with grant number 268248.

In addition, energy data of the local public buildings used in this work were supported by Trondheim Municipality. Energy data of the two residential buildings were voluntarily shared by two anonymous dwellers, who retrieved the data from the local power grid supplier.

ACKNOWLEDGEMENTS

From an energy consultant in China to a master's student in Sweden, and eventually a PhD candidate in Norway, I cannot express enough thanks to those who have given me a hand during the journey. I would always remember their support, encouragement, and friendship that helped me make it through the ups and downs.

First of all, I sincerely would like to express my deepest gratitude to my mentor and main supervisor, Professor Natasa Nord for providing me with this interesting topic and allowing me to have the opportunity of exploring unlimited sparkles in this area. More than that, no matter how busy she was, she always arranged meetings with me for checking my work progress and giving me valuable advice and encouraging feedbacks. During our discussion, in addition to getting scientific suggestions by her broad knowledge, I was impressed by her serious research and teaching attitudes, and inspired by her positive and generous attitudes to life. This has greatly helped me develop myself as a potential researcher.

My sincere thanks also go to my co-supervisors Professor Helge Brattebø and Associate Professor Shuqin Chen (陈淑琴). It was always witty and inspiring discussing research with Helge, who has helped me advance my research horizon and broaden my research views. Although the pandemic hindered me from having exchange study physically with Shuqin's group, online supervision and guidance from her worked undoubtedly successfully.

I gratefully acknowledge the support from the Department of Energy and Process Engineering at NTNU, the Research Council of Norway (Norges forskningsråd) (ExPOSe-programme), and Trondheim Municipality.

Special thanks to Qiang Liu (刘强) for giving me research and life advice when I needed it. And my appreciation goes to Qian Wang (王乾) and Thomas O. Timoudas for presenting me with great role models bridging academia and the industrial world.

I would like to take this opportunity to thank Professor Jan-Olof Dalenbäck and Professor Stavros Papadokonstantakis for showing me the beauty of research and for inspiring me to the research path.

Furthermore, during the four-year research and study period, I am very lucky and delighted having received great support and care from my colleagues and friends here and at home: especially Masab, Maria, Dmytro, Tomas, Milan, Bima, Elyas, Han Deng (邓晗), Huiting Yuan (袁慧婷), Renxia Sun (孙仁霞), Zhou Zhou (周舟), Rui'e Zhao (赵瑞娥), Kuankuan Li (李宽宽), Weifeng Liu (刘伟峰), Jiao Li (李娇), Haiquan Yu (于海泉), Xiaolan Ma (马小兰), Ting He (何婷), Yang Bi (毕扬). Wish them all the best for their future work and well-being.

Last but certainly not least, my heartfelt thanks to my beloved family who always support me and have my back with their endless love. You have always been my rock. 由衷感谢我的家人.

Written in October 2022, Happy birthday to myself!

Yiyu Ding,
Trondheim, October 2022

LIST OF PUBLICATIONS

Paper I

Ding, Y., Brattebø, H. and Nord, N., 2019. Energy analysis and energy planning for kindergartens based on data analysis. *1st Nordic conference on Zero Emission and Plus Energy Buildings*, *IOP Conference Series: Earth and Environmental Science*, Volume 352(1), p.012031.

Paper II

Ding, Y., Brattebø, H. and Nord, N., 2021. A systematic approach for data analysis and prediction methods for annual energy profiles: An example for school buildings in Norway. *Energy and Buildings*, 247, p.111160.

Paper III

Ding, Y., Ivanko, D., Cao, G., Brattebø, H. and Nord, N., 2021. Analysis of electricity use and economic impacts for buildings with electric heating under lockdown conditions: examples for educational buildings and residential buildings in Norway. *Sustainable Cities and Society*, 74, p.103253.

Paper IV

Ding, Y., Timoudas, T.O., Wang, Q., Chen, S., Brattebø, H. and Nord, N., 2022. A study on data-driven hybrid heating load prediction methods in low-temperature district heating: an example for nursing homes in Nordic countries. *Energy Conversion & Management*, p.116163.

Paper V

Xue, K., Ding, Y., Yang, Z., Nord, N., Barillec, M., et al, 2020. A Simple and Novel Method to Predict the Hospital Energy Use Based on Machine Learning: A Case Study in Norway. *International Conference on Neural Information Processing, ICONIP 2020: Neural Information Processing*, Part of the *Communications in Computer and Information Science book series*, CCIS, Volume 1332, pp.11-22.

Paper VI

Nord, N., Ding, Y., Skrautvol, O. and Eliassen, S., 2021. Energy Pathways for Future Norwegian Residential Building Areas. *Energies*, 14(4), p.934.

Paper VII

Ivanko, D., Ding, Y. and Nord, N., 2021. Heat use profiles in Norwegian educational institutions in conditions of COVID-lockdown. *REHVA European HVAC Journal*, pp.55 - 58, 02/2021.

Paper VIII

Ding, Y., Ding, Y. and Nord, N., 2021. Data-driven analysis of electricity use for office buildings: a Norwegian case study. *Cold Climate HVAC & Energy 2021*, *E3S Web of Conferences*, Volume 246, p.04005.

Paper IX

Ivanko, D., Ding, Y. and Nord, N., 2021. Analysis of heat use profiles in Norwegian educational institutions in conditions of COVID-lockdown. *Journal of Building Engineering*, 43, p.102576.

Paper X

Timoudas, T.O., Ding, Y. and Wang, Q., 2022. A novel machine learning approach to predict short- term energy load for future low-temperature district heating. *CLIMA 2022 Conference*.

Paper XI

Wang, S., Niu, Y., Zhu, G., Ding, Y., Guo, X. and Hui, S., 2021. NO formation and destruction during combustion of high temperature preheated pulverized coal. *Journal of the Energy Institute*, 99, pp.82-87.

Paper XII

Wang, S., Zhu, G., Niu, Y., Ding, Y. and Hui, S., 2021. Experimental and kinetic studies on NO emission during pulverized coal preheating-combustion process with high preheating temperature. *Journal of the Energy Institute*, 97, pp.180-186.

Abbreviation and Symbols

Abbreviation

ANN	Artificial neural network
ASHRAE	American Society of Heating, Refrigerating and Air-Conditioning Engineers
CPT	Changing point temperature
CV(RMSE)	Coefficient of variation of the root mean squared error
DH	District heating
DHW	Domestic hot water
EB	Electric boiler
ED	Euclidean distance
EH	Electric heating
ENS	Energy not supplied
ES curve	Energy signature curve
FV	Fjernvarme (district heating in Norwegian)
GESD	Generalized extreme studentized deviate
GMM	Gaussian Mixture Model
HDD	Heating degree day
HP	Heat pump
LTDH	Low-temperature district heating
LR	Linear regression
MAD	Median absolute deviation
MAE	Mean absolute error
(s)MAPE	(symmetric) Mean absolute percentage error
MET Norway	Norwegian Meteorological Institute
ML	Machine learning
M(N)LR	Multiple (non-)linear regression
MSE	Mean squared error
NMBE	Normalized mean bias error
nZEB	nearly zero-energy/emission buildings
OECD	Organisation for Economic Co-operation and Development
PAA	Piecewise aggregate approximation
PCC	Pearson correlation coefficient
P2H	Power-to-heat
PPP	Purchasing power parities
SAX	Symbolic aggregate approximation
SH	Space heating
TELP	Typical electricity load pattern
TMA	Temperature moving average
TMY	Typical meteorological year
WD	Weekday
WE	Weekend

Special letters

el	electricity
€	EUR (currency)
n	number of observation
R^2	coefficient of determination
t_τ	outdoor temperature at time instance τ (°C)
yr	year
f_{72}	ANN model with 72 input units defined in the thesis
g_{120}	ANN model with 120 input units defined in the thesis
μ	Mean value of a time-series
σ	Standard deviation of a time-series

Contents

List of Figures

List of Tables

1

INTRODUCTION

Men argue. Nature acts.

Voltaire

The Earth is a fine place and worth fighting for.

Ernest Miller Hemingway

This chapter presents the research motivation, research questions and tasks, thesis structure, and a list of publications that support the doctoral work.

1.1 Background and motivation

Building energy planning is part of energy planning and covers a wide range of topics. Energy demands of end-users for electricity, heating and cooling are met by the energy supply systems, which utilize conversion technologies to convert primary energy sources into different forms of delivered energy and deliver the energy via distribution systems. Finally, all of these contribute to emissions and pollutants to the environment. Building energy demand is usually influenced by two sets of factors, technical and physical factors, and human factors. During the operation phase, technical and physical factors cannot be easily changed. Instead, human influence can be altered and defined by the building's occupants. Proper maintenance is required to keep buildings running efficiently [1]. Additionally, social and economic factors also have a non-negligible impact on building energy use.

This section gives a brief introduction to the current and future situation of building energy use and supply in Norway and Norwegian public municipal buildings, as well as energy impacts under special circumstances.

1.1.1 Current building energy use in Norway

About 36-40% of the world's energy is used in building services each year. Specifically, for example, in 2019, the building sector accounted for 35% of global final energy use and 38% of energy-related CO_2 emissions [2]. Although CO_2 emissions declined in 2020, mainly due to the COVID-19 pandemic, the building sector's share

of final energy use and CO_2 emissions for the year was 36% and 37%, respectively, almost the same as in 2019 [3]. Norway has committed to reducing national greenhouse gas emissions by 30% from 1990 levels by 2020, 40% by 2030 and 80-95% by 2050, in order to achieve a low-emissions society. This is in line with the EU's desire to reduce emissions across all sectors [4]. Energy efficiency strategies for urban building stocks are expected to make a significant contribution to reducing energy use and greenhouse gas emissions.

In climates with high heating demand, such as in the Nordic countries, a large amount of building energy is used for heating purposes, such as space heating (SH) and domestic hot water (DHW). Due to the abundant hydro-power providing cheap and green electricity, this strong electricity production has been dominating and monopolizing the Norwegian energy system, making this country remains highly dependent on electricity for heating in residential and service buildings. According to statistics [5], nearly three-quarters of Norwegian households use electricity for heating in the form of electric radiator, electric floor heating, air source heat pump, or central electric heating. In the service sector, electricity accounts for about 77% of total energy use, mainly for heating purposes. Furthermore, in the Nordic countries, although heat pumps (HPs) are gradually replacing direct electric heating, electricity demand in the residential sector has been increasing over the last decade, according to a report by Nordic Energy Research [6].

Given the rapid electrification in buildings, as well as the transport sector in countries such as Norway, alternative heating methods should be promoted to alleviate the increasing stress on the grid. District heating (DH) systems play a vital role in reducing primary energy use and CO_2 emissions in the building sector. In general, primary energy factors may vary due to changes in fuel and incentives from national policies. On the European scale, the primary energy factor for electricity is 2-2.5 [7], while the DH is 0.6-1.3, depending on the mixed heat sources from renewables to fossil fuels [8]. Therefore, DH has great potential to relieve stress on the grid in this region. For example, in a neighboring country like Sweden, DH supplies 60% of their total building heating demand [9]. Driven by the economic and environmental benefits of DH, Norway has introduced relevant regulations and investment subsidies to expand the DH systems. Over the past decade, DH use in Norway has doubled, with 26.7% of DH production currently used for residential heating and 54.5% for service heating [10].

1.1.2 Benefits and challenges of low-temperature district heating

However, despite the higher efficiency of DH as introduced above, there are still two challenges that may hinder the DH expansion, the competition from individual HPs and the decrease in building heating demand. For the former, the high flexibility of individual HPs makes them favored by end-users; for the latter, as renovation of

existing buildings, low-energy buildings, passive houses and near-zero energy buildings account for an increasing proportion of the building market, the future building stock will feature a highly improved envelope and accordingly significantly reduced space heating (SH), as stated in e.g. the Norwegian standards [11] and regulations [12], and the European Union's legislative framework [13].

To stay economically and environmentally competitive in the heating market, the DH development needs a transition to low-temperature DH (LTDH) by decreasing the DH supply temperatures from the current 80-120°C level to a much lower level, e.g. 45-55°C. LTDH provides wider opportunities for integrating distributed renewable energy in the system, such as employing building-sized HPs or renewables for peak shaving [14]. Meanwhile, alternative economical piping materials, such as PEX/Aluminum/PE can also be employed in LTDH by reducing construction costs and heat loss through distribution networks. A pilot study of a renewable energy-based Danish municipality proved several benefits of LTDH with a supply and return temperature at 55°C and 25°C, that the reduction percentages of the primary energy demand, the thermal grid, and the costs were 4.5%, 6%, and 2.7%, respectively, comparing with the current 3rd generation DH system [15].

The desire for a circular economy and the increased power trading among neighboring countries has promoted LTDH expansion based on both political landscapes and energy efficiency directives requiring resource recovery and expansion of renewables [14]. On the transition to LTDH, the change in heating load is the fundamental premise. Therefore, analyzing the potentials and challenges by understanding the key heating loads from a planning and operational aspect is a stepping stone to accelerate the transition. Some examples addressing the challenges are shown below.

From the investigation of the current European low-temperature based 5th generation district heating and cooling (LTDHC) systems, the review study concluded that the LTDHC requires more advanced control strategies because of the bi-directional energy flows and decentralized interactions [16], which highlights the information and communication technologies will be required to advance LTDH [16]. For example, after coupling the LTDH to the electricity grid using power-to-heat (P2H) technologies, the heating and electricity load profiles and flow on demand side may change [17], which may cause operational problems and therefore require enhanced communication between the power supply and the DH system. Another example is shown with the analysis of the challenges and potentials for LTDH in the Nordic climate. The study found that an LTDH system is keen to the indoor set-point temperature, and the prediction of the outdoor temperature compensation curve needs to be optimized to benefit the indoor temperature and mass flow [18]. Briefly summarizing, there are certain challenges that need to be tackled in order to achieve the best performance for LTDH, and the establishment of viable tele-interaction between users and suppliers is one of the solutions. Therefore, LTDH and electricity grids require intelligent prediction of peak thermal loads and control systems.

1.1.3 Current status and future projection of municipal buildings

Local municipalities are responsible for monitoring and managing the operation of public buildings, and the energy data for such buildings are in most cases available. Among the public buildings, primary educational institutions such as schools and kindergartens, and special residential buildings such as nursing homes, their energy use has not been extensively studied, especially in the cold climate, as described in [19].

Educational buildings are designed to educate pupils and students to be intellectually and socially conscious in accordance with the laws of Norway and many other countries regarding daycare seating and the right to education. Besides that, the building operators are responsible to maintain the desired indoor environment in energy-efficient manners [20]. According to the construction situation of the local government in Norway [21], schools account for nearly 50% of the total local public building mass and are one of the most important building types. It has been found that energy expenditure is the second largest operation cost of American schools after employee salaries [22]. In Italy, 60% of educational buildings were constructed before 1976, and despite the extraordinary retrofits, most failed to meet the current energy performance requirements [23]. Population is one of the main drivers of educational building development. In anticipation of population growth and urbanization, there is a growing need for educational building expansions [24].

Currently, in Norway c.a.16% people over 65 reside in nursing homes, while the average level of OECD countries is 13% [25]. The Norwegian Institute of Public Health projects the population over 80 to double in two decades, similar to the expected average demographic growth in OECD countries. Approximately 90% of nursing homes in Norway are owned and managed by municipalities, along with a few private enterprises subsidized by the authorities. In 2018, the long-term care expenditure in Norway was 3.5% of GDP with 2250 USD PPP (purchasing power parities), compared to the OECD average expenditure of 1.5% with 800 USD PPP [26].

A modern nursing home usually covers a large floor area and includes residents' private rooms with round-the-clock occupancies, large common spaces (i.e. dining halls, activity rooms, etc.), on-site 24/7 nursing service, laundry and catering services, and administrative offices. The functions and characteristics of this building type make it an important public residential building for the advancement of social welfare and the caring needs of residents in the aging society. As most of the Nordic nursing homes are supplied by DH, it is important to study their energy needs during the transition to LTDH and improve building energy supply, for which reliable prediction methods are needed.

1.1.4 Special circumstances

To examine whether building operation strategies are energy efficient and resilient, it is necessary to study the energy impacts under special circumstances. The special circumstances may be caused by equipment failures and/or by sudden demand changes.

The supply-related special circumstances, such as the energy not supplied (ENS) caused by grid faults, are generally low in the Nordic countries with the exception of Iceland. Norway's ENS in 2013 was 10 801 MWh, and the annual average for the decade 2004-2013 was 3423 MWh. Grid disturbances happened 317 times in 2013, of which 92 led to ENS. The increased failures were mostly weather-related and reactive components. On July 27 of the same year, a lightning strike tripped two parallel 132 kV lines in neighboring Sweden, causing more than 43 000 customers to lose power for 45 minutes [27]. Therefore, diversification of energy sources, especially for heating, can enhance the thermal resilience of urban areas, which is very important for Nordic countries.

Regarding demand-related special circumstances, since the World Health Organization (WHO) declared the COVID-19 disease a pandemic in March 2020, many countries have adopted restrictive measures to tackle the pandemic and slow the spread of the coronavirus [28]. Occupancy schedules for buildings have been adapted to remote work due to partial or full lockdowns on public spaces, and commercial and industrial programs. The drastic changes have had a major impact on energy demand and put pressure on energy sector management and energy markets. An investigation of the magnitude of the impacts of various restrictions on total energy demand examined four European countries with strict containment measures and two European countries with less restrictive ones [29]. A comparison of total electricity demand based on resident activities shows that electricity demand has dropped significantly in the countries with strict lockdown measures [29]. These sudden changes in energy demand have affected energy production and utility companies' investment plans. The power sector in Southeast Asia was examined in [30] and the study finds the restrictions have exacerbated the vulnerability of the current power system there. It highlights the significance of buildings as resilient systems for this region. In addition to the economic strains on utility companies, changes balance and increased uncertainty have created new challenges for load forecasting and requirement for flexibility.

In order to comply with Norway's national lockdown regime, which was launched from March to May 2020, teaching activities on campus were severely disrupted and switched to remote learning, with many employees following the work-from-home regulations. Section 2.2 presents a literature review on the impacts worldwide and the thesis examined the techno-economic impacts of lockdowns on building energy demand.

1.2 Thesis objectives, research questions and research tasks

The main objective of this PhD research is to gain a deeper understanding of the energy use of Norwegian urban buildings. Primarily, the research aimed to develop appropriate prediction models and to identify representative energy load profiles for Norwegian urban buildings, which may be used to improve the efficiency of urban building energy supply systems.

The study was carried out based on measured data obtained from schools, kindergartens, university buildings, nursing homes, and residential buildings. These buildings have diverse operating regimes and technological solutions for building energy supply systems. Therefore, the methods proposed in the PhD thesis were aimed to be applicable to the analysis of various building types. Finally, the following questions were addressed to achieve the research purpose:

- **Research Question 1:** What are the environmental impacts of heating systems in future building development?
  - Task 1.1: Identify the typical annual CO_2 emissions from operating heating systems for certain building types.
  - Task 1.2: Project the CO_2 emissions for building development, with the consideration of different environmental background factors.

- **Research Question 2:** What factors shall be considered for building heating and electricity operation and what are the differences between the two delivered energy forms?
  - Task 2.1: Analyze the demand patterns for heating and electricity separately.
  - Task 2.2: Develop a systematic approach for predicting heating and electricity load profile separately on an annual basis.
  - Task 2.3: Evaluate the prediction performance of heating load and electricity load separately.

- **Research Question 3:** How can the methods for developing and predicting heating load profiles be improved for daily LTDH operation?
  - Task 3.1: Develop hybrid prediction methods for heating load prediction, including long-term sizing and short-term prediction.
  - Task 3.2: Evaluate and compare the heating load prediction performance of the hybrid methods.

- **Research Question 4:** What are the energy and economic impacts of the buildings under special circumstances?
  - Task 4.1: Compare the energy load profiles of the buildings before and after lockdowns.
  - Task 4.2: Identify and estimate energy and economic saving potentials in non-residential buildings.
  - Task 4.3: Identify and estimate energy and economic increase in the residential buildings regarding different household size and household members.

1.3 Thesis organization

According to the research tasks, the thesis was divided into seven main chapters, as listed in the following content:

- Chapter 2 presents a literature review of energy load prediction methods and the impacts of lockdowns on energy and economy.
- Chapter 3 provides the data information of the observed buildings.
- Chapter 4 explains the theory and principal methods of data analysis, energy load prediction and prediction quality evaluation criteria, as well as CO_2 emissions calculation.
- Chapter 5 describes the research examples of using the above methods to bring about the thesis purpose.
- Chapter 6 presents the key results of the research examples.
- Chapter 7 demonstrates the main conclusions, acknowledges the limitation, and recommends future research.

The main findings and results of the research work are shown in the collected papers, as listed in Section 1.4.

1.4 Publications

The PhD thesis is built on four main papers including one conference paper and three journal papers. The main papers address the research questions and are appended in the thesis. During the PhD study, the author also contributed to six additional papers extending the research questions and bringing new ideas to the project, and two other papers reflecting the author's previous working experience. An overview of the main papers and additional papers is illustrated in Figure 1.1, which presents how the 10 papers related to each research question and the addressed aspects.
The papers' publication information and the author's contribution to each paper are as follows.

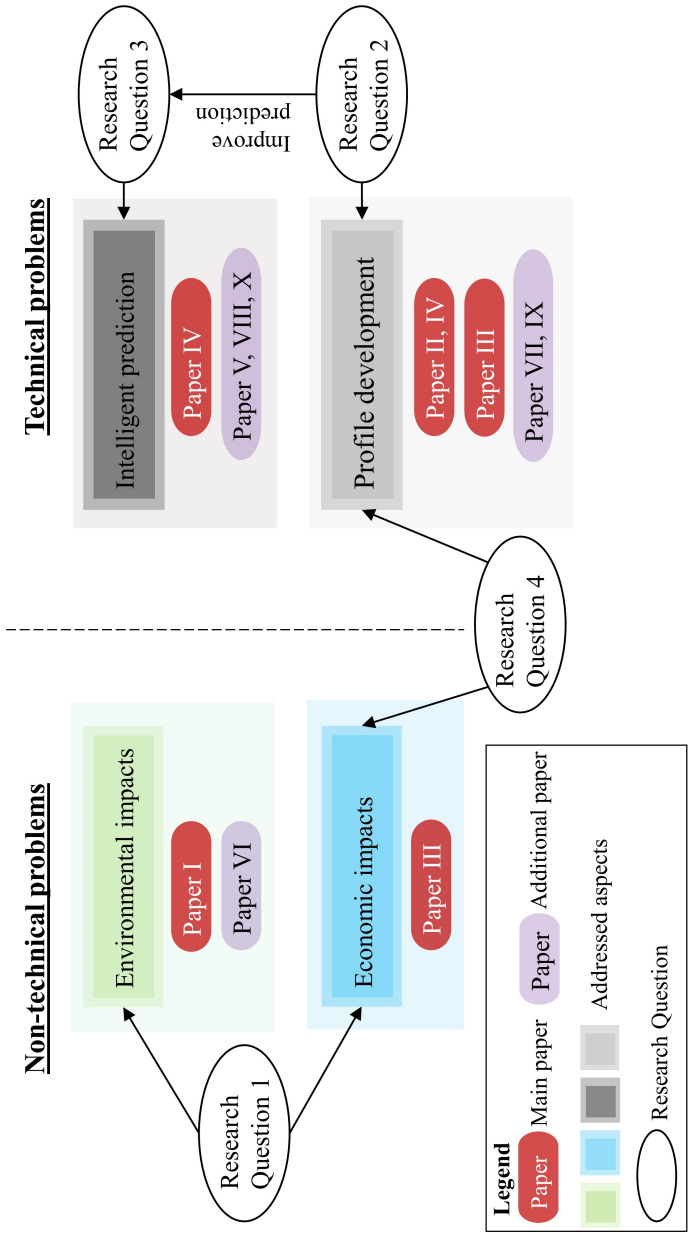

Figure 1.1: Overview of the publications

Main papers by the author INCLUDED in the thesis:

Paper I

Ding, Y., Brattebø, H. and Nord, N., 2019. Energy analysis and energy planning for kindergartens based on data analysis. *1st Nordic conference on Zero Emission and Plus Energy Buildings*, *IOP Conference Series: Earth and Environmental Science*, Volume 352(1), p.012031.

Author contribution: This paper is a full-length article. The conceptualization of this paper was initiated by the author and Natasa Nord. The author conducted a formal analysis, methods, and the original draft. Helge Brattebø and Natasa Nord supervised the work, reviewed and commented on the paper.

Paper II

Ding, Y., Brattebø, H. and Nord, N., 2021. A systematic approach for data analysis and prediction methods for annual energy profiles: An example for school buildings in Norway. *Energy and Buildings*, 247, p.111160.

Author contribution: This paper is a full-length article. The conceptualization of this paper was initiated by the author and Natasa Nord. The author conducted a formal analysis, methods, and the original draft. Helge Brattebø and Natasa Nord supervised the work, reviewed and commented on the paper.

Paper III

Ding, Y., Ivanko, D., Cao, G., Brattebø, H. and Nord, N., 2021. Analysis of electricity use and economic impacts for buildings with electric heating under lockdown conditions: examples for educational buildings and residential buildings in Norway. *Sustainable Cities and Society*, 74, p.103253.

Author contribution: This paper is a full-length article. The conceptualization of this paper was initiated by the author, Dmytro Ivanko, and Natasa Nord. The author conducted a formal analysis, methods, and the original draft. Dmytro Ivanko and Guangyu Cao reviewed and commented on the paper. Helge Brattebø and Natasa Nord supervised the work, reviewed and commented on the paper.

Paper IV

Ding, Y., Timoudas, T.O., Wang, Q., Chen, S., Brattebø, H. and Nord, N., 2022. A study on data-driven hybrid heating load prediction methods in low-temperature district heating: an example for nursing homes

in Nordic countries. *Energy Conversion and Management*, p.116163.

Author contribution: This paper is a full-length article. The conceptualization of this paper was initiated by the author, Qian Wang, and Natasa Nord. The author conducted a formal analysis and methods with the assistance of Thomas O. Timoudas and Qian Wang. The original draft of the paper was written by the author. Shuqin Chen, Helge Brattebø, and Natasa Nord supervised the work, reviewed and commented on the paper.

Additional papers by the author not included in the thesis:

Paper V

Xue, K., Ding, Y., Yang, Z., Nord, N., Barillec, M., et al, 2020. A Simple and Novel Method to Predict the Hospital Energy Use Based on Machine Learning: A Case Study in Norway. *International Conference on Neural Information Processing, ICONIP 2020: Neural Information Processing*, Part of the *Communications in Computer and Information Science book series*, CCIS, Volume 1332, pp.11-22.

Author contribution: This paper is a full-length article. The author contributed parts of the methods, reviewed and commented on the paper.

Paper VI

Nord, N., Ding, Y., Skrautvol, O. and Eliassen, S., 2021. Energy Pathways for Future Norwegian Residential Building Areas. *Energies*, 14(4), p.934.

Author contribution: This paper is a full-length article extended from the paper published in Cold Climate HVAC Conference 2018, pp. 505–517, part of the Springer Proceedings in Energy book series (SPE). The author conducted the extension draft of this paper.

Paper VII

Ivanko, D., Ding, Y. and Nord, N., 2021. Heat use profiles in Norwegian educational institutions in conditions of COVID-lockdown. *REHVA European HVAC Journal*, pp.55 - 58, 02/2021.

Author contribution: This paper is a short communication article. The author reviewed and commented on the paper.

Paper VIII

Ding, Y., Ding, Y. and Nord, N., 2021. Data-driven analysis of electricity use for office buildings: a Norwegian case study. *Cold Climate HVAC & Energy 2021*, *E3S Web of Conferences*, Volume 246, p.04005.

Author contribution: This paper is a full-length article. The author reviewed and commented on the paper.

Paper IX

Ivanko, D., Ding, Y. and Nord, N., 2021. Analysis of heat use profiles in Norwegian educational institutions in conditions of COVID-lockdown. *Journal of Building Engineering*, 43, p.102576.

Author contribution: This paper is a full-length article. The author contributed parts of the methods, reviewed and commented on the paper.

Paper X

Timoudas, T.O., Ding, Y. and Wang, Q., 2022. A novel machine learning approach to predict short-term energy load for future low-temperature district heating. *CLIMA 2022 Conference*.

Author contribution: This paper is a full-length article. The author contributed parts of the methods, reviewed and commented on the paper.

Other papers by the author not included in the thesis:

Paper XI

Wang, S., Niu, Y., Zhu, G., Ding, Y., Guo, X. and Hui, S., 2021. NO formation and destruction during combustion of high temperature preheated pulverized coal. *Journal of the Energy Institute*, 99, pp.82-87.

Author contribution: This paper is a full-length article. The author reviewed and commented on the paper.

Paper XII

Wang, S., Zhu, G., Niu, Y., Ding, Y. and Hui, S., 2021. Experimental and kinetic studies on NO emission during pulverized coal preheating-combustion process with high preheating temperature. *Journal of the Energy Institute*, 97, pp.180-186.

Author contribution: This paper is a full-length article. The author reviewed and commented on the paper.

2
LITERATURE REVIEW

> Facts are stubborn things, but statistics are pliable.
>
> *Mark Twain*

> All models are wrong, but some are useful.
>
> *George Box*

This chapter introduces literature reviews of energy load prediction methods including short-and-long-term prediction, as in Section 2.1, and the energy and economic impacts on building energy demand under special circumstances, as in Section 2.2.

2.1 Previous studies on load prediction methods

By leveraging large amounts of measured data, data-driven methods such as statistical methods and machine learning (ML) have shown advantages in energy load prediction.

2.1.1 Short-term prediction methods

In response to the challenges of LTDH as well as its integration with renewables, smart tools and methods shall be employed to understand the heating load. The ML research studies presented below consider their promising results and current limitations. Section 2.1.1.1 briefly introduces the knowledge of Artificial neural network (ANN) and afterward, Section 2.1.1.2 presents studies on the ANN-based models, as ANN is one of the two load prediction methods used in the thesis, see the mathematical description in Section 4.2; several other ML methods are introduced in Section 2.1.1.3, which aims at presenting a more comprehensive literature search on smart load prediction.

2.1.1.1 Introduction of artificial neural network

Artificial neural network (ANN) is one of the ML methods found to be the most widely used in energy planning, followed by Support Vector Machines (SVM) and

Auto-regressive Integral Moving Average (ARIMA) methods, and Statistical methods like Linear Regression (LR) [31].

The history of ANN can be traced back to the 1940s when Warren McCulloch and Walter Pitts founded neural networks based on mathematics and an algorithm called threshold logic. Later, the research of neural networks split into two directions, one focuses on biological processes in the brain, and the other focuses on the application of neural networks in artificial intelligence. The latter one is the method adopted in the thesis. In the field of ML and cognitive science, ANN is a mathematical model or computational model that imitates the structure and function of the biological neural network, and is used to estimate or approximate functions. Neural networks are calculated by connecting a large number of artificial neurons. A modern neural network is a nonlinear statistical data modeling tool and is usually optimized by a learning method based on mathematical statistics type. Figure 2.1 shows a basic schematic of a feed-forward neural network architecture with three basic layers, an input layer, a hidden layer, and an output layer [31]. The number of hidden layers can be increased depending on the complexity of the tasks.

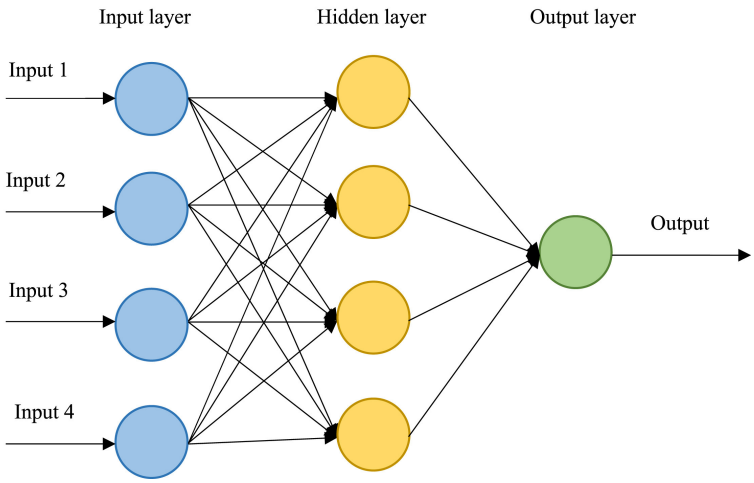

Figure 2.1: A basic ANN schematic architecture

Each neuron is connected to every other neuron in the previous layer through adaptive synaptic weights. Regardless of the ANN architecture, a training process is needed for building an ANN model. With the available data inputs, the training process is to train the ANN by modifying and adjusting the connection weights and biases to learn the relationship among the inputs and capture the key information, and finally, the desired output may be acquired.

2.1.1.2 Artificial neural network-based studies

Mainly because of the early implementation of smart meters, ANN and other data-driven approaches have focused primarily on electricity use rather than heat use. For example, to estimate the occupancy-related electricity demand of air-conditioning systems in non-residential buildings, using occupancy as input, an ANN-based model was developed, which was identified by blind system identification, thereby improving the accuracy of electricity prediction [32]. However, the proposed model needed validation over a period of at least one year to account for seasonal variations in the interaction of occupancy with electricity profiles [32]. Another ANN-based model compared two back-propagation learning algorithms (Bayesian regularization and Levenberg-Marquardt) for day-ahead and hour-ahead electricity load prediction in a downtown area involving many building types [33]. Aggregating prediction for heterogeneous building types in the area improved day-ahead load prediction performance by 7.9-11.9% compared to the total predicted load for the area [33].

The recent widespread implementation of smart heat meters to collect (sub)-hourly heat use data has greatly promoted the quality of heating load prediction and clustering studies for heating use data analysis [34]. As highlighted in [35], the knowledge and experience obtained from the studies of building electricity demand data can be used for heating demand analysis and uncertainty (such as weather forecast). Two models, auto-regressive multiple linear regression (MLR) and auto-regressive multiple non-linear regression (MNLR), were first established to predict the DH load curves of reference buildings, and then the defined reference load curves were aggregated to urban district level [36]. The work showed that the ANN-based MNLR outperforms MLR in terms of 4.2% reduction in mean squared error (MSE) for predicting buildings with high daily load variation, such as office buildings [36]. Three ML methods, SVM, deep neural network (DNN) and extreme gradient boosting (XGBoost), were respectively employed to establish a multi-step ahead forecasting model of DH load, which also considered direct strategy and recursive strategy [37]. All three ML methods using both strategies may accurately predict the next day's DH load by using the previous day's influencing factors. Finally, it was recommended to further explore the potential of these heating load predictions to optimize the DH systems operation. A Gaussian Mixture Model (GMM) clustering defined four typical DH operation modes in office buildings in a semi-arid climate (having cold and dry winters) by considering sub-patterns related to temperature and occupant behaviors [38]. Combining the GMM clustering with regression and ANN models, respectively, the accuracy of hourly heating load prediction was greatly improved by 38.7-75.7% [38]. However, it was still difficult to predict peak heating loads from night to morning because of the possible random operating behaviors. As presented in [39], the prediction model established on Convolutional Neural Network Long Short-Term Memory (CNN-LSTM), outperformed other ML methods in solving the thermal inertia problem in DH systems, mainly thanks to the model's combination of the feature extraction capability of CNN and the advantages of LSTM's 2D space

ability. However, this model required a large number of sensors, a large amount of data storage, and needs daily re-training [39].

In conclusion, the ANN-based prediction models have enhanced energy load prediction, especially the heating load prediction performance, such as computation time and prediction quality, has been largely improved. However, problems such as lack of big data for model training, difficulty in peak load prediction, regular re-training and others, shall be solved.

2.1.1.3 Other machine learning-based studies

Additionally, a few research explored the uncertain potentials of reinforcement learning (RL) applied to energy prediction. As proposed in [40], three deep RL techniques, asynchronous advantage actor-critic (A3C), deep deterministic policy gradient (DDPG), and recurrent deterministic policy gradient (RDPG) models were compared with three supervised models for building cooling energy forecasting. RDPG gave the best performance as improving the mean absolute error (MAE) by 16-32%, whereas it requires over 100 times the model training time [40]. To identify the typical electricity load patterns (TELPs) at an individual building level, a method with two-step clustering analysis was suggested in [41]. The first step was to use the Density-based spatial clustering application with noise (DBSCAN) algorithm clustering technique to locate daily outliers, and the second step employed the k-means algorithm to group similar TELPs. The effectiveness of this framework was verified by the time-series electricity data of several in-use office buildings. A transfer learning-based approach was proposed in [42] to predict other buildings by leveraging massive well-measured building operating data. Quantitative assessment of 24-hour ahead building energy demand predicted by this method was studied on office, school, and university building types. Compared to those individual models, this approach could reduce prediction errors by 15-78% and provide insights for realizing the value of existing data in building energy management [42]. The Q-algorithm was used to develop a data-driven model by dividing the data into two parts by using a reference load Q_{REF} under three-level decision trees [35]. This model is robust to district-wide heating load prediction. Nevertheless, the satisfied accuracy results (R^2) claimed in [35] are significantly below the common value, which is 0.75 [43].

2.1.2 Long-term prediction methods

From the literature search, the main efforts on load prediction have been focused on short-term prediction, contributing to optimal scheduling of building energy supply systems, meanwhile mid- to long-term load prediction for typical building types has not been addressed well. Mid- to long-term energy load forecasts for typical building types can be used for efficient operation/maintenance strategies of local energy systems and building energy planning policies. A few studies on annual load profiles for certain building types are introduced below.

A method to automatically generate and reproduce the annual heating demand of residential buildings was proposed in [44]. However, in order to achieve recoverability of the relevant buildings and system parameters, data from reference buildings are needed, and scaling the proposed method to a larger set of buildings has not been validated yet. By involving tens of thousands of generation outputs from weather data files by Monte Carlo simulations, a probabilistic approach was proposed to formulate an annual cooling load profile for office buildings [45]. This prediction method can save substantial over-cooling time, which has been verified by measurement. A heating load weather normalization was proposed in [46], which segmented the weather data and heating load with heating degree days (HDDs) and performed multivariable linear regression. However, the method was only validated in two multi-family residential buildings.

2.2 Energy and economic impacts under lockdowns

2.2.1 Impacts on the energy load profiles

Energy profile is a useful tool for energy system planning and management. They reflect the customers' total energy demand and energy use pattern requirements. The COVID-19-related demand changes and corresponding energy load profiles are worth studying for different grid levels and sizes.

In an analysis of electricity use trends during the pandemic in Ontario, Canada, it was found that by April 2020, electricity had dropped by 14% and CO_2 emissions had decreased significantly [47]. The hourly-based load curve showed a shift in peak weekly electricity demand from the second half of the week to the first half of the week. Meanwhile, the morning and evening peaks were avoided, and the curve was obviously flattened [47]. Based on an analysis of electricity data covering millions of customers in Illinois, U.S., the results showed that the weekday load curves for residential buildings were more likely to be weekend curves [48]. By extrapolating the results of total load profiles, COVID-19-related profiles may alter long-term work schedules and further influence peak hourly loads [48].

Four simulation scenarios of typical household energy use in Serbia were defined in [49]: S1–reference case, S2–mild protection measures, S3–semi-quarantine measures, S4–complete quarantine to the relationship between user behavior and energy source uses. Using the building's occupancy profiles as inputs, the simulation models showed that heating and electricity use increased during the pandemic due to the increase in the users' presence. Compared to normal conditions, the scenario-based models implied heating and electricity use might increase by 31-32% and 54-58%, respectively [49].

2.2.2 Impacts on the energy demand

The Brazilian power system and its four subsystems were analyzed before and after distancing measures became effective [50]. A comparison of weekly electricity use and weekly change percentage showed a significant reduction in energy demand. Additionally, the energy use trends of subsystems were observed in different dynamics according to geographic location [50]. A data-driven analysis was carried out on the U.S. bulk power systems and electricity markets during the pandemic in [51]. The power sector was severely affected from March to May 2020. From the perspective of market analysis, the power operation and economic interests in the Northeast region were most seriously affected. Accordingly, it is suggested that possible shocks and disproportionate effects between energy companies and consumers deserve more attention and effort. According to an in-depth study of the global power system operation [52], many countries have suffered considerable revenue losses due to an 8%-30% reduction in total electricity demand. The sharp decrease was mainly due to the temporary suspension of industrial, commercial, and public transport activities. The conventional nuclear power generation suffered a reduction, while the contribution from renewables increased by 3.5-72%, depending on the countries [52]. In addition to the economic problems of traditional utilities, the challenges of load forecasting and the need for flexibility due to balance changes and increased uncertainty were highlighted in [53].

2.3 Summary of literature review

In short, previous research focused on improving energy systems has looked at measured energy data as a package of information, while most energy forecasts have not yet been conducted on sizing or energy demand requirements for typical building types. This may lead to two negative effects. First, without energy data mining or energy use pattern identification for different building types, abnormal energy use may be misled as inputs and thus deviate from anticipated benefits. Second, specifically with regard to LTDH, as only a few researchers have so far addressed the problems of LTDH prediction and improved operations using data mining methods, there may be a gap between smart heat meters and DH suppliers that requires bridges in between.

On the other hand, regarding the handling of special circumstances, the literature review indicates that there are many investigations of COVID-19-related energy use in non-cold climate regions. However, buildings in Norway and a similar climate lack real-world data analysis and scenario-based modelling of electric heating use.

Therefore, the primary aim of the thesis was to understand and identify load profiles of typical Norwegian urban buildings under normal conditions, with the consideration of estimating annual CO_2 emissions for typical building types, speculating normal building energy operation strategies, and improving load prediction quality.

Moreover, taking into account personal interests and municipal public expenditures, the secondary aim was to investigate the energy use behavior and economic impacts of buildings with electric heating in Norway during the COVID-19 pandemic, as well as unforeseen future disturbances, which may also have implications for local energy planning.

3

BUILDING AND ENERGY DATA INVENTORY

The studied buildings were divided into two cohorts depending on their connection to district heating (DH), Cohort 1 - buildings without DH and Cohort 2 - buildings with DH.

3.1 Building information

- **Cohort 1 - Buildings without DH**

  For buildings without district heating, electricity is their main energy supply source, for instance, space heating (SH), domestic hot water (DHW), ventilation, lighting, computers, and other electric appliances. In the thesis, 14 kindergartens, eight schools, one apartment, and one residential house were used to analyze impacts on energy use in buildings with electric heating (EH) under COVID-lockdowns, see Section 5.4. For SH supply, the kindergartens and schools use electric panel heaters and ventilation heating, the apartment with natural ventilation uses electricity for radiators, and the residential house also with natural ventilation is heated by a radiant wood stove, electric radiators, and an air-source heat pump (HP) for assistant heating.

  The floor areas of Cohort 1 buildings are as follows, kindergarten buildings ranged from 279 to 1143 m^2, school buildings from 2157 to 5443 m^2, the apartment and residential are 40 m^2 and 133 m^2, respectively.

- **Cohort 2 - Buildings with DH**

  For buildings with district heating, DH supplies SH and DHW needs. In the thesis, 40 schools with DH were used to analyze for typical annual load profiles, see Section 5.2, and 20 nursing homes with DH were used to improve load prediction in low-temperature district heating (LTDH), see Section 5.3.

  The floor areas of Cohort 2 buildings are as follows, school buildings ranged from 1822 to 8996 m^2, and nursing home buildings from 1350 to 10 940 m^2, respectively.

3.2 Energy data inventory

The historical hourly DH and electricity use data of the public buildings were retrieved from the energy monitoring platform of Trondheim Municipality [54], which is responsible for the operation and maintenance of local public buildings and institutions. Besides the observed buildings in the thesis, other public buildings such as sports centers, public libraries, and fire stations, are also monitored in the platform. Weather impacts (mainly outdoor temperature) were considered in the energy analysis and prediction, and the local historical weather data during the corresponding years were obtained from the Norwegian Meteorological Institute (MET Norway) [55]. Electricity data for the two residential buildings were voluntarily shared by the dwellers, who retrieved the data from local grid provider Tensio AS [56].

Most of the buildings have been evaluated for energy performance. Building construction year and energy labelling result of those buildings were obtained from the Norwegian Energy Efficiency Agency (Enova) [57]. The energy labelling scheme goes from A (best building energy performance) to G (worst performance) by considering the calculated delivered energy to each building. Table 3.1 summarizes the building information regarding energy label, construction year, and energy data duration [1].

Overall, Cohort 2 buildings were constructed more recently than Cohort 1 buildings and were better documented in the energy labelling scheme. As the buildings cover different floor areas and are featured with different energy efficiencies, the energy analysis was performed on the average specific load (W per m^2) across buildings within each building type, in a search for defining the representative energy use of each studied building type in the Nordic climate, by concerning buildings with different characteristics.

[1] Due to a different aspect, the study shown in Section 5.1 did not address the in-depth analysis of building energy use as the other three examples, and the detailed building information of the study in Section 5.1 was not included.

Table 3.1: List of observed buildings' information, Cohort 1 and Cohort 2 are included

Cohort 1 - Buildings without DH							
Schools Data duration (Y/M/D): 2018.01.01- 2020.12.31; Location: Trondheim							
Construction year	Before 1950	1950- 1979	1980- 1999	2000- 2010	After 2010		No infor.
Building number	/	4	2	/	/	/	2
Energy labels	A	B	C	D	E	F, G	No infor.
Building number	/	/	/	5	1	/	2
Kindergartens Data duration (Y/M/D): 2018.01.01- 2020.12.31; Location: Trondheim							
Construction year	Before 1950	1950- 1979	1980- 1999	2000- 2010	After 2010		No infor.
Building number	/	4	/	/	1	/	9
Energy labels	A	B	C	D	E	F, G	No infor.
Building number	/	/	1	/	4	/	9
Apartments Data duration (Y/M/D): 2018.10.01- 2020.12.31; Location: Trondheim							
Construction year	Before 1950	1950- 1979	1980- 1999	2000- 2010	After 2010		No infor.
Building number	/	/	1	/	/	/	/
Energy labels	A	B	C	D	E	F, G	No infor.
Building number	/	/	/	1	/	/	/
Townhouses Data duration (Y/M/D): 2018.10.01- 2020.12.31; Location: Trondheim							
Construction year	Before 1950	1950- 1979	1980- 1999	2000- 2010	After 2010		No infor.
Building number	/	1	/	/	/	/	/
Energy labels	A	B	C	D	E	F, G	No infor.
Building number	/	/	/	/	1	/	/

Cohort 2 - Buildings with DH							
Schools Data duration (Y/M/D): 2015.01.01- 2018.12.31; Location: Trondheim							
Construction year	Before 1950	1950- 1979	1980- 1999	2000- 2010	After 2010		No infor.
Building number	3	8	10	10	5		4
Energy label	A	B	C	D	E	F, G	No infor.
Building number	1	5	8	14	7	1	4
Nursing homes Data duration (Y/M/D): 2016.01.01- 2018.12.31; Location: Trondheim							
Construction year	Before 1950	1950- 1979	1980- 1999	2000- 2010	After 2010		No infor.
Building number	/	/	7	9	3		1
Energy label	A	B	C	D	E	F, G	No infor.
Building number	/	4	6	6	3	/	1

4

METHODS

This chapter explains the principal methods of this thesis. Section 4.1-4.2 introduces the two energy load prediction methods, namely Method 1 and Method 2, with a focus on long-term and short-term load prediction, respectively. Section 4.3 presents the load prediction performance evaluation by following quality criteria and cluster methods. Finally, the economic costs and environmental impacts of building energy systems are introduced in Section 4.4.

4.1 Prediction Method 1 - Long-term energy load prediction with energy signature curve models

In the thesis, long-term heating load prediction was made up of energy signature curve (ES curve) models with the consideration of heating degree days (HDDs) and temperature moving average (TMA), as introduced in Section 4.1.1-4.1.3, respectively. Prediction Method 1 was designed for the following purposes: 1) to size the heating system, 2) to evaluate building energy performance, and 3) to check the boundary for the prediction load by prediction Method 2, which is described in Section 4.2.

4.1.1 Energy signature curve model

The energy signature curve (ES curve) model is one of the important applications of linear regression, which is normally used to describe the relationship between two variables (predictor and response) by fitting a linear equation to the observed data [31], here refers to outdoor temperature and heating load. This method has been applied in building energy planning and management by efficiently utilizing measured data. Generally, ES curve consists of two parts, namely the temperature-dependent part and temperature-independent part, which are divided by the changing point temperature (CPT) or heating effective temperature. The ES curve may be expressed as:
If $t_\tau \leq$ CPT,

$$P(t_\tau) = p_1 \cdot t_\tau + p_2 + \epsilon \tag{4.1}$$

If $t_\tau >$ CPT,

$$P(t_\tau) = p_1 \cdot t_\tau + p_2 + \epsilon; = p_2 \tag{4.2}$$

In Eqs.(4.1) and (4.2), p_1 and p_2 are the coefficients of each ES curve model, $P(t_\tau)$ is the heating load for a certain outdoor temperature t at time instance τ, and ϵ is the residual error. The heating load follows the linear growth under the slope of p_1. When the outdoor temperature is below the CPT, the heating load highly depends on the ambient condition, as shown in Eq.(4.1); when the outdoor temperature is above the CPT, the heating load is either under a mild slope p_1 or at a small and constant volume as shown in Eq.(4.2). The building operation schedules are considered for establishing ES curve models for the corresponding periods. The ordinary least squares method is adopted to identify the coefficients aiming to minimize the error between predicted and observed values. A higher coefficient of determination (R^2) implies the model fits the data better. Technically, R^2 shall not be less than 0.75 for a satisfactory model [58, 43]. From this, the identified ES curve models may be applied to estimate building heating energy demand by combining the regression coefficients in Eqs.(4.1) and (4.2) with the corresponding weather data. ES curve model has been applied to the examples described in Section 5.2-5.3, and the corresponding results are shown in Section 6.2-6.3.

4.1.2 Heating degree days

A degree day is a measurement to quantify the heating and cooling demand during a certain period and assess the climate for different regions. In the thesis, heating degree day (HDD) was used to segregate heating seasons, which compares the daily difference between heating balance temperature t_{bal} (assumed at 15°C) and hourly outdoor temperature $\frac{1}{24}\sum_{\tau=1}^{24}(t_{bal} - t_\tau)$, the negative values were set to zero without including cooling effects [46, 59]. Days with HDDs smaller than $\frac{5}{24}$°C were treated as the summer, between $\frac{5}{24}$°C and $\frac{100}{24}$°C as the transition season, between $\frac{100}{24}$°C and $\frac{510}{24}$°C as the heating season, and over $\frac{510}{24}$°C as the very cold season. The application of HDD is shown in Section 5.3.

4.1.3 Temperature moving average

By considering time delay due to building thermal inertia, the concept of temperature moving average (TMA) was used to define a more accurate mathematical relation between outdoor temperature and heating load with adjustment. Depending on building physics, buildings' temporary heat storage capacities can be various. For example, better-insulated buildings coupled with internal heat gains may experience longer time lags. The practices of TMA in studies [60, 61] present that the lag time shall be considered in accordance with building physical characteristics. When involving TMA, the empirical lag hour such as 24 and 48 hours were used as the reference range values. A search for the highest correlation between the outdoor temperature and heating load was performed by shifting the outdoor temperature backward hour by hour until reaching the reference range limits. A higher abso-

lute value of the correlation implies a better fit between the heating load and the moved outdoor temperature. The effect of temperature lag is presented in Figure 4.1, where the highest correlation is located at five hours for the analyzed building group [62]. Therefore, the linear regression between the outdoor temperature and the heating load was identified with the outdoor temperature five-hour ago. TMA has been considered in the examples using ES curve model.

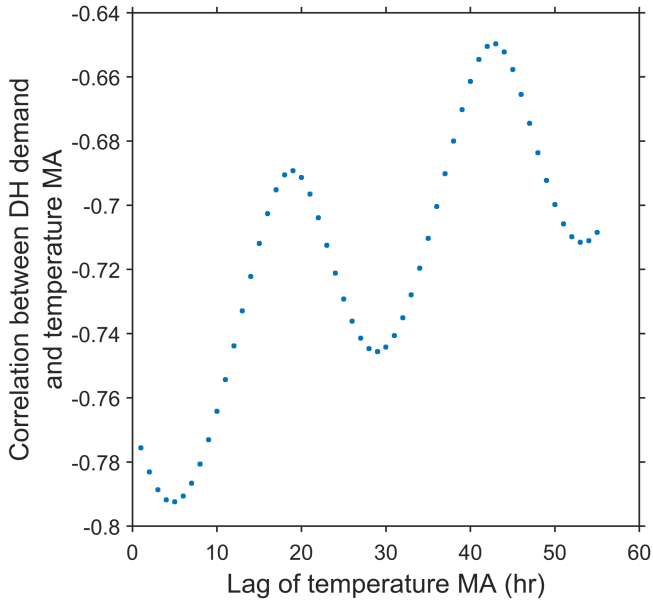

Figure 4.1: Temperature lag moving average, where 5-hour lag yielded the highest correlation between heating needs and outdoor temperatures

4.2 Prediction Method 2 - Short-term energy load prediction with Artificial neural network models

In the thesis, prediction Method 2 refers to short-term prediction, which deals with day-ahead prediction to solve the problem of predicting DH load for the next 24-hour period at a given daily time point. The models may improve short-term DH production planning and operation purposes. Two individual Artificial neural network (ANN) prediction models were developed using different input parameters, to compare the parameters' impacts on the prediction accuracy. Method 2 has been mainly applied to the example described in Section 5.3, and the corresponding results are shown in Section 6.3.

4.2.1 Inputs to Artificial neural network models

The first ANN model considered only the impacts from outdoor temperature, by using the measured outdoor temperature for certain hours p preceding the prediction time point τ and the forecasted outdoor temperature for the following 24 hours. In addition to the outdoor temperature considered in the first model, the second ANN model contained the historical DH load, which is the measured DH load for certain hours p preceding the prediction time point τ.

When considering the two categories of input, weather data both the historical data and forecasted data are usually publicly accessible via meteorological institutions, however, historical energy load data are in some cases either accessible with delays and limitations or of low data quality. Therefore, the first model may be useful when these challenges occur.

4.2.2 Mathematical description of Artificial neural network models

The mathematical expression of the two ANN models are formulated as follows, Q_τ and t_τ respectively represent the measured energy load and measured outdoor temperature at hour τ, $\widehat{Q}_{\tau,s}$ and $\widehat{t}_{\tau,s}$ respectively represent to the predicted energy load and forecasted outdoor temperature, from hour τ for each hour till hour $\tau + s$, defined for $s = 1, \ldots, 24$. The prediction and historical inputs are expressed as the following:

$$\widehat{Q}_\tau^{24} = (\widehat{Q}_{\tau,1}, \ldots, \widehat{Q}_{\tau,24}), \tag{4.3}$$

$$\widehat{t}_\tau^{24} = (\widehat{t}_{\tau,1}, \ldots, \widehat{t}_{\tau,24}), \tag{4.4}$$

$$Q_\tau^p = (Q_{\tau-p+1}, \ldots, Q_\tau), \text{and} \tag{4.5}$$

$$t_\tau^p = (t_{\tau-p+1}, \ldots, t_\tau) \tag{4.6}$$

where Q_τ^p and $\widehat{Q}_\tau^{24}$ represent, at hour τ, the measured DH load for the previous p hours (including τ) and the targeted predicted DH load for the next 1 to 24 hours, respectively, meanwhile t_τ^p and $\widehat{t}_\tau^{24}$ represent, at hour τ, the measured outdoor temperature for the previous p hours and the forecasted outdoor temperature for the next 1 to 24 hours, respectively. With these notations, the two ANN models may be described as:
a. considering only outdoor temperature as the predictor of the model,

$$\widehat{Q}_\tau^{24} = f(\widehat{t}_\tau^{24}, t_\tau^p), \tag{4.7}$$

b. considering both energy load and outdoor temperature as the predictors of the

model,

$$\widehat{Q}_{\tau}^{24} = f(\widehat{t}_{\tau}^{24}, t_{\tau}^{p}, Q_{\tau}^{p}), \tag{4.8}$$

Mean squared error (MSE) was used as the loss function, and *Adam* was used for the parameter optimization, in other words, to minimize a loss function. The two ANN models were examined with 24, 48, and 72 hours of historical data (outdoor temperature and/or DH load) in the search for the optimal historical p hours. Regarding the loss function, between using 24 and 48 hours of historical data was found a significant difference, while between using 48 and 72 hours it was found a minor difference. Benefiting from the faster speed of running the models, the number of historical hours p was determined to be 48. Therefore, 48 hours of historical data were selected. Structure of the both ANN models was built with one input layer, one hidden layer, and one output layer, as depicted in Figure 2.1. The notation f_{72} represents model $f(\widehat{t}_{\tau}^{24}, t_{\tau}^{48})$ in Eq.(4.7) and notation g_{120} represents model $f(\widehat{t}_{\tau}^{24}, t_{\tau}^{48}, Q_{\tau}^{48})$ in Eq.(4.8), and the two notations were used in the thesis for simplicity.

4.3 Prediction performance evaluation

To examine the quality of the prediction models and the possibility of employing the model for future use, a quality evaluation shall be performed. Four criteria are introduced in Section 4.3.1, and they are Mean absolute percentage error (MAPE), symmetric Mean absolute percentage error (sMAPE), Normalized mean bias error (NMBE), and Coefficient of variation of the Root mean squared error (CV(RMSE)). Evaluation results of using the quality criteria are shown in Section 6.2-6.3. In addition, cluster methods of Piece-wise aggregate approximation (PAA) and Symbolic aggregate approximation (SAX) are suggested for further evaluation if the prediction model cannot satisfy the quality criteria evaluation, see Section 4.3.2, the corresponding results are shown in Section 6.2.

4.3.1 Quality criteria

MAPE summarizes the relative mean error between the actual(measured) and predicted data in absolute value, which avoids the possible offsets between positive and negative errors. The expression of MAPE is given as:

$$MAPE = \frac{1}{n}\sum_{i=1}^{n}|\frac{A_i - F_i}{A_i}| \cdot 100\% \tag{4.9}$$

sMAPE is defined by modifying the original MAPE. sMAPE and can be used as a supplementary criterion of MAPE, by setting lower and upper bounds. sMAPE is given as:

$$sMAPE = \frac{1}{n}\sum_{i=1}^{n}|\frac{A_i - F_i}{(|A_i| + |F_i|)/2}| \cdot 100\% \tag{4.10}$$

NMBE calculates the total error percentage over the examined data, and its directionality implies either an over-prediction or under-prediction. A negative result

of NMBE means an over-prediction is made, and conversely, an under-prediction. NMBE is given as:

$$NMBE = \frac{1}{n}\frac{\sum_{i=1}^{n}(A_i - F_i)}{\overline{A}} \cdot 100\% \tag{4.11}$$

Root mean square error (RMSE) assesses the standard deviation of the prediction errors, and CV(RMSE) normalizes the RMSE with the average value over the examined data. NMBE and CV are commonly used together to indicate whether the model can reflect the real load shape. CV(RMSE) is given as:

$$CV(RMSE) = \frac{\sqrt{\frac{1}{n}\sum_{i=1}^{n}(A_i - F_i)^2}}{\overline{A}} \cdot 100\% \tag{4.12}$$

In the expressions above, A_i is the measured value, $\overline{A}$ is the average measured value, F_i is the predicted value, and n is the number of the observations.

As indicated by guidelines and handbook, when hourly data are utilized as the case of the thesis, MAPE and sMAPE results shall be smaller than 20%, NMBE within ±10%, and CV smaller than 30% for verifying a satisfied prediction model [58, 63, 64].

4.3.2 Cluster methods of discretization evaluation

Moreover, cluster methods of piece-wise aggregate approximation (PAA) and symbolic aggregate approximation (SAX) were also used for evaluating the prediction models in the thesis. First, the annual load profile was extracted on a seasonal daily average basis. Every 24-h was considered as a time-series. Second, the daily average DH load was initially Z-normalized with $\frac{C_i - \mu}{\sigma}$, where μ and σ refer to the mean value and the standard deviation of the time-series, respectively. The Z-normalized time-series $C = C_1, C_2, \ldots, C_n$ were proceeded through the PAA approximation, which aimed to reduce the dimensionality of the raw time-series by splitting them into equally sized intervals [65, 66]. Each interval was then calculated by averaging the values within the interval. The raw time-series C may be represented by a dimensionally reduced new series as $\overline{C} = \overline{C_1}, \overline{C_2}, \ldots, \overline{C_w}$. The number of data in the new time-series, w, shall be much smaller than the original number n, typically $w \ll n$. The ith element of new time-series $\overline{C}$ may be expressed as:

$$\overline{C_i} = \frac{w}{n} \sum_{j=\frac{w}{n}(i-1)+1}^{\frac{w}{n}i} C_j \tag{4.13}$$

Therefore, here the 24-hour data (n) of each day was equally split into 8 (w) segments in the new time-series, aiming at approximating the raw 24-hour time-series by a linear combination of eight boxes.

Lastly, the PAA coefficients were given with a string representation graph through the symbolization process of SAX. In each interval, when the compared data (the

measured and predicted data) have the same SAX strings, they may be clustered as the same group, and their PAA coefficients do not have to be the same. According to [67], the binding of PAA and SAX may accelerate fault tracking and energy performance when dealing with the fast growth of building data amount.

4.4 Economic and environmental impact assessment

In the thesis, the electricity costs were considered in the economic aspect, and its price model is introduced in Section 4.4.1; the environmental impacts were considered as expressed tonne CO_2 for heating use per year, under different CO_2 factors of local DH production, as presented in Section 4.4.2.

4.4.1 Economic impact assessment

The current electricity price model contains fixed grid rent, tax, and variable power market prices. Consequently, the monthly electricity cost was calculated as:

$$C_{mon} = (1 + 0.25) \cdot \sum_{t=1}^{720 \ or \ 744} v_\tau \cdot \dot{E}_\tau + f \cdot \sum_{t=1}^{720 \ or \ 744} \dot{E}_\tau + \frac{F}{12} \tag{4.14}$$

where 0.25 is the tax rate on the electricity spot price, v_τ the variable spot price at time instance τ, $\dot{E}_\tau$ is the electricity use at time instance τ, f is the grid rent, and lastly F is the annual grid fee to ensure customers' access to electricity including the costs associated with power grid operation. The price charging models in many European countries are similar to the one described in Eq.(4.14) [68]. Tax is generally determined by the authority, and grid rent and annual grid fee are determined by the grid supplier. These values can vary depending on user and industry type, and can be updated by the authorities from time to time. Additionally, a surcharge may be applied for high peak load during winter season in some cases. In the thesis, the local historical spot price was used as the variable price and retrieved from NordPool [69]. The annual electricity expense was therefore calculated by summarizing the monthly cost as shown in Eq.(4.14). The economic impacts were considered in the example Section 5.4 and the corresponding results are shown in Section 6.4.

4.4.2 Environmental impact assessment

The environmental impact considered CO_2 emissions for DH production mix. Because of the large transmission loss of the heating system, DH is unsuitable for long-distance transport. Therefore, the equivalent energy and environmental factors associated with DH production are usually locally specified based on the fuel source composition. From the information of Norsk Fjernvarme [70], during the last decade more than half of the DH has been provided through waste-to-energy in Trondheim and the whole Norway, followed by fossil gas with a 10 % contribution,

and the rest production is made from electricity, bio-energy, ambient heat, and fossil oil. In accordance with the Norwegian National Standard NS 3720-2018 [71], the CO_2 emissions associated with energy production (electricity and DH) from municipal solid waste have been allocated to the waste management sector, rather than to the energy sector. Meanwhile, the CO_2 factor of electricity shall be considered within a certain border, as various CO_2 values may occur through the transmission. For example, the abundant hydro-power contributed to a low CO_2 factor of 10 gCO_2 per kWh electricity (named as $CO_{2\text{-EL1}}$) within the Norwegian border, however, the involvement of fossil fuels in the Nordic electricity production mix yield a high CO_2 factor of 110 gCO_2 per kWh electricity (named as $CO_{2\text{-EL2}}$) within the Nordic region.

Accordingly, based on the annual production mix of energy sources, the local CO_2 factors of DH production may be calculated giving the expression of gCO_2 per kWh heat. As listed in Table 4.1, three typical CO_2 factors of local DH production were found, they are the average value from 2010 to 2018 (named as $CO_{2\text{-DH1}}$), the value of 2015 as the 9-year's lowest one (named as $CO_{2\text{-DH2}}$), and value of 2010 as the 9-year's highest one ($CO_{2\text{-DH3}}$); additionally, the CO_2 values for fossil gas, bio-energy, and fossil oil can refer to Norsk Energi [72]. The three factors were respectively used as the background data for comparably estimating CO_2 emissions. The CO_2 emissions were considered in the example Section 5.1 and the corresponding results are shown in Section 6.1.

Table 4.1: CO_2 factors of DH production mix in Trondheim

		2010-2018: $CO_{2\text{-DH1}}$	2015: $CO_{2\text{-DH2}}$	2010: $CO_{2\text{-DH3}}$
Fuel source composition (%)	Waste incineration	74.0	83.1	61.0
	Fossil gas	10.8	5.9	20.0
	Electricity	8.5	5.0	6.0
	Bio-energy	4.0	4.0	5.0
	Fossil oil	1.9	1.0	7.0
	Ambient heat	0.8	1.0	1.0
CO_2 factors (gCO_2/kWh heat)		41.7	23.5	76.3

5

RESEARCH EXAMPLES

This chapter describes how the principal methods introduced in Chapter 4 may be applied for certain research purposes. Research examples include the CO_2 emissions based on current building heating status to future building area planning as presented in Section 5.1, the approach for identifying typical annual heating and electricity load profiles as presented in Section 5.2, the hybrid heating load prediction for utility production planning as presented in Section 5.3, and finally the electricity and economic impacts of buildings with electric heating under lockdowns as presented in Section 5.4.

5.1 CO_2 emissions considering different environmental factors in future planning

This example analyzed the current energy use of a typical building type and forecasted the impact of future building area development on CO_2 emissions, based on well-measured DH and electricity data of kindergartens in Trondheim. The key steps are introduced below, for detailed description, see **Paper I**.

5.1.1 Energy share between electricity and district heating in buildings

In buildings connected to DH, heating demand was provided by DH, and electricity was mainly used for ventilation, lighting, computers, and other electric appliances. To see the contribution from the two energy supply ways, Figure 5.1 demonstrates the energy shares between electricity and DH in the analyzed buildings. From the chart, three cases were defined, named DH average share, DH high share, and DH low share, accounting for nearly 60.0%, 76.9%, and 31.4% of total energy use, respectively.

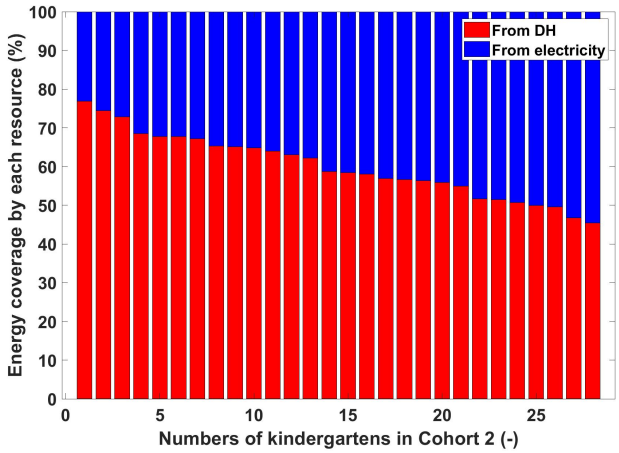

Figure 5.1: Energy share between electricity and DH in each building

5.1.2 Annual CO_2 emissions of one typical kindergarten and future assumption

The three cases of energy share were respectively considered for calculating the annual CO_2 emissions of a typical 700 m^2 kindergarten. Next, a future new building area of 10 000 m^2 (A_{new}) was assumed to assess future CO_2 emissions. Taking the current total building area 70 413 m^2, the building area growth rate is 14.2% (r), which was used as the reference line and compared with the CO_2 emissions growth rate by varying the percentage of new building area connected to DH (x in percentage) under different CO_2 factors, as introduced in Section 4.4.2. For the building area not connected to DH (100 - x), their electricity demand was assumed as the demand sum of the DH and electricity of the building area that was connected to DH.

The comparison (α) between building area growth rate (r) and CO_2 emissions growth rate ($\frac{CO_{2\text{-added}}}{\overline{CO_2}}$) for new building area is expressed as:

$$\alpha = r - \frac{CO_{2\text{-added}}}{\overline{CO_2}} \cdot 100\% \tag{5.1}$$

$$CO_{2\text{-added}} = [A_{\text{new}} \cdot (1-x) \cdot E_{\text{EL}} + A_{\text{new}} \cdot x \cdot E_{\text{DH-EL}}] \cdot CO_{2\text{-EL2}} + A_{\text{new}} \cdot x \cdot E_{\text{DH-DH}} \cdot CO_{2\text{-DHi}} \tag{5.2}$$

$\overline{CO_2}$ refers to the average annual average CO_2 emissions of all the local kindergartens, x refers to the percentage of new building area connected to DH, i refers to the different DH production CO_2 factors, E_{EL} and $E_{DH\text{-}EL}$ refer to the electricity demand of building area not connected to DH and connected to DH, respectively,

and $E_{DH\text{-}DH}$ refers to the DH demand of building area connected to DH. When $\alpha = 0$, there is a break-even point that the growth rate of CO_2 emissions is the same as the growth rate of the new building area. When $\alpha < 0$, it means if the new building area was increased by 14.2%, it would generate more than 14.2% CO_2 emissions. Contrarily, when $\alpha > 0$, it implies that slower CO_2 emissions growth could be achieved.

5.2 Approach for data analysis and prediction for annual energy load profiles

This example developed a systematic approach for data analysis and prediction Method 1 for annual electricity and DH load profiles, based on well-measured DH and electricity data of 40 schools in Trondheim, see Table 3.1 Cohort 2. The workflow is illustrated in Figure 5.2, and the key steps are introduced below. For detailed description, see **Paper II**.

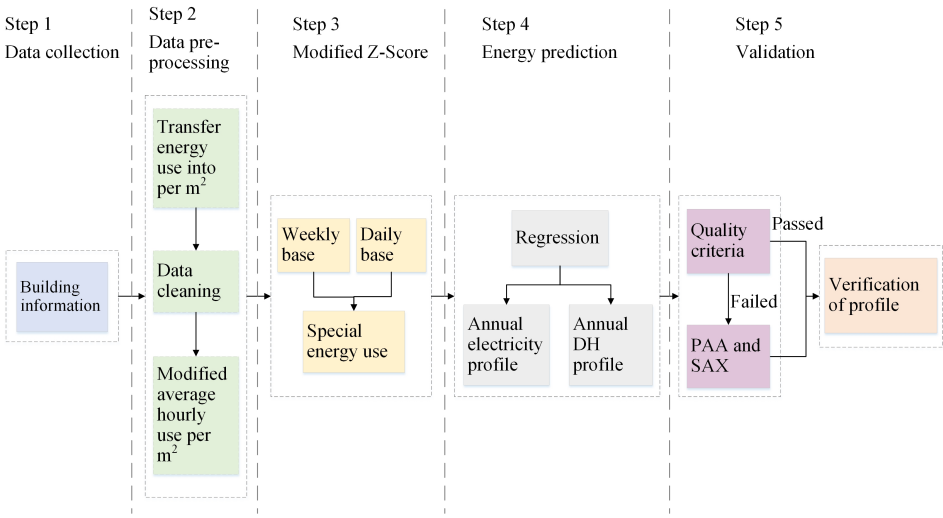

Figure 5.2: Workflow of the data analysis of energy load profiles

5.2.1 Modified Z-Score

A modified Z-Score method defined in [73] is preferred to identify possible outliers over the common practice of Z-Score. The modified Z-Score is expressed as:

$$M_i = \frac{0.6745 \cdot (x_i - \widetilde{x})}{MAD} \tag{5.3}$$

where x_i refers to the measured data point, $\widetilde{x}$ refers to the median value of the data samples, and MAD denotes the median absolute deviation in the dataset, see below:

$$MAD = median(|x_i - \widetilde{x}|) \tag{5.4}$$

If the absolute value of M_i to one data point is higher than 3.5, the point shall be flagged as a potential outlier. In the thesis, this method explored whether the building operation followed the schedule by considering the energy differences between normal days and special periods, showing the energy load profile trends by observing "unusual" energy conditions, such as school weeks, public holidays and so on. For instance, if there was an "unusually" low energy demand during the school week noted with a negative M_i in a series, this might indicate the building operation followed the low attendance. Contrarily, if a high positive M_i was in a series, high energy use might be required.

5.2.2 Annual district heating load profiles

Figure 5.3 is a logic diagram of correlation coefficients under different conditions. The typical annual hourly DH load profile can be acquired by substituting typical meteorological year (TMY) weather data and the corresponding coefficients into Eqs.(4.1) and (4.2). The analyzed outdoor temperature ranged from -18 to 26°C, covering the cold design temperatures of several major Nordic cities, such as Stockholm (-18°C), Copenhagen (-11°C), Gothenburg (-17°C), and so on [74].

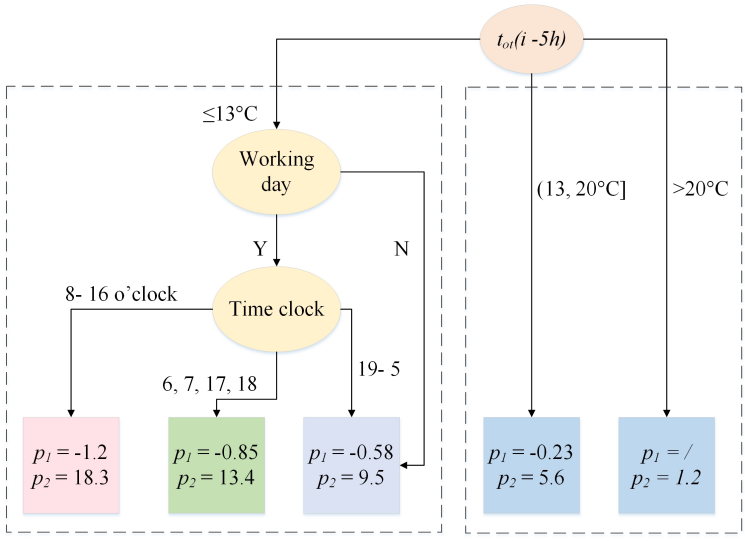

Figure 5.3: Logistic diagram of predicting DH demand under different conditions

5.2.3 Annual electricity load profiles

The correlation of every two years' electricity load profile between Week 1 and 52 (Week 2 to 53 in 2015 only) examined the similarity of electricity use over the four years. The high correlation within every two years shown in Figure 5.4 implied similar electricity use patterns over the four-year period. The small deviations can be explained by the fact that study trips, activities, and public holidays were scheduled on different days and weeks of the year.

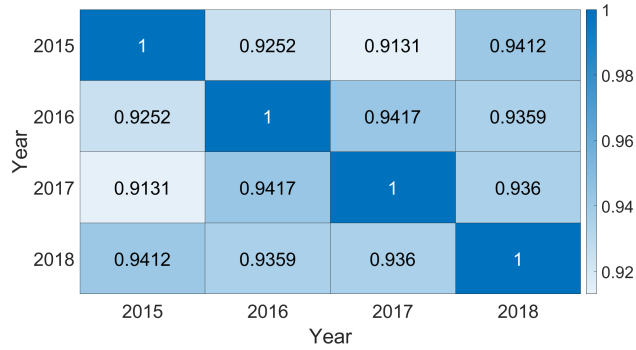

Figure 5.4: Correlation of electricity load profile 2015-2018 (52 weeks)

From the modified Z-Score mentioned in Section 5.2.1, typical profiles for normal and special days can be identified, separately. The four-year values as the predictor and their average value as the response, and they were together trained in the linear regression learner, with cross-validation for increasing the accuracy of the final model. These typical profiles can be combined to extrapolate and estimate the demand for future years.

5.3 Hybrid heating load prediction in low-temperature district heating

This example developed hybrid heating energy prediction methods by combining prediction Method 1 for plant sizing and the advanced prediction Method 2 for optimizing daily operation, based on well-measured DH data of 20 nursing homes in Trondheim, see Table 3.1 Cohort 2. The work flow is illustrated in Figure 5.5, and the key steps are introduced below. For detailed description, see **Paper IV**.

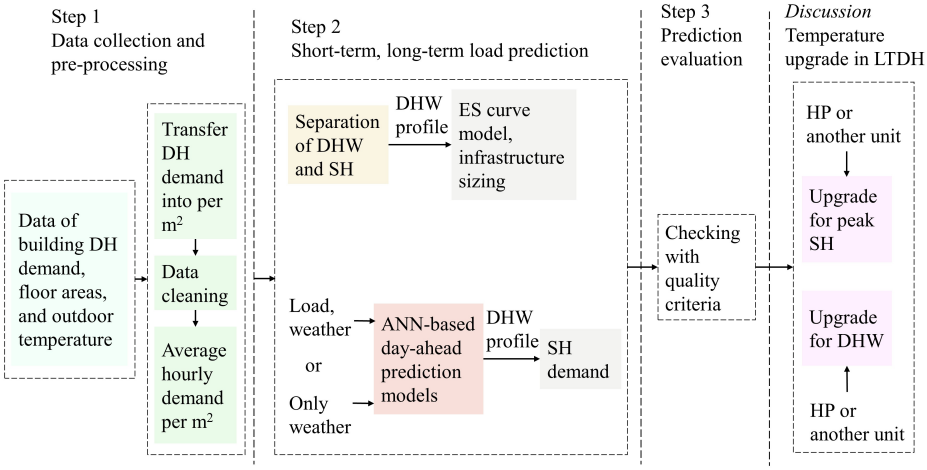

Figure 5.5: Workflow of the data analysis and modelling of DH load prediction in low-temperature district heating

5.3.1 Typical domestic hot water use

Depending on building standards, the domestic hot water use (DHW) heat use in nursing homes ranges from 15-20% to 40-65% of their total annual heat use [75]. Since DHW heat use is less sensitive to climate than SH, it is reasonable to separate DHW from the total DH load to explore a more accurate relationship between outdoor temperature and SH load. Profiles of typical daily DHW heat use in Norwegian nursing homes were identified in [19] with regard to the effects of season and day type. These typical daily profiles provide representative DHW use patterns for the given climate and resident type, and were used as reference profiles in the thesis.

The differences between the weekdays (WD as a shortcut) and weekends (WE as a shortcut) in the same season are noted in Figure 5.6. These four typical daily DHW profiles were extrapolated into an annual DHW profile and then extracted from the total DH to obtain space heating (SH) use. A Danish study for demand side management in DH networks also addressed the necessity and challenges of separating SH and DHW in the total heating load [76].

5.3.2 Sizing the heating supply system

Using the Heating degree day (HDD) introduced in Section 4.1.2, the obtained SH use was clustered into four heating seasons, as shown in Figure 5.7. It can be concluded that the daily SH operation generally followed the daily weather and was not affected by the day type (weekdays or weekends), nor by manual false operation. Therefore, the (energy signature) ES curve models for SH prediction were estab-

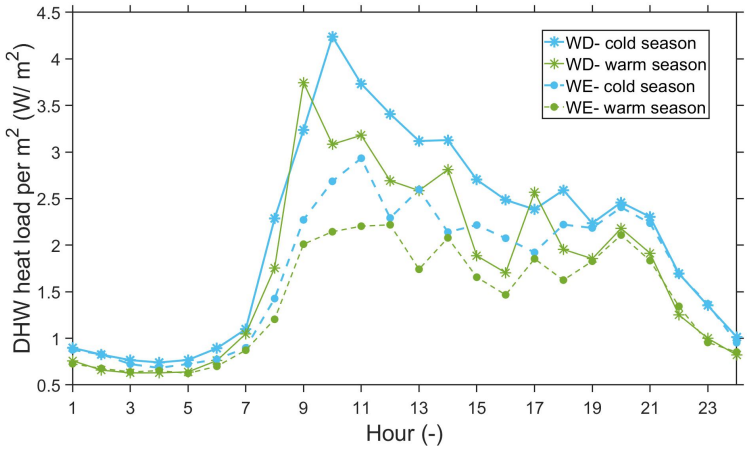

Figure 5.6: Daily domestic hot water heat load profiles in the nursing homes, divided by day of week and seasons

lished according to working hours and non-working hours, respectively, following Eqs.(4.1) and (4.2), similar to the example in Section 5.2.

The regression line shows a good correlation between daily heating degree day (HDD) and daily space heating (SH) demand in general, however, it might have over-predicted the SH use during the short and very cold season, as shown by the dark red diamond points.

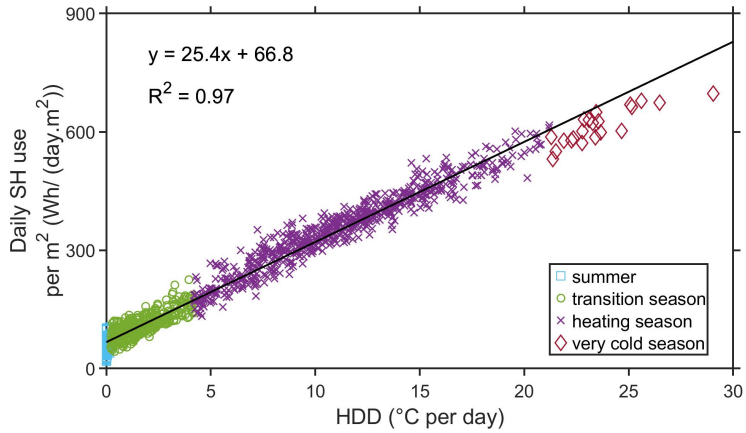

Figure 5.7: Daily SH use vs. daily HDD, based on four different heating seasons, summer, transition season, heating season, and very cold season (high-heating season)

5.3.3 Accumulation of daily load prediction from prediction Method 2

Due to the thermal and hydraulic inertia of DH systems and fuel availability, daily operations are normally planned and scheduled beforehand based on heating energy demand prediction to economically meet end-users' heating needs. As introduced in Section 4.2, the two ANN models f_{72} and g_{120} were respectively developed to generate the next 24-hour heating load prediction at any hour τ, and the same hour τ of each day can be chosen to schedule production for the following day. By accumulating the daily prediction at the same hour τ from prediction Method 2, a summed deviation between the measured and the predicted data over a time span may be acquired. The deviation accumulated during the (high) heating season is particularly important for evaluating the peak load prediction performance, which can critically affect the balance between peak load supply and demand. Therefore, the generated 24-hour ahead prediction made at 0 o'clock (τ) each day from January 1 to December 31 was accumulated for obtaining an annual DH load profile.

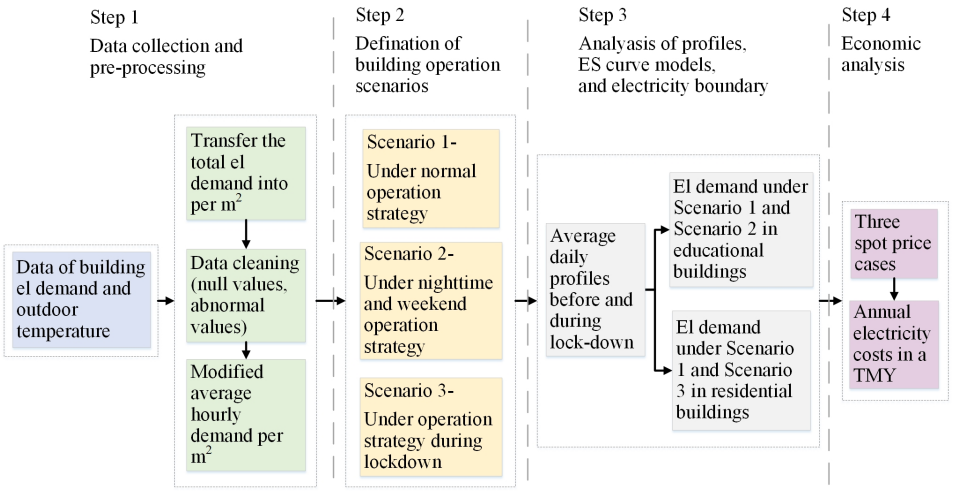

Figure 5.8: Workflow of the electricity and economic analysis under lockdowns

5.4 Analysis of electricity use and economic impacts for buildings with electric heating under lockdowns

This example shows how the confinement measures affected the electricity and economic costs of educational and residential buildings, based on well-measured electricity data of 14 kindergartens, eight schools, one apartment, and one residential

house in Trondheim, see Table 3.1 Cohort 1. The workflow is illustrated in Figure 5.8, and the key steps are introduced below. For detailed description, see **Paper III**. Another example regarding the lockdown-related impacts on educational buildings with DH can be found in **Paper IX**.

5.4.1 Daily electricity profiles before and during COVID-19 lockdown

Similar to the previous examples, the analysis was performed on the average specific energy use, here W_{el}/m^2, to define the representative electricity use for buildings with different characteristics.

To compare the average daily electricity demand and load profiles for each building type from March to May 2018(2019)-2020, the profiles with and without normalization, and Euclidean Distance (ED) was used. The normalization was performed by Pearson Correlation Coefficient (PCC) to identify the similarities discarding the possible influence from outdoor temperature to electricity profile shapes, given as:

$$PCC(X,Y) = \frac{cov(X,Y)}{S_X S_Y} = \frac{\sum_{i=1}^{n}(x_i - \overline{x})(y_i - \overline{y})}{\sqrt{\sum_{i=1}^{n}(x_i - \overline{x})^2}\sqrt{\sum_{i=1}^{n}(y_i - \overline{y})^2}} \tag{5.5}$$

ED was to measure whether the big outdoor temperature difference led to a higher electricity demand difference, given as:

$$d_{ED}(X,Y) = \sqrt{\sum_{i=1}^{n}(x_i - y_i)^2} \tag{5.6}$$

5.4.2 Three scenarios regarding different building operation strategies

The different campus activities and attendance between normal weekdays and weekends generate remarkable energy use in the educational buildings. However, unlike kindergartens and schools, residential buildings usually have lower energy demand during working hours and higher demand when residents are at home. According to different electricity use habits and patterns, three scenarios were proposed considering different operation strategies under lockdowns, as expressed below. The electricity demand for each scenario was calculated.

- **Scenario 1** considered the building operation under normal conditions without disturbances from lockdown. This scenario applied to both educational and residential buildings.
- **Scenario 2** considered the energy-saving mode and assumed a temporarily limited operation under a low electricity demand setting during normal weekdays' nighttime and weekend, when electricity was typically observed at mini-

mum levels for maintaining the acceptable indoor air quality under nearly zero attendance. This scenario applied only to educational buildings with an aim to estimate the electricity savings potential.

- **Scenario 3** considered the operation of residential buildings under work-from-home conditions. This scenario aimed to find the possible electricity increase caused by lockdowns and to examine energy robustness regarding dwelling scale.

5.4.3 Economic impact assessment

As shown in Figure 5.9, the electricity spot price fluctuated greatly from 2016 to 2020. Thus, three price cases were made, the spot price in 2018 was taken as the case of the highest price level (shown by the yellow line), the spot price in 2020 as the case of the lowest price level (shown by the green line), and the median values of the remaining years as the case of the moderate price level (by the thick blue line). These three levels were assumed to be representative of the electricity market in recent years.

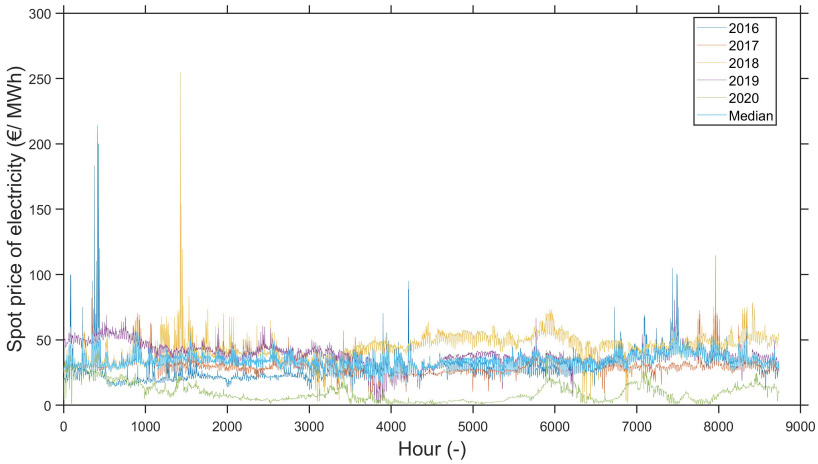

Figure 5.9: Annual electricity spot prices in Trondheim 2016-2020

By combining annual electricity profiles with each of the three price levels, the annual electricity costs of the observed buildings under the three operation scenarios may be calculated and further compared.

6

RESULTS AND DISCUSSION

This chapter summarizes the publications during the PhD work by presenting the main findings and contributions of the *main papers*. Each section in this chapter corresponds to the research example in Chapter 5 and is dedicated to a specific paper, presenting the main results and discussions.

6.1 Results of CO_2 emissions considering different environmental factors for heating systems in future planning

This section shows the main findings of the current energy use of a typical kindergarten and the impact of future building area development on CO_2 emissions. This example answers **Research Question 1**, corresponding to the example described in Section 5.1. A detailed explanation of the method and results are shown in **Paper I**.

6.1.1 Comparison results of annual CO_2 emissions of one typical Nordic kindergarten

Figure 6.1 compares the annual CO_2 emissions of a typical kindergarten with and without DH connection. In Figure 6.1, the two separate bars on the right side represent the building without DH. When the CO_2 factor of electricity was changed from the Norwegian electricity production 10 to the Nordic electricity production 110 gCO_2/kWh, the annual CO_2 emissions increased substantially from 1.2 tCO_2 to 13.6 tCO_2, which was the worst case. Within the dashed green square, three cases of DH shares (from low to high share) were compared with four different CO_2 factor combinations. It can be seen that if electricity took on more energy supply, the total annual CO_2 emissions would vary greatly according to the CO_2 factor of electricity. Meanwhile, in the case of a high share of DH, the changes of CO_2 emissions under different CO_2 background data were relatively small.

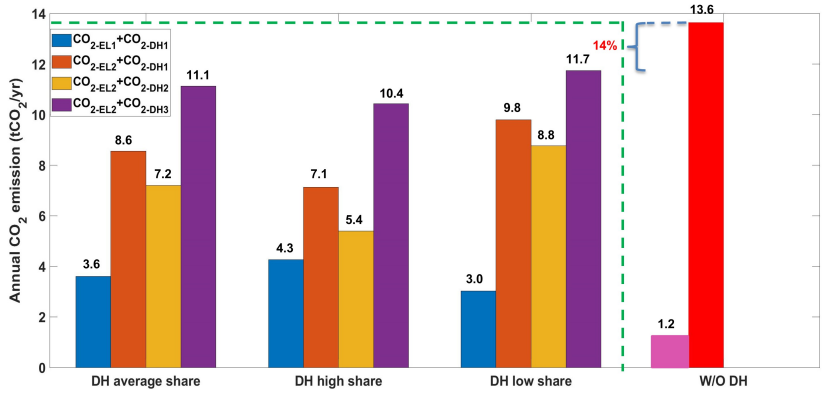

Figure 6.1: Annual CO_2 emissions of one kindergarten of 700 m^2; within the dashed green square, blue bars for the Norwegian electricity ($CO_{2\text{-EL1}}$) with the DH average production ($CO_{2\text{-DH1}}$), orange bars for the Nordic electricity ($CO_{2\text{-EL2}}$) with the DH average production ($CO_{2\text{-DH1}}$), yellow bars for $CO_{2\text{-EL2}}$ with DH production in 2015 ($CO_{2\text{-DH2}}$), and purple bars for $CO_{2\text{-EL2}}$ with DH production in 2010 ($CO_{2\text{-DH3}}$); outside of the green square, the pink bar for the Norwegian electricity and red bar for the Nordic electricity

6.1.2 Impact of future building area development on CO_2 emissions

By varying the penetration (x) of new buildings with DH between 0 and 100%, three new annual trends in CO_2 emissions were calculated based on the DH production CO_2 factors.

As shown in Figure 6.2a), when all new building area was powered only with electricity, the annual increase in CO_2 emissions was 194.9 tCO_2/yr, and this was same for the three growing trends. When half of the new building area was connected to the DH system, the annual CO_2 reduction was between 22.5 and 49.7 tCO_2/yr. Since CO_2 was expected to decrease linearly with changes in DH penetration, annual CO_2 emissions would double if all new construction area was connected to DH. The orange line represents the best case as 2015 has the smallest DH production CO_2 factor, while the yellow line had the mildest slope of decline due to the selection of the highest DH production CO_2 factor, while the blue line for the average DH production CO_2 factor was in between.

In Figure 6.2b), the building area growth rate, 14.2%, was shown as the purple reference line. Above the reference line, the CO_2 increase rate was higher than the building area growth rate, which means that if the building area was increased by

14.2%, the CO_2 emissions would increase by more than 14.2%; below the reference line, the CO_2 increase rate was less than the building area growth rate, which is the expected result of slower carbon footprint growth in the future. The orange line representing the smallest DH production CO_2 factor ($CO_{2\text{-DH2}}$) had the steepest slope. A slower rate of CO_2 increase may be achieved after using DH on more than half of the new building area. While using the highest DH production CO_2 factor ($CO_{2\text{-DH3}}$), the break-even point reached 67%, as shown by the yellow line. Therefore, under different CO_2 background data, the break-even point may be between 50 and 67% of the new building area connected to DH.

The results may be useful for future planning of building development where slower CO_2 increases may be achieved when appropriate energy supply methods are chosen.

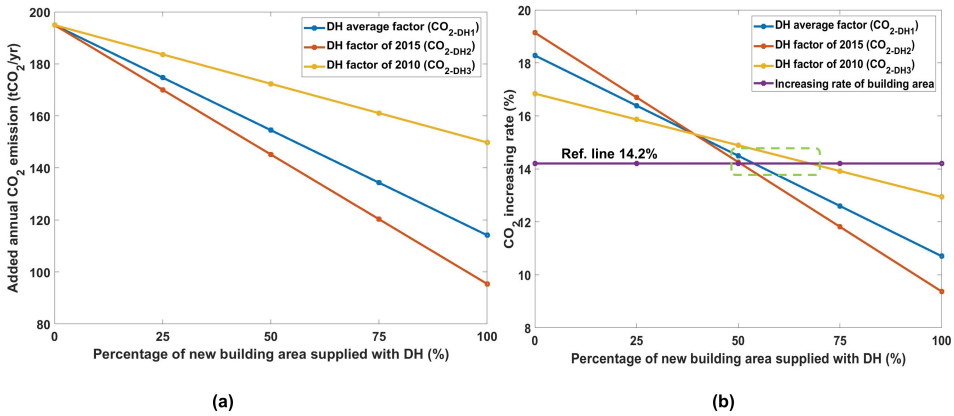

Figure 6.2: (a) Annual CO_2 addition of 10 000 m^2 new building area; (b) CO_2 increasing rate of 10 000 m^2 new building area

6.2 Results of data analysis and prediction for annual energy load profiles: an example for Nordic school

This section shows the main findings of the annual heating and electricity profile for a typical Nordic school and answers **Research Question 2**, corresponding to the example described in Section 5.2. A detailed explanation of the method and results are shown in **Paper II**.

6.2.1 Results of modified Z-Score

For heating operations on short holidays and one-day holidays, the analysis was carried out within a week (five weekdays) by comparing with the adjacent days as usually there was not much difference in outdoor temperature between adjacent days. In Figure 6.3, there were five days in each line marked with a week number. Most DH demand was below the upper threshold, only No.6 in 2017 had an unusually high demand when it was supposed to close on Whit Monday. Only No.1 and 3 in 2015, No.1 in 2016, No.1, 4, and 5 in 2017, and No.1 and 6 in 2018 followed public holiday expectations for low DH demand, although some did not yet reach the lower threshold compared to adjacent days.

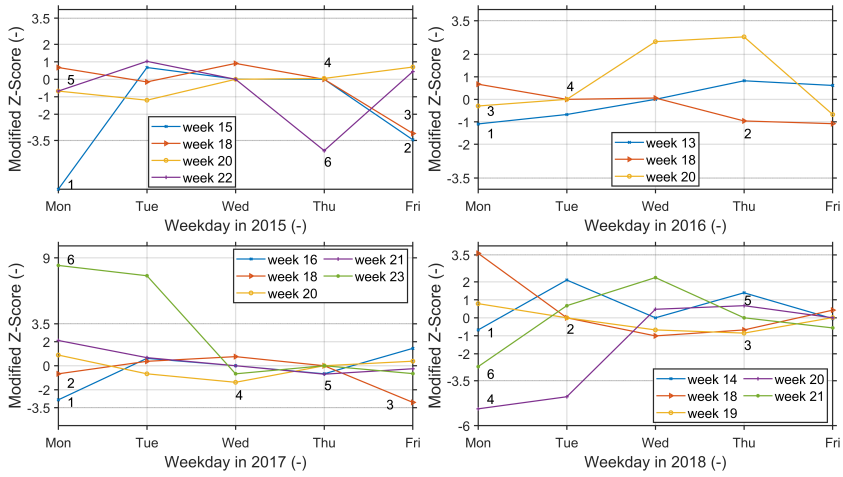

Figure 6.3: Modified Z-Score of the district heating use regarding short holidays during 2015-2018

As suggested in [77], for days with similar occupancy to previous days, the previous days can be selected as their reference days. Therefore, the electricity demand for short-day holidays was analyzed by comparing the same weekday number within each season. Since electricity use was less sensitive to the outdoor temperature, it was assumed that the electricity use followed a weekday schedule in each season. In Figure 6.4, each line presents 13 points of the same weekday. Except for the abnormally high use of No.4 in 2015, all other electricity demand was under the upper threshold line. All the public holidays were detected as "outliers" or local minima for the low electricity demand, compared to the DH use. Also, when a one-day holiday was on Thursday, it was likely that the following Friday was also in holiday mode or reduced school hours.

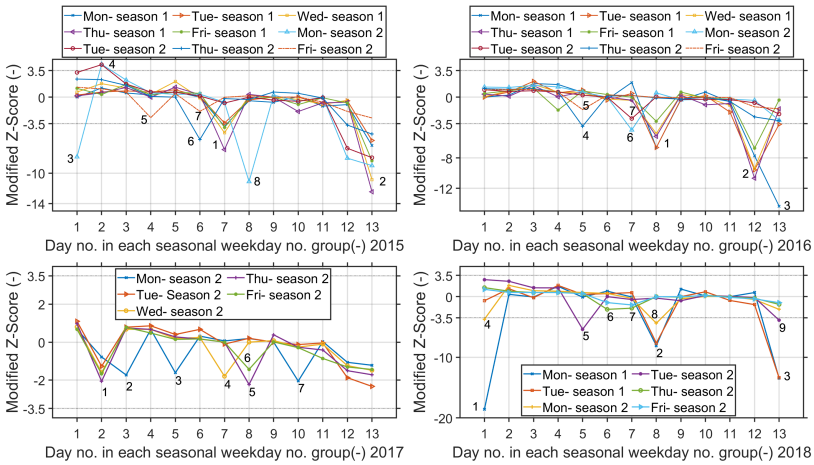

Figure 6.4: Modified Z-Score of the electricity use regarding short holidays during 2015- 2018

It can be concluded that the control of electrical appliances in the schools made reasonably fast responses by closely following the attendance and schedule. Nevertheless, the response of hydronic DH systems was a relatively slow process mainly due to the long transport of heating fluid and complex control of the DH sub-stations, as mentioned by others [74].

6.2.2 Profile results of district heating and electricity in a typical Nordic school

The (energy signature) ES curve for DH load is shown in Figure 6.5, where the critical point for changing point temperature (CPT) was found 13°C, obtained by an adequate piece-wise approximation for an average school building. In the area below 13°C, it was further segmented into three parts, the stable working hour, the ramping hour, and the non-working hour. In the area above the CPT, the heating needs were negligible and the impact on the energy supply system was small. Figure 6.5 shows the strong heating load differences.

Finally, the measured and predicted annual DH load profiles are compared in Figure 6.6 and the predicted typical annual DH load profile in a typical year is presented in Figure 6.7. Due to the strong dependence on outdoor temperature, the DH load fluctuated throughout the year with peak fluctuations. The peak load was around 48 W/m^2, the minimum load was close to 1 W/m^2, and the total annual heat demand was 72 kWh/m^2.

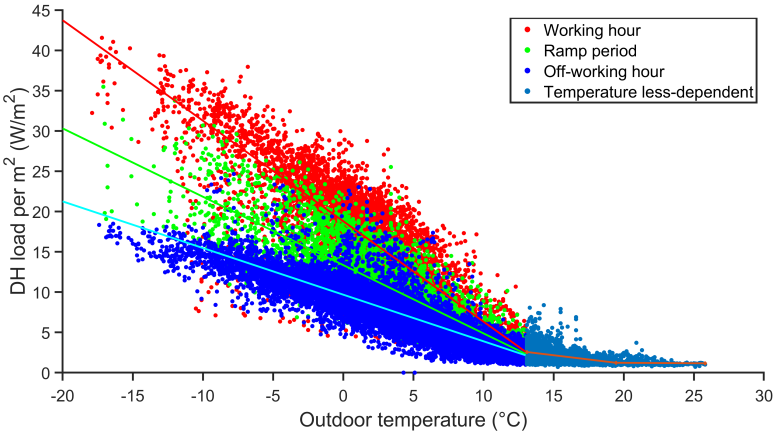

Figure 6.5: Energy signature curve models of DH load considering different operation periods; below CPT, working hour period, ramp period, off-working hour; above CPT, temperature less-dependent period

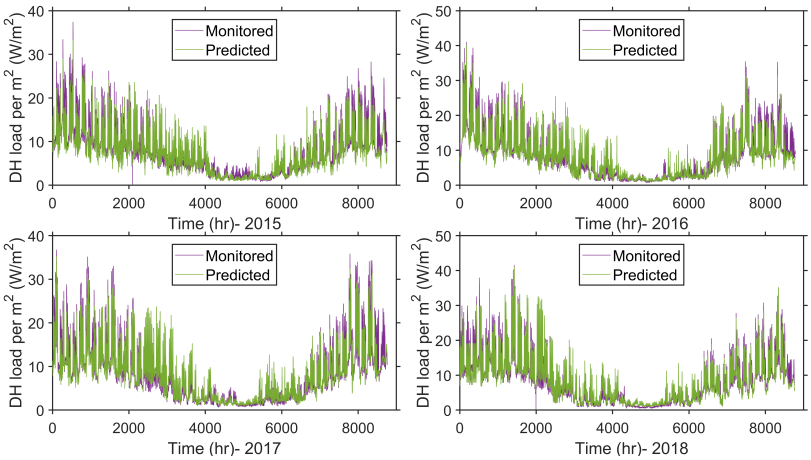

Figure 6.6: Measured vs. predicted DH load profile during 2015-2018

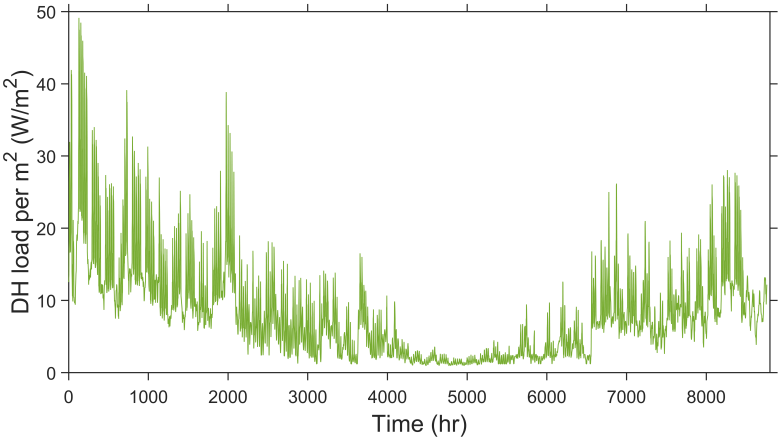

Figure 6.7: Predicted typical annual DH load profile under typical meteorological weather

Figure 6.8 shows the overview of 4-year monitored and predicted annual profiles of electricity. The identified typical hourly profiles for school week, Easter week, short holidays, and the remaining normal days (excluding the above special days) are shown in Figure 6.9. The peak load was around 18 W/m^2, the minimum load was 2 W/m^2, and the total annual demand was 57 kWh/m^2. The minimum load was mainly used for some plug-in devices and low ventilation during the unoccupied period. The peak load of electricity was only one-third of the peak load of DH (48 W/m^2), and the total demand was 79% of that of DH (72 kWh/(m^2· yr)). Therefore, the power grid stress may be significantly reduced in buildings with DH compared to buildings with electricity supply alone. This is especially important in winter when both heating and electricity require a high energy supply. In addition, by analyzing the heat and power profiles separately, the different requirements of heat and power grids in terms of sizing and output are presented.

The energy density for the observed average school was 129 kWh/(m^2·yr), with nearly 56% for heating needs. The energy share for the heating purposes was almost the same as the average situation [24], while the total density was slightly lower than the annual average energy use in Norwegian schools [24, 78], but the same as the mean value of Swedish schools [79], and approach to the proposed nZEB energy performance target level for Finnish educational buildings in FInZEB project, 104 kWh/(m^2·yr) [80].

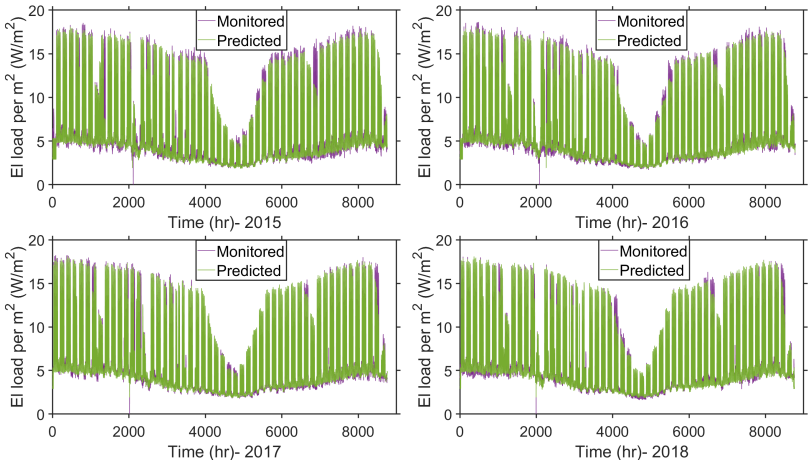

Figure 6.8: Measured vs. predicted electricity load profile during 2015-2018

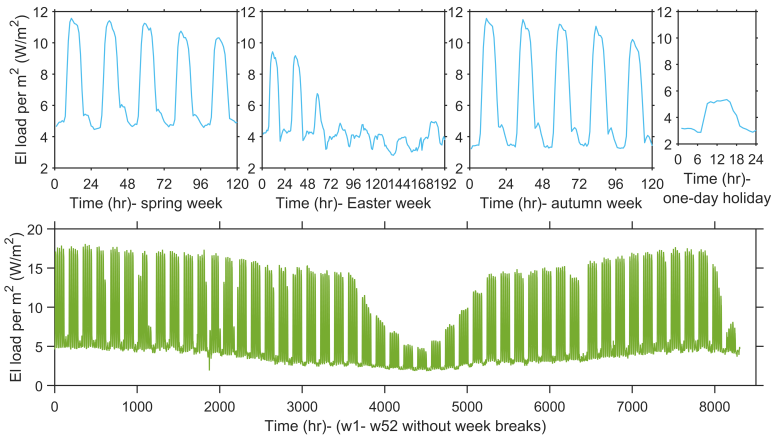

Figure 6.9: Typical hourly load profiles for the school week, Easter week, short holiday, and the normal days without these special days; for easy reading, the load profiles for Easter week, autumn week, and one-day holiday have the same Y-axis label of spring week

6.2.3 Results of prediction performance evaluation of a typical Nordic school

The prediction performance evaluation is summarized in Table 6.1. The mean absolute percentage error (MAPE) results of the electricity prediction were less than 10%, the normalized mean bias error (NMBE) within ±1%, and the coefficient of variation of the root mean squared error (CV(RMSE)) less than 20%, meeting the criteria upper limits [58, 63, 64]. However, the MAPE results of the DH prediction were higher than 20%. It can be said that the ES curve model was to some extent convincing but not very accurate and further validation was therefore needed.

Table 6.1: Evaluation results of the energy forecast by three criteria

	prediction of DH load profile			prediction of electricity load profile		
Year	MAPE (%)	NMBE (%)	CV(RMSE) (%)	MAPE (%)	NMBE (%)	CV(RMSE) (%)
2015	20.2	2.9	25.7	8.8	0.9	16.0
2016	23.2	-1.4	26.7	6.8	0.2	10.6
2017	24.0	-2.4	26.9	6.6	-0.3	11.7
2018	29.6	-4.9	30.2 (↑)	7.5	-0.4	10.1

The predicted DH profiles were further evaluated by the cluster methods of PAA and SAX, introduced in Section 4.3.2. As recommended in [66], three breakpoints (-0.67, 0, 0.67) were selected. The PAA coefficients for those below -0.67 were symbolized with the string "a", the PAA coefficients between -0.67 and 0 with "b", the PAA coefficients between 0 and 0.67 with "c", and those higher than 0.67 with "d". In each interval, if the compared data from different datasets have the same SAX strings, they may be clustered as the same group, at the same time the PAA coefficients do not have to be the same. Figure 6.10 shows the comparison of the PAA coefficients of the predicted and measured DH daily profiles by considering the seasonal and weekday influences, and the corresponding SAX symbols are listed in Table 6.2. In the SAX table, those with different SAX strings within the same PAA interval are shown in italics, indicating that they cannot be clustered into the same group. It can be concluded that the predicted and measured load curves for Winter season had a very high similarity, as all the eight intervals between the predicted and measured load curves for each weekday had the same clustering strings, more importantly, Winter required most of the heating energy. However, the similarities in other seasons were not as strong as in Winter. The reason for the large deviations and errors in Spring and Autumn might be caused by seasonal changes and unstable outdoor temperatures, which might lead to large temperature differences.

From the approximation of the PAA and SAX symbol results, the predicted DH profiles for the average school turned out to be convincing and representative. In addition to the advantages of using PAA for time series discretization and magnitude normalization, it allowed us to present seasonal load patterns and shape comparisons by extracting the desired day types.

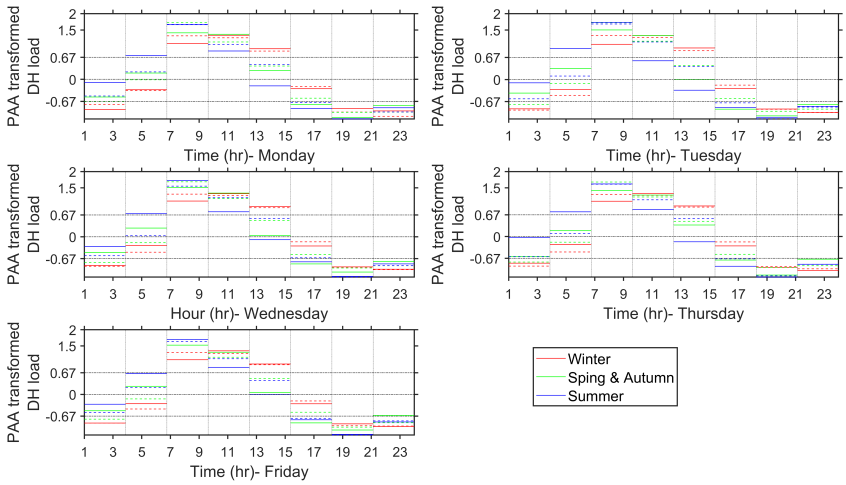

Figure 6.10: PAA coefficients results, considering different seasons in each working day

Table 6.2: PAA coefficients results in Figure 6.10 transferred into SAX symbols

Weekday		Winter	Spring & Autumn	Summer
Monday	predicted	a b d d d b a a	*b c* d d c *a* a a	b *d* d d *b* a a a
	measured	a b d d d b a a	*a b* d d c *b* a a	b *c* d d *c* a a a
Tuesday	predicted	a b d d d b a a	*b c* d d *b a* a a	b *d* d *c b* a a a
	measured	a b d d d b a a	*a b* d d *c b* a a	b *c* d *d c* a a a
Wednesday	predicted	a b d d d b a a	*b c* d d c *a* a a	b *d* d d *b a* a a
	measured	a b d d d b a a	*a b* d d c *b* a a	b *c* d d *c d* a a
Thursday	predicted	a b d d d b a a	*b c* d d c *a* a a	b *d* d d *b* a a a
	measured	a b d d d b a a	*a b* d d c *b* a a	b *c* d d *c* a a a
Friday	predicted	a b d d d b a a	*b c* d d c *a a b*	b c d d *b* a a a
	measured	a b d d d b a a	*a b* d d c *b* a *a*	b c d d *c* a a a

6.2.4 Discussion and limitation

This example identified the representative annual DH and electricity load profiles for a typical Nordic school.

The identified annual typical load profiles may be used as input to energy supply simulation models to locate the key impacts of peak loads and determine energy savings potentials. This is different from the previous studies, which usually used packaged energy data from utility companies as input for optimal modeling of energy supply systems. Moreover, it would be interesting to further cluster buildings into typical high energy-density, typical medium energy-density (mostly likely to be the profiles identified in this example), and typical low-energy-density buildings, and then to predict their corresponding energy profiles. Although the proposed approach

is robust and transferable to other building types, the prediction accuracy shall be further improved, for example, by using more advanced prediction techniques for comparison. Meanwhile, source data quality and building energy management behavior (such as manual interference, random operation, or regular routine) are also important for prediction accuracy.

6.3 Results of hybrid heating load prediction in low-temperature district heating: an example for nursing homes in Nordic countries

This section shows the main findings of the developed hybrid heating load prediction in LTDH and answers **Research Question 3**, corresponding to the example described in Section 5.3. A detailed explanation of the method and results are shown in **Paper IV**.

6.3.1 Results of long-term district heating load prediction

The ES curve models for the SH load are shown in Figure 6.11, where the CPT was found around 12°C to provide a suitable piece-wise approximation. During 77.6% of the time, the outdoor temperatures were below the CPT, falling into the high-heating season; while the remaining 22.4% of the time, the small space heating (SH) loads were less temperature dependent and could be described by one regression line regardless of working hours and non-working hours. Compared to buildings with distinct clock-controlled operations as shown in the example of school buildings, the SH differences between working and non-working hours in nursing homes were less pronounced, it is still worth analyzing them separately.

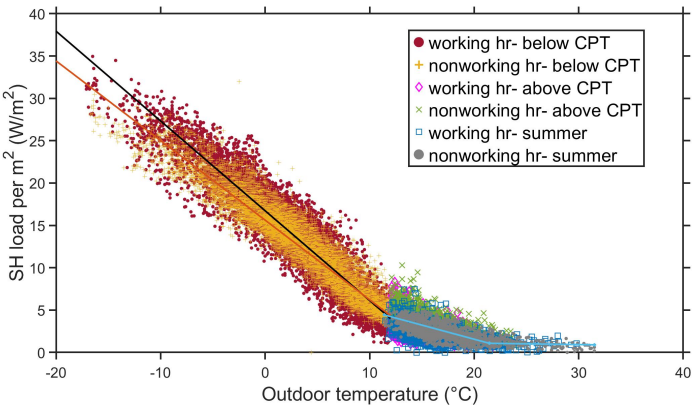

Figure 6.11: Energy signature curve models of SH load considering different operation periods; below CPT, the black line represents working hours and red line non-working hours; above CPT, temperature less-dependent period

Figure 6.12 presents a breakdown of the space heating (SH) and domestic hot water (DHW) heat load profile. At outdoor temperatures of -11.6 – -9.3°C, the peak SH load was 29–31 W/m^2, while the minimum load was close to 0.9 W/m^2 for the network circulation; and DHW use was considered to be process heat with seasonally stable usage patterns. The predicted total annual DH demand was 114 kWh/m^2, of which 15% was for DHW, following the statistical data of heat use demand as well as the share for DHW heat use in nursing home [75].

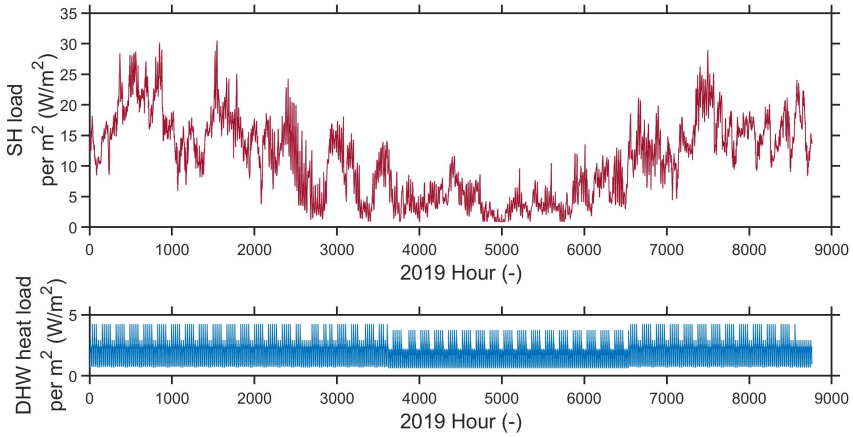

Figure 6.12: Predicted DH load profile for 2019 with a breakdown of space heating load profile (top row subplot) and domestic hot water heating load profile (bottom row subplot)

6.3.2 Results of short-term district heating load prediction

Figures 6.13 and 6.14 compare the day-ahead prediction performance of the two ANN models f_{72} (with 72 inputs) and g_{120} (with 120 inputs), in the examples from different heating seasons. In both models, the next 24-hour heating load prediction for the whole 2019 was made from 0 'clock (τ) on January 1 to 0 o'clock (τ) on December 31, giving a total of 8737 forecast results, respectively [1].

[1]Since 2020 weather was not included in the modelling, the prediction finished at 0 o'clock (τ) on December 31 with the weather input by 23 o'clock on December 31. Therefore, each ANN model ran 8737 times prediction (excluding 1-23 o'clock (τ) on December 31) and generated 8737 predictions, separately.

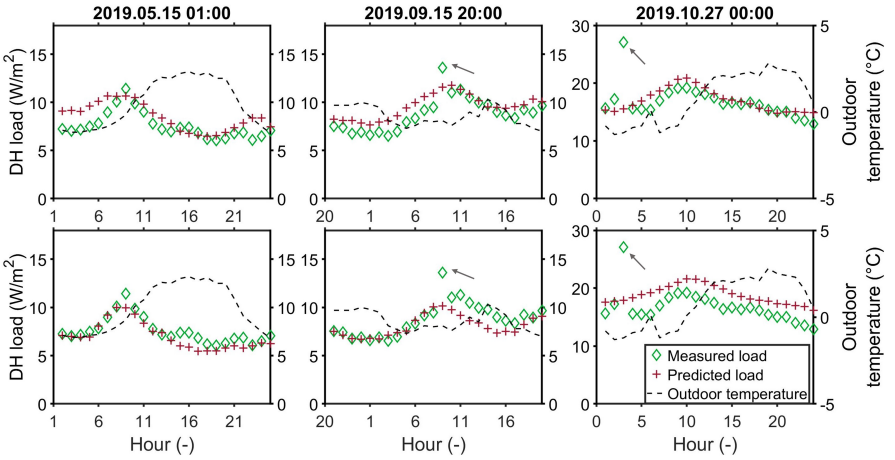

Figure 6.13: Predicted DH load for the 24-hour period following the date indicated above each column, showing the randomly selected three dates prediction results by model f_{72} (top row subplots) and by model g_{120} (bottom row subplots)

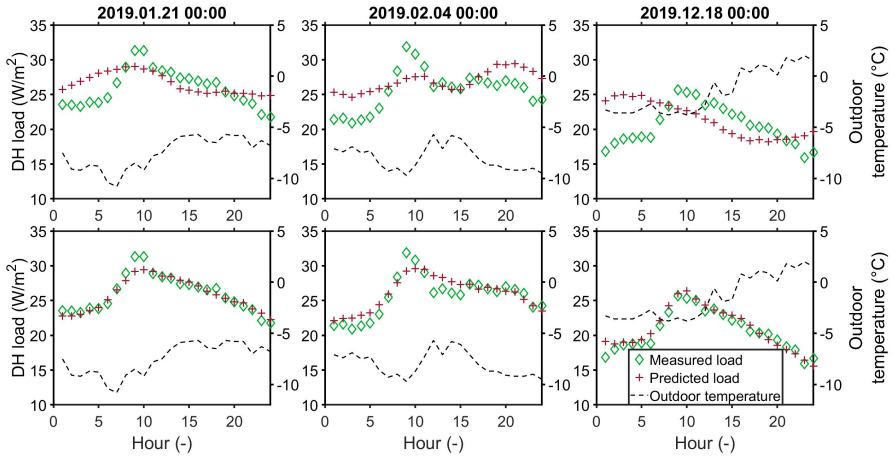

Figure 6.14: Predicted DH load for the 24-hour period following the date indicated above each column, showing the selected three dates prediction results by model f_{72} (top row subplots) and by model g_{120} (bottom row subplots)

In Figures 6.13 and 6.14, each column subplot shows the prediction for the next 24-hour period following the time instance indicated at the top, e.g. the prediction of the heating load $\widehat{Q}_\tau^{24} = (\widehat{Q}_{\tau,1}, \ldots, \widehat{Q}_{\tau,24})$ is plotted for the τ on the given date. By looking at each column of subplots, it is easy to compare the performance of f_{72} and g_{120} on the same time instance. To hold statistical reliability, three prediction outcomes out of the 8737 instances τ were randomly selected from the 2019 testing

data using a uniform probability distribution. As shown in Figure 6.13, there were two DH load spikes, one measured at 9 o'clock on September 16 and the other at 3 o'clock on October 27, see the green diamonds being pointed by grey arrows. In Figure 6.14, the prediction results for three dates during January, February, and December (high heating season) were randomly selected, covering the outdoor temperature from -11 to 2°C. In all the seasons, the load predicted by g_{120} was significantly closer to the measured load than the one predicted by f_{72}, both in the curve patterns and load values.

6.3.3 Prediction evaluation of different prediction methods

Since f_{72} and g_{120} respectively generated the next 24-hour heating load prediction at (any) hour τ, the same hour τ of each day can be chosen to schedule production for the next day. On this basis, the 24-hour ahead prediction results generated at 0 o'clock every day from January 1 to December 31 were accumulated to obtain the annual load profile prediction for 2019, and a summed deviation between the predicted and the measured data throughout a year may be visualized. Deviation accumulated during (high-) heating seasons is particularly important for evaluating peak load forecast performance. The deviation between the measured load and the predicted load is considered as $\Delta(\tau) = \textit{measured}\ Q(\tau) - \textit{predicted}\ \widehat{Q}_{\tau}$. Figure 6.15 shows the deviation for the three prediction models for 2019, and Table 6.3 summarizes the prediction accuracy evaluation.

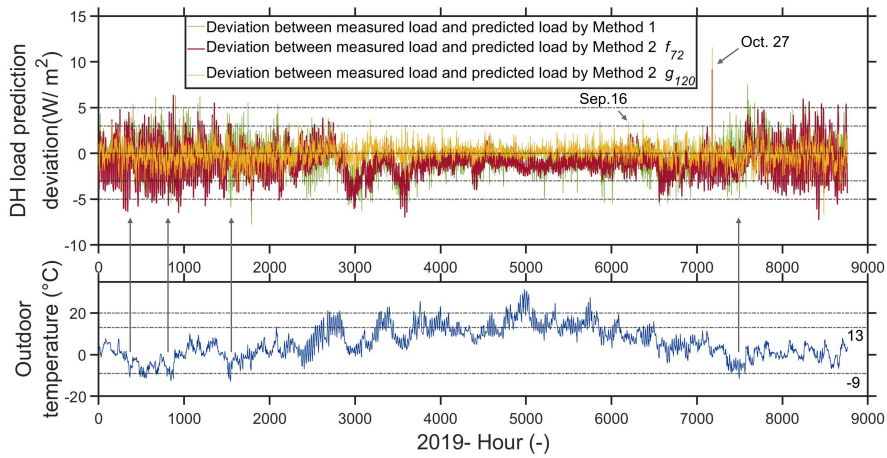

Figure 6.15: Deviation plot between measured and predicted DH load by the three models for 2019 (top row subplot), corresponds to the outdoor temperature for 2019 (bottom row subplot)

In the comparison in Figure 6.15, g_{120} held the prediction deviation within ± 3 W/m^2 most of the time, f_{72} had the highest deviation in the cold periods either

over-predicting DH load or under-predicting DH load, and the ES curve kept the prediction deviation in between. The high deviation spikes on October 27 were mainly caused by a measurement failure, see Figure 6.13, when a sudden high DH load was measured.

Figure 6.16 presents four examples of peak heating load periods. In the figure, the model f_{72} was least sensitive to the outdoor temperature changes by under-predicting the peak load and over-predicting the load during other time, also seen in Figure 6.15; the ES curve model and g_{120} captured most of the peak load periods, while the ES curve model might have over-predicted the peak load compared to the model g_{120}.

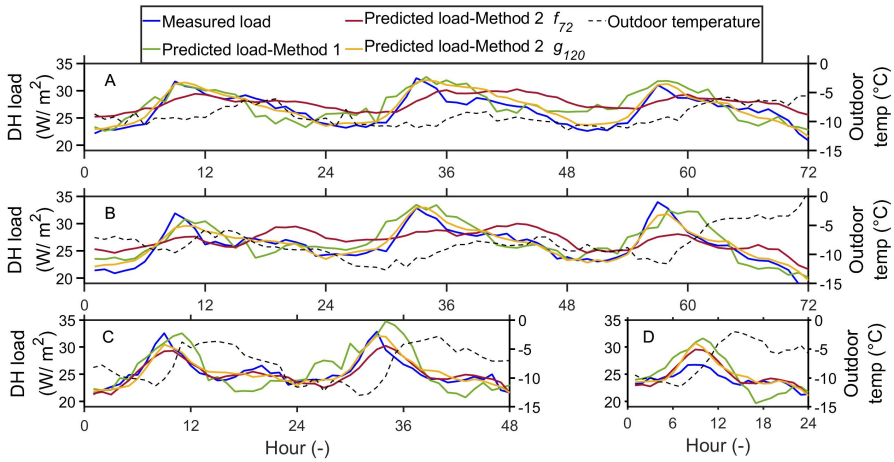

Figure 6.16: Four examples of peak load periods in 2019, measured vs. predicted DH profiles by the three prediction models. Subplot A represents the load profiles comparison from 1 o'clock on January 22 to 24 o'clock on January 24. Subplot B represents the load profiles comparison from 1 o'clock on February 4 to 24 o'clock on February 6. Subplot C represents the load profiles comparison from 1 o'clock on March 5 to 24 o'clock on March 6. Subplot D represents the load profiles comparison from 1 o'clock to 24 o'clock on November 9

As listed in Table 6.3, the MAPE and sMAPE results of the three models were less than 20%, NMBE within ±10%, and CV less than 20%, meeting the criteria upper limits [58, 63, 64]. Despite using the same training set for f_{72} and g_{120}, g_{120} showed the best prediction performance benefiting from using both historical heating load and outdoor temperature as inputs, while f_{72} only considered the ambient condition as inputs and its prediction accuracy was reflected in the poorest results regarding all the criteria. However, as the criterion CV(RMSE) result of f_{72} was much lower than the limit, 30%, it was still good to notice that the load predicted by f_{72} was somehow able to capture the patterns from the measured load curves even without the historical DH load as inputs. Besides setting the load boundary, the heating

load prediction quality of the ES curve model was in the middle of the three models.

This means that the models and their predicted DH load curves provided high accuracy for subsequent work, regardless of the different input settings and algorithms of the three prediction models.

Table 6.3: Evaluation results of 2019 DH load forecast produced by the three models. The criteria, namely MAPE, sMAPE, NMBE, and CV(RMSE) are used for quality evaluation

Prediction method	MAPE (%)	sMAPE (%)	NMBE (%)	CV(RMSE) (%)
Method 1 - ES curve model	13.94	12.81	-3.91	13.79
Method 2 - f_{72}	16.77	14.75	-8.13	15.51
Method 2 - g_{120}	7.23	7.28	-0.36	7.90

6.3.4 Discussions of the models' rationality and future study of temperature upgrade in low-temperature district heating

6.3.4.1 Rationality of the models

By making good use of big data, data-driven models were selected over physical models. As shown in Figure 6.13, there were two DH load peaks, while the load profiles predicted by the two ANN models showed a smoother trend. After checking outdoor temperatures for the two days, no "sudden" weather changes were recorded. Therefore, these abnormal data values might have been caused by metering failures or mishandling. Nonetheless, the established models showed more reasonable predictions. In addition to the proper algorithms, the three-year large data for training/validation also contributed to achieving the appropriate predictions.

6.3.4.2 Temperature upgrade in low-temperature district heating

In addition to improving DH load prediction quality, when the building is connected to LTDH system, the above heating load profiles for DHW and SH may be used respectively utilized for the building energy supply operation. For example, integrating two building-sized boosting heat pumps (HPs) in LTDH enables the system to respond to the minimum supply temperature requirements of DHW and SH. This may be considered a promising solution to one of the LTDH challenges. One possible application may be proposed as shown in Figure 6.17, where from left to right side are the emerging heat source from datacenter's waste heat, the temperature upgrade process, and the building user.

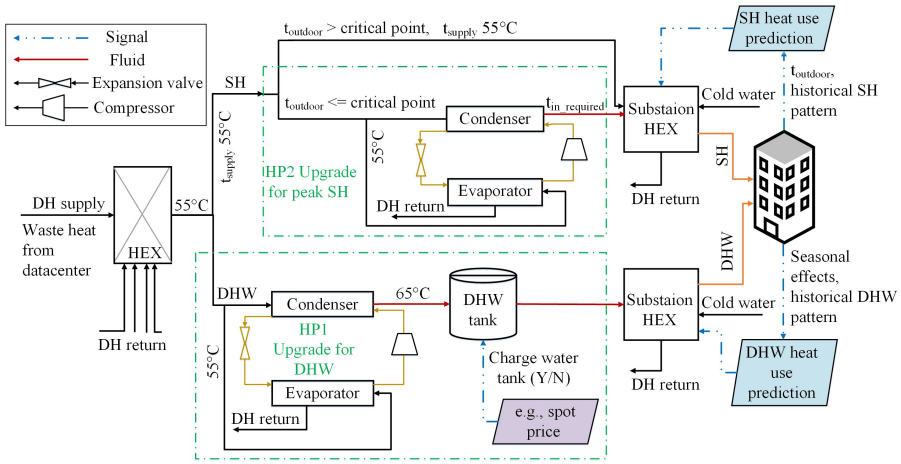

Figure 6.17: Schematic diagram of integrating two building-sized boosting heat pumps for space heating and domestic hot water use

According to the Norwegian regulation, the DHW temperature should be maintained at not lower than 65°C to prevent Legionella's growth when a water storage tank is included at substation [81]. One booster HP (HP1) may be accordingly employed to upgrade the heat source temperature e.g. 55°C to 65°C for DHW heating. The second booster HP (HP2) may be employed to upgrade the heat source for satisfying the peak SH load, when the outdoor temperature reaches a critical point that the source temperature is unable to maintain thermal comfort. For example, when using the conventional radiators in Nordic housings, the critical point may be determined as in [82] giving the equation as:

$$t_{in} = -0.75 \cdot t_{\tau} \tag{6.1}$$

where t_{τ} is the outdoor temperature and t_{in} is the minimum heating supply temperature. Moreover, the selection of critical points shall also consider the energy system's flexibility and use of building thermal inertia as shown [83, 84]. Finally, when boosting units are applied in LTDH, their annual costs for the heat source upgrade process may be calculated and compared, for example using Eq.(4.14).

6.4 Results of lockdown impacts on electricity use and economic costs for buildings with electric heating

This section shows the main findings of the electricity use and economic impacts for buildings under lockdowns and answers **Research Question 4**, corresponding to the example described in Section 5.4. A detailed explanation of the method and results are shown in **Paper III**.

6.4.1 Comparison results of daily electricity profiles before and during lockdowns

The average daily electricity profiles for kindergartens and the apartment from March to May 2018(2019)-2020 are compared in Figures 6.18 and 6.19, respectively.

For the educational buildings shown in Figure 6.18, the electricity use followed the opening hours and schedules. On weekdays, the demand generally arose between 6 and 17 o'clock with the peak demand at around 8 or 9 o'clock. The demand rising ahead of the teaching activities aimed to extend thermal comfort and improve indoor air quality. From 19 to 6 o'clock the next day, the energy supply systems maintained low demand. It may be observed that the shapes of the three-year electricity profiles from March to May were quite similar [2]. Meanwhile, the electricity use pattern was different in the apartment. As shown in Figure 6.19, demand during the weekday day in 2020 was significantly higher than in 2019 and the weekday (WD) values were similar to the weekend (WE) values, which was also mentioned in [48]. This may indicate that the effect of occupants on private buildings plays a more important role than in public buildings, and that household energy demand varies by resident behavior, as discussed in [85, 86].

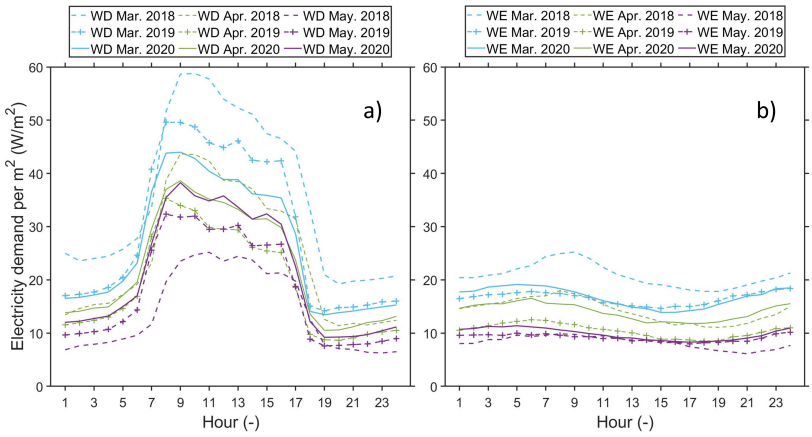

Figure 6.18: The average daily electricity load profiles for kindergartens from March to May 2018-2020, where a) are profiles on weekdays and b) are profiles on weekends

[2]Results of schools are similar to kindergartens and schools results are thus not shown in this section.

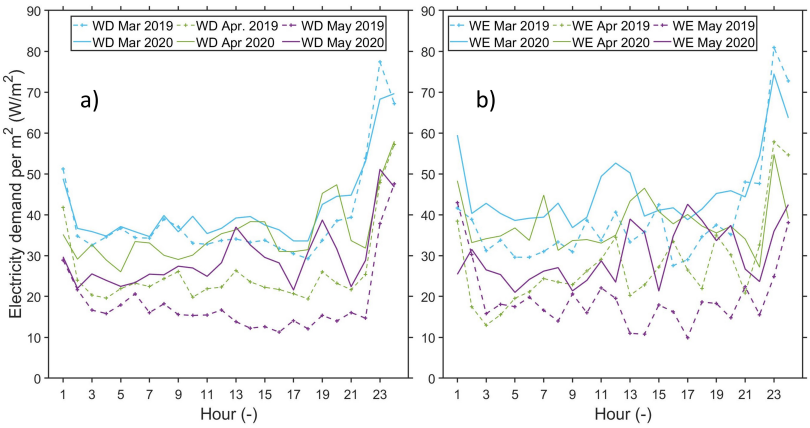

Figure 6.19: The average electricity load profiles for the single apartment from March to May 2019-2020, where a) are profiles on weekdays and b) are profiles on weekends

Further, the results of Euclidean distance (ED) and Pearson correlation coefficient (PCC) measures within every two years for kindergartens and the residential buildings are compared in Figures 6.20 and 6.21. The PCCs are plotted by the red lines with dots, and each dot refers to the same year of the bar where it is located. By discarding the real energy demand scales influenced by the outdoor temperature, it was observed that the PCC results from March to May during the three years were higher than 0.93 in kindergartens on weekdays, and the highest PCCs were even found within 2019-2020. This again demonstrated that the patterns and operation of the three-year average daily energy use were of high similarity. The daily electricity profiles and ED results for kindergartens showed there were much lower demands on weekends than on weekdays. This is mainly because Norwegian educational institutions usually do not carry out teaching activities on weekends, but occasionally can rent buildings to maximize the use of public resources [24].

Regarding the residential buildings, the ED and PCC results of the townhouse and the apartment between 2019 and 2020 were compared in Figure 6.21. The ED values of the townhouse were lower and more stable than those of the apartment within the three months on weekdays and weekends, only with the exception of March when the two were close. Additionally, the EDs of the townhouse on weekends were smaller than on weekdays, which was backed by the high average PCC values. It mostly implied that the residents kept their usual weekend plans and the occupant behavior in smaller dwelling sizes had higher energy impacts and less robustness.

From the above findings, the operation in educational buildings might not shift to night/weekend settings as the hypothesis. For practical reasons, the schools and kindergartens remained open during the period to support parents working in key

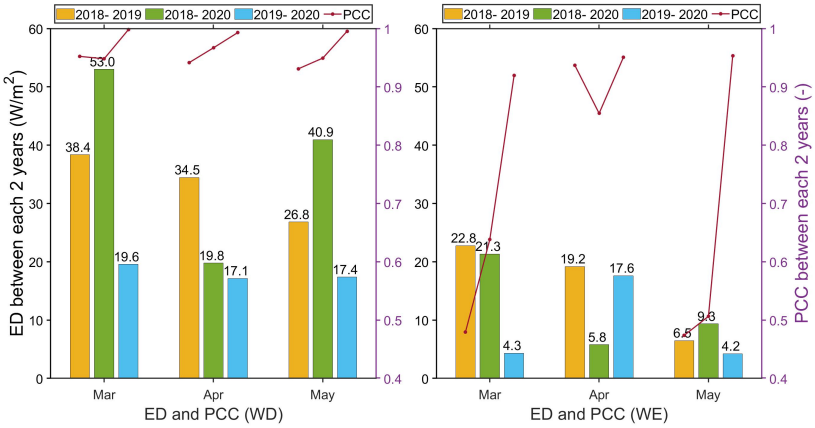

Figure 6.20: The ED and PCC results of kindergartens in 2018-2020, where the left is for weekdays, the right for weekends

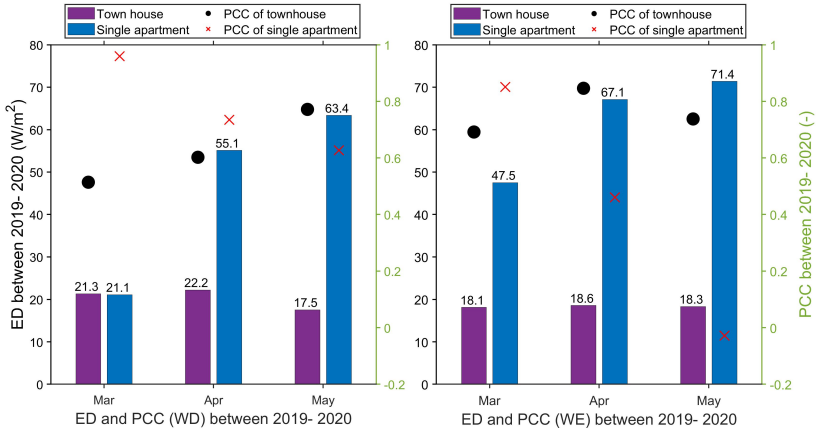

Figure 6.21: The ED and PCC results of townhouse and single apartment in 2019-2020, where the left is for weekdays, the right for weekends

positions such as the health system, police station, transportation and so on. This is similar to the heat use examined in the educational buildings [87], however unlike the electricity use examined in the university laboratory building [88] and the nursery school and elementary school buildings [89]. Meanwhile, as projected, the residential buildings were affected by the changes in the dweller's working schedule during the period. Moreover, an apartment with a smaller floor area and one dweller may be more sensitive to changes in use.

6.4.2 Results of scenario-based electricity profiles

Figures 6.22 and 6.23 illustrate the possible electricity profiles for kindergartens, the apartment, and the townhouse in a typical weather year.

In Figure 6.22, under the normal operation settings (**Scenario 1**), kindergartens may need 172 kWh/m^2 per year as indicated by the red line; while under the energy-saving mode (**Scenario 2**), only 112 kWh/m^2 may be needed, as indicated by the green line. Therefore, by reasonably setting up the building service systems and improving the arrangement of the educational institutions, the electricity use may be reduced by approximately 35% in the kindergartens. The scenario comparison of the residential buildings is shown in Figure 6.23. Under the normal conditions of low-daytime attendance (**Scenario 1**), the annual electricity demand of a typical year may be 222 kWh/m^2 and 126 kWh/m^2 in the apartment and townhouse, respectively, as indicated by the solid lines. However, when the work-from-home rule came into effect (**Scenario 3**), 26.9% more electricity may be needed in the apartment, while the townhouse may only require 1.3% more electricity, as shown by the dashed lines. The higher electricity density in the apartment made it more sensitive to the changes.

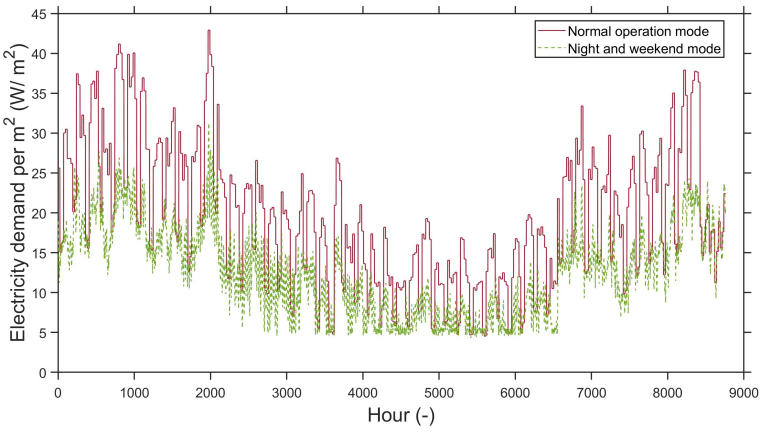

Figure 6.22: Annual electricity load profiles for kindergartens under Scenario 1 and Scenario 2

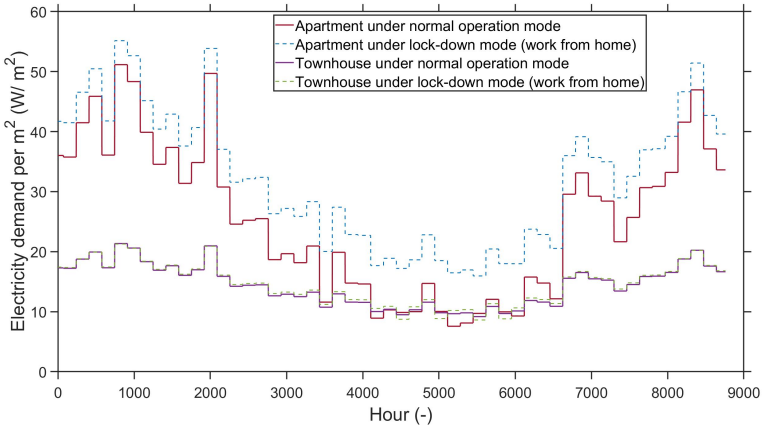

Figure 6.23: Annual electricity load profiles for the single apartment and the townhouse under Scenario 1 and Scenario 3

6.4.3 Results of economic impact assessment

By combining the above electricity profiles with the three price levels described in Section 5.4.3, the annual electricity costs for the analyzed building types were estimated based on the three price cases.

Figure 6.24 compares the annual electricity costs of one 700 m^2 representative kindergarten and one 4000 m^2 representative school under the normal operation mode (**Scenario 1**) and the night and weekend mode (**Scenario 2**), where moderate *el* price, highest *el* price, and lowest *el* price are the shortcuts of the cases of moderate, highest, and lowest electricity price. For the kindergarten, the cost reductions between the two operation modes varied from 1461 €/yr (equivalent to 2.1 €/(m^2·yr)) under the case of lowest electricity price to 2873 €/yr (4.1 €/(m^2·yr)) under the case of highest electricity price, see Figure 6.24a). For the school, Figure 6.24b) exhibits that between 5658 €/yr (1.4 €/(m^2·yr)) and 10 946 €/yr (2.7 €/(m^2·yr)) may be saved if the building was shifted to the night and weekend settings during the lockdown. It is worth noting that the economic savings potential of switching operating modes was greater when electricity prices were higher.

In the residential buildings, due to more time spent at home by the dwellers (**Scenario 3**), between 78-164 € (2.0 €/(m^2·yr)-4.1 €/(m^2·yr)) more money may be needed in the apartment annually, see Figure 6.25a), while the increase would be less than 15 € (0.1 €/(m^2·yr)) in the townhouse, see Figure 6.25b). Although the large dwelling with multifamily members required higher overall electricity expenditures than the small apartment, they might be more resilient and robust to changes in use patterns.

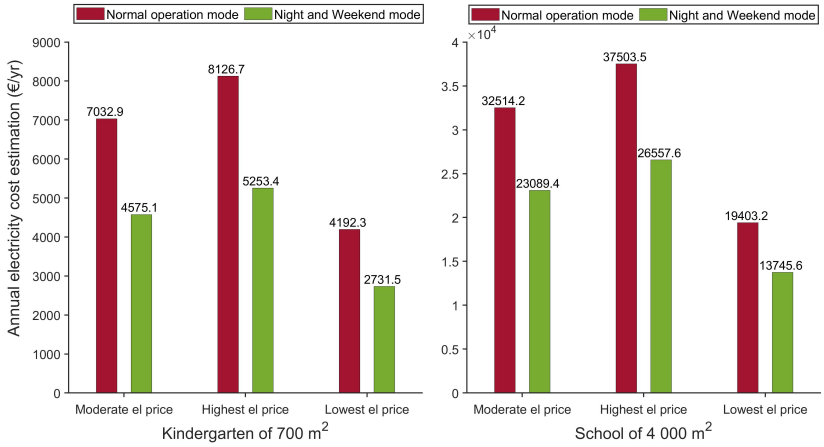

Figure 6.24: Annual electricity cost estimation of kindergartens and schools under Scenario 1 and Scenario 2, where the left is for the annual cost of kindergartens, the right is for the annual cost of schools

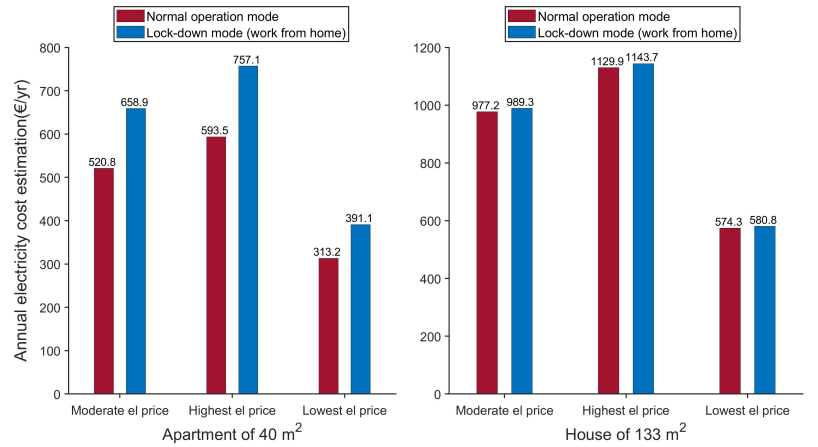

Figure 6.25: Annual electricity cost estimation of the single apartment and the townhouse under Scenario 1 and Scenario 3, where the left is for the annual cost of the apartment, the right is for the annual cost of the townhouse

6.4.4 Discussions of aggregation and consequence on energy planning

Analysis of energy use under special situations (e.g. lockdowns) may help local energy planning. An imaginary community was assumed consisting of one kindergarten, one school, and one residential area composed of 40% of apartments and 60% of townhouses. By aggregating the annual electricity demand for the four building types in a normal year (**Scenario 1**) and lockdown year (**Scenario 2-3**), the annual total electricity use for this community may be compared. By varying the residential area and the work-from-home adoption percentage, the electricity demand, especially the peak demand and the capacity factor may be affected. The energy plant capacity factor is the ratio of the actual total energy output to the maximum output over a period of time, and it measures the overall utilization rate of the power plant [90].

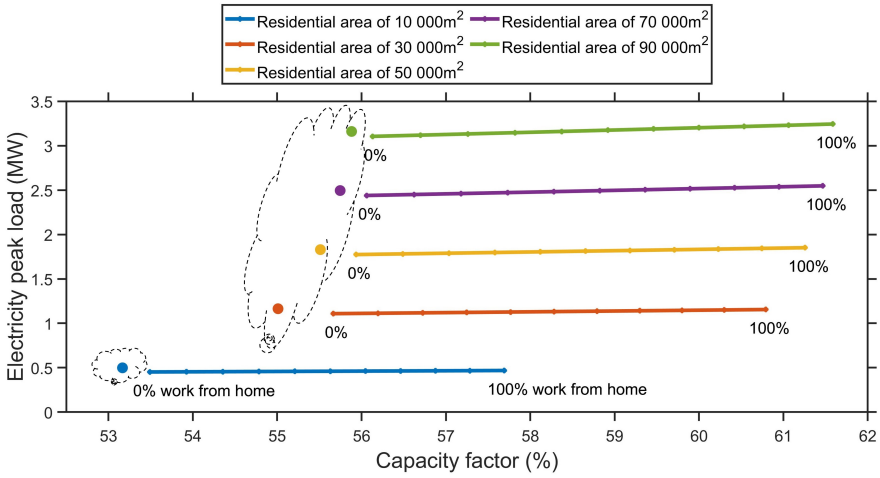

Figure 6.26: Capacity factor vs electricity peak load for different residential building areas, comparing normal year with lockdown year when varying percentages of work-from-home adoption

Figure 6.26 shows the possible consequence of energy planning in terms of the capacity factor with the electricity peak demand by changing the work-from-home adoption percentages from 0% to 100%, as indicated by the solid line, in the variation of residential areas between 10 000-90 000 m^2. The solid circles in the dashed cloud line represent the normal year conditions, which had a lower plant capacity factor and needed higher peak demand than some of the work-from-home conditions for the smaller residential areas (e.g. 10 000–50 000 m^2). Interestingly, the energy facilities may not be fully utilized in normal years, which may lead to uneconomical production. While in larger residential areas (e,g. 70 000–90 000 m^2), the plant ca-

pacity can be better utilized through a higher capacity factor, however higher peak demand may be required during lockdowns. It may be explained that the electricity savings from the closed kindergarten and school may not be comparable to the more electricity use, when most of the residents stay at home, in larger residential areas.

7

CONCLUSIONS AND OUTLOOKS

Never confuse education with intelligence, you can have a PhD and still be an idiot.

Richard Phillips Feynman

Stay hungry, stay foolish.

From "Whole Earth Catalog"

This chapter concludes the main findings of the thesis, as presented in Section 7.1, acknowledges the limitations, and recommends future study, as presented in Section 7.2.

7.1 Main conclusions and contributions

The main objective of this PhD research is to gain a deeper understanding of the energy use of Norwegian urban buildings and to help improve the efficiency of urban buildings' energy systems. The following issues were addressed: analyzing heating and electricity use data, locating factors that may affect the building energy operation, identifying representative load profiles for heating and electricity for different building types, developing appropriate models for long-term sizing and short-term prediction, and estimating environmental and economic costs for future development and special circumstances. The main findings are highlighted as follows.

The study was carried out based on measured data obtained from municipal and residential buildings with different operating regimes and technical solutions for building energy supply systems. For buildings featured with distinct night setback control operations and different attendance levels between the weekdays and the weekends, such as educational buildings, the heating operators most likely set mode between weekdays and weekends, as well as long holiday mode during summer vacation and Christmas, with a slow control response to short breaks, which caused part of heating energy being wasted. This implied that the DH demand was more

likely prone to the outdoor temperature over the schedule on short breaks, while the control of electrical appliances responded closely by following the attendance and schedule. The energy density for the identified typical school was 129 kWh/(m^2·yr), of which nearly 56% was for heating needs. The energy density was slightly lower than the average annual energy use in Norwegian schools, but on par with the Swedish school average and close to the nZEB energy performance target level for Finnish educational buildings. While for buildings featured with relatively stable occupancy, such as nursing homes, the heating load profiles exhibited milder peak load during the working hours and relatively higher levels during the non-working hours. The DH density of a typical Nordic nursing home was found around 111-114 kWh/(m^2·yr), almost twice that of a typical Nordic school. Additionally, from the analysis of buildings with electric heating under lockdowns, the electricity demand of the educational buildings was almost the same as in previous years, while the electricity demand of the residential buildings changed significantly. The scenario-based analysis showed that with proper building operation during a temporary closure, the electricity use could be reduced by 35% for kindergartens and by 29% for schools, equivalent to 2.1-4.1 €/(m^2·yr) for kindergartens, and 1.4-2.7 €/(m^2·yr) for schools, as estimated in the three spot price level cases. Meanwhile, electricity demand for the apartment and the townhouse increased by around 27% and 1.3%, respectively, equivalent to 2.0-4.1 €/(m^2·yr) for the apartment and negligible for the townhouse. The small apartment with higher electricity density was more electricity sensitive than the large house. In general, the energy demand of the observed buildings has shown the average demand level in Nordic countries.

Regarding future building expansion, the analysis of the aggregated electricity demand showed that the size of local infrastructure may be affected by building area, area composition of different building types, energy operation mode, and unintended conditions. For the small residential area of i.e. 10 000 m^2, the percentage changes in peak demand were between -9.3% and -6.1% from 0% to 100% of work-from-home adoption, and these changes for the large residential area of i.e. 90 000 m^2 were between -1.8% and 2.6%. As suggested in a study of one university campus with multiple building types [91], an appropriate building type ratio may help reduce the overall load and load fluctuation of a district. Therefore, it is important to analyze the energy demand under different scenarios to discover the optimal sizing for future planning. In addition to infrastructure sizing, based on the current energy demand, a slower CO_2 growth rate and enhanced energy resilience may be achieved for future building area expansion, as long as diverse low-carbon energy resources are involved.

For short-term, such as the day-ahead heating load prediction, it is important to include historical heating load, such as the previous one-to-three days' load, to predict the next day's load, as shown by the defined ANN model g_{120} (with 120 inputs) compared to the ANN model f_{72} (with 72 inputs). However, historical heating load data are unfortunately either accessible with delays or low data quality, i.e. low time resolution. This is different from historical weather information, which is often

publicly accessible via meteorological institutions. Although f_{72} showed a worse prediction quality performance than g_{120} and the ES curve model, f_{72} can still contribute a good heating load prediction even without previous days' load as inputs. Another potential contribution of the results is to map load prediction to other relevant buildings, either existing buildings without high-quality data or new ones without adequate training data. For example, the gained knowledge may be useful in understanding new or existing nursing homes in need of renovation assessment, by transferring the developed energy prediction models for a typical building type to individual buildings through the Transfer Learning (TL) method, a state-of-the-art machine learning (ML) technique [42].

The methods and results proposed in the thesis were constructed and evaluated based on a certain amount of measured data for different building functions, taking into account normal and unforeseen disruptions, and they may contribute to future infrastructure development and better insight into building energy management.

7.2 Limitations and future recommendations

In the thesis, both long-term and short-term heating load prediction employed the actual measured outdoor temperature (predictor) as the forecasted outdoor temperature for prediction. In practice, such weather forecasts are however somewhat inaccurate and may consequently lead to worse performance than observed here. Therefore, it is important to build the base model as accurately as possible to reduce the possible spread and impacts of such weather uncertainties.

The accuracy of long-term heating load prediction for such as schools, shall be improved. Currently, the ES curve was divided into four parts according to different time periods and outdoor temperatures, and the prediction performance for transition and summer seasons was unsatisfactory, mainly due to the less dependence on outdoor temperatures. Other methods shall be considered. Regarding the accuracy of short-term heating load prediction for such as nursing homes, only one-layered ANN model was employed. To cope with the small amount of training data available and the intelligent prediction of peak load and control systems required by low-temperature district heating (LTDH) and electricity networks, newer types of ANN architectures and other machine learning methods shall be examined.

For the analysis of lockdowns, Norway's lockdown regime was in effect from mid-March to mid-May 2020, and the outdoor temperature during this period (0-21°C on weekly base) did not cover the local historical outdoor temperature range throughout the year (e.g. -7 -21°C on weekly base in 2019), especially the low outdoor temperature recorded in winter. Therefore, extrapolation of the Scenario 3-based models to the typical year might not fully represent the annual household electricity use profile. By extrapolating power characteristics over the limited outdoor temperature range during lockdowns, the annual increase in household electricity demand,

especially in winter, may be higher than the estimation made in the thesis. To better address future unforeseen disruptions and trends in workplace and lifestyle, further research using more data and seasonal correction factors is needed, for example, to take experiments on home office activities involving more dwellings. This may provide more comprehensive insights through more accurate prediction models and better knowledge.

As discussed in Section 6.3.4.2, integrating separate temperature boosting units may solve one of the challenges in LTDH, which is the different minimum allowable temperature requirements for domestic hot water and space heating. To analyze the impacts of different prediction models on the overall costs of the building heating system, an in-depth study shall be carried out addressing several key factors, e.g. types of boosting heat pumps (HPs) compressors driving force, operation optimization strategy, the sizing of the boosting HPs and water storage tank.

The thesis mainly focused on building energy analysis, prediction, and supply in buildings. When intermittent renewables and short-to-medium-term energy storage are integrated into the district network, which is likely to come more in the near future, it would be interesting to examine the interactive response between the energy plant/network and the building side, and to optimize the network as a whole.

Bibliography

[1] H. Yoshino, T. Hong, and N. Nord. IEA EBC annex 53: Total energy use in buildings—analysis and evaluation methods. *Energy and Buildings*, 152:124–136, October 2017.

[2] U.N. Environment. 2020 global status report for buildings and construction, 2020.

[3] U.N. Environment. 2021 global status report for buildings and construction, 2021.

[4] Norwegian Ministry of Climate and Environment. Climate Change Act, 2017.

[5] Statistics Norway. Energy and manufacturing.

[6] A. Kofoed-Wiuff, K. Dyhr-Mikkelsen, I. S. Rueskov, and K. Brunak. Tracking nordic clean energy progress 2019. *Nordic Energy Research*, 2019.

[7] EGEC geothermal European Biomass Association and European Solar Thermal Industry Federation. Primary energy factor for electricity in the energy efficiency directive, 2017.

[8] E. Latõšov, A. Volkova, A. Siirde, J. Kurnitski, and M. Thalfeldt. Primary energy factor for district heating networks in european union member states. *Energy Procedia*, 116:69–77, June 2017.

[9] IEA. Energy policies of iea countries: Sweden 2019 review, 2019.

[10] Statistics Norway. District heating and district cooling.

[11] Standard Norge. Ns 3700: Kriterier for passivhus og lavenergibygninger–boligbygninger; 2013, 2013.

[12] Directorate of Building Quality. Tek17. veiledning om tekniske krav til byggverk/building technology regulations, norway; 2017, 2017.

[13] EU Commission. Energy performance of buildings directive.

[14] H. Averfalk, H. Benakopoulos, I. Best, F. Dammel, C. Engel, R. Geyer, O. Gudmundsson, K. Lygnerud, N. Nord, J. Oltmanns, K. Ponweiser, D. Schmidt, H. Schrammel, D.S. Østergaard, S. Svendsen, M. Tunzi, and S. Werner. *Low-Temperature District Heating Implementation Guidebook: Final Report of IEA DHC Annex TS2. Implementation of Low-Temperature District Heating Systems*. Fraunhofer IRB Verlag, 2021.

[15] P. Sorknæs, P. A. Østergaard, J. Z. Thellufsen, H. Lund, S. Nielsen, S. Djørup, and K. Sperling. The benefits of 4th generation district heating in a 100% renewable energy system. *Energy*, 213(119030):119030, December 2020.

[16] S. Buffa, M. Cozzini, M. D'Antoni, M. Baratieri, and R. Fedrizzi. 5th generation district heating and cooling systems: A review of existing cases in europe. *Renewable and Sustainable Energy Reviews*, 104:504–522, April 2019.

[17] J. Wang, H. Cai, S. You, Y. Zong, C. Zhang, and C. Træholt. A framework for techno-economic assessment of demand-side power-to-heat solutions in low-temperature district heating. *International Journal of Electrical Power & Energy Systems*, 122(106096):106096, November 2020.

[18] N. Nord, E. K. Løve Nielsen, H. Kauko, and T. Tereshchenko. Challenges and potentials for low-temperature district heating implementation in norway. *Energy*, 151:889–902, May 2018.

[19] D. Ivanko, H. T. Walnum, and N. Nord. Development and analysis of hourly DHW heat use profiles in nursing homes in norway. *Energy and Buildings*, 222:110070, September 2020.

[20] L. Dias Pereira, D. Raimondo, S. P. Corgnati, and M. Gameiro da Silva. Energy consumption in schools – a review paper. *Renewable and Sustainable Energy Reviews*, 40:911–922, December 2014.

[21] A. O. Hopland and S. Kvamsdal. Building conditions in norwegian local governments: trends and determinants. *Facilities*, 37(3/4):141–156, February 2019.

[22] Alliance to Save Energy. Ee noon: Back to school with energy efficiency.

[23] L. Pistore, G. Pernigotto, F. Cappelletti, A. Gasparella, and P. Romagnoni. A stepwise approach integrating feature selection, regression techniques and cluster analysis to identify primary retrofit interventions on large stocks of buildings. *Sustainable Cities and Society*, 47(101438):101438, May 2019.

[24] Norges vassdrags-og energidirektorat. Analyse av energibruk i undervisningsbygg, 2014.

[25] OECD. *Health at a Glance 2017*. Health at a glance. OECD, November 2017.

[26] OECD. Spending on long-term care brief, 2020.

[27] European network of transmission system operators for electricity. NORDIC GRID DISTURBANCE STATISTICS- 2013, 2014.

[28] World Health Organization. Coronavirus (covid-19) events as they happen.

[29] A. Bahmanyar, A. Estebsari, and D. Ernst. The impact of different COVID-19 containment measures on electricity consumption in europe. *Energy Research & Social Science*, 68(101683):101683, October 2020.

[30] T. Lowder, N. Lee, and J. Leisch. Covid-19 and the power sector in southeast asia: Impacts and opportunities. *NREL/TP-7A40-76963*, June 2020.

[31] K. B. Debnath and M. Mourshed. Forecasting methods in energy planning models. *Renewable and Sustainable Energy Reviews*, 88:297–325, May 2018.

[32] Y. Wei, L. Xia, S. Pan, J. Wu, X. Zhang, M. Han, W. Zhang, J. Xie, and Q. Li. Prediction of occupancy level and energy consumption in office building using blind system identification and neural networks. *Applied Energy*, 240:276–294, April 2019.

[33] H. Dagdougui, F. Bagheri, H. Le, and L. Dessaint. Neural network model for short-term and very-short-term load forecasting in district buildings. *Energy and Buildings*, 203(109408):109408, November 2019.

[34] P. Gianniou, X. Liu, A. Heller, P. S. Nielsen, and C. Rode. Clustering-based analysis for residential district heating data. *Energy Conversion and Management*, 165:840–850, June 2018.

[35] M. Lumbreras, R. Garay-Martinez, B. Arregi, K. Martin-Escudero, G. Diarce, M. Raud, and I. Hagu. Data driven model for heat load prediction in buildings connected to district heating by using smart heat meters. *Energy*, 239(122318):122318, January 2022.

[36] B. Talebi, F. Haghighat, and P. A. Mirzaei. Simplified model to predict the thermal demand profile of districts. *Energy and Buildings*, 145:213–225, June 2017.

[37] P. Xue, Y. Jiang, Z. Zhou, X. Chen, X. Fang, and J. Liu. Multi-step ahead forecasting of heat load in district heating systems using machine learning algorithms. *Energy*, 188(116085):116085, December 2019.

[38] Y. Lu, Z. Tian, P. Peng, J. Niu, W. Li, and H. Zhang. GMM clustering for heating load patterns in-depth identification and prediction model accuracy improvement of district heating system. *Energy and Buildings*, 190:49–60, May 2019.

[39] J. Song, L. Zhang, G. Xue, Y. Ma, S. Gao, and Q. Jiang. Predicting hourly heating load in a district heating system based on a hybrid CNN-LSTM model. *Energy and Buildings*, 243(110998):110998, July 2021.

[40] T. Liu, Z. Tan, C. Xu, H. Chen, and Z. Li. Study on deep reinforcement learning techniques for building energy consumption forecasting. *Energy and Buildings*, 208(109675):109675, February 2020.

[41] X. Liu, Y. Ding, H. Tang, and F. Xiao. A data mining-based framework for the identification of daily electricity usage patterns and anomaly detection in building electricity consumption data. *Energy and Buildings*, 231(110601):110601, January 2021.

[42] C. Fan, Y. Sun, F. Xiao, J. Ma, D. Lee, J. Wang, and Y. C. Tseng. Statistical investigations of transfer learning-based methodology for short-term building energy predictions. *Applied Energy*, 262(114499):114499, March 2020.

[43] S. Menard. Coefficients of determination for multiple logistic regression analysis. *The American Statistician*, 54(1):17–24, February 2000.

[44] A. Melillo, R. Durrer, J. Worlitschek, and P. Schütz. First results of remote building characterisation based on smart meter measurement data. *Energy*, 200(117525):117525, June 2020.

[45] Y. Bao, W. L. Lee, and J. Jia. Probabilistic assessment of overcooling risk for a novel extra-low temperature dedicated outdoor air system for hong kong office buildings. *Building Simulation*, 14(3):633–648, June 2021.

[46] L. Lundström and F. Wallin. Heat demand profiles of energy conservation measures in buildings and their impact on a district heating system. *Applied Energy*, 161:290–299, January 2016.

[47] A. Abu-Rayash and I. Dincer. Analysis of the electricity demand trends amidst the COVID-19 coronavirus pandemic. *Energy Research & Social Science*, 68(101682):101682, October 2020.

[48] C. Burleyson, A. D. Smith, J. S. Rice, N. Voisin, and A. Rahman. Changes in electricity load profiles under COVID-19: Implications of "the new normal" for electricity demand. July 2020.

[49] D. Cvetković, A. Nešović, and I. Terzić. Impact of people's behavior on the energy sustainability of the residential sector in emergency situations caused by COVID-19. *Energy Build.*, 230(110532):110532, January 2021.

[50] M. Carvalho, D.B.de M. Delgado, K.M.de Lima, M.de C. Cancela, C.A.dos Siqueira, and D.L.B.de Souza. Effects of the covid-19 pandemic on the brazilian electricity consumption patterns. *International Journal of Energy Research*, 45(2):3358–3364, September 2020.

[51] G. Ruan, J. Wu, H. Zhong, Q. Xia, and L. Xie. Quantitative assessment of U.S. bulk power systems and market operations during the COVID-19 pandemic. *Applied Energy*, 286(116354):116354, March 2021.

[52] R. Madurai Elavarasan, G. M. Shafiullah, K. Raju, V. Mudgal, M. T. Arif, T. Jamal, S. Subramanian, V. S. Sriraja Balaguru, K. S. Reddy, and U. Subramaniam. COVID-19: Impact analysis and recommendations for power sector operation. *Applied Energy*, 279:115739, December 2020.

[53] H. Zhong, Z. Tan, Y. He, L. Xie, and C. Kang. Implications of COVID-19 for the electricity industry: A comprehensive review. *CSEE Journal of Power and Energy Systems*, 6(3):489–495, September 2020.

[54] Esave AS. iEOS - Planning.

[55] Norsk Klimaservicesenter. https://seklima.met.no/observations/.

[56] Tensio NTE Nett og TrønderEnergi Nett har blitt til Tensio. https://tensio.no/.

[57] Enova Offentlig søk etter energiattester. https://attest.energimerking.no/.

[58] American Society of Heating Refrigerating and Air Conditioning Engineers. Ashrae handbook: fundamentals. 2013.

[59] M. Carragher, M. De Rosa, A. Kathirgamanathan, and D. P. Finn. Investment analysis of gas-turbine combined heat and power systems for commercial buildings under different climatic and market scenarios. *Energy Conversion and Management*, 183:35–49, March 2019.

[60] T. Tereshchenko, D. Ivanko, N. Nord, and I. Sartori. Analysis of energy signatures and planning of heating and domestic hot water energy use in buildings in norway. *E3S Web of Conferences, CLIMA 2019 Congress*, 111, August 2019.

[61] K. B. Lindberg and G. Doorman. Hourly load modelling of non-residential building stock. In *2013 IEEE Grenoble Conference*. IEEE, June 2013.

[62] Y. Ding, H. Brattebø, and N. Nord. A systematic approach for data analysis and prediction methods for annual energy profiles: An example for school buildings in norway. *Energy and Buildings*, 247(111160):111160, September 2021.

[63] J. Granderson, S. Touzani, C. Custodio, M. Sohn, S. Fernandes, and D. Jump. *Assessment of Automated Measurement and Verification (Mamp;V) Methods*. Building Technology and Urban Systems Division, Lawrence Berkeley National Laboratory, July 2015.

[64] N. Meade. Industrial and business forecasting methods, lewis, c. d. *Journal of Forecasting*, 2(2):194–196, January 1983.

[65] E. Keogh, J. Lin, and A. Fu. HOT SAX: Efficiently finding the most unusual time series subsequence. In *Fifth IEEE International Conference on Data Mining (ICDM'05)*. IEEE, 2006.

[66] J. Lin, E. Keogh, L. Wei, and S. Lonardi. Experiencing SAX: a novel symbolic representation of time series. *Data Mining and Knowledge Discovery*, 15(2):107–144, August 2007.

[67] C. Miller, Z. Nagy, and A. Schlueter. Automated daily pattern filtering of measured building performance data. *Automation in Construction*, 49:1–17, January 2015.

[68] EU Commission. Electricity price statistics Statistics Explained. https://ec.europa.eu/eurostat/statistics-explained.

[69] See market data for all areas. https://www.nordpoolgroup.com/market-data1/.

[70] Norsk Fjernvarme. http://www.fjernkontrollen.no/.

[71] Standard Norge. Ns 3720: 2018- method for greenhouse gas calculations for buildings.

[72] Norsk Energi. Klimaregnskap for fjernvarme, 2014.

[73] B. Iglewicz and D. C. Hoaglin. *How to detect and handle outliers: Vol 16*. ASQC/Quality Press, Milwaukee, WI, December 1997.

[74] S. Frederiksen and S. Werner. *District Heating & Cooling*. Studentlitteratur, Lund, Sweden, August 2013.

[75] Enova. Hensiktsmessige varme- og kjøleløsninger i bygninger (Appropriate heating and cooling solutions in buildings), 2013.

[76] H. Cai, C. Ziras, S. You, R. Li, K. Honoré, and H. W. Bindner. Demand side management in urban district heating networks. *Applied Energy*, 230:506–518, November 2018.

[77] Y. Sun, S. Wang, and F. Xiao. Development and validation of a simplified online cooling load prediction strategy for a super high-rise building in hong kong. *Energy Conversion and Management*, 68:20–27, April 2013.

[78] Enova. Rapport: Enovas byggstatistikk 2016.

[79] C. Hjortling, F. Björk, M. Berg, and T. af Klintberg. Energy mapping of existing building stock in sweden – analysis of data from energy performance certificates. *Energy and Buildings*, 153:341–355, October 2017.

[80] T. Niemelä, R. Kosonen, and J. Jokisalo. Cost-optimal energy performance renovation measures of educational buildings in cold climate. *Applied Energy*, 183:1005–1020, December 2016.

[81] TEK Building technical regulation. Inneklima og legionella- temaveiledning (indoor climate and legionella - topic guide).

[82] A. Ploskić, Q. Wang, and S. Sadrizadeh. Mapping relevant parameters for efficient operation of low-temperature heating systems in nordic single-family dwellings. *Applied Science*, 8(10):1973, October 2018.

[83] Y. Li, C. Wang, G. Li, J. Wang, D. Zhao, and C. Chen. Improving operational flexibility of integrated energy system with uncertain renewable generations considering thermal inertia of buildings. *Energy Conversion and Management*, 207(112526):112526, March 2020.

[84] D. Romanchenko, J. Kensby, M. Odenberger, and F. Johnsson. Thermal energy storage in district heating: Centralised storage vs. storage in thermal inertia of buildings. *Energy Conversion and Management*, 162:26–38, April 2018.

[85] T. Hong, D. Yan, S. D'Oca, and C. Chen. Ten questions concerning occupant behavior in buildings: The big picture. *Building and Environment*, 114:518–530, March 2017.

[86] V. M. Barthelmes, R. Li, R. K. Andersen, W. Bahnfleth, S. P. Corgnati, and C. Rode. Profiling occupant behaviour in danish dwellings using time use survey data. *Energy and Buildings*, 177:329–340, October 2018.

[87] D. Ivanko, Y. Ding, and N. Nord. Analysis of heat use profiles in norwegian educational institutions in conditions of COVID-lockdown. *Journal of Building Engineering*, 43(102576):102576, November 2021.

[88] C. Birch, R. Edwards, S. Mander, and A. Sheppard. Electrical consumption in the Higher Education sector, during the COVID-19 shutdown. In *2020 IEEE PES/IAS PowerAfrica*, pages 1–5, August 2020.

[89] M. S. Geraldi, M. V. Bavaresco, M. A. Triana, A. P. Melo, and R. Lamberts. Addressing the impact of COVID-19 lockdown on energy use in municipal buildings: A case study in florianópolis, brazil. *Sustainable Cities and Society*, 69(102823):102823, June 2021.

[90] J. Morales Pedraza. Current status and perspective in the use of coal for electricity generation in the North America region. In *Conventional Energy in North America*, pages 211–257. Elsevier, 2019.

[91] S. Chen, X. Zhang, S. Wei, T. Yang, J. Guan, W. Yang, L. Qu, and Y. Xu. An energy planning oriented method for analyzing spatial-temporal characteristics of electric loads for heating/cooling in district buildings with a case study of one university campus. *Sustainable Cities and Society*, 51(101629):101629, November 2019.

A

APPENDIX

A.1 Paper I

Energy analysis and energy planning for kindergartens based on data analysis

Ding, Y., Brattebø, H. and Nord, N.

1st Nordic conference on Zero Emission and Plus Energy Buildings, Trondheim, Norway, IOP Conference Series: Earth and Environmental Science, Volume 352(1), p.012031, 2019

IOP Conf. Series: Earth and Environmental Science **352** (2019) 012031 doi:10.1088/1755-1315/352/1/012031

Energy analysis and energy planning for kindergartens based on data analysis

Yiyu Ding*, Helge Brattebø, Natasa Nord

Department of Energy and Process Engineering, Norwegian University of Science and Technology, NO-7491 Trondheim, Norway

e-mail: yiyu.ding@ntnu.no

Abstract. The aim of the study was to utilize different building data for prediction of development in energy use of a typical building type. In this study, energy use and its future development for kindergartens in Trondheim, Norway, were analyzed. The energy use data were retrieved from the energy monitoring platform of Trondheim Municipality. The total area of all the kindergartens was about 76 000 m^2, where the area of each kindergarten was ranging from 100 – 4 471 m^2. Firstly, typical heat and electricity duration curves per m^2 of kindergartens in Trondheim within six years were identified. Secondly, the kindergartens were divided into two cohorts based on their connection to district heating (DH). The average total annual energy use was 177 kWh/m^2 for kindergartens without DH, and 168 kWh/m^2 for kindergartens connected to DH. The peak load values were similar for both cohorts, about 140 W/m^2. Analysis of the duration curves showed a bigger electricity load variation for the kindergartens without DH connection. Within the building cohort with DH, three cases were found depending on the energy share from DH; i.e. DH high share, DH average share, and DH low share. By following different background data for CO_2 factors of electricity and local DH, the kindergarten with DH high share had almost the lowest annual CO_2 emission. Contrarily, the annual CO_2 emission of a kindergarten with lower share of DH, or without DH, usually had a wider range of emissions due to its dependence of the electricity production mix. Finally, a prediction was made by assuming 14.2 % growth rate of kindergartens on the ground of the average six-year total kindergarten area. The result showed that if more than 50- 67 % of the new building area would be connected to DH, a smaller increase of CO_2 emission from the projected area could be achieved, depending on the relevant CO_2 factors. This proved that buildings with DH were more robust than the one without DH concerning CO_2 emission. The suggested analysis method and identified duration curves could be used to as a reference example for defining energy profiles of other building types. These profiles are necessary for diversifying and upgrading local energy supply pathways, infrastructure sizing, and improving urban energy planning.

1. Background

Approximately 36-40 % of energy is consumed in building service around the world each year, and it is responsible for nearly 40 % of direct and indirect CO_2 emissions [1]. Therefore, urban building stocks are expected to make high contribution for low energy use and reduction of greenhouse gas emissions. In Norway, due to cheap and green electricity power from the abundant hydro-power, coverage rate of district heating (DH) system is small. DH only contributes approximately 11 % of total heating demand

Content from this work may be used under the terms of the Creative Commons Attribution 3.0 licence. Any further distribution of this work must maintain attribution to the author(s) and the title of the work, journal citation and DOI.
Published under licence by IOP Publishing Ltd

in Norway [2]. Norwegian residential and service buildings are highly reliant on electricity for space heating (SH) and domestic hot water (DHW). Whereas, driven by the motivation of economic and environmental benefits of DH, relevant regulations and investment subsidies have been introduced to expand the build-up of DH system in Norway. As the third largest city in Norway, Trondheim municipality has been committed improving urban plans for better living environment under the pressure of urbanization, population growth, and mitigation of anthropological carbon footprint [3].

The aim of this article was to identify energy profiles of one typical building type in Trondheim. Typical profiles of energy use can be used as input to building simulations and model calibration. The historical energy use data of kindergartens from 2013 to 2018 was retrieved from the energy monitoring platform of Trondheim Municipality [4]. The outdoor weather data and energy use was given in hourly resolution. Besides kindergarten, school, heath/nursing center, sports center and others are also monitored.

2. Methods

2.1. Building general information

During the six years, numbers of total kindergartens have been increased from 83 to 99. Based on the connection to DH, the kindergartens were divided into two cohorts, Cohort 1 and Cohort 2. In Cohort 1, the buildings are not connected to DH, and supplied by electricity only, and in Cohort 2, the buildings are connected to DH. The yearly building numbers and building area of the two cohorts were compared in Table 1. In total, there were 559 hourly files of kindergartens being used in the analysis.

Table 1. Building numbers and area of Cohort 1 and Cohort 2.

		2013	2014	2015	2016	2017	2018
Building numbers (-)	Cohort 1	66	66	68	68	71	71
	Cohort 2	21	23	26	27	28	28
	Total	83	89	94	95	99	99
Building area (m^2)	Cohort 1	36979	38855	40890	40890	43259	43259
	Cohort 2	24623	26317	30105	31766	32768	32768
	Total	61602	65172	70995	72656	76027	76027

It shows that generally the share of Cohort 2 is smaller than Cohort 1 but growing, especially when it comes to the building area. As shown in Figure 1, the blue square stands for Cohort 1 and the red for Cohort 2, and the green line demonstrates the percentage of Cohort 2, Cohort 2 covers around 43 % of total building area till 2018. This can be explained in Figure 2 by plotting the relation between building area and weekly-based load needs. Most of the kindergartens in Cohort 1 were built within small to medium size (in blue stars), while kindergartens in Cohort 2 were within medium to large size (red circles). The area of each kindergarten varies largely from 100 to 4471 m^2.

2.2. Energy duration curve per m^2

There is a big variety of the building area of each kindergarten, hence, the load duration curves were analyzed based on energy demand per m^2. For buildings in Cohort 1, the duration curves were made only by electricity use. For buildings in Cohort 2, the duration curves of electricity and DH were analyzed separately. Yearly duration curve of each building was obtained by sorting annual load hourly profile from highest to lowest values, and average duration curve was made by the mean values of all the curves. From the average energy use under its outdoor temperature, energy signature was established to imply the relation between energy demand per m^2 and outdoor temperature. MATLAB was used for energy data analysis.

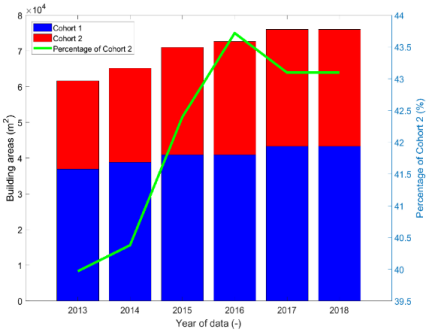

Figure 1. Building area comparison of Cohort 1 and Cohort 2.

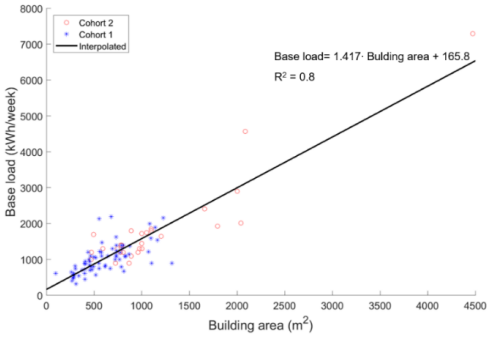

Figure 2. Building area vs Building weekly base load of Cohort 1 and Cohort 2.

2.3. Energy coverage rate in Cohort 2

In Cohort 2, heating demand was provided by DH and the other energy demand by electricity. In order to see the contribution from the two energy supply ways, Figure 3 demonstrates the energy coverage rates from DH and electricity in Cohort 2. In Figure 3, DH was marked in red and electricity in blue, each bar stands for the average energy use situation of one kindergarten from 2013 to 2018, and all the 28 kindergartens were included. From the bar chart, three cases were defined, they were named as DH average share, DH high share and DH low share. In the case of DH high share, nearly 76.9 % of total energy use comes from DH, 31.4 % higher than the case of DH low share. On average, DH supports 60.0 % of total energy use, as listed in Table 2.

Table 2. Energy coverage rate of three cases in Cohort 2.

	From DH (%)	From electricity (%)
DH average share	60.0	40.0
DH high share	76.9	23.1
DH low share	45.5	54.5

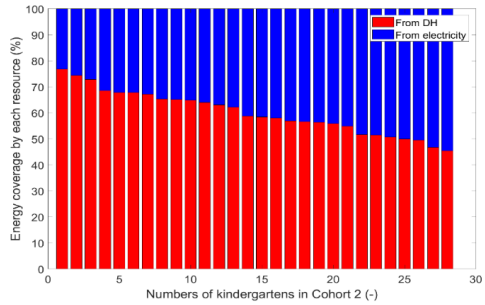

Figure 3. Energy coverage rates of DH and electricity in Cohort 2.

2.4. CO_2 factors of electricity and DH production

Benefitting from the modern transmission technology and the characteristic of electricity, electricity is capable of long-distance transmission with less than 5 % of loss. Norway is connected in the Nordic power grid and further expanded into the wider European grid, and electricity is traded in the free market. Within the Norwegian border, CO_2 factor of electricity can be as low as 10 gCO_2/kWh (named as $CO_{2\text{-}EL1}$), which is mainly contributed by the abundant hydro-power, however this factor can be high up to 110 gCO_2/kWh ($CO_{2\text{-}EL2}$) in the Nordic region since fossil fuels are involved in the electricity production mix. Distinguished from electricity, the transmission loss of heating can be quite high, which makes DH not suitable for long-distance transport. Therefore, the equivalent energy and environmental factors of DH is mostly locally specified. From the information of Norsk Fjernvarme, during 2010 to 2018 most of the DH in Trondheim has been provided by waste incineration, followed by fossil gas with the

contribution of around 10 %, and the small rest comes from flexible electricity, bio-energy, ambient heat, and fossil oil [5]. In Norway, in accordance to NS 3720-2018, the CO_2 emission from waste-to-energy for energy production (electricity and DH) has been allocated to the sector of waste management instead of energy sector [6]. The CO_2 factors of DH production in Trondheim were calculated based on the annual production composition of energy sources. Three typical CO_2 factors of DH were found, they are the average value from 2010 to 2018, value of 2015 as the 9-year lowest, and value of 2010 as the 9-year highest. These factors were used as background data for the assessment of CO_2 emission, respectively. The CO_2 factors of DH production in Trondheim are listed in Table 3, and the CO_2 data of fossil gas, bio-energy and fossil oil can be found in Norsk Energi [7].

Table 3. CO_2 factors of DH production in Trondheim.

		2010-2018: $CO_{2\text{-DH1}}$	2015: $CO_{2\text{-DH2}}$	2010: $CO_{2\text{-DH3}}$
Composition of energy sources (%)	Waste incineration	74.0	83.1	61
	Fossil gas	10.8	5.9	20
	Flexible electricity	8.5	5.0	6
	Bio-energy	4.0	4.0	5
	Ambient heat	0.8	1.0	1
	Fossil oil	1.9	1.0	7
CO_2 factors (gCO_2/kWh)		41.66	23.5	76.3

2.5. Annual CO_2 emission of one typical kindergarten and future prediction

From Figure 2, a typical kindergarten in Trondheim was determined at 700 m^2 concerning the main size ranges the two cohorts. For the buildings in Cohort 1, as addressed above regarding the difficulty of splitting energy share from heating and electricity, therefore, the annual CO_2 emission comparison of one typical kindergarten between Cohort 1 and Cohort 2 was made based on the annual average energy demand of Cohort 1. For Cohort 2, the three cases regarding DH shares were considered separately.

After the annual CO_2 emission calculation of one typical kindergarten was made and compared, the impact of new building area was predicted. In this article, 10 000 m^2 of new building area of kindergarten (A_{new}) was assumed to be added in Trondheim. The building area growth rate (r) was defined as the ratio between (A_{new}) and the annual average total building areas of kindergarten throughout the six years, which is 70 413 m^2. The increasing building area rate is 14.2 %. This growth rate was used as the reference line, and compared with the CO_2 growth rate based on different background data by varying the percentage of new building area connected to DH (x). For simplicity, the annual CO_2 emission was calculated based on the CO_2 factor of Nordic electricity ($CO_{2\text{-EL2}}$) and the three DH production factors. Meanwhile, for the new area connected to DH, the case of DH average share was used. In Function (1), as the denominator, the average annual average CO_2 emission of all the kindergartens ($\overline{CO_2}$) was calculated from the annual average energy use of Cohort 1 and Cohort 2 within the six years. The comparison between growth rates of building area and CO_2 can be explained as:

$$r - \frac{CO_{2-added}}{\overline{CO_2}} \cdot 100\% \tag{1}$$

$$CO_{2-added} = [A_{new} \cdot (1-x) \cdot E_{EL} + A_{new} \cdot x \cdot E_{DH-EL}] \cdot CO_{2-EL2} + A_{new} \cdot x \cdot E_{DH-DH} \cdot CO_{2-DHi} \quad (i = 1, 2, 3)$$

When Function (1) = 0, there is a break-even point that the increasing rates of CO_2 emission and new building area are same. When Function (1) < 0, it means if increasing new building area by 14.2 %,

more than 14.2 % more CO_2 emission would be produced. On the contrary, when Function (1) > 0, it implies that slower CO_2 emission growth could be achieved.

3. Results

3.1. Results of energy duration curve and Energy signature per m²

The annual average duration curves were presented in Figure 4, Figure 5, and Figure 6, and the annual energy demand were summarized in Table 4. Average duration curves were plotted in black thick lines. The peak load for the two cohorts are almost same. The maximum deviation from the average curves are 27.2 % in Cohort 1 and 24.3 % in Cohort 2. The deviation considers 0- 4000 hour in the duration curve. Energy loads during the last 4760 hours are small, and have minor influence of the grid and plant sizing. Moreover, peak load for Cohort 1 can only expect from electricity; while the peak load for Cohort 2 can be satisfied by DH and electricity, it releases the maximum demand of power grid. Although electricity use in Cohort 2 has weak relation with outdoor temperature, the duration curves of six years have similar pattern except higher use in 2013. It may be explained that fewer kindergartens were used for the analysis, and it caused the large deviation. The detailed annual duration curves can be found in Appendix Figure A 1 to Figure A 6, and there were several unknown high peak loads in Cohort 1.

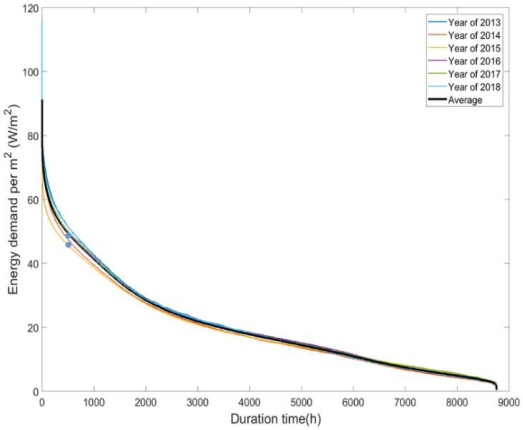

Figure 4. Average total energy duration curves of Cohort 1.

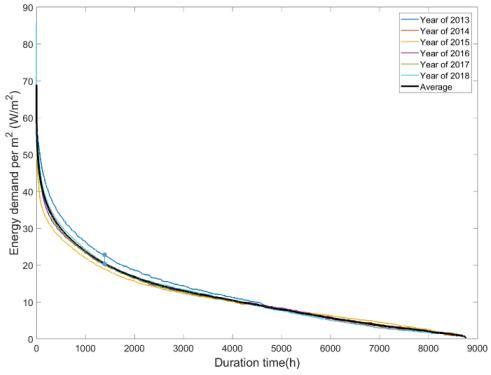

Figure 5. Average heating energy duration curves of Cohort 2.

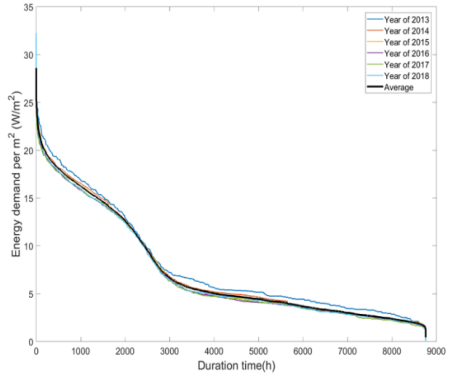

Figure 6. Average electricity duration curves of Cohort 2.

Table 4. Average annual energy use of Cohort 1 and Cohort 2.

		2013	2014	2015	2016	2017	2018	Average
Cohort 1	E_{EL} (kWh/yr)	182.3	169.6	169.6	180.9	180.8	179.8	177.2
Cohort 2	E_{DH-DH} (kWh/yr)	111.6	100.9	98.8	102.2	101.6	102.9	103.0
	E_{DH-EL} (kWh/yr)	69.9	65.4	64.6	62.9	62.5	63.1	64.7

Moreover, to see if the energy use followed the outdoor temperature (t_{od}), heating degree days (HDD)/ heating degree hours (HDH) and energy signature were adopted as rough measurements.

Firstly, heating degree days (HDD)/ heating degree hours (HDH) is the integral of difference between indoor and outdoor temperatures, and is robust tool of predicting space heating. 12- 18 °C are commonly used as the effective indoor temperature to avoid oversizing of heating plants [8]. In this article 18 °C was chosen to roughly estimate the colder and milder weather conditions. The HDH of the six years can be found in Table 5. The average annual heating use of Cohort 2 (E_{DH-DH}) better followed the outdoor temperature (t_{od}) than the average annual energy use of Cohort 1 (E_{EL}).

Table 5. Heating degree hours of six years.

	2013	2014	2015	2016	2017	2018
°C·h	107562.4	94982.4	99146.4	106567.2	105487.2	106156.8

Secondly, energy signature curve can be used as a function of t_{od} to describe and predict heating energy demand [8] [9]. Figure 7 and Figure 9 were made by average hourly energy demand of six years (105 168 hourly data). For buildings in Cohort 1, it is rather difficult to draw one interpolation curve to describe the relation between energy demand $P(t_{od})$ and (t_{od}) in the whole temperature range. There was a break around 5 °C, and energy demand turning back and forth with t_{od}. The appearance of break has been discussed before in caused by changing of heating equipment under different t_{od} [10]. In this article, it can be explained that some electric heating equipment may be shut down during off- work hours in Cohort 1. For example, electric resistant heater has little thermal inertia, which makes it unnecessary to keep on with non-appearance of occupants. Since electricity is used both for heating and other electric appliances, it is not easy to make accurate calculation of energy consumption share for heating and other electric uses. To know the daily operation routine of these buildings is needed. For buildings in Cohort 2 of hydronic DH system, SH and DHW are measured in one meter. The DHW use of one kindergarten was assumed as constant as its six-year average use, and its annual use followed the Norwegian statistic data [12], which is around 9 kWh/m^2 in most of Norwegian kindergarten. Figure 8 presents the distribution of the ratio between the annual hot water use and total heating needs within the six years. Clearly, DHW accounted for less than 9 % of total heating demand in most of the kindergartens and had a small influence in the whole picture. In this article, to describe the relation between SH and t_{od} more accurately, DHW use was deducted from the total DH needs. DHW use profile was roughly assumed as the DH use when t_{od} higher than 18 °C (the effective indoor temperature) in May, June, and August (kindergartens are mostly closed in July). For weekends, coefficient of 0.2 was considered. As shown in Figure 9, it is relatively easy to establish the energy demand function of t_{od} in polynomials through the entire outdoor temperature range. The function was written as:

$$P(t_{od}) = p_1 {t_{od}}^{i} + p_2 {t_{od}}^{i-1} + p_3 {t_{od}}^{i-2} + p_4 \quad (2)$$

$$(i = 1, 2, 3. If\ i - 2 < 0, p_{3,}\ p_4 = 0;\ if\ i - 2 = 0, p_4 = 0\ )$$

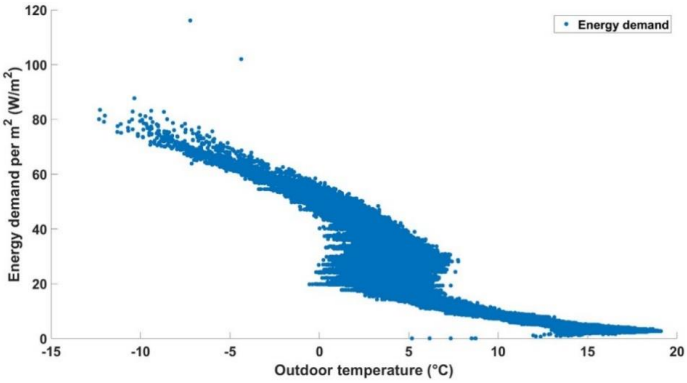

Figure 7. Energy demand vs Outdoor temperature of Cohort 1.

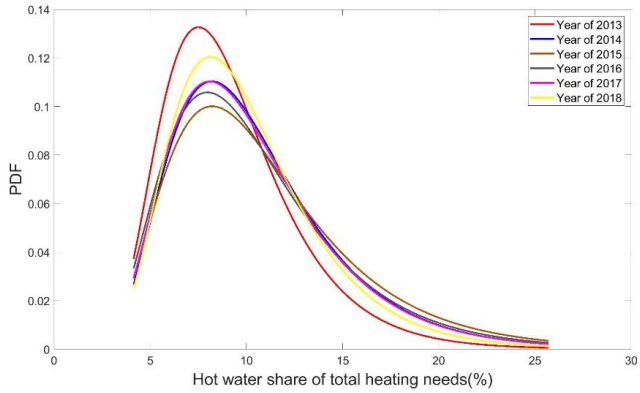

Figure 8. Distribution of hot water use in total DH needs of six years.

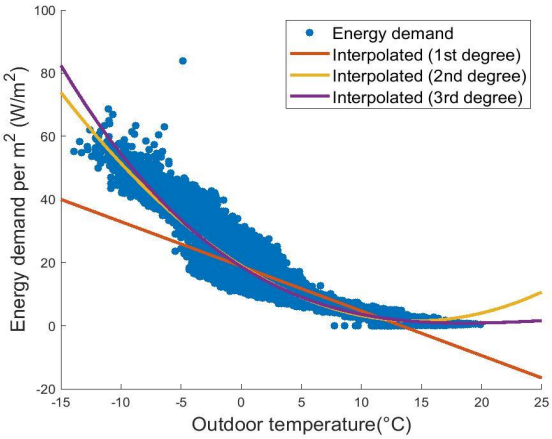

Figure 9. Energy signature curve of DH demand of Cohort 2 under 1st degree, 2nd degree, and 3rd polynomial.

To make sure of the goodness-of-fit of the model, the coefficients of determination R^2 was used. The value of R^2 should not be less than 0.75 as a rule of thumb in the analysis of building energy [12]. The coefficients of Function (2) and R^2 of each polynomial were shown in Table 6. It can be seen that even the simplest 1st degree polynomials satisfies the requirement of R^2 and fulfil the prediction of energy demand. This can be used to predict hourly heating load in the accordance with reference weather year, which is developed based on decades of weather data and can be found in database library [13]. The load profile can be used as input to energy system modelling, such as EnergyPLAN [14].

Table 6. Coefficients of Function (2) and R^2

	p_1	p_1	p_3	p_4	R^2
1st degree	-1.414	18.82	/	/	0.7927
2nd degree	0.08309	-2.412	19.02	/	0.8977
3rd degree	-0.001359	0.1027	-2.403	18.72	0.8995

3.2. Calculation of CO_2 emission of one typical kindergarten

In Figure 10, the stand-alone two bars at right side represent the building without DH. The annual CO_2 emission can be hugely increased from 1.2 tCO_2/yr to 13.6 tCO_2/yr when CO_2 factors of electricity changed from 10 to 110 gCO_2/kWh by making it the worst case. In the green square, three cases of different DH shares were compared, and their combinations regarding CO_2 factors were made as: blue bars of Norwegian electricity ($CO_{2\text{-EL1}}$) with average DH production ($CO_{2\text{-DH1}}$), orange bars of Nordic electricity ($CO_{2\text{-EL2}}$) with average DH production ($CO_{2\text{-DH1}}$), yellow bars of $CO_{2\text{-EL2}}$ with DH production of 2015 ($CO_{2\text{-DH2}}$), and purple bars of $CO_{2\text{-EL2}}$ with DH production of 2010 ($CO_{2\text{-DH3}}$). All the blue bars still gave the smallest values in each case since CO_2 factor electricity was 10 gCO_2/kWh. From the results, it can be seen that if electricity shoulders more energy supply, the total annual CO_2 emission can be varied a lot depending on the CO_2 factor of electricity. While in the case of DH high share, the variation of CO_2 emission under different background data was relatively small. Generally speaking, in the comparison of building with and without DH by using the same total energy demand, even in the case of DH low share under the highest DH production factor ($CO_{2\text{-DH3}}$), the total annual CO_2 emission (11.7 tCO_2/yr) can still be lower than the case without DH (13.6 tCO_2/yr) by 14 %.

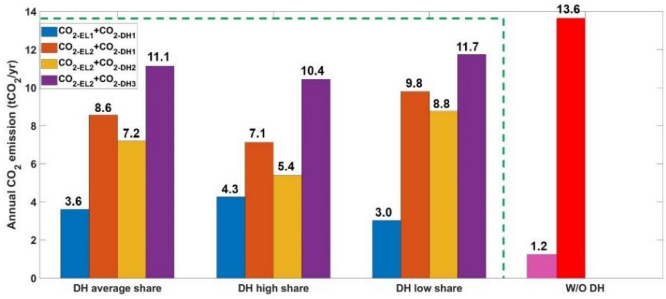

Figure 10. Annual CO_2 emission of one kindergarten of 700 m^2.

3.3. Assessment of CO_2 impact of new building area

After 10 000 m^2 of new building area of kindergartens was assumed to be built in Trondheim, the calculation of annual CO_2 emission regarding the new area was made. Through changing the penetration rates of new building area supplied by DH (x) between 0 % and 100 %, three kinds of growing trends of added annual CO_2 emission were calculated by following each DH production factor. As plotted in Figure 11, when all new buildings had only electricity, the added annual CO_2 emission would be 194.9

tCO_2/yr, and this is same for the three growing trends. When half of the new building area being connected to DH system, annual CO_2 reduction would be between 22.5 and 49.7 tCO_2/yr. Since it was predicted to follow linear CO_2 reduction with variation of DH penetration, the annual CO_2 emission would be double if all the new building area being connected to DH. The orange line represents the best case since DH production factor in 2015 was smallest, while the yellow line has mildest reduction slope due to the choice of highest DH production factor, and the blue line of the average DH production factor is in between.

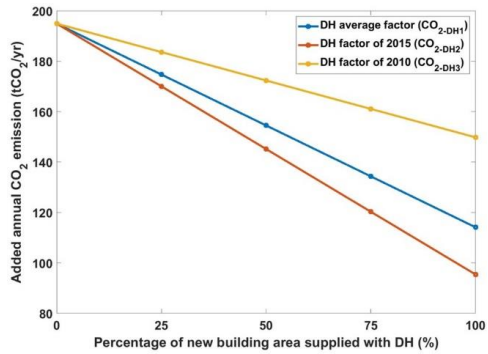

Figure 11. Annual CO_2 addition of 10 000m^2 new building area.

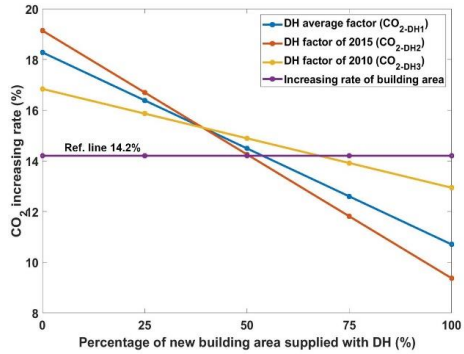

Figure 12. CO_2 increasing rate of 10 000m^2 new building area.

On the ground of the 6-year average annual area, the growth rate of building area, 14.2 %, was shown as the purple reference line in Figure 12. The region above the horizontal line had higher increasing rate of CO_2 than that of building area. It means if 14.2 % more building area being introduced, more than 14.2 % more CO_2 would be emitted; while the region below the line had smaller CO_2 increasing rate than the building area increasing rate, and this is what is expected to happen in the future to slower carbon footprint growth. The orange line representing the smallest DH production factor ($CO_{2\text{-}DH2}$) had the steepest slope. After more than half of new building area using DH, slower CO_2 increasing rate can be realized. When using the highest DH production factor ($CO_{2\text{-}DH3}$), the break-even point can reach at 67 % as shown in the yellow line of the mildest slope. Therefore, the breaking point located between 50 % and 67 % of new building area connected to DH under different CO_2 background data.

4. Summary and Future work

In this article, a typical energy profile of kindergarten in Trondheim was identified. The energy use data was retrieved from energy monitoring platform of Trondheim Municipality in total 559 hourly files. Two cohorts, namely Cohort 1 (not connected to DH) and Cohort 2 (connected to DH) were analyzed and compared. Under various building areas of the kindergartens, energy profile per m^2 of all kindergartens from 2013 to 2018 was defined and the average profile of each cohort was obtained. For Cohort 1, it is difficult to draw a robust energy signature regarding the energy demand and outdoor temperature, other issues and scheduling may be considered. While for Cohort 2, hot water use can be estimated as the only DH use in summer period and deducted from the total heating needs, in order to establish energy signature more accurately. Within the six- year duration curves, the annual average energy use of Cohort 1 was 177.2 kWh/(m^2.yr), and annual average electricity and heating of Cohort 2 was 64.7 kWh/(m^2.yr) and 103.0 kWh/(m^2.yr), respectively. Within Cohort 2, there were three cases depending on the energy contribution from DH and electricity, from DH high share, DH average to DH low share. 700m^2 was chosen as the representative building area of one kindergarten. Its annual CO_2 was compared between with and without DH based on the same total annual energy use. For the background data of electricity, two CO_2 emission were used. The one within Norwegian border gave the best results in all cases; when extended the border to the Nordic region, CO_2 emission jumped to higher level. For the CO_2 factors of DH production in Trondheim, the average factor from 2010 to 2018, the

factor in 2015 as lowest, and the factor in 2010 as highest, were used. The kindergarten with DH high share had lowest annual CO_2 emission and smaller CO_2 variation. By using the DH factor in 2015, it supported the lowest emission. For the kindergarten had low share of DH or even without DH, the CO_2 emission had a wider range. This is mainly caused by their higher dependence of the electricity production mix since electricity can be traded in the free market. Moreover, the building with only electricity is more likely to have unknown high peak load. As a mild prediction, 10 000 m^2 was assumed to be built in Trondheim. On the ground of average total kindergarten area within six- year, the growth rate of building area, 14.2 %, was used as the reference line. The growth rate of CO_2 emission could be slower than that of the building area, if more than 50 % and 67 % of new building area would be connected to DH. The break-point locates depending on the energy sources of local DH production, which determines the CO_2 factor.

The results of this article showed that building connected to DH system was more competent than the building of only- electricity concerning the CO_2 emission, and its energy demand easier to be predicted. In the future work, energy data and profiles of other building types and reference weather data in Trondheim shall be defined and analyzed. These profiles can be used to diversify and upgrade energy supply ways and improve urban energy planning.

Appendices

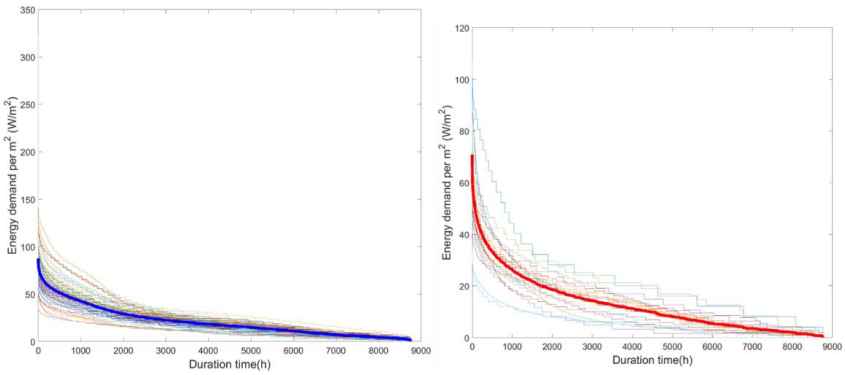

Figure A 1. Annual energy duration curves of Cohort 1 and Cohort 2 (only DH) in 2013.

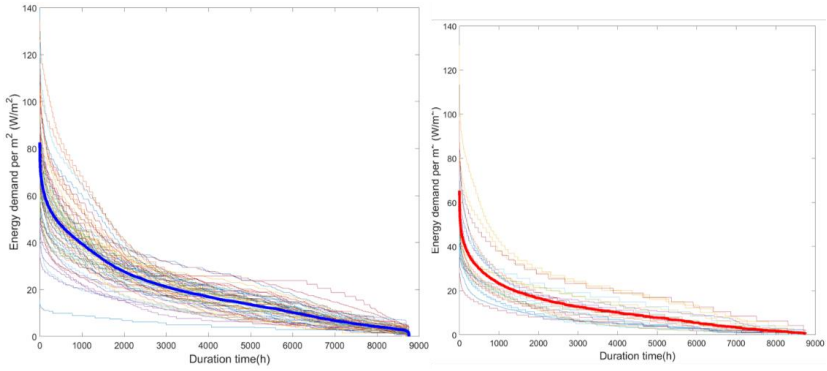

Figure A 2. Annual energy duration curves of Cohort 1 and Cohort 2 (only DH) in 2014.

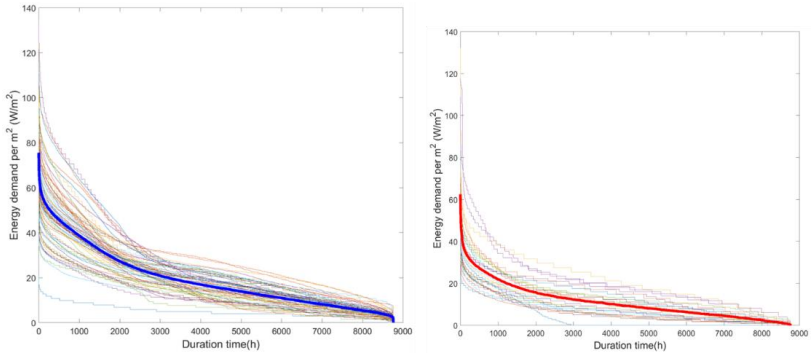

Figure A 3. Annual energy duration curves of Cohort 1 and Cohort 2 (only DH) in 2015.

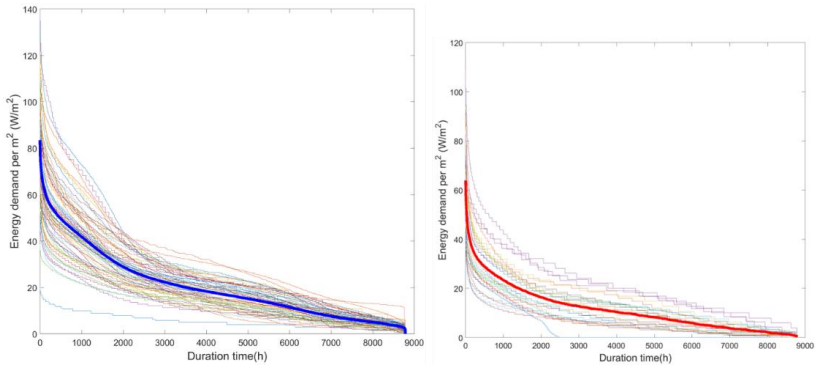

Figure A 4. Annual energy duration curves of Cohort 1 and Cohort 2 (only DH) in 2016.

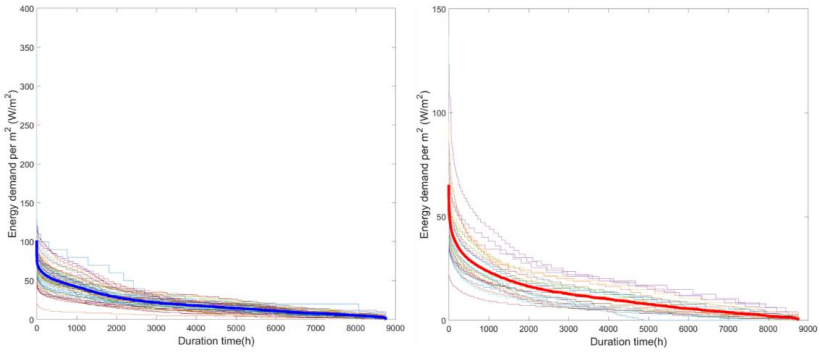

Figure A 5. Annual energy duration curves of Cohort 1 and Cohort 2 (only DH) in 2017.

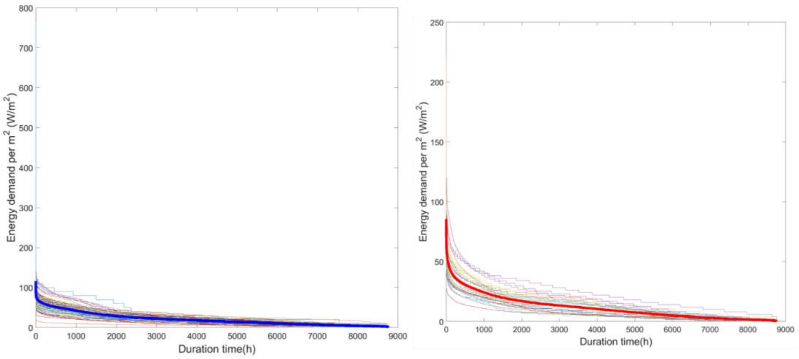

Figure A 6. Annual energy duration curves of Cohort 1 and Cohort 2 (only DH) in 2018.

References

[1] International Energy Agency. Energy Efficiency: Buildings.
[2] Patronen J, Kaura E and Torvestad C 2017 Nordic heating and cooling.
[3] SSB Statistics Norway 2018 Population projections.
[4] Energy monitoring platform of Trondheim Municipality. http://www2.esave.no.
[5] Norsk Fjernvarme. http://www.fjernkontrollen.no/.
[6] Climate Agency. NS 3720: 2018- Method for greenhouse gas calculations for buildings.
[7] Norsk Energi 2014 Klimaregnskap for Fjernvarme.
[8] Frederiksen S and Werner S 2014 *District heating and cooling* (Lund: Studentlitteratur) chapter 4.
[9] Hitchin R and Knight I 2016 Daily energy consumption signatures and control charts for air-conditioned buildings. *Energy and Buildings*, 112.
[10] Djuric N and Novakovic V 2010 Correlation between standards and the lifetime commissioning. *Energy and Buildings*, 42(4).
[11] Norwegian Water Resources and Energy Directorate (NVE) 2014 Analyse av energibruk i undervisningsbygg, RAPPORT.
[12] Menard S 2000. Coefficients of determination for multiple logistic regression analysis. *The American Statistician 54*: 17-24.
[13] Hensen J and Lamberts R 2011 *Building Performance Simulation for Design and Operation* (Spon Press) chapter 3.
[14] Sustainable Energy Planning Research Group. EnergyPLAN-Advanced Energy Systems Analysis Computer Model Documentation Version 14.

A.2 Paper II

A systematic approach for data analysis and prediction methods for annual energy profiles: An example for school buildings in Norway

Ding, Y., Brattebø, H. and Nord, N.

Energy and Buildings, 247, p.111160, 2021.

Energy & Buildings 247 (2021) 111160

Contents lists available at ScienceDirect

Energy & Buildings

journal homepage: www.elsevier.com/locate/enb

A systematic approach for data analysis and prediction methods for annual energy profiles: An example for school buildings in Norway

Yiyu Ding *, Helge Brattebø, Natasa Nord

Department of Energy and Process Engineering, Norwegian University of Science and Technology (NTNU), Kolbjørn Hejes vei 1 a, Trondheim 7491, Norway

ARTICLE INFO

Article history:
Received 20 March 2021
Revised 12 May 2021
Accepted 31 May 2021
Available online 4 June 2021

Keywords:
District heating
Electricity
modified Z-Score
Hourly profile
Regression analysis
Schools

ABSTRACT

Current research on energy supply systems and building energy demand presents positive impacts from the two sides, with potentials of combining top-down and bottom-up modelling. Mostly, the energy demand input has been employed directly from energy utility companies as a package of information, without considering energy use patterns regarding building type. There lacks a bridge between demand profiles on building stock functions and urban energy supply systems. Accordingly, this article proposes a framework that enables the prediction of annual energy profiles, applied to one educational building type on an hourly basis. The work consists of five steps: (1) getting energy information of 40 district heating (DH) supplied schools in Norway, (2, 3) processing data for getting the modified average hourly demand per m^2 and holiday breakpoints through a modified Z-Score, (4) energy forecast of DH and electricity load profiles through temperature moving average, correlation, and linear regression analysis, (5) validation of the predicted yearly profiles by three criteria, and further with the cluster methods for DH profiles. The results showed that the suggested methods for annual energy forecast were satisfying. The defined load profiles might represent the current energy demand of the Nordic school and the methods could be transferred to other building types. With energy analysis of typical building types, the proposed method enables the planners to better understand the energy needs for different building functions.

© 2021 The Author(s). Published by Elsevier B.V. This is an open access article under the CC BY license (http://creativecommons.org/licenses/by/4.0/).

1. Introduction

1.1. Background

Every year approximately 36–40% of the energy supply is used to serve buildings around the world, which is responsible for nearly one-third of global CO_2 emissions [1]. Energy efficiency strategies in urban building stocks are expected to make a high contribution to reductions in energy use and greenhouse gas emissions.

There is fruitful research suggesting how to make positive impacts from both energy system side and building side on the total building stock use. Several relevant publications are introduced below. Thellufsen et al. [2] investigated the possibilities of achieving a smart energy city within a 100% renewable energy context of Denmark and Europe. Averfalk et al. [3] found that lower distribution temperatures provide higher profitability and would facilitate transition to renewable and recycled heat supply in district heating (DH) systems. Lund et al. [4] gave perspectives on 5th generation DH that has a strong focus on combined heating and cooling as the main driver and may coexist with 4th generation technologies. From the view of enhancing building energy efficiency, Moschetti et al. [5] proposed a pathway for transiting building from zero energy to zero emission with a life cycle assessment on the most influential buildings' factors. When the techno-economic benefits analysis of building refurbishment is performed, Ascione et al. [6] emphasized the uncertainty in building occupant behavior shall not be neglected.

However, the energy demand input has usually been employed directly from utility companies as a package of information for energy system modelling. Without energy data mining or targeting energy use patterns on different building types, abnormal energy use could be misleadingly used as the input, which may deviate the anticipated benefits. According to the International Energy Agency Energy in Buildings and Communities Programme Annex 53, the offset issues from the designed demand to the real building energy were analyzed on different climates [7]. Meanwhile, Reynders et al. [8] explored the methodologies that enable residential buildings to offer flexibility to the energy system by utilizing building thermal storage. Therefore, a better understanding of energy usage and profiles in different building categories is needed and possible, with the aim to treat energy system and building in a holistic view.

* Corresponding author.
E-mail address: yiyu.ding@ntnu.no (Y. Ding).

https://doi.org/10.1016/j.enbuild.2021.111160
0378-7788/© 2021 The Author(s). Published by Elsevier B.V.
This is an open access article under the CC BY license (http://creativecommons.org/licenses/by/4.0/).

Nomenclature

CV(RMSE)	coefficient of variation of the root mean squared error
DH	district heating
DHW	domestic hot water
ES curve	energy signature curve
GESD	generalized extreme studentized deviate
MAD	median absolute deviation
MAPE	mean absolute percentage error
NMBE	normalized mean bias error
PAA	piecewise aggregate approximation
SAX	symbolic aggregate approximation
SH	space heating
TMA	temperature moving average
TMY	typical meteorological year

el	Electricity
no.	Number
t_{ot}	outdoor temperature
R^2	coefficient of determination
N	number of observations
W	number of data in the new series in PAA

Greek letters

σ	standard deviation
μ	average value

1.2. Previous studies

As an important subset of non-residential buildings, the educational building aims to educate students with knowledge and social mind, on the basis of laws on day-care seats and rights to education in Norway and many other countries. This building category contains kindergarten, school, and college/university. Meanwhile, the building operators are responsible to maintain the required indoor environment in energy-efficient ways [9]. It has been found that energy spending is the second biggest operating cost for schools in the U.S., only beneath the employees' salaries [10]. In Italy, 60% of the educational buildings were built before 1976, most of which fail to meet the current energy performance requirements despite of extraordinary retrofit [11].

According to the building conditions in Norwegian local governments [12], schools make up nearly 50% of the total local public building mass and constitute the most important building type. Population is one of the key drivers for developing educational buildings. Under the expectation of population increase and urbanization to come, there is a growing need for educational building expansion [13].

The aim of this study was to understand and identify load profiles of one typical Norwegian educational building type: the district heating supplied school buildings. Local municipalities are responsible to monitor and manage the operation of public buildings, hence energy data for such buildings are often available. Finding appropriate energy statistical methods and prediction methods are needed to achieve the study goal.

Sun et al. [14] developed a cooling load prediction strategy for a super high-rise building in Hong Kong, by combining selection of reference day, calibration with weather data, and model accuracy enhancement. This method requires low computation load and is feasible for online application of building load prediction in order to optimize equipment operation and guide load shifting [14].

Fan et al. [15] proposed a transfer learning-based methodology by utilizing the massive well-measured building operational data to predict other buildings. A quantitative assessment of this methodology for 24-hour ahead building energy demand was studied on building types of office, schools, and universities. Comparing with individual models, this methodology could reduce 15–78% of prediction errors and give insights to realize the value of existing data in building energy management [15].

Liu et al. [16] suggested a method with two-step clustering analysis to identify the typical electricity load patterns (TELPs) at individual building level. Density-based spatial clustering application with noise (DBSCAN) algorithm clustering technique is used in the first step to detect daily outliers. The second step uses the k-means algorithm to group similar TELPs. The effectiveness of this framework was confirmed with the time-series electricity data of office buildings in Chongqing [16]. Another k-means algorithm-based clustering analysis was made by Gianniou et al. [17] for studying residential district heating data. These single-family houses in Aarhus were segmented based on heat use intensity and representative patterns, by examining with the characteristics of buildings and occupants, load profiles of households, and use behavior changes.

Raza et al. [18] reviewed a number of artificial intelligence based short term load forecasting techniques, among which artificial neural network (ANN) was praised with great performance for complex problems. The findings show that improvement of training capability of neural network is needed to achieve promising forecasting results.

From the literature study, the main efforts regarding prediction have been put on short term energy load forecasting (time-series based techniques and artificial intelligence based techniques), with the contribution to optimal scheduling of energy equipment, spinning reserve, evaluation of economic dispatch, etc. Medium to long term load forecast for typical building types has not been stressed well. Medium to long term load forecast, especially for the public buildings, can be used for efficient operation/maintenance of the local energy system and building energy planning policies. However, there are few studies on annual load profiles for specific building types. Melillo et al. [19] suggested a method enabling to automatically generate and reproduce the annual heat demand for residential buildings. However, data from a reference building is required for achieving the recoverability of relevant building and system parameters, and scaling up the proposed method to a larger building set has not been validated yet. Bao et al. [20] proposed a probabilistic approach to formulate annual cooling load profile for office building, by involving tens of thousands of generation outputs from weather data files by Monte Carlo simulations. This prediction method can save much more overcooling hours, which was validated by measurements. Lundström et al. [21] proposed a heat load weather normalization, by segmenting the weather data and heat load with heating degree days and performing multivariable linear regression. The work was validated with two multi-family residential buildings.

The novel contributions of this work may be summarized as follows. The defined specific hourly-based load profiles were built on the analysis of a group of schools. These typical load profiles give an insight to the general energy situation of schools and they can be used for building simulations and model calibration. The proposed systematic approach is simple and robust, and it can be easily transferred to a large number of other public buildings in a fast way. The findings and method are thought to benefit public administrations and energy planners regarding local energy planning.

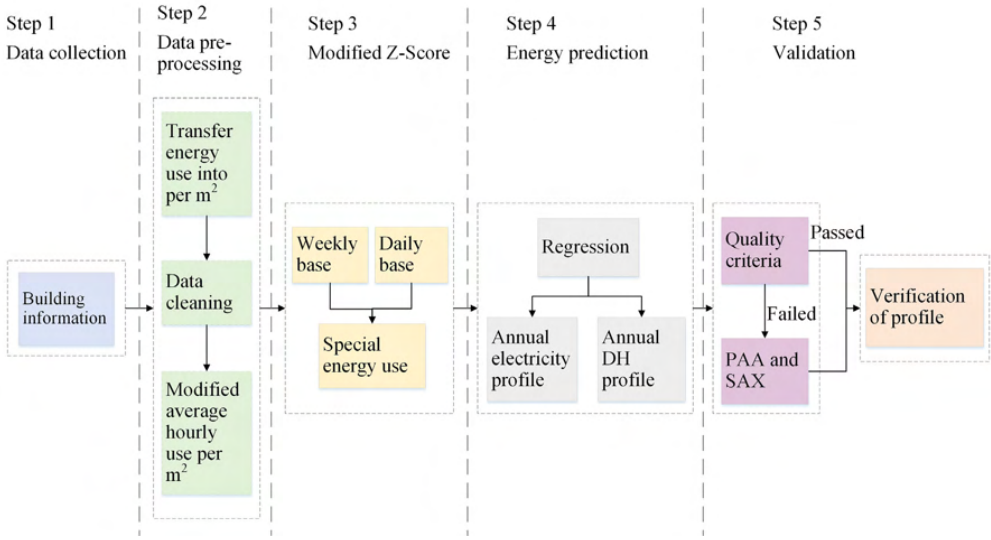

Fig. 1. The workflow of the data analysis of energy use profiles.

The rest of the article is organized as follows. Section 2 briefs the study methods about the data information of the observed buildings and the prediction process of energy profiles. Section 3 shows the periods of special energy use by adopting a modified Z-Score. Section 4 shows the prediction results of the typical annual DH profile and electricity profile. The accuracies of the predicted profiles were evaluated in Section 5. The application and limitations were discussed in Section 6. Finally, Section 7 concludes the main findings of this study.

2. Methodology

The outline of the five main steps of the energy analysis is illustrated in Fig. 1. Section 2.1 gives the building information. Section 2.2 explains how the energy data of the observed buildings were processed for getting the modified specific hourly demand for an average school building. Section 2.3 presents a modified Z-Score method to describe the energy use trend, which can identify the possible holiday breakpoints. Section 2.4, 2.5, and 2.6 describe the specific energy use forecast of DH and electricity that was proceeded through regression analysis, by using the modified specific hourly demand and considering the energy differences between normal days and holiday. Finally, Section 2.7 briefly introduces three quality criteria and cluster methods for validation. MATLAB was used for the energy data analysis.

2.1. Description of the observed buildings

The observed DH supplied schools are located in Trondheim, Norway. As the third largest city in Norway, Trondheim Municipality has been committed to improving strategies for a better living environment under the pressure of urbanization, population growth, and mitigation of anthropological carbon footprint.

The historical data of schools from 2015 to 2018 were retrieved from the energy monitoring platform of Trondheim Municipality [22]. Besides schools, other public buildings such as kindergartens, health/nursing centers, sports centers are also monitored in the platform. During the four years, the number of these schools registered in the monitoring platform increased from 36 to 40. The retrieved annual data file of each building included annual DH demand, electricity demand, and outdoor temperature in hourly resolution [22]. A total of 153 annual data files were used in the analysis. Table 1 summarizes the building information regarding average measured energy demand, energy labelling, building year, and building number in the data platform. The building year and energy labelling of the buildings were obtained from the Norwegian Energy Efficiency Agency (Enova) [23], which provides the information of the energy labelling scheme. Most of the buildings were built between 1980 and 2010 and labelled with C and D[1]. This building composition of school group can represent the current Norwegian situation that most of the schools have medium aged buildings and medium energy demand.

In the observed buildings, DH delivered the space heating (SH) and domestic hot water (DHW), while electricity was mainly used for ventilation, lighting, computers, and other electric appliances. The building area of each school varied from 1 822 m^2 to 8 996 m^2, and their average annual demand for DH and electricity of each building are shown in Fig. 2. The buildings regarding areas versus their annual demand were clustered with k-means.

It can be seen that a larger building floor area accounted for higher annual demand in general, but the relationship cannot be simply explained by linear regression models, due to a poor correlation. Hence, the energy analysis was performed on specific energy use (kWh per m^2) and the hourly resolution, in a search for representative energy use profiles for the school building in the Nordic climate.

2.2. Representative hourly energy demand

To find the representative hourly energy use, the simple way is to use the average hourly energy value of the n buildings as $\frac{\sum_{i=1}^{n} e_i}{n}$,

[1] The energy labelling was performed during 2011–2015, and possible update of equipment operation might happen afterwards, which may explain the building number difference when considering the measured annual energy demand in the platform and the labelling requirement. Contrarily, new buildings may have nevertheless higher energy use than stipulated by the building code [24]. Hereby the energy labelling result was used as reference.

Table 1
Information of the observed buildings.

Average measured annual energy demand (kWh/m²)	≤70	≤100	≤135	≤175	≤220	≤280	
Building number	/	5	17	14	4	/	
Energy labelling	A	B	C	D	E	F, G	No infor.
Building number	1	5	8	14	7	1	4
Building year	Before 1950	1950–1979	1980–2010	After 2010			No infor.
Building number	3	8	20	5			4
Monitored year in data platform	2015	2016	2017	2018			
Building number	36	38	39	40			

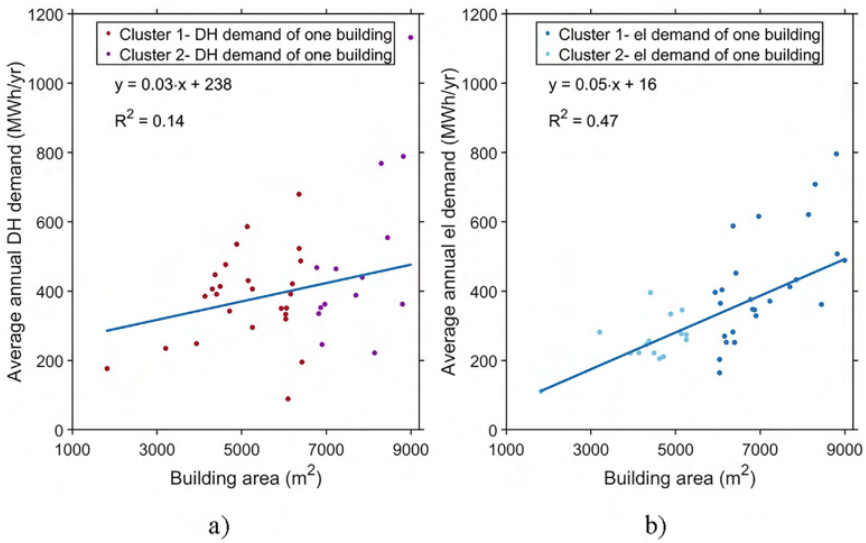

Fig. 2. a) Average annual DH demand vs building area, b) Average annual electricity demand vs building area.

where e_i is the hourly energy demand of building i, n is the total building numbers. However, this might mislead to high or low energy use. As stated in [15], the overall power use distribution of buildings (including schools and universities) is observed as right skewed, as few buildings have extremely high powers. The authors considered such rare measurements should be removed to avoid undesired model instability, with a threshold of maximum 10% extreme data of high powers being removed. In this study, there was one possible situation leading to atypical energy use. According to the report from Norwegian Water Resources and Energy Directorate (NVE) [13], student halls and canteens can be rented out for catering during evenings and weekends, which is meant to maximize the utilization of public resources. In other countries, such as the UK and the U.S., it is also seen opening part of schools to the public after normal school hours [25]. Educational buildings "can be used as communication means towards students and their families, and can thus reach many different society groups" [26]. Additionally, the working paper [12] addressed the importance of maintenance of public buildings. The annual report of Oslo [27], the Norwegian capital, specially emphasized the development and maintenance of schools must be planned and implemented with good functionality. Therefore, it was reasonably assumed some atypical energy might be caused by renting out and maintaining schools.

There is no widely accepted method to clear outliers automatically. Several methods of locating the outliers have been developed, such as the methods of median, mean, grubbs, generalized extreme studentized deviate (GESD), and observations beyond the range of quartiles, and each method has its own characteristics [28]. In this study, the method of "quartiles" was used. By following this method, data beyond 1.5 inter-quartile ranges of the upper (75 percentile) and lower quartiles (25 percentile) were detected as outliers. This method has proved useful when data is not normally distributed [29,30], which also fits the monitored dataset of the school group.

After clearing outliers of each hour, the average value of the remaining dataset was used. The typical energy demand for each hour was calculated as $\frac{\sum_{i=1}^{n'} e_i}{n'}$, where e_i is the hourly energy demand of building i among the remaining datasets, and n' is the total remaining building numbers. For simplicity, this modified, but still monitored average hourly energy demand was named as modified average energy demand in this study. This process was applied to both DH use and electricity use. By comparing the raw average hourly energy demand $\frac{\sum_{i=1}^{n} e_i}{n}$ in the original datasets with the modified average hourly energy demand $\frac{\sum_{i=1}^{n'} e_i}{n'}$ in the remaining datasets during the four years, only 9.5% of the differences ($|\frac{\sum_{i=1}^{n} e_i}{n} - \frac{\sum_{i=1}^{n'} e_i}{n'}| / \frac{\sum_{i=1}^{n} e_i}{n}$) were higher than 10% and most of the differences were minor. Hereby, it is appropriate to use the modified average hourly energy demand without a bias.

2.3. Modified Z-Score

The Z-Score is the number of standard deviations from the mean value, by subtracting the mean value from a raw data point and then dividing the difference by the standard deviation. If the absolute value of Z-Score is higher, it implies the raw data point is farther than the average. In this study, a modified Z-Score method defined by Iglewicz et al. was introduced.

As recommended by Iglewicz et al., this modified Z-Score is preferred to identify possible outliers over the common practice of Z-Score [31]. The modified Z-Score is defined as Eq. (1), x_i refers to the value of monitored sample, where $\tilde{x}$ refers to the median value of the samples, and MAD denotes the median absolute deviation in the dataset, see Eq. (2). The detailed information regarding this method can be found in [31].

$$M_i = \frac{0.6745 \cdot (x_i - \tilde{x})}{MAD} \tag{1}$$

$$MAD = median(|x_i - \tilde{x}|) \tag{2}$$

If the absolute value of the M_i to one data point is higher than 3.5, the point shall be marked as a potential outlier. This method is robust to detect outliers ranging from small to large sample size [31]. Accordingly, this method was used in this study to explore whether the building operation followed the schedule by considering the energy difference between the normal days and special periods, by showing the energy profile trend and observing "unusual" energy conditions during each year, such as school weeks, public holidays and so on. For instance, if there was an "unusually" low energy demand during school week noted with a negative M_i in a series, it might indicate the building operation followed the low attendance. Contrarily, if a high positive M_i in a series, a high energy use might be needed.

2.4. Temperature moving average and energy signature curve

Energy demand for DHW is much less sensitive to outdoor temperature than SH, and its use is relatively stable throughout a year. According to the report from NVE, the energy demand for the annual DHW in schools is less than 6% of their total heating needs (SH + DHW) [13]. The DH meter in the platform did not have submeters for monitoring DWH and SH, separately, thus energy for DHW was not excluded in the heating analysis. Unlike other building types such as nursing home, where DHW may account for over 20% of total heating needs and shall be exclusively studied, such as the work by Ivanko et al. [32].

Besides thermal inertia of the piping system, by considering the impact of building thermal inertia, the concept of a temperature moving average (TMA) was introduced to define a more accurate mathematical relation between outdoor temperature and DH demand. Depending on building physics, there is a big variety of capacity for temporary heat storage. It is simply saying that better insulation plus internal heat gains may yield longer time lag. The practices of considering TMA have been addressed in literature [33,34], and it is proven that the time lag hour shall be estimated as per the building physical characteristics [33]. The empirical time lag hour such as 24 or 48 h [33,34] was initially used as the reference range, and extended to 55 h. Within the range, the outdoor temperature was shifted backward by each hour to find the highest correlation between the outdoor temperature and the DH demand and to get accurate model. When the correlation has a higher absolute value, it implies a better fit between the moved outdoor temperature by TMA and the DH demand. Fig. 3a) compares the temperature lag with the highest correlation of each building. Fig. 3b) presents the effect of temperature lag on the DH based on the 4-year modified average hourly values. It can be found that the lag of five hours yielded the highest correlation for the building group in this study. Therefore, the outdoor temperature of five hours ago at each time clock was used to identify the relationship between outdoor temperature and DH demand. Meanwhile, there was a second peak noted at 29 h, implying the outdoor temperature of 29 h ago might also have a good correlation with DH demand. Similar finding was at 53 h. This may be explained that the outdoor temperature at the same time clock between neighboring days are usually similar. However, these correlations were not as high as at five hours. This differed from both the empirical number and the lag of 14 h found in [33], where a low-energy building of better building physics was analyzed.

Instead of constructing a physical model with the detailed building input data and parameters, data-driven approach defines building energy demand through statistical relationships. Among the data-driven approaches, there are regression analysis and advanced techniques such as artificial neural networks and decision trees by requiring long computation time and sophisticated knowledge. One of the important applications of linear regression is the energy signature curve (ES curve), which is a function of the outdoor temperature to predict heating energy demand [35–37]. It has been applied to fruitful research and is welcomed by utility companies. From the ES curve model, the DH use is usually described by the composition of two parts, temperature-dependent and temperature-independent. These two parts are divided by heating effective temperature or changing point temperature (CPT). The ES curve models may be expressed as:

$$\text{If } t_{ot} \le \text{CPT},\ P(t_{ot}) = p_1 \cdot t_{ot} + p_2 + \varepsilon \tag{3}$$

$$\text{If } t_{ot} > \text{CPT},\ P(t_{ot}) = p_1 \cdot t_{ot} + p_2 + \varepsilon; \approx p_2 \tag{4}$$

In Eqs. (3) and (4), p_1 and p_2 are the coeffiients of each ES curve model. p_1 denotes the slope, p_2 denotes the intercept, and ε is the residual error. The regression model of $P(t_{ot})$ as a function of t_{ot} may be used to estimate heat use. When the outdoor temperature is above the CPT, the heating demand is usually either at a small and constant volume or under a mild slope with the outdoor temperature. To solve the equations above, the ordinary least squares method is traditionally adopted. The coefficients are determined through the aim that the error between predicted and observed values is minimized. The higher the R^2, the better the model fits the data. Technically, R^2 shall not be less than 0.75 for a satisfying model in accordance with ASHRAE [38,39].

Boxplot method can reveal descriptive statistics about dispersion [30]. As illustrated in Fig. 4, these boxplots for the daily DH profiles were used to separate working and off-working hours, in order to segment ES curve models with each operational period. The observed DH data were assigned into four groups by considering seasonal and operational issues. Group I was for January, February, March, and December. Group II was for April, October, and November. Group III was for May, first-half June, second-half August, and September. Group IV was for the whole July. Fig. 4 shows the considerable heat variation between the working and off-working hours, the weekdays and weekends (without other short or long holidays). It also shows the heating loads during nights and weekends were close. From the boxplots, the DH system was generally under operation from 6 to 18 o'clock on weekdays. This is similar as depicted in [15], where the schools' daily power use typically rises at 6 and fall at 17 o'clock. It is a common practice that building operators start the system early before occupants arrive, and reduce the heat supply after they leave, to provide satisfying thermal comfort. Ma et. al mentioned the extended heating hours for coping with the complaints of freezing mornings [40].

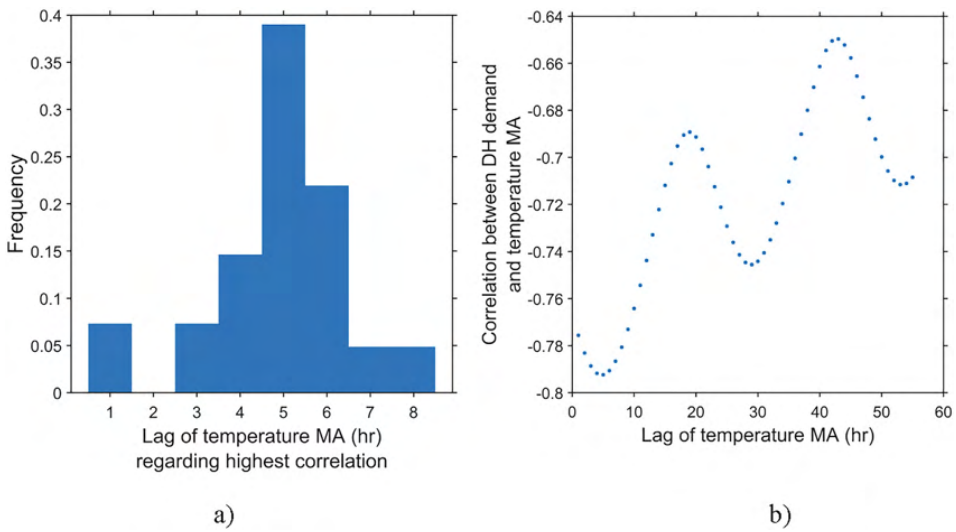

Fig. 3. a) Distribution of temperature lag regarding highest correlation of each building, where 5-hour lag had the highest frequency among the building group; b) Temperature lag moving average based on the modified average DH demand, where 5-hour lag yielded the highest correlation.

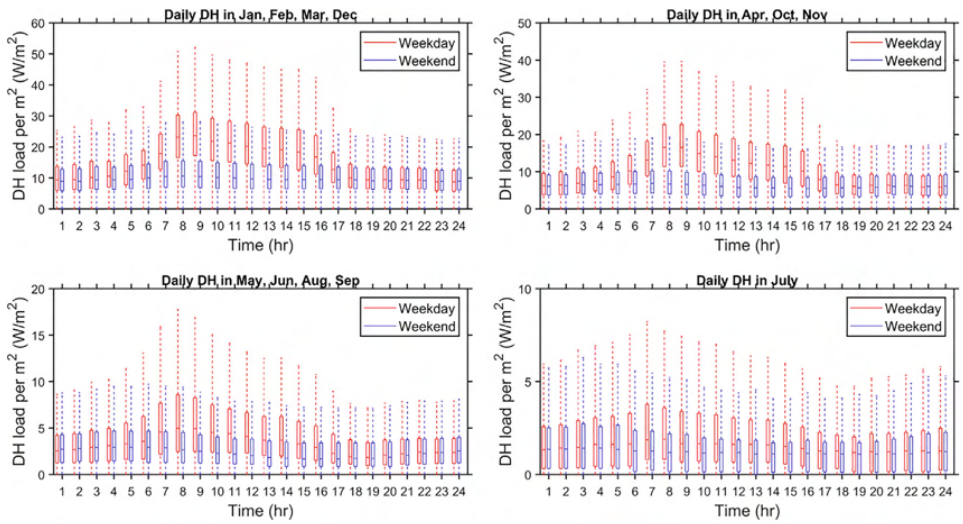

Fig. 4. Boxplots for the daily DH profiles on weekdays and weekends during four groups, from top left to bottom right, they are Group I, Group II, Group III, and Group IV.

The minor heat fluctuation of demand in July reflected the minimum water flow circulating in the piping system of the DHW system when the school was normally closed for the summer holiday.

2.5. Typical meteorological year and prediction of DH profile

The importance of typical meteorological year (TMY) that allows estimation of long term performance from a single year analysis is elaborated in literature [41]. From the European Union website, TMY 2007–2016 for Trondheim was retrieved and used for heating prediction in this study [42]. The calendar of 2025 in Norway was used as a reference year for acquiring information on public holidays, and the methods can be adopted to calendars of other years.

2.6. Electricity profile

It is acknowledged that each year starts and ends with different day numbers. For example, it started with Friday in 2016 and with Monday in 2018. Therefore, the 4-year similarity regarding the electricity use was examined with the correlation for every two years' electricity profile between the week 1 and the week 52 (only week 2 to week 53 for 2015). The remaining 1 or 2 days were discarded, the correlation plot is shown in Fig. 5. The high correlation numbers within every two years imply the similar electricity use

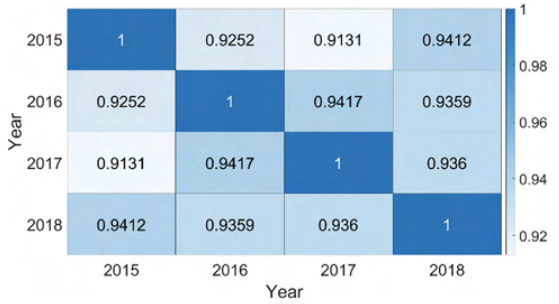

Fig. 5. Correlation of electricity profile during 2015–2018 (52 weeks).

during the four years. The small deviations can be explained by the situation that study trips, activities, and public holidays were arranged on different dates and weeks in each year. After the modified Z-Score mentioned in Section 2.3, typical profiles for normal days and special days can be separately identified. The 4-year value was treated as the predictor and their average value was treated as the response, and they were together trained in the linear regression learner. Additionally, cross-validation was selected for increasing the accuracy of the final model by using the full data. Then these typical profiles can be combined to extrapolate and estimate the demand for future years.

2.7. Validation procedures

To prove that the predicted energy profiles are convincing, an evaluation process is needed for measure and verification. In this study, all the profile models were verified through three mostly-used quality criteria as the following: mean absolute percentage error (MAPE), normalized mean bias error (NMBE), and coefficient of variation of the root mean squared error (CV(RMSE)). If the model meets the requirements of all the three criteria, it may be regarded as a satisfying model. If the model fails to one of the criteria, it is further checked with the cluster methods of piecewise aggregate approximation (PAA) and symbolic aggregate approximation (SAX). The explanation and validation results of these indices are presented in Section 5.1 and 5.2.

3. Results of modified Z-Score

The daily DH and electricity demand on weekdays are shown in Fig. 6a) and Fig. 6b), separately, which was made based on the equal division of every year's 52 weeks into four seasons. It can be seen that there were considerable seasonal energy demand variations and different requirements for DH and electricity. The red and pink boxes for the winter and early spring required very high energy demand, while the demand in the green boxes was lowest and the blue boxes in between. The DH and electricity use was then analyzed on seasonal and weekly base, separately, see Section 3.1 and 3.2.

3.1. Analysis of DH use

The weekly DH demand based on the modified average DH demand from 2015 to 2018 is shown in Fig. 7a), and the modified Z-Scores within each season are given in Fig. 7b). A summary of the seasonal Z-Scores is given in Appendix Table A1, and the abnormal DH use with $|Z| \geq 3.5$ are highlighted with numbers.

From the weekly DH aspect, most of the data were within the threshold of ± 3.5. The high DH demand marked with No. 1, 2, 3 and 4 was mainly due to the extremely cold condition. From Fig. 7a) and b), it was obvious to identify seasonality, but it was not clear to detect the breaking points of weekly breaks such as the school week, Easter week, when the DH demand was expected to be low during the temporary low attendance. There was only No. 6 of 2018 found with very low DH demand even though the weekly coldest temperature was −11.1 °C.[2]

As for the heating operation of short and one-day holiday, the analysis was performed within the week by comparing with the adjacent days. This concerned that heat demand was dependent on the outdoor temperature, while the outdoor temperature difference between neighboring days were not big. Thus, in Fig. 8 there were five days in each line, and their modified Z-Scores are given in Appendix Table A2, where the holidays were marked with numbers. Most of the DH demand was under the upper threshold, only No.6 in 2017 had an abnormally high demand when it was supposed to be closed for Whit Monday. There were only No. 1 and 3 in 2015, No. 1 in 2016, No. 1, 4 and 5 in 2017, and No. 1 and 6 in 2018 followed the expectation of the low DH demand on public holidays, although some of them were not as low as to achieve the lower threshold by comparing with neighboring days.

3.2. Analysis of electricity use

The 4-year weekly electricity is given in Fig. 9a). The corresponding modified Z-Scores during each season are given in Fig. 9b), and the breaking points are listed in Appendix Table A3. Although the electricity demand also had seasonal variation, the demand was much lower than DH, especially in early spring and winter.

By comparing with the DH use, there was no weekly electricity demand beyond the upper threshold, moreover, it was straightforward to distinguish the breaking points where weekly low demand occurred on holidays.

As suggested in [14], for the days having similar occupancies as their previous days, the previous days can be selected as their reference days. For example, the previous Tuesday is selected as the reference day of this Tuesday due to their similar occupancy periods for electric chiller operation management [14]. Hence, regarding the electricity demand during a short and one-day holiday, the analysis was made by comparing the same weekday number within each season. Since the electricity use was less sensitive to the outdoor temperature, it was assumed that the electricity use followed weekday schedule in each season. For example, all the Mondays in season 1 were assumed having similar electricity use if there were no holidays. Accordingly, in Fig. 10 each line presents 13 points of the same weekday. Except for the abnormally high use of No. 4 in 2015, the other electricity demand was under the upper threshold line. In contrast to the DH use, all the public holidays were detected with the low electricity demand as the "outliers" or the local minimum. Besides that, when the one-day holiday was on Thursday, it would be probably that the following Friday was also on holiday or had reduced school hours. For example, No. 7 in 2015, No. 5 in 2016, and No. 6 in 2017 were found with a local minimum, see Fig. 10. The corresponding modified Z-Scores are given in Appendix Table A4.

3.3. Similarities and dissimilarities from the modified Z-Scores on DH and electricity

Based on the weekly energy use diagrams of the DH and the electricity use above, it was found that both Spring and Autumn

[2] Week 2 to week 53 of 2015 was in the analysis, the week number of 2015 in Fig. 7a) and b) shall be plus 1 accordingly.

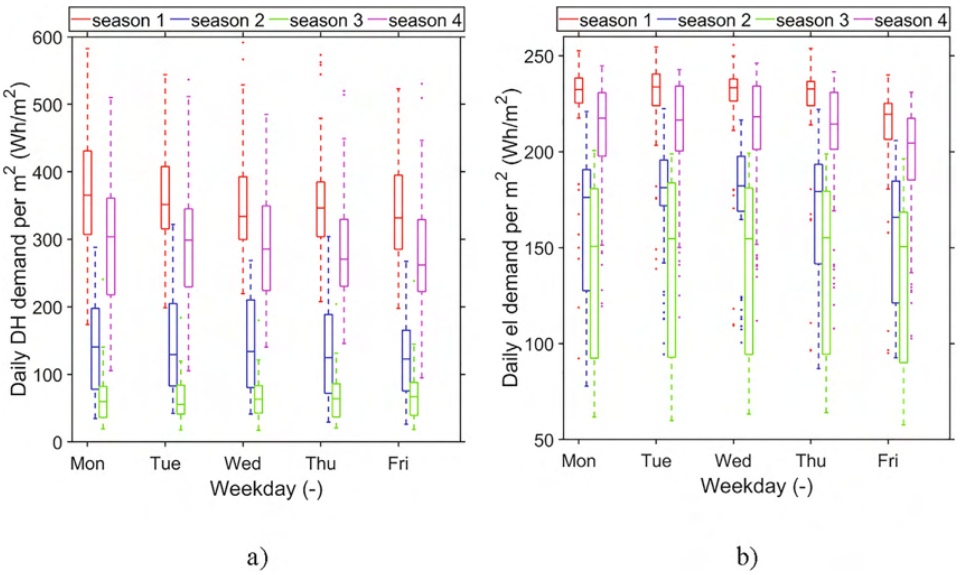

Fig. 6. Boxplots of energy use on weekdays, where a) DH use, b) electricity use. The red box refers to season 1 (week 1–13), the blue box refers to season 2 (week 14–26), the green box refers to season 3 (week 27–39), and the pink box refers to season 4 (week 40–52). (For interpretation of the references to color in this figure legend, the reader is referred to the web version of this article.)

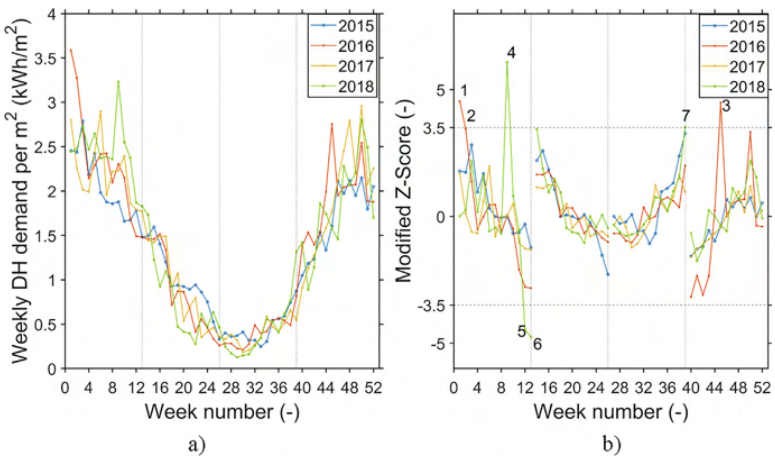

Fig. 7. a) Weekly DH use 2015–2018, b) Modified Z-Score I of weekly DH use during 2015–2018.

school week were arranged in the same week number during the four years, week 8 and week 41, respectively, while the Easter weeks and other public holidays were of different week numbers, causing various energy impacts on the neighboring weeks. The school closure for summer vacation was approximately arranged from week 26 to week 32, and the Christmas holiday during week 51 and week 52.

There was no extremely high electricity use generally, but pit low use during the breaks. Season 1 and Season 2 had more "outliers" since most of the holidays were in the first half of the year, see Fig. 9a) where there were considerable variations of weekly electricity use, and Fig. 9b) where there were six out of eight "unusually" low demand. However, the modified Z-Scores for the DH demand could not disclose the holiday breaks as in the case of the electricity use, as shown in Fig. 7a) and b) where most of the points were not below −3.5.

Based on the above introductory analyses, it can be concluded that the control of electrical appliances in the school made reasonably fast responses by closely following the attendance and schedule. Nevertheless, the response of hydronic DH systems was a relatively slow process mainly due to the long transport of heating fluid and complex control of the DH sub-stations, as mentioned by others [36,43]. From the modified Z-Scores, it was most likely that the heating operators in the school set mode between weekdays and weekends, and long holiday mode for Summer vacation and Christmas week, without disturbing for

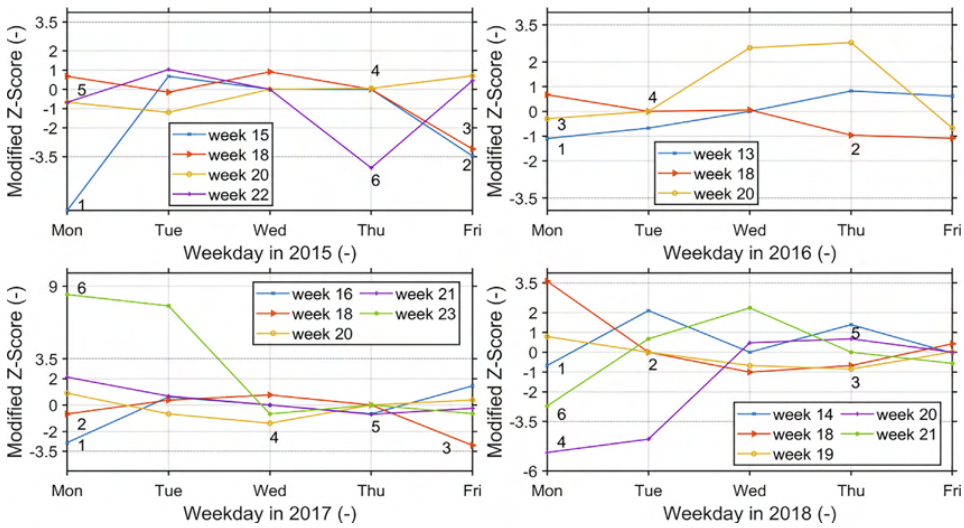

Fig. 8. Modified Z-Score I of DH use regarding short holidays during 2015–2018.

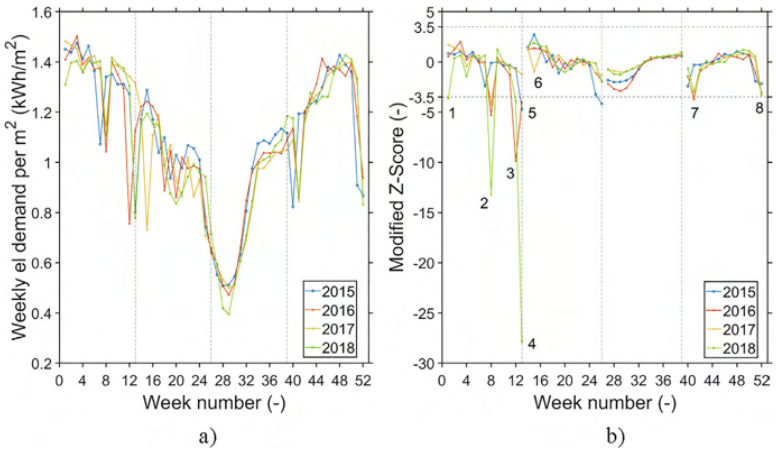

Fig. 9. a) Weekly electricity use during 2015–2018, b) Modified Z-Score I of weekly electricity use during 2015–2018.

the short public holidays. This implied that the DH demand was more likely prone to the outdoor temperature over the schedule on short breaks.

4. Results on energy prediction

4.1. Results on ES curve models and prediction of DH profiles

The ES curve for DH demand is illustrated in Fig. 11, where the CPT was found at 13 °C by giving the adequate piece-wise approximation for an average school building. This CPT is in the range of typical average national threshold temperatures for the current European building stock, which vary between 10 and 15 °C [36]. In the area below 13 °C, it was the temperature-dependent DH part. In Fig. 11, the red dots represent the stable working hour from 8 to 16 o'clock, the green dots represent the ramping hour at 6, 7 17, and 18 o'clock, and the blue dots represent the non-working hour. The non-working hours included weekends and nights on weekdays, since these two parts had close demand as mentioned in Section 2.4. In the area above the CPT, the light blue dots only covered a small share of the DH demand.

Fig. 11 shows the strong differences in energy demand among the four parts, from dominating high to nearly negligible heating use. The coefficients of Eqs. (3) and (4), and R^2 of each part are given in Table 2. In the outdoor temperature dependent area, only the model of ramp period showed a bit weaker fitting and the other two models were capable to predict the DH demand well. In the area above CPT, the heating needs were trivial and had minor impact on energy supply system. Fig. 12 is the logistic diagram by giving the relevant coefficients under different conditions. Then by inserting the weather data of TMY (see Section 2.5) and the coeffects into Eqs. (3) and (4), the typical annual hourly DH load can be predicted. The outdoor temperatures in the analysis were

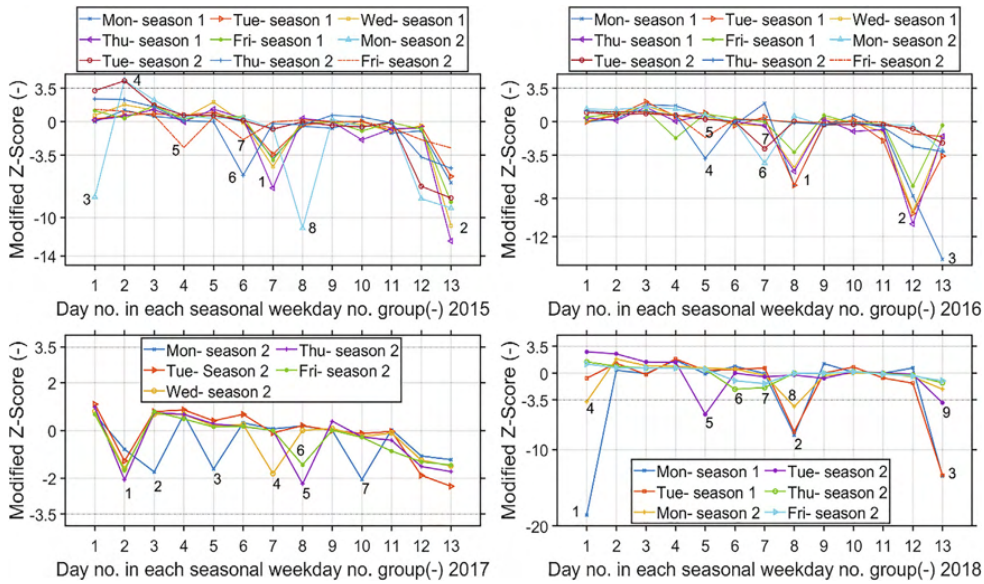

Fig. 10. Modified Z-Score I of electricity use regarding short holidays during 2015–2018.

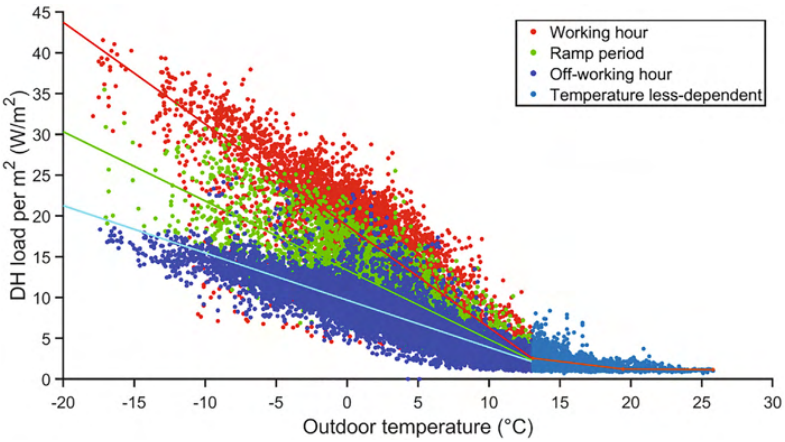

Fig. 11. Energy signature curve models of DH demand.

Table 2
Coefficients of Eq.(3) and Eq.(4), and the corresponding R^2.

	Outdoor temperature dependent ≤ 13 °C			Outdoor temperature less dependent	
	Working hour	Ramp period	Off-working hour	(13, 20 °C]	>20 °C
p_1	−1.2	−0.85	−0.58	−0.23	/
p_2	18.3	13.4	9.5	5.6	1.2
R^2	0.76	0.73 (↓)	0.78	0.35 (↓)	

between −18 and 26 °C, covering the cold design temperature of several major Nordic cities, such as Stockholm (−18 °C), Copenhagen (−11 °C), Gothenburg (−17 °C), etc. [36].

Finally, the monitored and the predicted annual profiles for the DH demand from 2015 to 2018 are compared in Fig. 13, where the purple lines present for the monitored profiles and the green lines present the predicted profiles. Meanwhile, the predicted typical annual DH load profile in TMY is presented in Fig. 14. Owing to the large dependence on the outdoor temperature, the heat load fluctuated throughout the year with oscillation of peaks. The peak load was around 48 W/m^2 and the minimum load was close to 1 W/m^2, and the total annual heat demand was 72 kW h/m^2.

4.2. Prediction of electricity profiles

Fig. 15 shows the 4-year monitored and predicted annual profiles of electricity. The comparison plots were of the same color pattern as in Fig. 13. There was one hour at around 2000-hour with

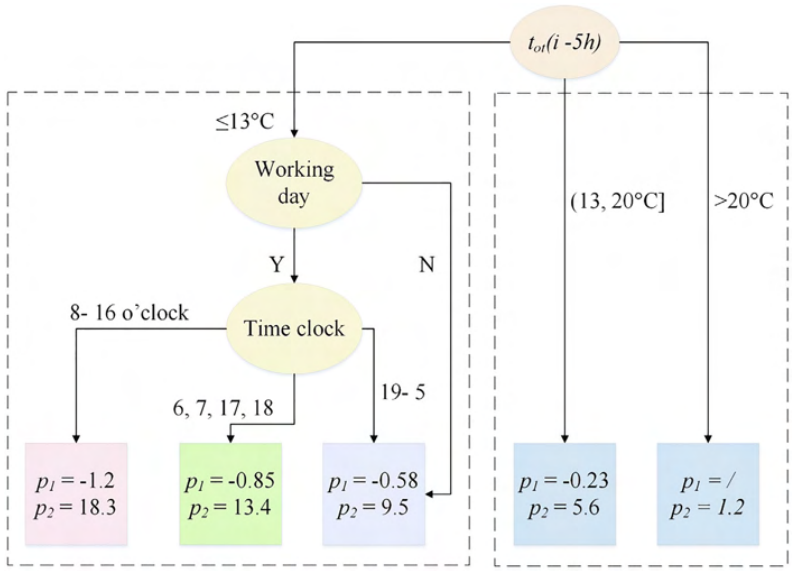

Fig. 12. Logistic diagram of predicting DH demand under different conditions.

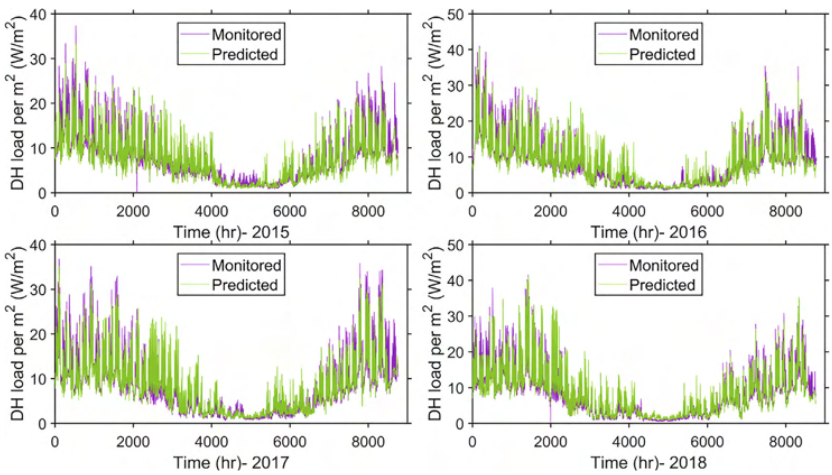

Fig. 13. Monitored vs. predicted DH profile during 2015–2018.

a monitoring failure, and this was fixed in the prediction model. There were 3.2–8.6% of predicted load differed from the monitored load by 30–40% in the four years, and most of the predicted load were close to the monitored load. The defined typical hourly profiles for school week, Easter week, short holiday, and the remaining normal days (without the above special days) are shown in Fig. 16.

The predicted typical annual electricity load profile is presented in Fig. 17, which showed the relatively stable pattern of electricity. The peak load was around 18 W/m^2 and the minimum load was 2 W/m^2, and the total annual demand was 57 kWh/m^2. The minimum 2 or 3 W/m^2 electricity load was mostly used for some plug-in equipment and low ventilation in meeting the air quality requirement during the unoccupied period. Additionally, it is seen as a conventional custom in the Nordic region that a few lights in the main entrance or hallways are kept on after a school is closed. The peak load for electricity was only one-third of the peak DH load (48 W/m^2), and the total demand was 79% of the DH demand (72 kWh/(m^2·yr)). Hence, it remarkably reduced the strains of the power grid for the buildings with DH comparing with the buildings those were solely supplied with electricity. It was of significance especially in the winter season when both heating and electricity called for high energy supply. Moreover, by analyzing heat and electricity profile separately, it presents the different requirements for thermal and power grid in relation to sizing and production.

The total specific energy demand for the observed average school was 129 kW h/(m^2·yr), with nearly 56% for heating needs. The energy share for heating purpose was almost the same as the average situation [13]. The total energy demand was slightly

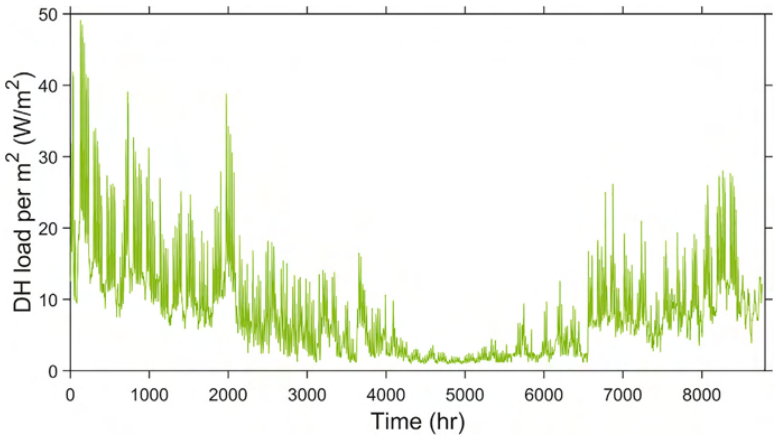

Fig. 14. Predicted typical annual DH load profile.

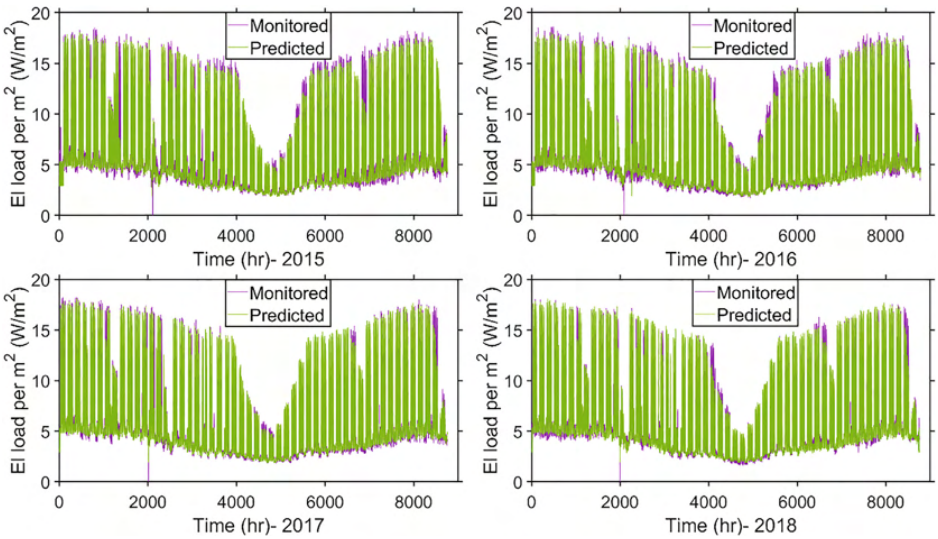

Fig. 15. Monitored vs. predicted electricity profile during 2015–2018.

lower than the annual average energy use in Norwegian schools [13,44], but same as the mean value of Swedish schools according to the Energy Statistics [24]. This predicted demand was also approaching to the proposed nZEB energy performance target level for Finnish educational buildings in FInZEB project, 104 kW h/(m^2·yr) [45].

5. Validation results

5.1. Criteria results of MAPE, NMBE, and CV(RMSE)

After the regression analysis, the deviations between the predicted and observed profiles were examined through the verification process with MAPE, NMBE, and CV(RMSE). If the verification results are within the recommended range, it means the prediction methods are reliable to be used for future modelling.

MAPE means the average error between the actual and predicted data to the actual data, and it is usually expressed in relative numbers. The expression of MAPE is given as:

$$MAPE = \frac{1}{n}\sum_{i=1}^{n}\left|\frac{A_i - F_i}{A_i}\right| \cdot 100\% \quad (5)$$

where A_i is the actual and monitored value, F_i is the predicted value, and n is the number of the observations. The absolute value of MAPE avoids the possible offset among positive and negative errors. MAPE is used as a common measure in the forecast of wide areas such as finance, business, energy sectors and so on [18,46,47]. Table 3 lists the prediction quality when using MAPE criterion, where the MAPE result is recommended less than 20% to verify an accurate model [47].

NMBE calculates the total percentage of the error during the evaluation period and this criterion is given as:

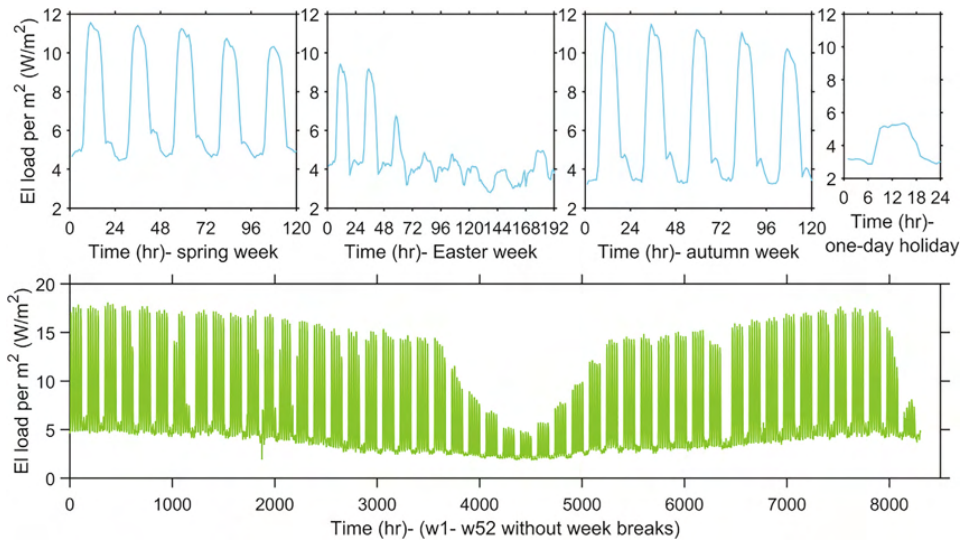

Fig. 16. Typical hourly profiles for school week, Easter week, short holiday, and the normal days without these special days; for easy reading, the profiles for Easter, autumn week, and one-day holiday have the same Y-axis title of spring week.

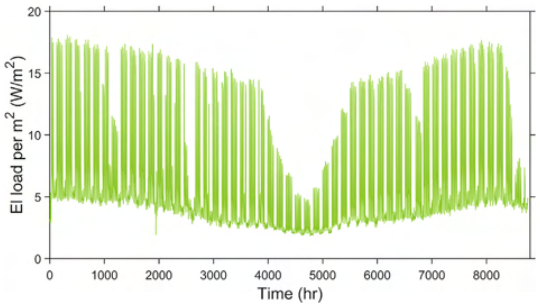

Fig. 17. Predicted typical annual electricity load profile.

$$NMBE = \frac{1}{n}\frac{\sum_{i=1}^{n}(A_i - F_i)}{\bar{A}} \cdot 100\% \quad (6)$$

where $\bar{A}$ refers to the average value of the monitored data, the other denotations are the same as for the MAPE. If a negative result is obtained for the NMBE, it implies that the energy demand is over-predicted, on the contrary, an under-prediction is made. The directionality of the NMBE shows the difference between the actual and predicted use [46,48].

The Root Mean Squared Error (RMSE) assesses the mean squared error, and CV(RMSE) normalizes the RMSE with the average energy demand during the evaluation time [46,48]. CV(RMSE) is given as:

Table 3
MAPE criterion of evaluating forecast quality.

MAPE (%)	Forecast quality
<10	Highly accurate forecasting
10–20	Good forecasting
20–50	Reasonable forecasting
>50	Inaccurate forecasting

$$CV(RMSE) = \frac{\sqrt{\frac{1}{n}\sum_{i=1}^{n}(A_i - F_i)^2}}{\bar{A}} \cdot 100\% \quad (7)$$

CV(RMSE) indicates whether the forecast model can reflect the real load shape. The two metrics, NMBE and CV are commonly used together to find out prediction performance. Under ASHRAE Guideline 14, the hourly criteria of NMBE and CV are limited within ± 10% and 30% respectively for verifying a satisfying model [38,39].

As listed in Table 4, all the MAPE results regarding the electricity demand were less than 10%, NMBE were with ±1%, and CV were less than 20%, which meant the forecast of the electricity profile was of high accuracy. Accordingly, it was reliable to estimate the future profile for electricity by extrapolating the regression results with adjustment of the calendar considering such as school weeks, public holidays, etc., as mentioned in Section 3.2. However, from the validation results on the DH profile that MAPEs were higher than 20% and CV in 2018 was slightly beyond the ASHRAE criterion, it can be said that the ES curve model was to some extent convincing but not very accurate. Further validation was thus needed for the DH profile.

5.2. Discretization results for PAA and SAX

Since the prediction of the electricity profile passed via all the three quality criteria, only the predicted DH profile was further checked with piecewise aggregate approximation (PAA) and symbolic aggregate approximation (SAX). In this study, weekdays from the predicted typical annual DH profile were extracted to compare with the 4-year monitored weekdays on Winter, Spring and Autumn, and Summer, respectively. Each weekday (24-h) was treated as a time-series.

First, Fig. 18 illustrates the comparison of the daily DH profiles during weekdays between the predicted profile (shown in Fig. 14) and the 4-year monitored profiles. In Fig. 18, the red lines show the Winter season, the greens line show the Spring and Autumn season, and the blue lines show the Summer season. In addition, the thick lines depict the predicted profiles, while the thin dashed lines describe the monitored profiles. It was noted that there was a peak

Table 4
Evaluation results of the energy forecast by three criteria.

Year	prediction of DH load profile			prediction of electricity load profile		
	MAPE (%)	NMBE (%)	CV(RMSE) (%)	MAPE (%)	NMBE (%)	CV(RMSE) (%)
2015	20.2	2.9	25.7	8.8	0.9	16.0
2016	23.2	−1.4	26.7	6.8	0.2	10.6
2017	24.0	−2.4	26.9	6.6	−0.3	11.7
2018	29.6	−4.9	30.2 (↑)	7.5	−0.4	10.1

load arising at 9 o'clock. After manually adding 2 W/m^2 at 9 o'clock during the heating season (thick dotted line), the predicted profile was seen closer to the observed one for the Winter season. The peak heat load at 9 o'clock was also seen in the average weekly heat load patterns of public administration buildings in [49]. However, since the outdoor temperature in the measured years and TMY were not same, the predicted profile was not anticipated to be the same as the measured ones.

Second, during the approximation process of PAA, the predicted data in the time-series were initially Z-normalized with $\frac{C_i-\mu}{\sigma}$, where μ and σ referred to the mean value and the standard deviation of the time-series, respectively. More specifically, in this study the μ and σ were the daily average DH load and daily standard deviation, respectively; and the daily DH load were normalized to [−2, 2]. It is an essential step allowing the mining algorithm to focus on the patterns' similarities/dissimilarities instead of on the data amplitudes in the time-series. This normalization step is different from the modified Z-score in Section 2.3. Next, the Z normalized time-series $C = C_1, C_2, \cdots, C_n$, proceeded through the PAA. PAA is one of the algorithms that is designed to reduce the dimensionality of the raw time-series, and the basic idea is to split them into equally sized intervals [50,51]. Each interval is computed by averaging the values within the interval. The time-series C is represented by a dimensionally reduced new series as $\overline{C} = \overline{C_1}, \overline{C_2}, \cdots, \overline{C_w} (w \leq n)$, w is the number of data in the new series. Theoretically, if w is close to n, it has a high accuracy of data representation, however, it would lose the meaning of dimensionality reduction from the PAA. On the contrary, if w is very small with for example only one or two intervals, it would hardly make a sounding representation of the original dataset. Typically, it has $w \ll n$. The ith element of new time-series $\overline{C}$, or say the mean value of the data falling within the ith interval, is calculated as Eq.(8) [51]:

$$\overline{C_i} = \frac{w}{n} \sum_{j=\frac{n}{w}(i-1)+1}^{\frac{ni}{w}} C_j \tag{8}$$

Accordingly, in this study the 24-hour data (n) of each weekday was split into 8 (w) equally sized segments in the new time-series. The representation was aimed at approximating the raw 24-hour time-series by a linear combination of 8 box functions.

Finally, after deciding the value of w that suits the dataset, the PAA coefficients are assigned with a string representation graph through symbolization process of SAX. As recommended in literature [51], three breakpoints (−0.67, 0, 0.67) were chosen here. The PAA coefficients for those below the −0.67 were symbolized with the string "a", the coefficients between −0.67 and 0 were with "b", the coefficients between 0 and 0.67 were with "c", and those higher than 0.67 were with "d". In each interval, if the compared data from different datasets have the same SAX strings, they may be clustered as the same group and the PAA coefficients do not have to be exactly same.

The comparison of the PAA coefficients between the predicted and the monitored DH daily profiles is shown in Fig. 19, and the corresponding SAX symbols are listed in Table 5. The PAA coefficients and the SAX symbols of the predicted profile were calculated based on the thick dotted line in Fig. 18. In the SAX Table, those had different SAX strings within the same PAA interval were marked with the italic font, implying they cannot be clustered as the same group. It can be concluded that the predicted and monitored load profile for the whole Winter had very high similarity, since all the eight intervals between predicted and monitored load profile on each weekday had same clustering strings. And Winter also consumed most of the heating energy. However, the similarities for the other seasons were not as strong as Winter, but there were still more than half belonged to the same group within the same

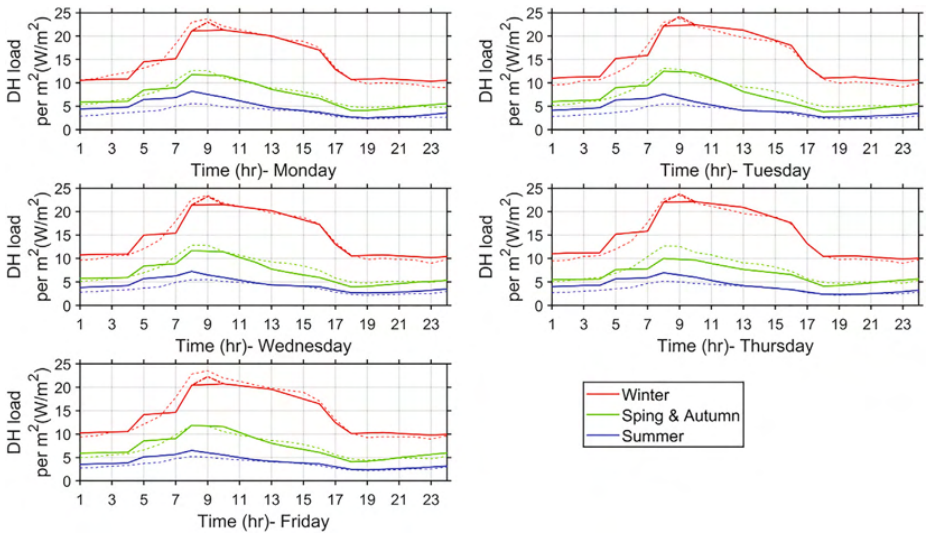

Fig. 18. Comparison between the predicted and monitored DH profiles.

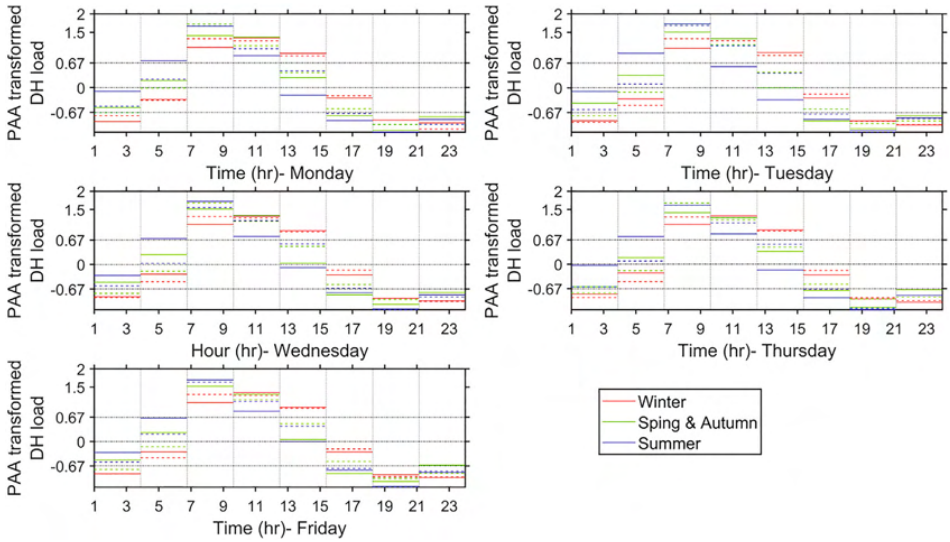

Fig. 19. PAA coefficients results of the comparison related to Fig. 18.

interval, (23 + 29) out of (40 + 40). The relatively large deviation and error during the Spring and Autumn seasons might be explained by the changing seasons with unstable outdoor temperatures, which might cause larger temperature differences. From the approximation of the PAA and the SAX symbol results, the predicted DH profile for the average school was proved convincing and representative. Besides the advantages of using PAA for time-series discretization and amplitude normalization, it also enabled us to present seasonal load patterns and shape comparisons through extracting the required day types. For example, from the transferred SAX strings, it shows the daily heat load varies in all the seasons with peak intervals "d", valley intervals "a", and transition intervals "b" and "c", even when the heat load was low in Summer. Miller et al. praised the benefits of the PAA and SAX, which may accelerate clustering building performance for building commissioning and fault tracking in response to the rapid increase of building data amount [52].

6. Application and limitations

The suggested analysis method for the ES curves and identified load profiles could be used as a reference example for stating energy use of other building types in the Nordic climate. An artificial urban area may be aggregated and synthesized by involving different building types. The method may be used as input data for modelling energy supply optimization.

Electricity has been traded freely in the European market after the regulation being removed since the 1990s, and the CO_2 emission of electricity counts on market production. To estimate the annual CO_2 emission and economic cost of electricity use in an urban area, there are two approaches to follow. The first one is to use the annual energy demand multiplied with the annual average CO_2 factor and average electricity price. For example, within the Nordic region, the CO_2 factor is approximately 110 g CO_2/kWh and the number can be higher in the wider European region when fossil fuels are involved [53]. The second approach is to adopt the hourly energy demand multiplied with the hourly CO_2 factor and price in the spot market. The real-time data of the CO_2 factor of electricity and spot price can be retrieved from electricityMap and Nord Pool separately [54,55]. The benefit of employing the hourly energy demand with spot market information is that it can better locate the critical impacts from the peak load and define the energy-saving potentials, for example how to perform load shedding and energy storage, and transition to higher DH coverage system and so on.

Due to the length of this paper, only the most representative load profiles for the average Nordic school were identified, without separating the buildings with typical high energy–density profiles and typical low energy–density profiles. In addition, the evaluation

Table 5
PAA coefficients results in Fig. 19 transferred into SAX symbols.

weekday		Winter	Spring& Autumn	Summer
Mon	predicted	a b d d d b a a	*b* c d d c *a* a a	b d d d *b* a a a
	monitored	a b d d d b a a	*a b* d d c *b* a a	b c d d c a a a
Tue	predicted	a b d d d b a a	*b* c d d *b a* a a	b *d* d c *b* a a a
	monitored	a b d d d b a a	*a b* d d c *b* a a	b c d *d* c a a a
Wed	predicted	a b d d d b a a	*b* c d d c *a* a a	b d d d *b a* a a
	monitored	a b d d d b a a	*a b* d d c *b* a a	b c d d c *b* a a
Thur	predicted	a b d d d b a a	*b* c d d c *a* a a	b d d d *b* a a a
	monitored	a b d d d b a a	*a b* d d c *b* a a	b c d d c a a a
Fri	predicted	a b d d d b a a	*b* c d d c *a a b*	b c d d *b* a a a
	monitored	a b d d d b a a	*a b* d d c *b a* a	b c d d c a a a

process was made by using the modified average data that were extracted for the regression analysis. It may also be necessary to use the current statistically typical profiles and individual buildings to compare and reflect the energy use trend and load scales. And the selection of the sample individual buildings shall be carefully considered with regards to sample sizes, representativeness, etc.

Although the proposed approach is robust and transferable, the model accuracies for annual heat load profiles shall be further improved. More advanced statistical based techniques and artificial intelligence based prediction techniques shall be selected. These AI methods are mostly developed for short term load prediction, it is still worthwhile to extrapolate the time-series prediction to yearly ones.

7. Conclusions

This study proposed a systematic approach to identify the typical energy load profiles of the average Nordic school connected to the DH system, which was made up of the modified average load of the 40 schools. The observed buildings involved different building ages, areas, energy labelling levels, and operation in the Nordic climate.

The work was done through five steps, including data collection and processing, detection of special energy use period, prediction of annual DH and electricity load profiles, and validation process. The main findings are the following:

- The selected modified Z-Score may point out the special energy use periods and show the energy demand trend. The electric appliances in the schools might be concluded with reasonably fast responses by following the attendance. While the DH demand mainly followed the outdoor temperature and the daily work schedule, with a slow control response to the short holidays, which caused part of heating energy being wasted.
- The ES curve models combining temperature moving average and segmented piece-wise linear regression gave satisfying descriptive results.
- The identified specific load profiles may present the current energy use of schools in the Nordic climate. The predicted peak load of DH was 48 W/m^2 and the annual demand was 72 kWh/m^2. The predicted peak load of electricity was 18 W/m^2 and the annual demand was 57 kWh/m^2. Accordingly, the buildings with DH may largely reduce the power grid strains.
- The symbolization cluster methods of PAA and SAX were efficient and robust for validating building energy prediction.
- The suggested approach does not require much time-consumed computation and can be efficiently applied to other public buildings under the similar climate. This benefits public administrations to have a better understanding of energy needs for different building functions and project future demand changes by varying penetration of various building types.

In the future work, the authors are going to synthesize an artificial urban area by aggregating representative load profiles for different building types, which is to be used as input for modelling and optimization of the energy system. Advanced statistical and

Table A1
Results of modified Z-Score of unusual weekly DH use.

Year	No. in figure	Week no.	Remarks	|Modified Z-Score| ≥3.5 (Y/N)
2016	1	1	Coldest temp was −17.3 °C	Y
	2	2	Coldest temp was −15 °C	Y
	3	45	Coldest temp was −10.9 °C	Y
2018	4	9	Coldest temp was −17.5 °C	Y
	5	12		Y
	6	13	Easter; Coldest temp was −11.1 °C	Y
	7	39		Y

Table A2
Results of modified Z-Score of DH use regarding short holidays 2015–2018.

Year	No. in figure	Date	Week no.	Holiday (Y/N)	|Modified Z-Score|≥3.5 (Y/N)	Remarks
2015	1	4.6	W15	Y	Y	Easter
	2	4.10	W15	N	Y	
	3	5.1	W18	Y	N (but local minimum)	Labor Day
	4	5.14	W20	Y	N	Ascension Day
	5	5.25	W22	Y	N	Whit Monday
	6	5.29	W22	N	Y	
2016	1	3.28	W13	Y	N (but local minimum)	Easter
	2	5.5	W18	Y	N	Ascension Day
	3	5.16	W20	Y	N	Whit Monday
	4	5.17	W20	Y	N	Constitution Day
2017	1	4.17	W16	Y	N (but local minimum)	Easter
	2	5.1	W18	Y	N	Labor Day
	3	5.5	W18	N	N (but local minimum)	
	4	5.17	W20	Y	N (but local minimum)	Constitution Day
	5	5.25	W21	Y	N (but local minimum)	Ascension Day
	6	6.5	W23	Y	Y	Whit Monday, abnormally high demand
2018	1	4.2	W14	Y	N (but local minimum)	Easter
	2	5.1	W18	Y	N	Labor Day
	3	5.10	W19	Y	N	Ascension Day
	4	5.14	W20	N	Y	Abnormally low demand
	5	5.17	W20	Y	N	Constitution Day
	6	5.21	W21	Y	N (but local minimum)	Whit Monday

Table A3
Results of modified Z-Score of unusual weekly electricity use.

Year	No. in figure	Week no.	Remarks	|Modified Z-Score|≥3.5 (Y/N)
2018	1	1	Involve holiday	Y
2015–2018	2	8	School week	N in 2015 (local minimum); Y
2016	3	12	Easter	Y
2018	4	13	Easter	Y
2015, 2016	5	14 in 2015; 13 in 2016	Easter	Y
2017	6	15	Easter	N (local minimum)
2015–2018	7	41	School week	N in 2015 (local minimum); Y
2015–2018	8	53 in 2015; 52	Christmas	N in 2015 (local minimum); Y

Table A4
Results of modified Z-Score of electricity use regarding short holidays during 2015–2018.

Year	No. in figure	Date	Week no.	Holiday (Y/N)	|Modified Z-Score|≥3.5 (Y/N)	Remarks
2015	1	2.16–2.20	W8	Y	Y	school week
	2	3.30–4.3				
6.29–7.3	W14; W27	Y	Y	Easter; summer vacation		
	3	4.6	W15	Y	Y	Easter
	4	4.13, 4.14	W16	N	Y	Abnormally higher use
	5	5.1	W18	Y	N (but local minimum)	Labor Day
	6	5.14	W20	Y	Y	Ascension Day
	7	5.15	W20	N	N (but local minimum)	After holiday 5.14, some schools might have reduced school hour
	8	5.25	W22	Y	Y	Whit Monday
2016	1	2.22–2.26	W8	Y	2.22–2.25 Y; 2.26 N (but local minimum)	school week
	2	3.21–3.25	W12	Y	Y	Easter
	3	3.28	W13	Y	Y	Easter
	4	5.5	W18	Y	Y	Ascension Day
	5	5.6	W18	N	N (but local minimum)	After holiday 5.5, some schools might have reduced school hour
	6	5.16	W20	Y	Y	Whit Monday
	7	5.17	W20	Y	N (but local minimum)	Constitution Day
2017	1	4.11–4.14	W15	Y	N (but local minimum)	Easter
	2	4.17	W16	Y	N (but local minimum)	Easter
	3	5.1	W18	Y	N (but local minimum)	Labor Day
	4	5.17	W20	Y	N (but local minimum)	Constitution Day
	5	5.25	W21	Y	N (but local minimum)	Ascension Day
	6	5.26	W21	N	N (but local minimum)	After holiday 5.25, some schools might have reduced school hour
	7	6.5	W23	Y	N (but local minimum)	Whit Monday
2018	1	1.1	W1	Y	Y	
	2	2.19, 2.20	W8	Y	Y	school week
	3	3.26, 3.27	W13	Y	Y	Easter
	4	4.2	W14	Y	Y	Easter
	5	5.1	W18	Y	Y	Labor Day
	6	5.10	W19	Y	N (but local minimum)	Ascension Day
	7	5.17	W20	Y	N (but local minimum)	Constitution Day
	8	5.21	W21	Y	Y	Whit Monday
	9	6.26	W26	Y	Y	summer vacation

artificial intelligence based techniques shall be selected and performed to enhance the accuracies of the load profiles. Moreover, in order to make more precise energy planning, on the trend of more efficient buildings into the market, which is dominated by the medium-aged buildings, it is needed to make dynamic building stock forecast and separate the representative load profiles based on building energy density.

CRediT authorship contribution statement

Yiyu Ding: Conceptualization, Methodology, Formal analysis, Software, Investigation, Validation, Visualization, Writing - original draft. **Helge Brattebø:** Formal analysis, Supervision, Writing - review & editing. **Natasa Nord:** Conceptualization, Formal analysis, Funding acquisition, Project administration, Supervision, Writing - review & editing.

Declaration of Competing Interest

The authors declare that they have no known competing financial interests or personal relationships that could have appeared to influence the work reported in this paper.

Acknowledgement

This article has been written within the research project “Methods for Transparent Energy Planning of Urban Building Stocks–ExPOSe”. The authors gratefully acknowledge the support from the Research Council of Norway, Department of Energy and Process Engineering of NTNU, and Trondheim municipality.

Appendix

Table A1–A4 are listed in Appendix.

References

[1] T. Abergel, B. Dean, J. Dulac, "Towards a zero-emission, efficient, and resilient buildings and construction sector, Global status report (2017",) 48.

[2] J.Z. Thellufsen et al., Smart energy cities in a 100% renewable energy context, Renewable and Sustainable Energy Reviews 129 (Sep. 2020), https://doi.org/10.1016/j.rser.2020.109922 109922.

[3] H. Averfalk, S. Werner, Economic benefits of fourth generation district heating, Energy 193 (Feb. 2020), https://doi.org/10.1016/j.energy.2019.116727 116727.

[4] H. Lund et al., Perspectives on fourth and fifth generation district heating, Energy 227 (Jul. 2021), https://doi.org/10.1016/j.energy.2021.120520 120520.

[5] R. Moschetti, H. Brattebø, M. Sparrevik, Exploring the pathway from zero-energy to zero-emission building solutions: A case study of a Norwegian office building, Energy and Buildings 188–189 (Apr. 2019) 84–97, https://doi.org/10.1016/j.enbuild.2019.01.047.

[6] F. Ascione, N. Bianco, R.F. De Masi, M. Mastellone, G.M. Mauro, G.P. Vanoli, The role of the occupant behavior in affecting the feasibility of energy refurbishment of residential buildings: Typical effective retrofits compromised by typical wrong habits, Energy and Buildings 223 (Sep. 2020), https://doi.org/10.1016/j.enbuild.2020.110217 110217.

[7] H. Yoshino, T. Hong, N. Nord, IEA EBC annex 53: Total energy use in buildings—Analysis and evaluation methods, Energy and Buildings 152 (Oct. 2017) 124–136, https://doi.org/10.1016/j.enbuild.2017.07.038.

[8] G. Reynders, R. Amaral Lopes, A. Marszal-Pomianowska, D. Aelenei, J. Martins, D. Saelens, Energy flexible buildings: An evaluation of definitions and quantification methodologies applied to thermal storage, Energy and Buildings 166 (May 2018) 372–390, https://doi.org/10.1016/j.enbuild.2018.02.040.

[9] L. Dias Pereira, D. Raimondo, S. P. Corgnati, and M. Gameiro da Silva, "Energy consumption in schools – A review paper," Renewable and Sustainable Energy Reviews, vol. 40, pp. 911–922, Dec. 2014, 10.1016/j.rser.2014.08.010.

[10] "EE Noon: Back to School with Energy Efficiency," Alliance to Save Energy, Aug. 14, 2013. https://www.ase.org/events/ee-noon-back-school-energy-efficiency (accessed Feb. 24, 2021).

[11] L. Pistore, G. Pernigotto, F. Cappelletti, A. Gasparella, P. Romagnoni, A stepwise approach integrating feature selection, regression techniques and cluster analysis to identify primary retrofit interventions on large stocks of buildings, Sustainable Cities and Society 47 (May 2019), https://doi.org/10.1016/j.scs.2019.101438 101438.

[12] A.O. Hopland, S. Kvamsdal, Building conditions in Norwegian local governments: trends and determinants, Facilities 37 (3/4) (Jan. 2018) 141–156, https://doi.org/10.1108/F-10-2017-0101.

[13] Norges vassdrags- og energidirektorat, "Analyse av energibruk i undervisningsbygg," p. 120.

[14] Y. Sun, S. Wang, F. Xiao, Development and validation of a simplified online cooling load prediction strategy for a super high-rise building in Hong Kong, Energy Conversion and Management 68 (Apr. 2013) 20–27, https://doi.org/10.1016/j.enconman.2013.01.002.

[15] C. Fan et al., Statistical investigations of transfer learning-based methodology for short-term building energy predictions, Applied Energy 262 (Mar. 2020), https://doi.org/10.1016/j.apenergy.2020.114499 114499.

[16] X. Liu, Y. Ding, H. Tang, F. Xiao, A data mining-based framework for the identification of daily electricity usage patterns and anomaly detection in building electricity consumption data, Energy and Buildings 231 (Jan. 2021), https://doi.org/10.1016/j.enbuild.2020.110601 110601.

[17] P. Gianniou, X. Liu, A. Heller, P.S. Nielsen, C. Rode, Clustering-based analysis for residential district heating data, Energy Conversion and Management 165 (Jun. 2018) 840–850, https://doi.org/10.1016/j.enconman.2018.03.015.

[18] M.Q. Raza, A. Khosravi, A review on artificial intelligence based load demand forecasting techniques for smart grid and buildings, Renewable and Sustainable Energy Reviews 50 (Oct. 2015) 1352–1372, https://doi.org/10.1016/j.rser.2015.04.065.

[19] A. Melillo, R. Durrer, J. Worlitschek, P. Schütz, First results of remote building characterisation based on smart meter measurement data, Energy 200 (Jun. 2020), https://doi.org/10.1016/j.energy.2020.117525 117525.

[20] Y. Bao, W.L. Lee, J. Jia, Probabilistic assessment of overcooling risk for a novel extra-low temperature dedicated outdoor air system for Hong Kong office buildings, Build. Simul. 14 (3) (Jun. 2021) 633–648, https://doi.org/10.1007/s12273-020-0684-4.

[21] L. Lundström, F. Wallin, Heat demand profiles of energy conservation measures in buildings and their impact on a district heating system, Applied Energy 161 (Jan. 2016) 290–299, https://doi.org/10.1016/j.apenergy.2015.10.024.

[22] "iEOS - Planning." https://www2.esave.no/Esave.nsf/iEOS_Hovedbilde.xsp (accessed Feb. 24, 2021).

[23] "Enova Offentlig søk etter energiattester." https://attest.energimerking.no/ (accessed May 10, 2021).

[24] C. Hjortling, F. Björk, M. Berg, and T. af Klintberg, "Energy mapping of existing building stock in Sweden – Analysis of data from Energy Performance Certificates," Energy and Buildings, vol. 153, pp. 341–355, Oct. 2017, 10.1016/j.enbuild.2017.06.073.

[25] BRE Global, "BRE Environmental & Sustainability Standard, BES 5051: ISSUE 1.0, BREEAM Education 2008 Assessor Manual." [Online]. Available: https://tools.breeam.com/filelibrary/Non%20Domestic%20Manuals/BREEAM_Education_2008.pdf

[26] M. Davis, "Implementing the Energy Performance of Buildings Directive (EPBD) - Featuring Country Reports 2012," Build Up, Jul. 02, 2013. https://www.buildup.eu/en/practices/publications/implementing-energy-performance-buildings-directive-epbd-featuring-country-0 (accessed Mar. 12, 2021).

[27] "Årsberetning 2017," Oslo kommune. https://www.oslo.kommune.no/politikk/byradet/arsberetning-2017/ (accessed May 10, 2021).

[28] J.E. Seem, Using intelligent data analysis to detect abnormal energy consumption in buildings, Energy and Buildings 39 (1) (Jan. 2007) 52–58, https://doi.org/10.1016/j.enbuild.2006.03.033.

[29] S. Lydersen, Mean and standard deviation or median and quartiles?, Tidsskrift for Den norske legeforening (Jun. 2020), https://doi.org/10.4045/tidsskr.20.0032.

[30] M. Frigge, D.C. Hoaglin, B. Iglewicz, Some Implementations of the Boxplot, The American Statistician 43 (1) (Feb. 1989) 50–54, https://doi.org/10.1080/00031305.1989.10475612.

[31] B. Iglewicz, D.C. Hoaglin, How to detect and handle outliers, ASQC Quality Press, Milwaukee, Wis, 1993.

[32] D. Ivanko, H.T. Walnum, N. Nord, Development and analysis of hourly DHW heat use profiles in nursing homes in Norway, Energy and Buildings 222 (Sep. 2020), https://doi.org/10.1016/j.enbuild.2020.110070 110070.

[33] T. Tereshchenko, D. Ivanko, N. Nord, and I. Sartori, "Analysis of energy signatures and planning of heating and domestic hot water energy use in buildings in Norway," in E3S Web of Conferences, Les Ulis, France, 2019, vol. 111. http://dx.doi.org/10.1051/e3sconf/201911106009.

[34] K. B. Lindberg and G. Doorman, "Hourly load modelling of non-residential building stock," in 2013 IEEE Grenoble Conference, Jun. 2013, pp. 1–6. 10.1109/PTC.2013.6652495.

[35] R. Hitchin, I. Knight, Daily energy consumption signatures and control charts for air-conditioned buildings, Energy and Buildings 112 (Jan. 2016) 101–109, https://doi.org/10.1016/j.enbuild.2015.11.059.

[36] S. Frederiksen, S. Werner, *District Heating and Cooling*. Studentlitteratur AB (2013).

[37] C. Ghiaus, Experimental estimation of building energy performance by robust regression, Energy and Buildings 38 (6) (Jun. 2006) 582–587, https://doi.org/10.1016/j.enbuild.2005.08.014.

[38] American Society of Heating Refrigerating and Air Conditioning Engineers, ASHRAE handbook: fundamentals Accessed: Feb. 27, 2021. [Online]. Available: http://app.knovel.com/hotlink/toc/id:kpASHRAEC1/2013-ashrae-handbook 2013, 2013.

[39] S. Menard, Coefficients of Determination for Multiple Logistic Regression Analysis, The American Statistician 54 (1) (Feb. 2000) 17–24, https://doi.org/10.1080/00031305.2000.10474502.

[40] Z. Ma, R. Yan, N. Nord, A variation focused cluster analysis strategy to identify typical daily heating load profiles of higher education buildings, Energy 134 (2017) 90–102, https://doi.org/10.1016/j.energy.2017.05.191.

[41] J. L. M. Hansen and R. Lamberts, "Building Performance Simulation for Design and Operation," Routledge & CRC Press. https://www.routledge.com/Building-Performance-Simulation-for-Design-and-Operation/Hensen-Lamberts/p/book/9781138392199 (accessed Feb. 27, 2021).

[42] "JRC Photovoltaic Geographical Information System (PVGIS) - European Commission." https://re.jrc.ec.europa.eu/pvg_tools/en/tools.html#TMY (accessed Feb. 24, 2021).

[43] D. Rutz et al., "UpgradeDH: Upgrading the performance of district heating networks in Europe," Euroheat & Power, Jun. 14, 2018. https://www.euroheat.org/our-projects/upgradedh/ (accessed Mar. 12, 2021).

[44] "Rapport: Enovas byggstatistikk,, Mynewsdesk, (accessed Mar. 12 (2016",) 2021). https://presse.enova.no/documents/rapport-enovas-byggstatistikk-2016-73172.

[45] T. Niemelä, R. Kosonen, J. Jokisalo, Cost-optimal energy performance renovation measures of educational buildings in cold climate, Applied Energy 183 (Dec. 2016) 1005–1020, https://doi.org/10.1016/j.apenergy.2016.09.044.

[46] J. Granderson, S. Touzani, C. Custodio, M. Sohn, S. Fernandes, D. Jump, "Assessment of Automated Measurement and Verification (M&V), Methods" (2015).

[47] Nigel Meade, Industrial and business forecasting methods, Lewis, C.D., Borough Green, Sevenoaks, Kent: Butterworth, 1982. Price: £9.25. Pages: 144, Journal of Forecasting 2 (2) (1983) 194–196, https://doi.org/10.1002/(ISSN)1099-131X10.1002/for.v2:210.1002/for.3980020210.

[48] G. R. Ruiz and C. F. Bandera, "Validation of Calibrated Energy Models: Common Errors," Energies, vol. 10, no. 10, Art. no. 10, Oct. 2017, 10.3390/en10101587.

[49] H. Gadd and S. Werner, "Heat load patterns in district heating substations," Applied Energy, vol. 108, pp. 176–183, Aug. 2013, 10.1016/j.apenergy.2013.02.062.

[50] E. Keogh, J. Lin, and A. Fu, "HOT SAX: efficiently finding the most unusual time series subsequence," in Fifth IEEE International Conference on Data Mining (ICDM'05), Nov. 2005, pp. 8 pp.-. 10.1109/ICDM.2005.79.

[51] J. Lin, E. Keogh, L. Wei, S. Lonardi, Experiencing SAX: a novel symbolic representation of time series, Data Min Knowl Disc 15 (2) (Oct. 2007) 107–144, https://doi.org/10.1007/s10618-007-0064-z.

[52] C. Miller, Z. Nagy, A. Schlueter, Automated daily pattern filtering of measured building performance data, Automation in Construction 49 (Jan. 2015) 1–17, https://doi.org/10.1016/j.autcon.2014.09.004.
[53] Norsk Eenergi, "Klimaregnskap for fjernvarme." http://www.fjernvarme.no/uploads/Rapport_Klimaregnskap%20for%20fjernvarme_2.pdf (accessed Jan. 28, 2021).
[54] "Live CO_2 emissions of electricity consumption." http://electricitymap.tmrow.co (accessed Mar. 12, 2021).
[55] "See market data for all areas." https://www.nordpoolgroup.com/Market-data1/ (accessed Feb. 24, 2021).

A.3 Paper III

Analysis of electricity use and economic impacts for buildings with electric heating under lockdown conditions: examples for educational buildings and residential buildings in Norway

Ding, Y., Ivanko, D., Cao, G., Brattebø, H. and Nord, N.

Sustainable Cities and Society, 74, p.103253, 2021.

Sustainable Cities and Society 74 (2021) 103253

Contents lists available at ScienceDirect

Sustainable Cities and Society

journal homepage: www.elsevier.com/locate/scs

Analysis of electricity use and economic impacts for buildings with electric heating under lockdown conditions: examples for educational buildings and residential buildings in Norway

Yiyu Ding [a,*], Dmytro Ivanko [b], Guangyu Cao [a], Helge Brattebø [a], Natasa Nord [a]

[a] Department of Energy and Process Engineering, Norwegian University of Science and Technology (NTNU), Trondheim 7491, Norway
[b] Department of Electric Power Engineering, Norwegian University of Science and Technology (NTNU), Trondheim 7491, Norway

ARTICLE INFO

Keywords:
electricity use profile
educational buildings
residential buildings
COVID-19 lockdown
scenario-based analysis
energy planning

ABSTRACT

The COVID-19 pandemic has caused significant impacts on energy demand in Norway and many countries. It is important to improve the existing knowledge of building operation under unforeseeable disturbances. This study aimed to identify the potential problems of electricity use patterns for four building types with electric heating: kindergartens, schools, apartments, and townhouses. By comparing the electricity profiles for the lockdown period 2020 with the normal condition in previous years, it showed that the electricity demand in the two educational institutions was almost on the same level, while there were apparent changes for the residential buildings. To estimate the energy saving potential and increase, three scenarios were developed considering different operation strategies: Scenario 1 considered operation under normal settings; Scenario 2 considered operation of educational buildings under nighttime and weekend settings; Scenario 3 considered operation of residential buildings under work-at-home conditions. Energy signature curve models were built to predict yearly demand. The results showed that the electricity demand might be reduced by one-third in educational buildings by following Scenario 2. Meanwhile, the electricity density of small apartment varied more significant than the townhouse, causing an electricity increase of 27% for the apartment and 1.3% for the townhouse under Scenario 3.

1. Introduction

Since the World Health Organization (WHO) announced COVID-19 disease as the pandemic in March 2020, many countries have undertaken restrictive measures to tackle the pandemic and slow down the spread of the coronavirus [1]. Due to the partial or full lockdown imposed on public places, commercial, and industrial schemes, building occupancy schedules have been adapted into remote work. The drastic changes have led to significant impacts on energy demand and put pressure on energy sector management and energy market.

Energy profiles are powerful tools in energy system planning and management. They reflect the requirements of total demand and energy use patterns of the customers. The COVID-19 related demand variation and corresponding energy load profiles have been analyzed on different grid levels and scales in several publications.

In the analysis of electricity use trends during the pandemic in Ontario province, Canada, it is found a 14% of electricity decline with a considerable CO_2 reduction in April 2020 [2]. The hourly-based load curve shows the weekly highest electricity demands were moved from the latter part of the week to the earlier part. Meanwhile, the morning peak loads, and the evening peak loads were avoided, which yielded a noticeable flattened curve [2]. Peak load shift is also reported in other studies [3–6]. From the analysis of electricity data covering millions of customers in Illinois, USA, the results show that weekday load profiles for dwellings became more likely to weekend profiles [3]. Through extrapolation of the findings on total load profiles, COVID-19 related profiles may change long-term workplace arrangements and further influence peak hourly loads. In a study of a Canadian social housing building during the 4-month of lockdown, it was found out that on average the daily electricity use was slightly increased by 2% while the daily hot water use was slightly decreased by 3% [4]. The biggest impacts on energy use were mostly seen during the first two months (April and May) of the lockdown period, for example, in April the electricity use increased by 46% and the hot water increased by 103% during the middle of the day [4]. An online survey to explore the impacts of

* Corresponding Author:
E-mail address: yiyu.ding@ntnu.no (Y. Ding).

https://doi.org/10.1016/j.scs.2021.103253
Received 14 April 2021; Received in revised form 27 June 2021; Accepted 10 August 2021
Available online 13 August 2021
2210-6707/© 2021 The Author(s). Published by Elsevier Ltd. This is an open access article under the CC BY license (http://creativecommons.org/licenses/by/4.0/).

Nomenclature

ASHRAE	American Society of Heating, Refrigerating and Air-Conditioning Engineers
BAS	building automation systems
DHW	domestic hot water
ED	Euclidean distance
ES curve	energy signature curve
GESD	generalized extreme studentized deviate
MAPE	mean absolute percentage error
PCC	Pearson Correlation Coefficient
SH	space heating
TMY	typical meteorological year
WD	weekday
WE	weekend
el	electricity
n	number of observations
R^2	coefficient of determination
S	standard deviation
t_{ot}	outdoor temperature
yr	year
€	currency of Euro

California's Shelter-in-place order on energy activities in the residential buildings under the confinement measures was conducted in [5] and the responses indicate an increase of energy demand from 10 to 15 o'clock, which is also related to the characteristics of respondent and dwelling. The main findings present the relationship between such COVID-19 related changes and intention to adopt smart home technologies, which may benefit household practices in the future [5]. The Brazilian power system and its four subsystems before and after adopting the distancing measures were analyzed in [6]. The comparison results of the weekly electricity profiles and the weekly change percentages show a remarkable reduction of energy demand. And the energy use trends of the subsystems were observed with different dynamics depending on the geographic locations.

The energy use and energy profiles for certain building types were investigated in [7–10]. The impacts on energy use in residential aged care facilities were analyzed in [7]. From the comparison of electricity peak demand and profiles experiencing lockdown in four Australian climatic zones, the energy use and peak loads are shown greatly climatic related. Another study was performed on one energy-intensive laboratory building at a university campus [8]. After the lockdown, it was found that the unregulated electricity use in the laboratory reduced the power demand by half. The authors suggest a communication with the building managers about the typical building function and the actions taken during lockdown [8]. Four simulation scenarios of energy use in a typical Serbian household were analyzed in [9]: S1 – reference case, S2 – mild protection measures, S3 – semi-quarantine measures, S4 – complete quarantine, to assess the link between user behavior and energy source uses. By using the occupancy profiles in the building as input, the simulation models show that there was an increase in heating and electricity use during the pandemic due to the increased user presence. Compared with the normal conditions, the increase of heating and electricity use for the scenario-based models could be 31-32% and 54-58% respectively [9]. From the energy analysis in a southern Brazilian city, Florianópolis, during the lockdown [10], it was observed that the electricity use of administrative buildings, elementary schools, and nursery schools was reduced by 38.6%, 50.3%, and 50.4%, respectively, comparing with the same period of 2018-2019. These almost unoccupied municipal buildings do require considerable energy demand with nearly half of the energy being used regardless of the occupants' presence [10].

The extent of total energy demand influence from the various restrictive approaches was examined in [11]. The investigation contains four European countries with strict containment measures and two European countries with less restrictive ones. By comparing the total electricity demand depending on the residents' activities, it shows that there was a considerable electricity demand decline in the countries with severe lockdown measures [11]. These sudden changes of energy demand have influenced energy production and utility company's investment plans. Regarding the energy supply side, the following research has worked on the problems on energy production, economy, and security experiencing the confinement measures.

The power sector in Southeast Asia was examined in [12] and the study finds out the restrictive action has aggravated the vulnerabilities of their current power system. It highlights the significance of buildings as a resilient system in this region. A data-driven analysis was performed on the U.S. bulk power systems and electricity markets during the pandemic in [13]. The power sector was severely affected from March to May 2020. From the market-specific study, the northeast region suffered the most severe impacts on power operation and economic interests. Meanwhile, the authors believe more attention should be paid to possible shocks and disproportionate impacts between energy companies and consumers. From a thorough study of global power system operation [14], many countries have suffered considerable revenue loss due to a reduction of ca.8 to 30% of total electricity demand. The substantial decrease mainly came from the temporary halt of industrial, commercial, and public transportation activities. Power generation from the conventional nuclear power was affected, meanwhile it was noticed that the contribution from renewable energy increased by 3.5- 72% depending on the countries [14]. In addition to the economic problems of conventional utility companies, the authors in [15] underscore the challenges on load forecasting and required flexibility because of the changed balance and increased uncertainty.

The COVID-19 related indoor air quality issues have been studied as well. The indoor CO_2 concentration in residential buildings experiencing the home office regime was investigated in [16]. It shows that the adoption of a proper aeration process can minimize the increase of heating energy caused by changing the room function [16]. Another study shows that the mean daily PM2.5 concentration rose by approximately 12% and the mean volatile organic compound concentration by 37% to 559% comparing with the condition before and during the COVID-19 lockdown [17].

The literature review shows that there is a number of investigations regarding COVID-19 related energy use in non-cold climate region. However, the real data analysis and scenario-based modelling of electric heating use are missing for buildings in Norway and the similar climate zones. Therefore, the main objective of this study is to investigate the energy use behavior in Norwegian buildings with electric heating during the COVID-19 pandemic. The reason to study electric heating in buildings is that the country remains highly dependent on electricity. According to the statistics [18], nearly three quarters of Norwegian households are using electricity for heating purposes in the form of either electric radiator, electric floor heating, air source heat pump, or central electric heating. In the service sector, electricity accounts for approximately 77% of total energy use by supplying heating demand at a large extent. Moreover, within the Nordic region, although heat pumps are gradually replacing direct electric heating, the electricity demand in the residential sector has been increasing over the last decade, according to the report from the Nordic Energy Research [19].

As an important section of non-residential buildings at a municipal level, kindergartens and schools are commonly dispersedly located in cities or towns. Statistically, costs for building operation management become the second biggest expenditure of educational institutions, only beneath salaries of employees [20]. Building operators are therefore responsible for maintaining the required indoor environment in energy-efficient ways.

By complying with the Norwegian national lockdown regime

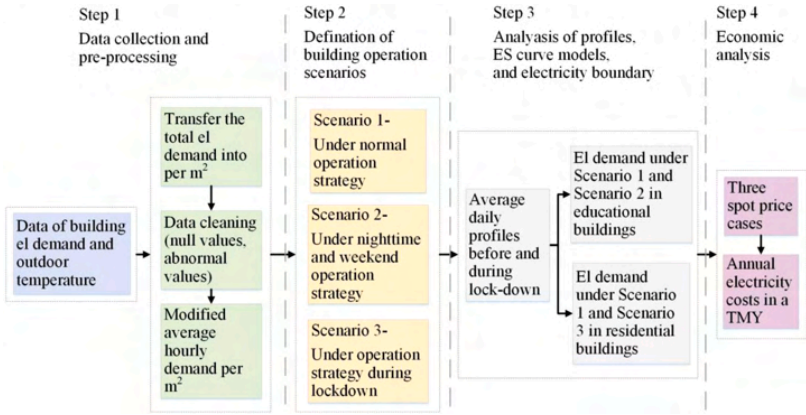

Figure 1. The workflow of the analysis of electricity use

Table 1
List of building information.

Building type	Floor area (m^2)	Data duration (Y/M/D)
Kindergarten	279- 1 143	2018.01.01- 2020.12.31
School	2 157- 5 443	2018.01.01- 2020.12.31
Apartment	40	2018.10.01- 2020.12.31
Townhouse	133	2018.10.01- 2020.12.31

initiated in March till May 2020, the teaching activities on campus were severely interrupted and transferred into remote learning, meanwhile many employees followed work-at-home rules. Therefore, this study focuses on the educational buildings and residential buildings in Norway and similar climatic regions. Concerning both for personal interests and municipality's public expenses, the secondary objective is to estimate the energy demand and economic impacts on the buildings with electric heating during the lockdown and future unforeseeable disturbances, which may also have influences on local energy planning.

To fulfill the research purposes, the three questions shall be answered: 1) whether the educational buildings were managed in an energy-efficient way during the temporary closure? 2) are there any energy and economic saving potentials in the educational buildings that might have been neglected and how much saving potentials may be reached? 3) how much electricity and economic impacts influenced the residential buildings with different household size and family members?

The novel contributions of this study may be summarized as follows. In our analysis, we utilized the measured electricity use data in real buildings during the lockdown and normal time. In such a way, the analysis was based on statistics rather than certain assumptions. It was found out that the common assumptions about energy use during COVID-lockdown in publications for public buildings were not always true and the household scale affected energy use in these buildings. Three scenario-based models were proposed, and they were used to discuss their impacts on energy management and local energy planning by varying building type ratio.

The rest of the paper is organized as the following. Section 2 introduces the study methods including the data information of the observed buildings, and the description of the three scenarios that were used to establish the energy models. The main results of the study are presented in Section 3. The electricity profiles under the three scenarios were analyzed and compared based on the measured data. The regression models' accuracies were evaluated by ASHRAE criteria. An economic analysis was further carried out to compare the annual electricity costs for the scenario-based models. Due to the different use characteristics between the educational buildings and the residential buildings, the feasible energy-saving strategies were proposed for the former ones, and the impacts on increased bill were studied for the latter ones. Lastly, the limitations, future work, and conclusions are discussed and summarized in Section 4 and Section 5.

2. Methodology

The outline of the main steps for this study is illustrated in Figure 1. Section 2.1 collects the building information. Section 2.2 – Section 2.4 explain the three scenarios regarding the different building operation strategies. In Section 2.5, the method for the economic analysis is introduced by considering the three levels of electricity spot price. Section 2.6 introduces the method for assessing the consequence on local energy planning.

2.1. Description of the observed buildings

During the lockdown, the educational buildings were supposed to be closed with minimum energy use, meanwhile the residential buildings were supposed to have higher energy demand under work-at-home conditions. To answer the above research questions, 14 kindergartens, eight schools, one apartment, and one residential house located in Trondheim, Norway, were analyzed in this study. The building areas of the kindergartens are between 279 and 1 143 m^2, while those of the schools are between 2 157 and 5 443 m^2, of which six are primary schools, one is a middle school, and one is a mixed one. All of them use electricity as their main building energy supply source, for instance, space heating (SH), domestic hot water (DHW), ventilation, and other electric appliances. About the space heating demand, there are electric panel heaters and ventilation heating in the kindergartens and schools. The maintenance and operation of these educational institutions are handled by Trondheim Municipality. The energy data were retrieved from the municipality's energy monitoring platform [21]. The historical annual demands of these observed buildings were close to the local average level. Therefore, these buildings may be representative to present the energy use changes and variations during the pandemic period. The residential house is a two-story townhouse with a floor area of 133 m^2, where accommodates a family of two adults and two pupils. The building is supplied by natural ventilation, and heated by a radiant wood stove, three electric radiators, and supplemented by an air source heat pump. In addition to the electric assistant heating, electricity is used for DHW, lighting, and other appliances. The apartment with natural ventilation has a floor area of 40 m^2, where accommodates an adult. It uses electricity for radiator (for SH), DHW, and other appliances. The electricity data of the two residential buildings were voluntarily shared

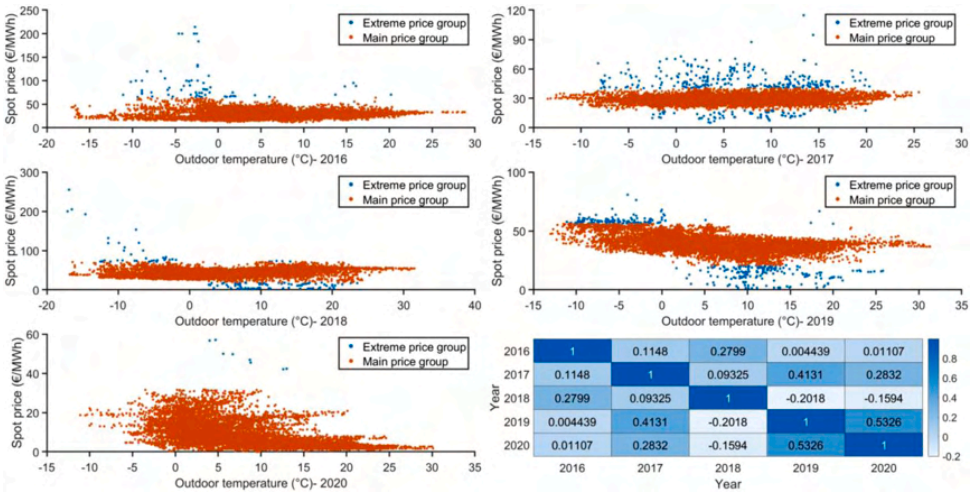

Figure 2. Electricity spot price vs Outdoor temperature, and Correlation of electricity spot price in 2016- 2020

by the dwellers who retrieved them from the local power grid supplier Tensio [22]. All these observed buildings have no submeter.

Weather conditions were considered in the energy analysis, and the historical weather data were obtained from the local meteorological station [23]. The electricity use of the educational buildings was from the beginning of 2018 to the end of 2020, while the electricity use of the two residential buildings was from October 2018 to the end of 2020 due to the upgrade into smart meter in September 2018. The data information is briefly explained in Table 1. The analysis was performed on average specific electricity use (kWh_{el}/m^2), to define the representative electricity use concerning buildings with different characteristics. MATLAB was used for the data analyses.

2.2. Scenario 1 - Electricity demand based on normal operation mode

Scenario 1 considered the electricity use under normal conditions without the disturbance from lockdown or other temporary disruption from 2018 to 2020 except March - May 2020. In the educational buildings, there is a remarkable difference in electricity demand between daytime on weekdays and off-work hours, which is mainly caused by the different campus activities and attendance between the two time slots. Whereas, the electricity use pattern in residential buildings is unlike kindergartens and schools. It generally has low demand during working hours and high demand when dwellers are at home.

As addressed before, large proportion of electricity is used for heating purposes in the electric-heated buildings in the cold climate areas. Accordingly, outdoor temperature (t_{ot}) may be regarded as the key predictor to determine the related heating electricity use in buildings under different operation strategies. To find the relationship between the electricity demand and outdoor temperature, energy signature curve (ES curve) was used in the study. ES curve has been widely utilized in building energy planning by researchers and engineers at all levels [24–26]. ES curve generally consists of two parts, the temperature dependent part and temperature independent part. They are divided by changing point temperature (CPT) or heating effective temperature. The formulas for the ES curve may be expressed as:

$$\text{If } t_{ot} \leq \text{CPT}, \quad P(t_{ot}) = p_1 \cdot t_{ot} + p_2 + \varepsilon \tag{1}$$

$$\text{If } t_{ot} > \text{CPT}, \quad P(t_{ot}) = p_1 \cdot t_{ot} + p_2 + \varepsilon; \approx p_2 \tag{2}$$

In Eqs.(1) and (2), p_1 and p_2 are the coefficients of each ES curve model, and ε is the residual error. The heating demand follows the linear growth under the slope of p_1. Besides the outdoor temperature, the work schedules also decide the operation settings and affect the electricity use. In the educational buildings, the ES curves were made for weekdays and weekends, separately. Concerning the possible random operation of electric appliances, which may cause irregular electricity use, the ES curves for the residential buildings were defined based on average weekly base.

The importance of using typical meteorological year (TMY) to estimate building energy performance from one single year analysis is highlighted in [27]. The outdoor temperature is made based on the most "representative" conditions over the last decade. In this analysis, TMY data 2007- 2016 of Trondheim were retrieved from the European Union website [28]. Combining the acquired energy signature under Scenario 1, the TMY data were applied to obtain the electricity use of the typical year. This scenario was applied to both the educational buildings and the residential buildings.

2.3. Scenario 2 - Electricity demand based on night and weekend operation mode in the educational buildings

This scenario referred to the energy-saving mode for a limited operation of buildings during a temporary closure. It was assumed that building management sector switched the energy supply operation to the settings of low demands during normal weekdays' nighttime and weekend to save energy. In the educational buildings, the electricity use was usually observed at minimum levels to maintain the acceptable indoor temperatures and air quality during weekends and off-work hours on weekdays, with the almost zero attendance. Similar as the study in [11], the weekday demand profiles for educational buildings during the pandemic were assumed to be identical as the weekend profiles of the reference week in 2019. Thus, Scenario 2 was only applied to the educational buildings in this study.

The hypothesis was made by considering the guidance of building operation in epidemic situations by the American Society of Heating, Refrigerating and Air-Conditioning Engineers (ASHRAE). It highlights that buildings equipped with or without a building automation systems (BAS) are not recommended to completely shut down the HVAC systems during the temporary closure or no occupancy [29]. The buildings shall be maintained "within a reasonable range of temperature and humidity" by setting the HVAC systems with relaxed temperature and humidity.

To find the electricity characteristics for Scenario 2, the ES curve was developed based on the hourly electricity use during the normal

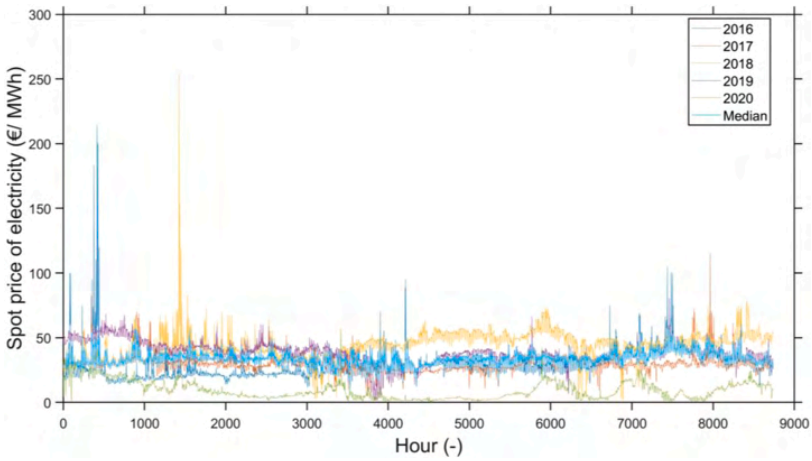

Figure 3. Annual electricity spot price profiles in 2016- 2020

weekdays' nighttime and weekends. After that, by following the similar way as Scenario 1, the electricity use of the TMY under Scenario 2 was acquired. It enables us to see the possible electricity reduction that may be achieved in the educational buildings when the building energy supply system runs at a low demand level.

2.4. Scenario 3 - Electricity demand based on lockdown operation mode in the residential buildings

When the rule of home office was in effect, the hypothesis of electricity use in the residential buildings might be higher than normal situation, especially during daytime since the work schedules of dwellers changed, similar as in the Canadian residential community [4]. Scenario 3 was to find the increased electricity use caused by the influence from lockdown in the residential buildings, and to study energy robustness by dwelling scale.

The ES curve was established based on the average weekly electricity use from March to May 2020. The electricity characteristics for this scenario were extrapolated to the whole typical year by using the coefficients acquired from this period. Then a yearly electricity use was obtained by using the similar methods for Scenario 1 and Scenario 2.

2.5. Economic impact assessment

In Norway, the specific electricity price contains two parts, the fixed grid rent price (f_i) and the variable price (v_i), see Eq.(3). This pricing mode is commonly adopted in many European countries [30, 31]. f_i refers to the fee and tax when using the grid, which is generally determined by the local authority and the value is normally constant within a certain amount of time, while v_i varies a lot based on the demand and supply in the power market.

$$p_i = f_i + v_i \tag{3}$$

Using the spot price as reference, each energy company charges with different price packages concerning their own interests. To calculate the annual electricity costs in this study, the fixed price was retrieved from Statistic Norway [18], and the variable price was considered with the spot price of Trondheim from NordPool (2016- 2020) [30].

The five-year spot price versus the outdoor temperature is plotted in Figure 2, where the orange dots represent the main price groups and the blue dots represent the extreme price groups (very high and low spot price). These extreme data points were separated from the main clouds by the method of Generalized extreme studentized deviate (GESD). The explanation and application of GESD can be found in [32, 33]. Moreover, as illustrated in the correlation heatmap at the bottom right in Figure 2, the five years had weak relation with each other. Most of the two-year correlation factors were smaller than 0.3. In Figure 3, it compares the annual spot price profile from 2016- 2020, showing the high-price level in 2018 in yellow line, the low-price level in 2020 in green line, and the others in between. Both the heat map and the annual spot price profiles were adjusted with the same starting day of the five years. As shown in Figure 2 and Figure 3, it is rather difficult to define a simple mathematical method explaining the variations of the five-year spot prices. Regarding the complex prediction of electricity prices, some examples are shown in [34–36]. Thus, in this study, three price cases were made. The spot price of 2018 was treated as the case of highest price level, that of 2020 for the case as the lowest price level, and the median values of the rest of the years as the case of moderate price level. The thick blue line is for the median values as shown in Figure 3. It was assumed that these three price levels were capable to represent the electricity market situation in recent years.

By combining the annual electricity profiles of a TMY and the three price levels, it allows us to calculate the annual electricity costs for the observed buildings regarding the three operation scenarios and further compared the costs.

2.6. Aggregation and consequence on energy planning

Local energy planning may be improved by analyzing the energy use during critical and special circumstances such as lockdown. An imaginary community could be assumed to be made up of one kindergarten, one school, and one residential area composed of 40% of apartment and 60% of townhouse. By aggregating the annual specific electricity demand for the four building types in a normal year (Scenario 1) and lockdown year (Scenario 2 and Scenario 3), the annual total electricity use for this community was calculated as

$$E_{nor\ yr} = e_{nor\ yr,kind}\cdot A_{kind} + e_{nor\ yr,\ sch}\cdot A_{sch} + e_{nor\ yr,\ apm}\cdot A_{resi}\cdot 40\% + e_{nor\ yr,\ house}\cdot A_{resi}\cdot 60\% \tag{4}$$

$$E_{ld\ yr} = e_{ld\ yr,\ kind}\cdot A_{kind} + e_{ld\ yr,\ sch}\cdot A_{sch} + e_{ld\ yr,\ apm}\cdot A_{resi}\cdot 40\%\cdot i + e_{nor\ yr,\ apm}\cdot A_{resi}\cdot 40\%\cdot(1-i) + e_{ld\ yr,\ house}\cdot A_{resi}\cdot 60\%\cdot i + e_{nor\ yr,\ house}\cdot A_{resi}\cdot 60\%\cdot(1-i) \tag{5}$$

where $e_{nor\ yr,\ kind}$, $e_{nor\ yr,\ sch}$, $e_{nor\ yr,\ apm}$, and $e_{nor\ yr,\ house}$ refer to the annual specific electricity use for kindergarten, school, the apartment, and the

Table 2
Monthly average temperature

	March	April	May
2018	-3.1 ℃	4.7 ℃	12.3 ℃
2019	-0.4 ℃	6.7 ℃	7.4 ℃
2020	1.4 ℃	3.5 ℃	6 ℃

townhouse in a normal year, respectively; $e_{ld\ yr,\ kind}$, $e_{ld\ yr,\ sch}$, $e_{ld\ yr,\ apm}$, and $e_{ld\ yr,\ house}$ refer to the annual specific electricity use for kindergarten (Scenario 2), school (Scenario 2), the apartment (Scenario 3), and the townhouse (Scenario 3) in a lockdown year, respectively; A_{kind}, A_{sch}, and A_{resi} refer to the building area of kindergarten, school, and the residential area, respectively; and i refers to the percentage of work-from-home adoption in the residential area. By varying the residential area A_{resi} and the work-from-home adoption percentage i, the electricity demand especially the peak demand and the capacity factor may be affected. Capacity factor of an energy plant is the ratio of the actual total energy production over a period to the maximum output if the plant operates at its rated capacity, and it measures the overall utilization of an energy plant [37]. These influences on local energy planning are discussed in Section 4.

3. Results

The analysis results of electricity daily profiles before and during COVID-19 lockdown are presented in Section 3.1, the scenario-based electricity demands are illustrated in Section 3.2, Section 3.3 shows the electricity profiles in a TMY under the three scenarios, and the yearly electricity costs under different scenarios and price levels are compared in Section 3.4.

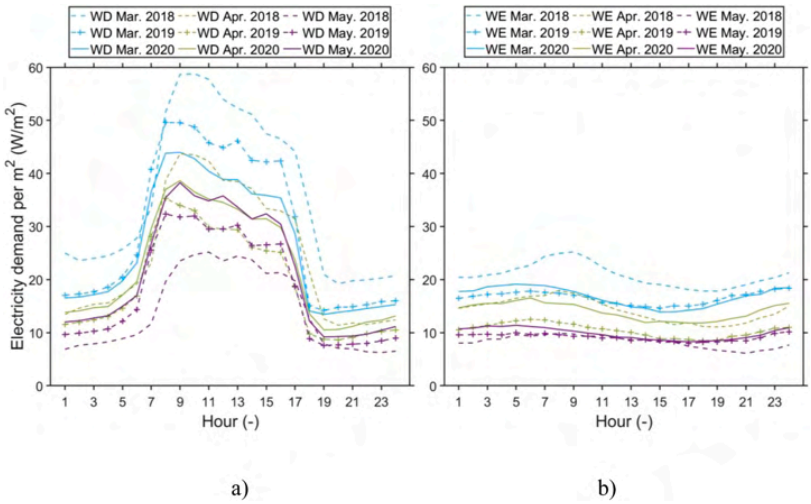

Figure 4. The average daily electricity profiles for kindergartens from March to May in 2018- 2020, where a) profiles on weekdays, b) profiles on weekends

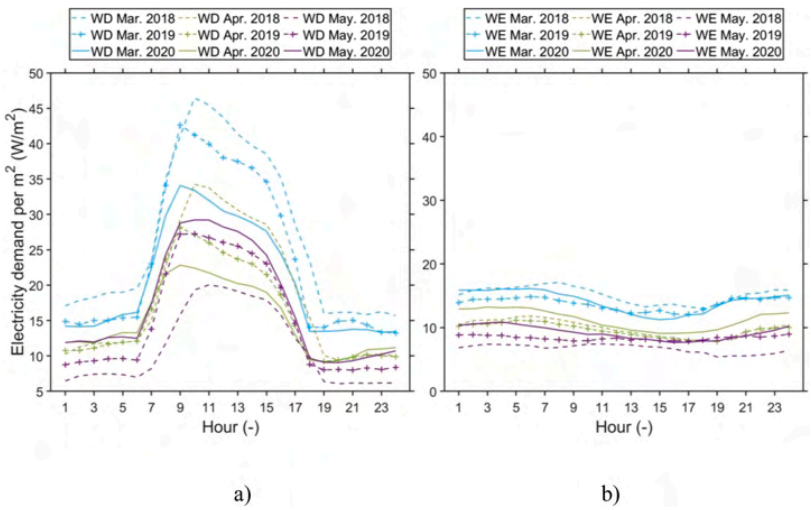

Figure 5. The average electricity profiles for schools from March to May in 2018- 2020, where a) profiles on weekdays, b) profiles on weekends

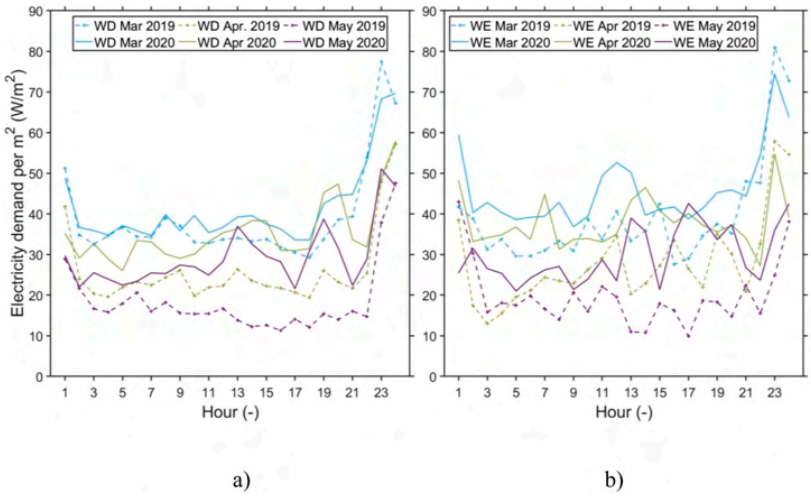

Figure 6. The average electricity profiles for the single apartment from March to May in 2019- 2020, where a) profiles on weekdays, b) profiles on weekends

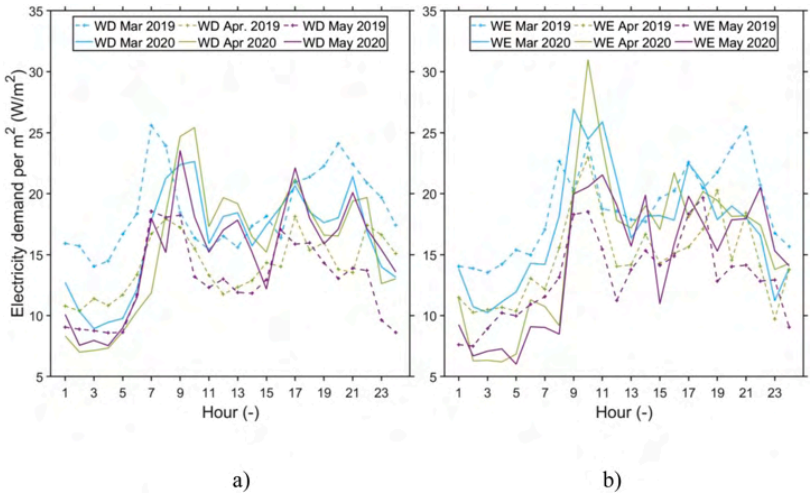

Figure 7. The average electricity profiles for the townhouse from March to May in 2019- 2020, where a) profiles on weekdays, b) profiles on weekends

3.1. Analysis of daily electricity profiles before and during COVID-19 lockdown

According to previous research and statistics, nearly half of energy use in buildings is used for heating in the cold climate. Therefore, the outdoor temperature has large influence on the total electricity use. The average monthly outdoor temperature between March and May during the three years are listed in Table 2, where 2018 had the coldest March and the warmest May, 2019 had the warmest April, and 2020 had the warmest March and the coldest April and May.

Considering different schedules and occupancy levels on weekdays and weekends, the electricity use profiles were therefore analyzed separately. The average daily electricity demand profiles for kindergartens, schools, and two residential buildings during March to May 2018- 2020 are compared in Figure 4 - Figure 7, respectively. In these figures, WD denotes weekday and WE denotes weekend, and the dashed lines stand for 2018, the dashed lines with plus symbol for 2019, and the solid lines for 2020.

For the educational buildings shown in Figure 4 and Figure 5, the electricity use followed the opening hours and schedules. On weekdays, the demand generally arose between 6 and 17 o'clock with the peak demand at around 8 or 9 o'clock. The demand rising ahead of the teaching activities was aimed extending the thermal comfort and improve the indoor air quality. From 19 to 6 o'clock next morning, the energy supply systems maintained at a low demand. It may be observed that the shapes of the three- year electricity profiles from March to May were quite similar. The average demands were mostly in line with the average monthly outdoor temperature. Also, kindergartens generally require higher energy demand than schools, which follows the statistical data due to the higher requirement of thermal comfort and hygiene in kindergartens [38].

Regarding the residential buildings, the electricity use patterns were different. In the apartment see Figure 6, there was distinct higher demand during the daytime on weekdays in 2020 than 2019. Meanwhile

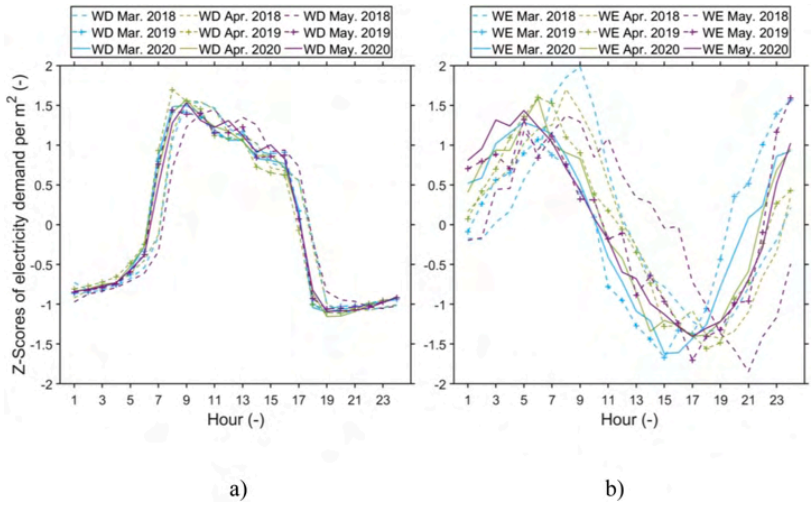

Figure 8. Z-Scores of average daily electricity profiles for kindergartens from March to May in 2018- 2020, where a) Z-Scores for weekdays, b) Z-Scores for weekends

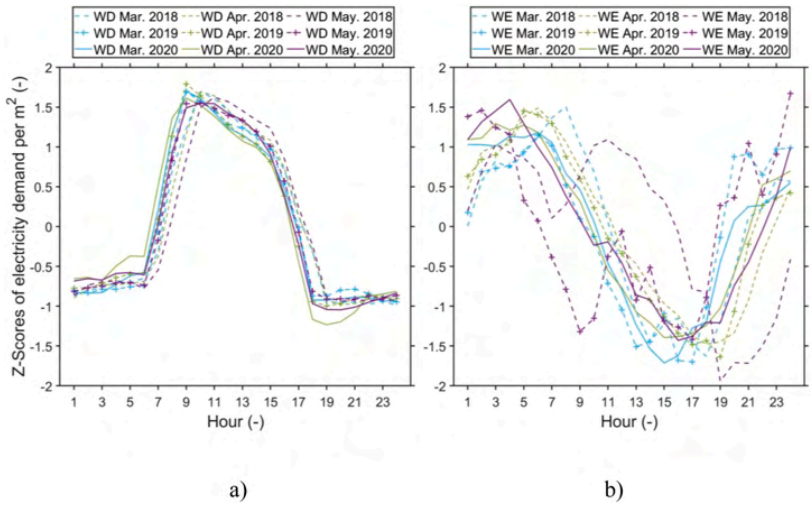

Figure 9. Z-Scores of average daily electricity profiles for schools from March to May in 2018- 2020, where a) Z-Scores for weekdays, b) Z-Scores for weekends

several local peak demands were noticed, such as 10, 13, and 14 o'clock in March, 14 and 15 o'clock in April, 9 and 13 o'clock in May. Additionally, the average higher demand in the evening was mainly due to the running of appliance, and the peak load in the midnight was used for recharging the hot water tank. The use pattern during weekends were similar with weekdays, but due to more time spent indoors there were several local peak loads both in 2019 and 2020. In the townhouse see Figure 7, March 2020 had slightly higher daytime electricity use, while April 2020 and May 2020 used more electricity during daytime than 2019. The morning peaks arising at 7 or 8 o'clock in 2019 was shifted later to 9 or 10 o'clock in 2020 due to the study- and- work- at home regime. Again, several local peak demands were also noted during the daytime on weekdays, such as around lunch period. The specific electricity demand in the single apartment was generally higher than the townhouse. The WD values were similar to the WE values in the residential buildings, which is also mentioned in [3]. This may indicate that the effect of occupants on private buildings plays a more important role than in public buildings, and the household energy demand varies based on residents' behavior, as mentioned in [39, 40].

In general, among the four building types, March claimed the highest electricity, May needed the lowest electricity, and April was in between, with an exception of the unusually cold May in 2020. To identify the effect from the outdoor temperature difference to the electricity, Euclidean Distance (ED) was calculated to prove that the larger outdoor temperature difference was supposed to yield the higher ED and vice versa. ED was calculated as:

$$d_{ED}(X,\ Y) = \sqrt{\sum_{i=1}^{n} (x_i - y_i)^2} \tag{6}$$

where X and Y refer the vector of the average daily profile in each year, x_i and y_i refer to the electricity demand at *i-th* hour in each year.

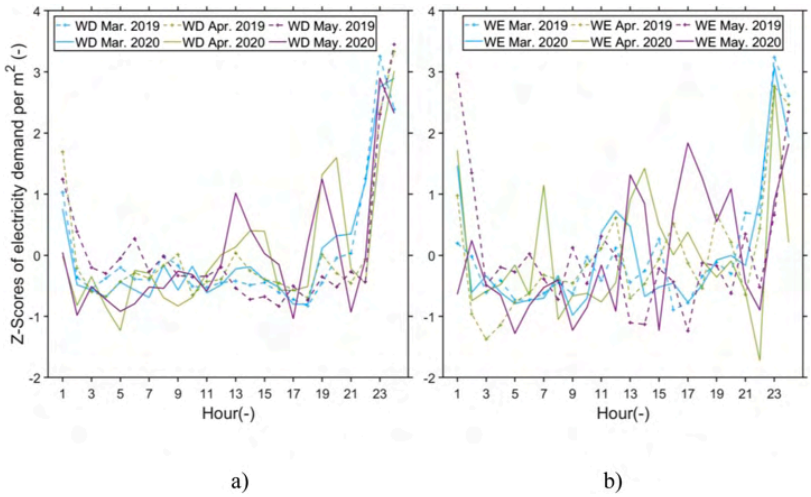

Figure 10. Z-Scores of average daily electricity profiles for the single apartment from March to May in 2019- 2020, where a) Z-Scores for weekdays, b) Z-Scores for weekends

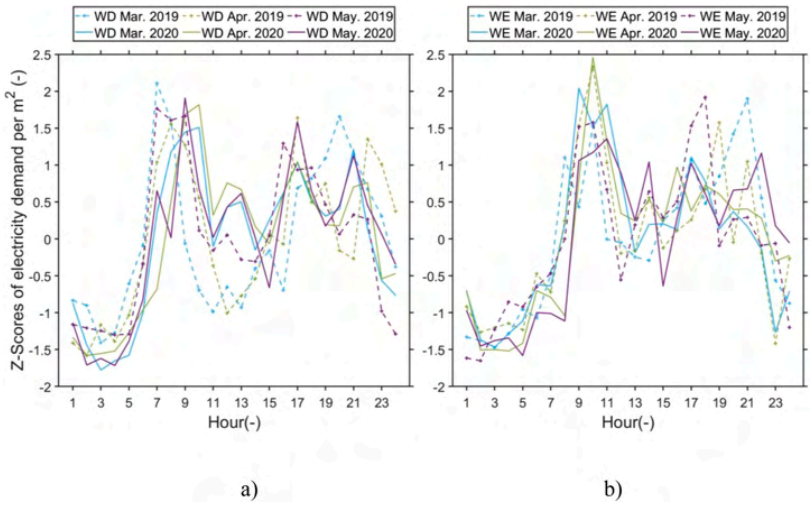

Figure 11. Z-Scores of average daily electricity profiles for the townhouse from March to May in 2019- 2020, where a) Z-Scores for weekdays, b) Z-Scores for weekends

Besides the difference defined by ED, the average daily profiles were further performed with Z standardization (Z-Score) and Pearson Correlation Coefficient (PCC) analysis to identify the similarities. Through the calculation of Z-Scores and PCC, the amplitudes of demand values were normalized by making the profiles of compatible scales, and the shape similarities of each two profiles can be measured by PCC. This may avoid the possible influence of the outdoor temperature to the energy profile shapes. The benefits of using the PCC measures to effectively recognize the profiles similarities were highlighted in [41].

The Z-score and PCC were calculated as Eqs.(7) and (8), respectively:

$$Z_i = \frac{x_i - \overline{x}}{S} \tag{7}$$

where x_i refers to the electricity demand at *i-th* hour, S refers to the standard deviation of the day (24 hours), $\overline{x}$ refers to the mean value of the day.

$$PCC(X,\ Y) = \frac{cov(X,\ Y)}{S_X S_Y} = \frac{\sum_{i=1}^{n}(x_i - \overline{x})(y_i - \overline{y})}{\sqrt{\sum_{i=1}^{n}(x_i - \overline{x})^2}\sqrt{\sum_{i=1}^{n}(y_i - \overline{y})^2}} \tag{8}$$

where *cov* means the covariance.

The Z-Scores of each average daily profile corresponding to Figure 4- Figure 7 are presented in Figure 8- Figure 11. When demand scales were normalized and discarded, the educational buildings reflected a highly similar pattern on weekdays during the three months from 2018 to 2020. However, the energy use on weekend varied from month to month. As for the residential buildings, the energy use patterns over the three months from 2019 to 2020 were quite different, with noticeable local peak demand during daytime on weekdays, for example from 12 to 16 o'clock in the single apartment 9 to 14 o'clock in the townhouse.

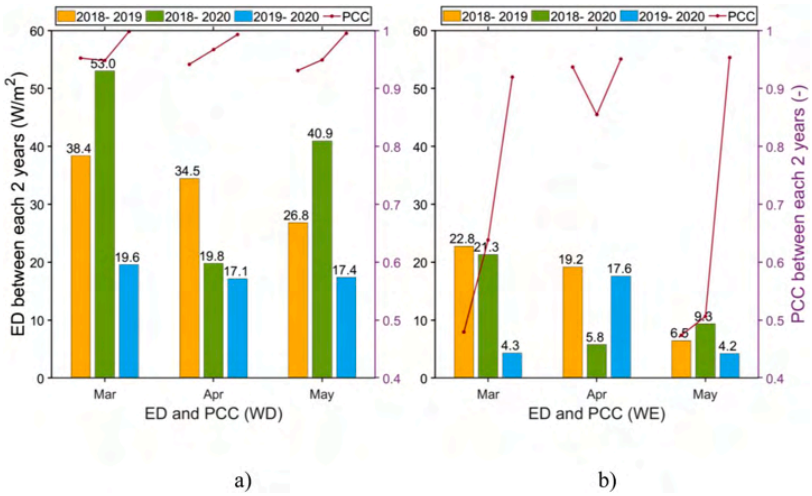

Figure 12. The ED and PCC results of kindergartens in 2018- 2020, where a) for weekdays, b) for weekends

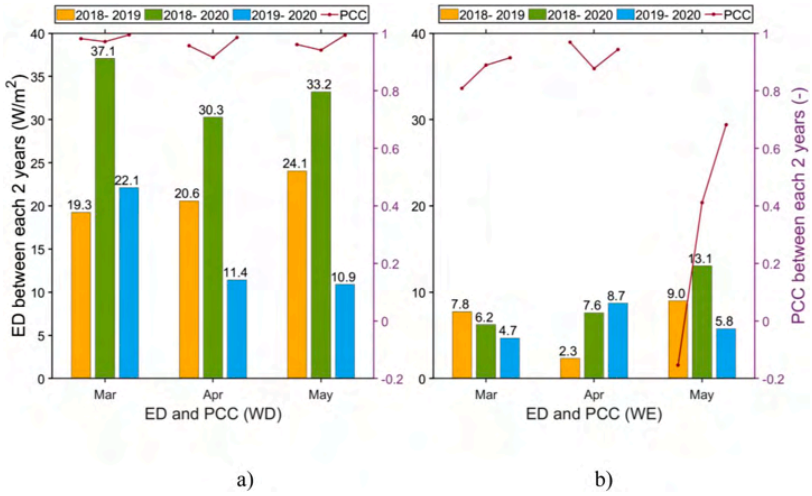

Figure 13. The ED and PCC results of schools in 2018- 2020, where a) for weekdays, b) for weekends

The results of ED and PCC measures within every two years for kindergartens and schools are compared in Figure 12 and Figure 13, where the yellow bars stand for the EDs within 2018- 2019, the green bars for the EDs within 2018- 2020, and the light blue bars for the EDs within 2019- 2020. The PCCs are plotted by the red lines with the dots, and each dot refers to the same year of the bar where it is located. By discarding the real energy demand scales influenced by the outdoor temperature, it was observed that the PCC results from March to May during the three years were higher than 0.93 in kindergartens and 0.91 in schools on weekdays, and the highest PCCs were even found within 2019- 2020 (the red dots located at the light blue bars). Even on weekends, there were also several PCCs beyond 0.7 between 2019 and 2020. This proved again that the patterns and operation of the three-year average daily energy use were of high similarity. The higher temperature deviation from 2018 to the other two years led to larger energy demand differences, which was reflected in the ED results. The closer outdoor temperature between 2019 and 2020 led to the smaller ED on weekdays. Comparing with weekdays, both the daily profiles and the ED results of electricity presented much lower demands on weekends in kindergartens and schools. This is mainly because the educational institutions in Norway usually do not carry out teaching activities on weekends, but the buildings can be occasionally rented out to maximize the public resource usage [38]. This explained the much lower impact from the outdoor temperature difference to the energy demand on weekends than that on weekdays, and the weekend demand was alike the night mode.

About the residential buildings, the ED and PCC results of the townhouse (purple columns and black dots) and the single apartment (blue columns and red crosses) between 2019 and 2020 are compared in Figure 14. The ED values of the townhouse were lower than those of the apartment within the three months both on weekdays and weekends, only with the exception in March when the two were close. Additionally, the EDs of the townhouse on weekends were smaller than on weekdays, which was also backed by the high average PCC values. It mostly implied

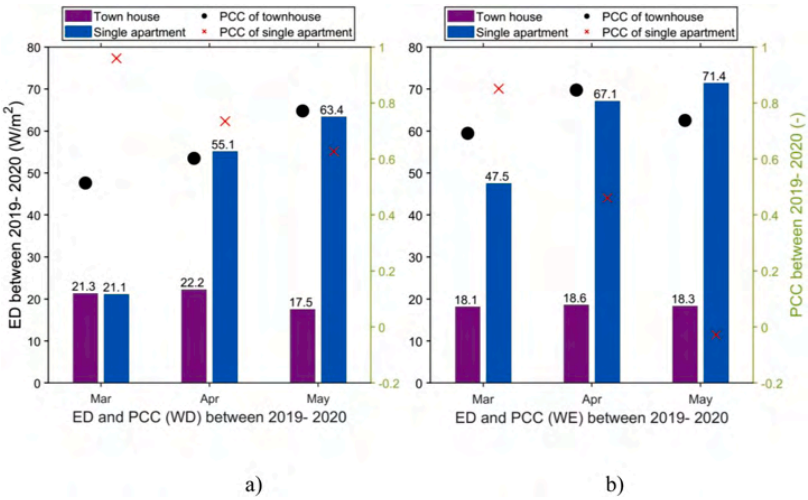

Figure 14. The ED and PCC results of townhouse and single apartment in 2019- 2020, where a) for weekdays, b) for weekends

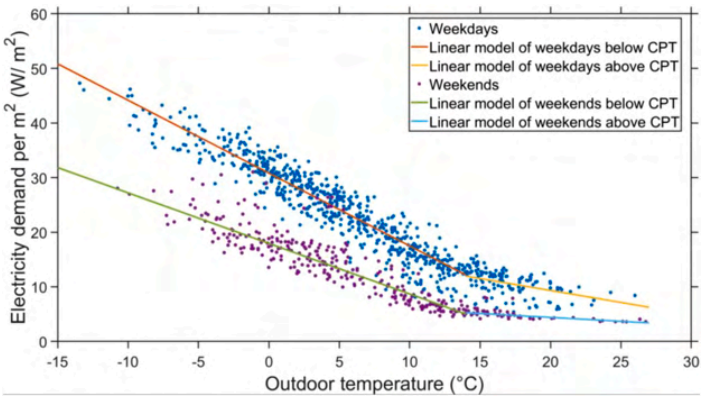

Figure 15. Energy signature curve models for kindergartens for Scenario 1

that the residents kept their usual weekend plans, for example the outdoor activities. Generally, EDs of the townhouse were rather stable. Whereas the apartment had much larger ED values and more various PCC values, which was similar with the findings in the average profiles in Figure 6 since more time was spent at home. The occupant behavior in smaller dwelling size had higher energy impacts.

Based on the findings from the weekday electricity profiles of kindergartens and schools during the lockdown period, the operation might not shift to night/weekend settings as the hypothesis. Due to the practical reasons, the schools and kindergartens were still open during the period to support the parents who were working in the critical positions such as health system, police station, transportation and so on. Both kindergartens and schools showed similar operation strategies between March and May from 2018 to 2020, by showing their similar electricity use patterns with the close average daily profiles and PCC results. This is unlike the electricity use examined in the university laboratory building [8] and the nursery school and elementary school buildings [10]. In the former building, most of the users are adults and able to take care of themselves [8]; in the latter buildings, although most of users are children same as in this study, nearly half of electricity demand was reduced [10].

Meanwhile the residential buildings showed a large variation influenced by the changes of the dweller's working schedule during the period as projected. Besides that, there was a bigger influence on specific electricity demand in the single apartment than the multi-member townhouse. Since the apartment has a smaller floor area and one dweller, it may be more sensitive with the changes. And the wood stove in the townhouse was not treated in the study.

3.2. Analysis of scenario-based electricity demands

This section studies the electricity use under the three scenarios in the observed buildings. All the ES curve models were established based on the measured data.

In the educational institutions, as shown above, the building energy systems were most likely maintained at normal level during the lockdown. Hence, the electricity use in kindergartens and schools during 2018- 2020 was treated under normal operation. In Scenario 1, the daily-based ES curve models of weekdays and weekends were built separately. The ES curve models of kindergartens are shown in Figure 15, where the weekdays (blue dots) and weekends (purple dots) have great demand differences. Since the ventilation, heating, and other

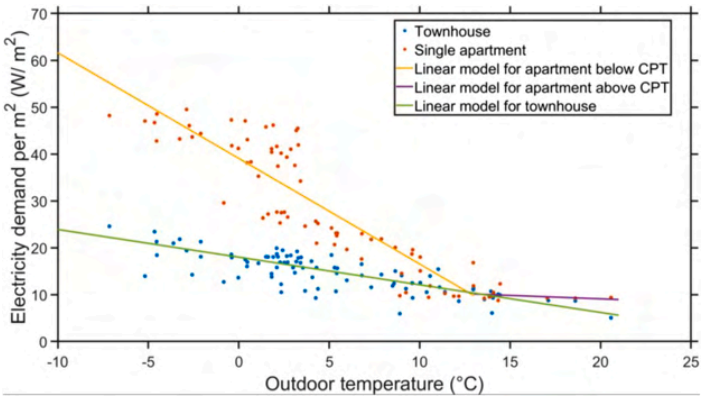

Figure 16. Energy signature curve models for the single apartment and the townhouse for Scenario 1

Table 3
Coefficients and Accuracy of the ES curve models for Scenario 1

Building type	Coefficients of model			Accuracy of model	
	CPT (°C)	p_1	p_2	R^2	MAPE (%)
Kindergarten (WD)	14	-1.3 (≤ 14°C) -0.4 (>14°C)	30.8 (≤ 14°C) 18.1 (>14°C)	0.90	11.9
Kindergarten (WE)	14	-0.9 (≤ 14°C) -0.1 (>14°C)	17.9 (≤ 14°C) 7.6 (>14°C)	0.79	
School (WD)	14	-1.2 (≤ 14°C) -0.3 (>14°C)	25.1 (≤ 14°C) 13.6 (>14°C)	0.82	18.2
School (WE)	14	-0.7 (≤ 14°C) -0.2 (>14°C)	15.1 (≤ 14°C) 7.7 (>14°C)	0.80	
Apartment	13	-2.3 (≤ 13°C) -0.2 (>13°C)	38.5 (≤ 13°C) 12.2 (>13°C)	0.80	18.2
Townhouse	/	-0.6	17.9	0.63 (↓)	14.6

appliances were much less operated on weekends, the electricity demand was lower than weekdays by around 35- 40%. The CPT was identified at 14°C both on weekdays and weekends by giving the adequate piece-wise approximation. The needs for electricity demand became less when the outdoor temperatures were above the CPT, that the regression lines had milder slopes than the ones below the CPT. This was mainly because of the reduction for electric space heating. Schools had similar electricity demand characteristics and their ES curve models are shown in Appendix Figure A1.

For the residential buildings in Scenario 1, the ES curve models for the single apartment and the townhouse were built on the weekly electricity use by excluding the lockdown period. Figure 16 presents their weekly-based ES curve models, where the orange dots are for the apartment and the blue dots for the townhouse. The CPT of 13°C gave a proper division between the temperature-dependent and temperature-independent electricity use in the apartment. Meanwhile, the relatively low electricity density in the townhouse made it follow the same linear relation over the whole outdoor temperature range without a CPT. When the outdoor temperature was below the CPT, the slope for the apartment was steeper than the townhouse. When the outdoor temperature was close and above the CPT, the slopes for the two residential buildings were close. This implied that when it was cold outside, the share of electricity used for space heating in the apartment was much higher than in the townhouse.

Table 3 gives the coefficients and the accuracy evaluation of the ES curve models for all the observed buildings for Scenario 1. Accuracy of

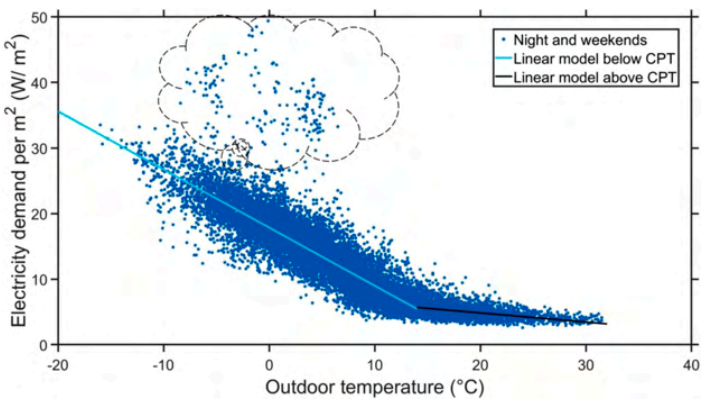

Figure 17. Energy signature curve models for kindergartens for Scenario 2

Table 4
Coefficients and accuracy of the ES curve models for Scenario 2

	Coefficients of model			Accuracy of model	
Building type	CPT (°C)	p_1	p_2	R^2	MAPE (%)
Kindergarten	14	-0.9 (≤ 14°C) -0.1 (>14°C)	17.9 (≤ 14°C) 7.6 (>14°C)	0.76	15.9
School	14	-0.7 (≤ 14°C) -0.1 (>14°C)	15.4 (≤ 14°C) 7.1 (>14°C)	0.75	19.4

the regression models were evaluated by two criteria, the coefficient of determination (R^2) and the mean absolute percentage error (MAPE). Except for the townhouse, the ES curve models for all the other building types had the R^2 higher than 0.75 and the MAPE lower than 20%, which meant they all satisfied the requirements of ASHEAE Guidelines for carrying out a satisfying model [42, 43]. The lower R^2 for the regression model in the townhouse might be explained by the relatively low share of electricity used for space heating purpose, while the other electric appliances accounted for a reasonably high share of electricity accordingly. It led to the linear relationship between the outdoor temperature and electricity not as strong as the other building types, where the space heating was only supplied by the electricity. However, according to the proposal from Henseler that R^2 with 0.5 is moderate in scholarly research as a rule thumb [44]. Also, the MAPE of the model for the townhouse was lower than 20% as required in [45] for a good forecasting. Therefore, the ES curve model for the townhouse was regarded qualified at some extent and may be utilized for a rough identification of profile in TMY in the following section.

As explained in Section 2.3, Scenario 2 considered the electricity demand level for buildings with low attendance during nighttime and weekends under normal situation. This energy-saving mode was regarded as the hypothesis of the operation mode that the kindergartens and schools should have adopted during the temporary closure.

The ES curve models for the kindergartens were carried out on hourly-based data, see Figure 17. It was noted that there were some outliers, marked within the dashed cloud. This must be caused by the occasional activities held during the weekends with high use of lighting, ventilation, and other appliances, as mentioned in Section 3.1. The ES curve models for schools were similar with kindergartens, and they are shown in Figure A2. The coefficients and the accuracy criteria of the ES curve models for kindergartens and schools under Scenario 2 are briefed in Table 4. The CPT of the two building types were still noted at 14°C with proper piecewise regression. The MAPE for the two building types were below 20%, and R^2 for the two building types are no less than 0.75. The ES curve models for the educational buildings meet the ASHRAE requirement of satisfying regression models.

Scenario 3 meant to identify the electricity use when the work-at-home regime was adopted. The weekly-based ES curve models for the two residential buildings under Scenario 3 are plotted in Figure 18. There was a noticeable higher electricity demand for the apartment under Scenario 3 than Scenario 1 (Figure 16), within the same outdoor temperature range. It indicated that there was higher electricity impact on the apartment, which was also consistent with the findings in the average daily profiles and ED results above. Because of the relatively small range of outdoor temperature during the work-at-home period, one linear model was sufficiently identified for the apartment without a CPT.

Table 5 gives the coefficients and the accuracy criteria of the ES curve models for the two residential buildings under Scenario 3. The R^2 for the two building types were higher than 0.8, and the MAPEs were below 10%, indicating these ES curve models were accurate to be used in the following work.

3.3. Scenario-based electricity profiles

A yearly electricity use profile may be predicted by combining the regression coefficients defined in Section 3.2 and the outdoor temperature in a typical weather year. Figure 19- Figure 21 illustrate the possible electricity profiles for kindergartens, schools, the single apartment, and the townhouse.

As shown by the solid red lines in Figure 19 and Figure 20, kindergartens and schools needed 172 kWh and 139 kWh electricity per m^2 in a typical year, under the normal operation settings (Scenario 1). These demand values were lower than the Norwegian Statistics, 183 kWh/(m^2•yr) for kindergartens and 167 kWh/(m^2•yr) for schools [38]. While under the energy-saving mode (Scenario 2), only 112 kWh/m^2 was needed in kindergartens and 99 kWh/m^2 in schools in a TMY, as shown by the green dashed lines. From the comparison between the two building management modes, it indicated that there was a remarkable energy saving potential during a temporary shutdown. By implementing proper settings for the building service systems and improving the arrangement of the educational institutions, the electricity use may be reduced by approximately 35% in the kindergartens and 29% in the

Table 5
Coefficients and Accuracy of the ES curve models for Scenario 3

	Coefficients of model			Accuracy of model	
Building type	CPT (°C)	p_1	p_2	R^2	MAPE (%)
Apartment	/	-1.6	41.9	0.88	8.1
Townhouse	/	-0.5	17.7	0.84	9.2

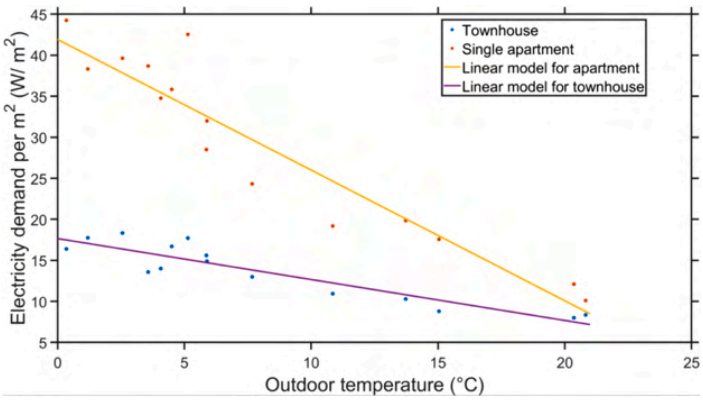

Figure 18. Energy signature curve models for the single apartment and the townhouse for Scenario 3

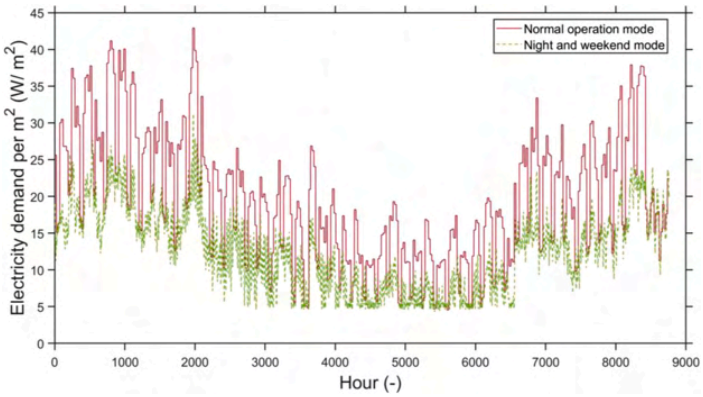

Figure 19. Annual electricity profiles for kindergartens under Scenario 1 and Scenario 2

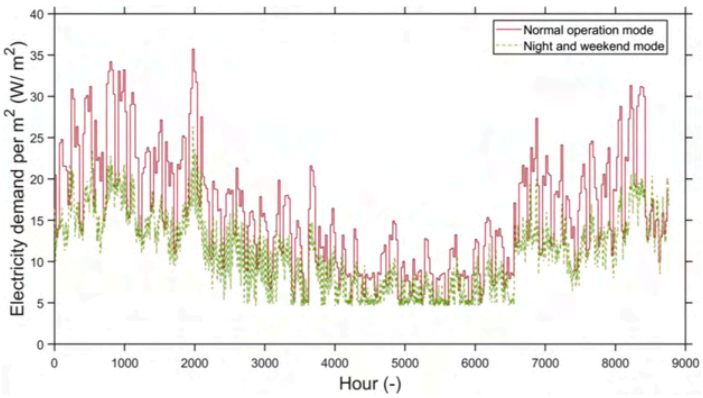

Figure 20. Annual electricity profiles for schools under Scenario 1 and Scenario 2

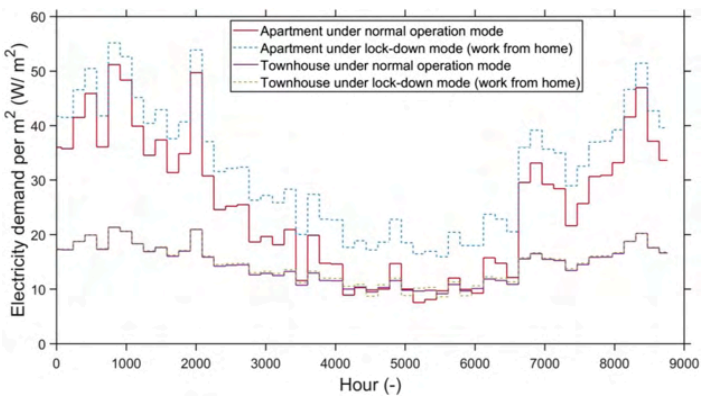

Figure 21. Annual electricity profiles for the single apartment and the townhouse under Scenario 1 and Scenario 3

schools. Since kindergartens usually have longer opening hour and higher indoor temperature requirements than schools, it explains kindergartens may have 6% more electricity reduction possibility than schools.

Regarding the scenario comparison in the residential buildings, the impact on the specific electricity demand was much higher in the single apartment than in the townhouse, as plotted in Figure 21. Under the normal situation when the daytime attendance was low, the annual electricity demand of a typical year was 222 kWh/m^2 and 126 kWh/m^2 in the apartment and townhouse, respectively, as shown in the solid

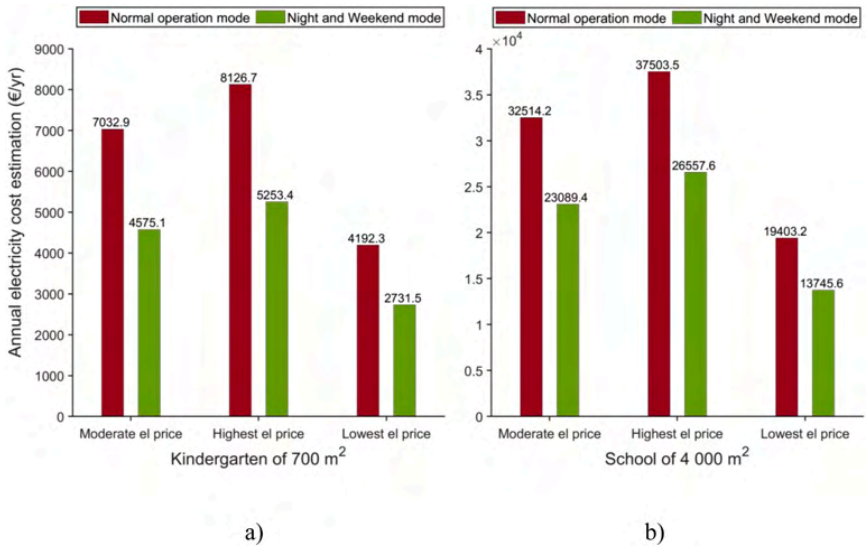

Figure 22. Annual electricity cost estimation of kindergartens and schools under two operation scenarios, where a) annual cost of kindergartens, b) annual cost of schools

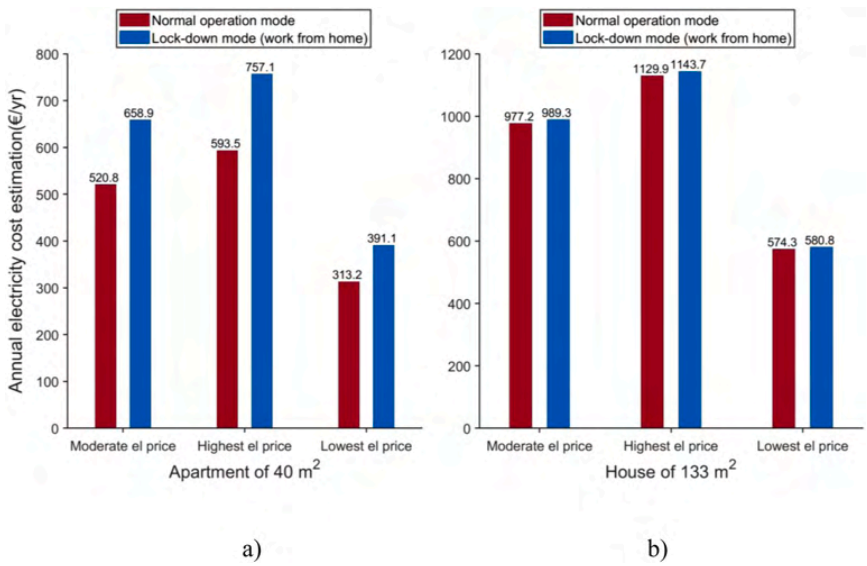

Figure 23. Annual electricity cost estimation of the single apartment and the townhouse under two operation scenarios, where a) annual cost of the apartment, b) annual cost of the townhouse

lines. Comparing with the Norwegian Statistics of the average energy use per household, this apartment used 20% more energy than the average level, and this townhouse used 14% less electricity than the average level (the fuel of wood was not considered) [18]. However, when the rule of work-at-home was in effect, 26.9% more electricity was needed in the apartment, while the townhouse only required 1.3% more electricity, as shown in the dashed lines. Again, the higher electricity density in the single apartment makes it more sensitive after the use pattern changed. Unlike the educational institutions, it may not be straightforward to point out the energy saving potential in the residential buildings. The possibilities and measures to save electricity can be realized by upgrading the building energy supply methods in the apartment building or its neighborhood community, for example, to introduce ground source heat pump, or connect to a district heating network if available [46–48].

3.4. Results of economic costs calculation

By combining the predicted electricity profiles defined in Section 3.3 and the three price levels described in Section 2.5, the annual electricity

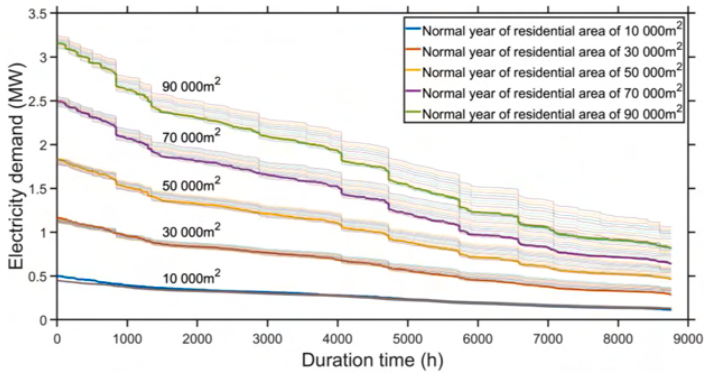

Figure 24. Electricity duration curves for different residential building areas, comparing normal year with lockdown year when varying percentages of work-from-home

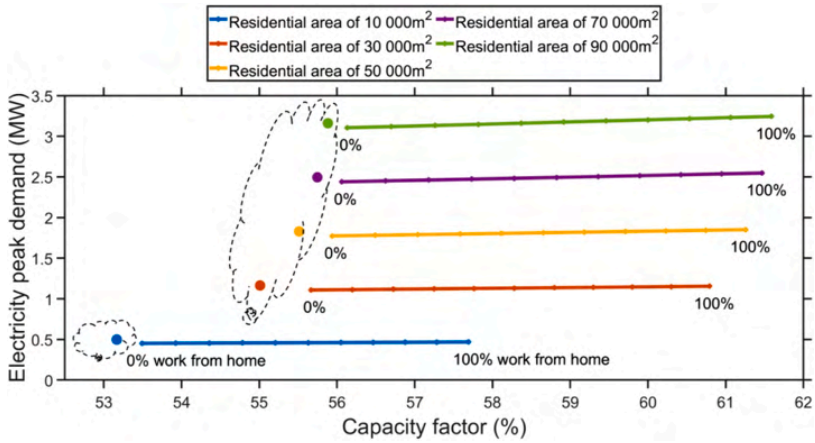

Figure 25. Capacity factor vs electricity peak demand for different residential building areas, comparing normal year with lockdown year when varying percentages of work-from-home adoption

costs for the four building types were estimated according to the three price cases.

In the educational buildings, the building area of kindergartens and schools was assigned with the Norwegian average area of 700 m^2 and 4 000 m^2, respectively [38]. Figure 22 compares the annual electricity costs of one representative kindergarten and one representative school under the normal operation mode (Scenario 1) and the night and weekend mode (Scenario 2), where moderate el price, highest el price, and lowest el price are the shortcuts of the cases of moderate, highest, and lowest electricity price. For the kindergarten, the cost reductions between the two running modes varied from 1 461 €/yr (equivalent as 2.1 €/(m^2.yr)) under the case of lowest electricity price to 2 873 €/yr (4.1 €/(m^2.yr)) under the case of highest electricity price, see Figure 22a. For the school, Figure 22b exhibits that between 5 658 €/yr (1.4 €/(m^2.yr)) and 10 946 €/yr (2.7 €/(m^2.yr)) may be saved if the building was shifted to the night and weekend settings during lockdown. It is worthy noted that the economic saving potential from switching operation mode was greater when the electricity price was higher. It further emphasized the importance of carrying out energy-efficient operation strategy during low attendance on campus.

In the residential buildings, the economic impacts were interpreted differently from the educational buildings. Due to more time spent at home by the dwellers, between 78 - 164 € (2.0 €/(m^2.yr) - 4.1 €/(m^2.yr)) more money may be needed in the apartment, see Figure 23a, while the increase would be less than 15 € (0.1 €/(m^2.yr)) in the townhouse, see Figure 23b. Although the larger dwelling of multi family members required higher total electricity expenditure than the smaller single apartment, they might act more robust in the changes of the use patterns.

To sum up, based on the findings from both energy and economic point of view, the yearly electricity costs were dependent both on the building management settings and the power market price. For example, at the lowest electricity price level, the expenses for normal operation in both kindergarten and school were still lower than the energy-efficient mode concerning the other two price cases. It was similar as in the residential buildings, the home office mode at the lowest price level might even cause less expenditures than the others.

4. Discussions and limitations of this study

In this study, there are three points worthy to be discussed.

Firstly, in these observed buildings, there are no submeters for separating the electricity used for heating purpose, lighting, and appliances. However, based on the evaluation results of the model accuracy, the R^2 and the MAPE, most of the developed ES curve models met the requirement of satisfying regression models, mainly because a large

Table A1
Peak demand and its changes regarding different residential area under normal condition and changing percentage of work-from-home adoption

Residential area (m^2)	Peak demand (MW) – normal condition	Percentage of work-from-home adoption (%)	Peak demand (MW) – work-from-home	Percentage changes of the peak demand (%)
10 000	0.498	0	0.452	-9.3
		10	0.453	-9.0
		50	0.460	-7.7
		100	0.468	-6.1
30 000	1.164	0	1.108	-4.8
		10	1.113	-4.4
		50	1.132	-2.8
		100	1.155	-0.8
50 000	1.829	0	1.774	-3.0
		10	1.782	-2.6
		50	1.813	-0.9
		100	1.851	1.2
70 000	2.495	0	2.439	-2.2
		10	2.450	-1.8
		50	2.494	-0.1
		100	2.548	2.1
90 000	3.160	0	3.105	-1.8
		10	3.119	-1.3
		50	3.175	0.5
		100	3.244	2.6

share of electricity goes to space heating. During the pandemic, the energy response of the buildings may be region and country related, which may be influenced by the building function, social aspects, and rule tightness [10, 11, 49]. Therefore, it is worthy using the ES curve models as a robust and fast method to predict the electricity demand based on different operation strategies, especially for buildings without submeters. However, the model accuracy may be weaker such as in low energy building and passive house, where space heating accounts for lower energy share.

Secondly, the COVID-19 related impacts on the buildings' annual CO_2 emissions were not included. It was considered adequate to identify the electricity demand changes and possible energy saving potential, because the change percentage of the CO_2 emissions would be the same as demand changes regardless of the CO_2 factors. However, it will still be interesting to find credible source of CO_2 factor and investigate the CO_2 emissions in response to future unforeseeable disruption.

Thirdly, the consequence on the local energy planning was discussed based on the example of the imaginary community by following Eqs.(4) and (5) in Section 2.6, where A_{kind}, A_{sch}, and A_{resi} were chosen with 700 m^2, 4000 m^2, 10 000 – 90 000 m^2 with each step of 20 000 m^2, respectively. As shown in Figure 24, the thick lines represent the electricity duration curves in the normal year, and the thin lines represent the electricity duration curves in the lockdown year by varying the percentages of work-from-home adoption from 0% to 100%. For each residential area group, the 0% of work-from-home adoption is shown with the lowest line, and the 100% is shown with the highest line. It is apparent that the duration curves in the normal year are steeper than most of the work-from-home conditions for all the residential area groups.

Figure 25 further compares the capacity factor with the electricity peak demand regarding different residential areas. The solid circles in the dashed cloud line stand for the normal year condition. The lockdown year's result for each residential area is shown with the solid line by varying work-from-home adoption from 0% to 100%. As noted in Figure 25, normal year had lower plant capacity factor and needed higher peak demand than some of work-from-home conditions for the smaller residential areas (e.g. 10 000 – 50 000 m^2). It is interesting to see the energy utilities may not be fully utilized in normal year, which may lead to uneconomic production. In the larger residential areas (e.g. 70 000 – 90 000 m^2), although the plant capacity can be better used with a higher capacity factor, it may require higher peak demand during the lockdown. For example, the percentage changes of the peak demand for the residential area of 10 000 m^2 were between -9.3% and -6.1% from 0% to 100% of work-from-home adoption, and these changes for the residential area of 90 000 m^2 were between -1.8% and 2.6% from 0% to 100% of work-from-home adoption. It may be explained as the saved electricity from the closed kindergarten and school may not be comparable with the more electricity being used when most of the residents stay at home, for a larger residential area. The detailed changes regarding each residential area are listed in Table A1.

From this example, it may be concluded that the local infrastructure sizing may be influenced by different aspects, such as the areas of residential and educational buildings, energy operation mode, and some unintended conditions. As suggested in a study of one university campus with multiple building functions [50], an appropriate building type ratio would be helpful to reduce the total load and load fluctuation of a district. Therefore, it is important to analyze the energy demand under different scenarios to discover the optimal sizing in the future planning.

Since the lockdown regime in Norway was in effect from mid-March to early May 2020, the outdoor temperature during this period (0 - 21°C on weekly base) did not cover the local historical outdoor temperature range throughout a year (such as -7 - 21°C on weekly base in 2019), especially the recorded low temperature in winter. Hence, the extrapolation of the Scenario 3 based ES curve models to the TMY might not fully represent the annual household electricity profile. The increased annual household electricity demand (especially in winter) may be higher than the estimation in this study, by extrapolating the electricity characteristics under the limited outdoor temperature range during the lockdown. Moreover, as shown in the results, the electricity use density to the outdoor temperature in the apartment was much higher than in the townhouse, making the deviation even larger for the apartment than for the townhouse. To better prepare for the future unforeseen disruptions as well as the trends of workplace and lifestyle, more data and/or seasonal correction factors are necessary for further study, for example, to take experiment of home office activities involving more dwellings. This may present a more comprehensive insight with more accurate forecasting models and better knowledge.

5. Conclusion

The COVID-19 pandemic has put heavy stress and crucial challenges around the world. Accordingly, many countries have carried out confinement regulation to hinder the infection spreading. Due to the changed work regime, the significant impacts on energy sectors have been seen in many countries. This study was focused to analyze the electricity profiles and the relevant changes in Norwegian buildings with electric heating. Two Norwegian educational building types at municipal level (kindergartens and schools) and two Norwegian residential buildings (a single apartment and a townhouse) during the lockdown were studied on the measured data.

The scenario-based analysis in this study was mainly made for identifying the possible electricity demand and corresponding electricity increase and saving potential at a macro scale if new disruption would be introduced. To achieve the aim, the article developed the three scenarios regarding the different building operation strategies. Scenario 1 modeled the electricity use under normal conditions, Scenario 2 modeled the electricity on settings during normal weekdays' nighttime and weekends for kindergartens and schools, and Scenario 3 modeled the household electricity use under the work-at-home conditions.

The work was conducted as follows. The average daily electricity profiles before and during the lockdown were identified. It was found that there were almost no changes of electricity use pattern in the two educational building types, but there was demand variation in the residential buildings. The ES curve models were then developed for describing the electricity characteristics under each scenario. Most of the models were qualified as satisfying regression models by evaluating

with the accuracy criteria R^2 and MAPE. These scenario-based ES curve models were used for making annual electricity profiles in a typical weather year. Under Scenario 1, around 172 kWh_{el}/m^2 and 139 kWh_{el}/m^2 were needed in a TMY for kindergartens and schools, respectively. These electricity use could be reduced by 35% for kindergartens and by 29% for schools, with proper building operation during a temporary closure, as suggested by Scenario 2. Meanwhile, when the dwellers' schedules changed into home office regime (Scenario 3), approximately 27% and 1.3% more electricity were required for the single apartment and the townhouse, respectively. The small apartment with higher electricity density made it more electricity sensitive than the large house, especially during the lockdown period. The annual power bills were estimated in three spot price level cases, showing that more expensive electricity yielded bigger driving forces to adopt better building management. With proper settings, between 2.1 - 4.1 €/(m^2.yr) may be saved for kindergartens, and 1.4 - 2.7 €/(m^2.yr) for schools. The apartment may spend 2.0 - 4.1 €/(m^2.yr) more for electricity, while the increased bill for the townhouse may be trivial.

The analysis on the aggregated electricity demand showed that the local infrastructure sizing may be influenced by the areas of residential and educational buildings, energy operation mode, and some unintended conditions. For the residential area of 10 000 m^2, the percentage changes of the peak demand were between -9.3% and -6.1% from 0% to 100% of work-from-home adoption, and these changes for the residential area of 90 000 m^2 were between -1.8% and 2.6%. Therefore, it is important to analyze the energy demand under different scenarios to discover the optimal sizing in the future planning.

The methods and results of this article may be useful to similar or other building types in response to future unforeseeable disruption, especially the buildings in the similar climatic conditions.

Declaration of Competing Interest

The authors declare that they have no known competing financial interests or personal relationships that could have appeared to influence the work reported in this paper.

Acknowledgement

This article has been written within the research project "Methods for Transparent Energy Planning of Urban Building Stocks– ExPOSe" and "Energy for domestic hot water in the Norwegian low emission society". The authors gratefully acknowledge the support from the Research Council of Norway (ExPOSe programme with funding number 268248 and ENERGIX-programme with funding number 267635), Department of Energy and Process Engineering of NTNU, and Trondheim Municipality.

Appendix A

Figure A1, A2 and Table A1

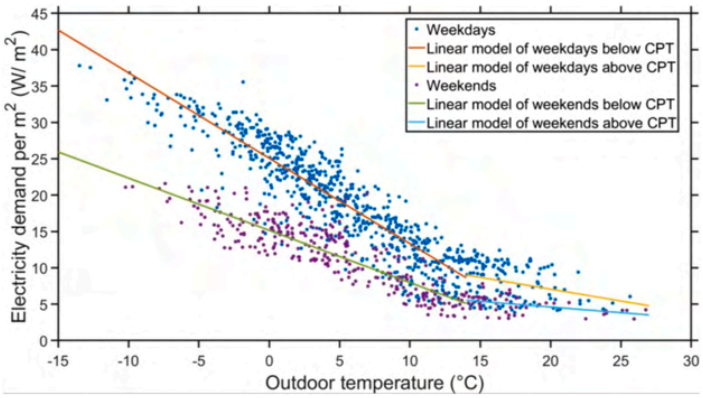

Figure A1. Energy signature curve models for schools for Scenario 1

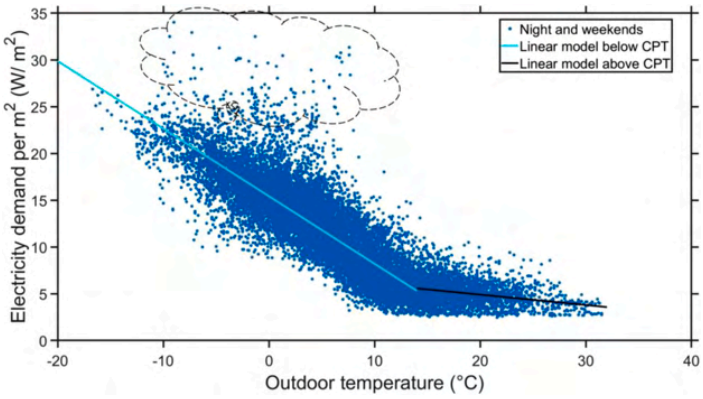

Figure A2. Energy signature curve models for schools for Scenario 2

References

[1] "Coronavirus (COVID-19) events as they happen." https://www.who.int/emergencies/diseases/novel-coronavirus-2019/events-as-they-happen (accessed Feb. 24, 2021).

[2] Abu-Rayash, A., & Dincer, I. (Oct. 2020). Analysis of the electricity demand trends amidst the COVID-19 coronavirus pandemic. *Energy Research & Social Science, 68*, Article 101682. https://doi.org/10.1016/j.erss.2020.101682

[3] Burleyson, C., Smith, A. D., Rice, J. S., Voisin, N., & Rahman, A. (Jul. 2020). Changes in Electricity Load Profiles Under COVID-19: Implications of 'The New Normal' for Electricity Demand. *engrXiv*. https://doi.org/10.31224/osf.io/trs57

[4] Rouleau, J., & Gosselin, L. (Apr. 2021). Impacts of the COVID-19 lockdown on energy consumption in a Canadian social housing building. *Applied Energy, 287*, Article 116565. https://doi.org/10.1016/j.apenergy.2021.116565

[5] Zanocco, C., Flora, J., Rajagopal, R., & Boudet, H. (Apr. 2021). Exploring the effects of California's COVID-19 shelter-in-place order on household energy practices and intention to adopt smart home technologies. *Renewable and Sustainable Energy Reviews, 139*, Article 110578. https://doi.org/10.1016/j.rser.2020.110578

[6] Carvalho, M., de M. Delgado, D. B., de Lima, K. M., de C. Cancela, M., dos Siqueira, C. A., & de Souza, D. L. B. (2021). Effects of the COVID-19 pandemic on the Brazilian electricity consumption patterns. *International Journal of Energy Research, 45*(2), 3358–3364. https://doi.org/10.1002/er.5877

[7] Liu, A., Miller, W., Crompton, G., & Zedan, S. (Mar. 2021). Has COVID-19 lockdown impacted on aged care energy use and demand? *Energy and Buildings, 235*, Article 110759. https://doi.org/10.1016/j.enbuild.2021.110759

[8] C. Birch, R. Edwards, S. Mander, and A. Sheppard, "Electrical consumption in the Higher Education sector, during the COVID-19 shutdown," in *2020 IEEE PES/IAS PowerAfrica*, Aug. 2020, pp. 1–5. doi: 10.1109/PowerAfrica49420.2020.9219901.

[9] Cvetković, D., Nešović, A., & Terzić, I. (Jan. 2021). Impact of people's behavior on the energy sustainability of the residential sector in emergency situations caused by COVID-19. *Energy and Buildings, 230*, Article 110532. https://doi.org/10.1016/j.enbuild.2020.110532

[10] Geraldi, M. S., Bavaresco, M. V., Triana, M. A., Melo, A. P., & Lamberts, R. (Jun. 2021). Addressing the impact of COVID-19 lockdown on energy use in municipal buildings: A case study in Florianópolis, Brazil. *Sustainable Cities and Society, 69*, Article 102823. https://doi.org/10.1016/j.scs.2021.102823

[11] Bahmanyar, A., Estebsari, A., & Ernst, D. (Oct. 2020). The impact of different COVID-19 containment measures on electricity consumption in Europe. *Energy Research & Social Science, 68*, Article 101683. https://doi.org/10.1016/j.erss.2020.101683

[12] T. Lowder, N. Lee, and J. Leisch, "COVID-19 and the Power Sector in Southeast Asia: Impacts and Opportunities," National Renewable Energy Lab. (NREL), Golden, CO (United States), NREL/TP-7A40-76963, Jun. 2020. doi: https://doi.org/10.2172/1665768.

[13] Ruan, G., Wu, J., Zhong, H., Xia, Q., & Xie, L. (Mar. 2021). Quantitative assessment of U.S. bulk power systems and market operations during the COVID-19 pandemic. *Applied Energy, 286*, Article 116354. https://doi.org/10.1016/j.apenergy.2020.116354

[14] Madurai Elavarasan, R., et al. (Dec. 2020). COVID-19: Impact analysis and recommendations for power sector operation. *Applied Energy, 279*, Article 115739. https://doi.org/10.1016/j.apenergy.2020.115739

[15] Zhong, H., Tan, Z., He, Y., Xie, L., & Kang, C. (Sep. 2020). Implications of COVID-19 for the electricity industry: A comprehensive review. *CSEE Journal of Power and Energy Systems, 6*(3), 489–495. https://doi.org/10.17775/CSEEJPES.2020.02500

[16] Kalmár, T., & Kalmár, F. (Mar. 2021). Investigation of natural aeration in home offices during the heating season – case study. *Journal of Building Engineering, 35*, Article 102052. https://doi.org/10.1016/j.jobe.2020.102052

[17] Domínguez-amarillo, S., Fernández-agüera, J., Cesteros-garcía, S., & R., A (2020). González-lezcano, "Bad air can also kill: Residential indoor air quality and pollutant exposure risk during the covid-19 crisis. *International Journal of Environmental Research and Public Health, 17*(19), 1–34. https://doi.org/10.3390/ijerph17197183

[18] Statistics Norway, "Energy and manufacturing," *ssb.no*. https://www.ssb.no/en/energi-og-industri (accessed Jan. 28, 2021).

[19] A. Kofoed-Wiuff, K. Dyhr-Mikkelsen, I. S. Rueskov, and K. Brunak, "Tracking Nordic Clean Energy Progress 2019," p. 28.

[20] "EE Noon: Back to School with Energy Efficiency," *Alliance to Save Energy*, Aug. 14, 2013. https://www.ase.org/events/ee-noon-back-school-energy-efficiency (accessed Feb. 24, 2021).

[21] "iEOS - Planning." https://www2.esave.no/Esave.nsf/iEOS_Hovedbilde.xsp (accessed Feb. 24, 2021).

[22] "Tensio - NTE Nett og TrønderEnergi Nett har blitt til Tensio," *Tensio.no*. https://tensio.no/(accessed Feb. 24, 2021).

[23] "Norsk Klimaservicesenter." https://seklima.met.no/observations/(accessed Feb. 24, 2021).

[24] Frederiksen, S., & Werner, S. (2013). District Heating and Cooling. *Studentlitteratur AB*.

[25] Hitchin, R., & Knight, I. (Jan. 2016). Daily energy consumption signatures and control charts for air-conditioned buildings. *Energy and Buildings, 112*, 101–109. https://doi.org/10.1016/j.enbuild.2015.11.059

[26] Ghiaus, C. (Jun. 2006). Experimental estimation of building energy performance by robust regression. *Energy and Buildings, 38*(6), 582–587. https://doi.org/10.1016/j.enbuild.2005.08.014

[27] J. L. M. Hansen and R. Lamberts, "Building Performance Simulation for Design and Operation," Routledge & CRC Press. https://www.routledge.com/Building-Performance-Simulation-for-Design-and-Operation/Hensen-Lamberts/p/book/9781138392199 (accessed Feb. 27, 2021).

[28] "JRC Photovoltaic Geographical Information System (PVGIS) - European Commission." https://re.jrc.ec.europa.eu/pvg_tools/en/tools.html#TMY (accessed Feb. 24, 2021).

[29] ASHRAE, "ASHRAE Epidemic Task Force Releases Updated Building Readiness Guide | ashrae.org." https://www.ashrae.org/about/news/2021/ashrae-epidemic-task-force-releases-updated-building-readiness-guide (accessed Feb. 27, 2021).

[30] "See market data for all areas." https://www.nordpoolgroup.com/Market-data1/(accessed Feb. 24, 2021).

[31] "Electricity price statistics - Statistics Explained." https://ec.europa.eu/eurostat/statistics-explained/index.php/Electricity_price_statistics#Electricity_prices_for_non-household_consumers (accessed Feb. 27, 2021).

[32] Seem, J. E. (Jan. 2007). Using intelligent data analysis to detect abnormal energy consumption in buildings. *Energy and Buildings, 39*(1), 52–58. https://doi.org/10.1016/j.enbuild.2006.03.033

[33] Rosner, B. (1983). Percentage Points for a Generalized ESD Many-Outlier Procedure. *Technometrics, 25*(2), 165–172. https://doi.org/10.2307/1268549

[34] Conejo, A. J., Plazas, M. A., Espinola, R., & Molina, A. B. (May 2005). Day-ahead electricity price forecasting using the wavelet transform and ARIMA models. *IEEE Transactions on Power Systems, 20*(2), 1035–1042. https://doi.org/10.1109/TPWRS.2005.846054

[35] Weron, R. (Oct. 2014). Electricity price forecasting: A review of the state-of-the-art with a look into the future. *International Journal of Forecasting, 30*(4), 1030–1081. https://doi.org/10.1016/j.ijforecast.2014.08.008

[36] Nowotarski, J., & Weron, R. (Jan. 2018). Recent advances in electricity price forecasting: A review of probabilistic forecasting. *Renewable and Sustainable Energy Reviews, 81*, 1548–1568. https://doi.org/10.1016/j.rser.2017.05.234

[37] J. Morales Pedraza, "Chapter 4 - Current Status and Perspective in the Use of Coal for Electricity Generation in the North America Region," in *Conventional Energy in North America*, J. Morales Pedraza, Ed. Elsevier, 2019, pp. 211–257. doi: 10.1016/B978-0-12-814889-1.00004-8.

[38] Norges vassdrags- og energidirektorat, "Analyse av energibruk i undervisningsbygg," p. 120.

[39] Hong, T., Yan, D., D'Oca, S., & Chen, C. (Mar. 2017). Ten questions concerning occupant behavior in buildings: The big picture. *Building and Environment, 114*, 518–530. https://doi.org/10.1016/j.buildenv.2016.12.006

[40] Barthelmes, V. M., Li, R., Andersen, R. K., Bahnfleth, W., Corgnati, S. P., & Rode, C. (Oct. 2018). Profiling occupant behaviour in Danish dwellings using time use survey data. *Energy and Buildings, 177*, 329–340. https://doi.org/10.1016/j.enbuild.2018.07.044

[41] Ma, Z., Yan, R., & Nord, N. (2017). A variation focused cluster analysis strategy to identify typical daily heating load profiles of higher education buildings. *Energy, 134*, 90–102. https://doi.org/10.1016/j.energy.2017.05.191

[42] American Society of Heating Refrigerating and Air Conditioning Engineers, *2013 ASHRAE handbook: fundamentals*.2013. Accessed: Feb. 27, 2021. [Online]. Available: http://app.knovel.com/hotlink/toc/id:kpASHRAEC1/2013-ashrae-handbook.

[43] Menard, S. (Feb. 2000). Coefficients of Determination for Multiple Logistic Regression Analysis. *The American Statistician, 54*(1), 17–24. https://doi.org/10.1080/00031305.2000.10474502

[44] J. Henseler, C. M. Ringle, and R. R. Sinkovics, "The use of partial least squares path modeling in international marketing," in New Challenges to International Marketing, vol. 20, R. R. Sinkovics and P. N. Ghauri, Eds. Emerald Group Publishing Limited, 2009, pp. 277–319. doi: 10.1108/S1474-7979(2009)0000020014.

[45] Meade, N. (1983). Industrial and business forecasting methods, Lewis, C.D., Borough Green, Sevenoaks, Kent: Butterworth, 1982. Price: £9.25. Pages: 144. *Journal of Forecasting, 2*(2), 194–196. https://doi.org/10.1002/for.3980020210

[46] Möller, B., Wiechers, E., Persson, U., Grundahl, L., Lund, R. S., & Mathiesen, B. V. (Jun. 2019). Heat Roadmap Europe: Towards EU-Wide, local heat supply strategies. *Energy, 177*, 554–564. https://doi.org/10.1016/j.energy.2019.04.098

[47] Østergaard, P. A., Jantzen, J., Marczinkowski, H. M., & Kristensen, M. (Aug. 2019). Business and socioeconomic assessment of introducing heat pumps with heat storage in small-scale district heating systems. *Renewable Energy, 139*, 904–914. https://doi.org/10.1016/j.renene.2019.02.140

[48] Soltani, M., et al. (Jan. 2019). A comprehensive study of geothermal heating and cooling systems. *Sustainable Cities and Society, 44*, 793–818. https://doi.org/10.1016/j.scs.2018.09.036

[49] Chen, C., et al. (Mar. 2020). Culture, conformity, and carbon? A multi-country analysis of heating and cooling practices in office buildings. *Energy Research & Social Science, 61*, Article 101344. https://doi.org/10.1016/j.erss.2019.101344

[50] Chen, S., et al. (Nov. 2019). An energy planning oriented method for analyzing spatial-temporal characteristics of electric loads for heating/cooling in district buildings with a case study of one university campus. *Sustainable Cities and Society, 51*, Article 101629. https://doi.org/10.1016/j.scs.2019.101629

A.4 Paper IV

A study on data-driven hybrid heating load prediction methods in low-temperature district heating: an example for nursing homes in Nordic countries

Ding, Y., Timoudas, T.O., Wang, Q., Chen, S., Brattebø, H. and Nord, N.

Energy Conversion and Management, p.116163, 2022.

Energy Conversion and Management 269 (2022) 116163

Contents lists available at ScienceDirect

Energy Conversion and Management

journal homepage: www.elsevier.com/locate/enconman

A study on data-driven hybrid heating load prediction methods in low-temperature district heating: An example for nursing homes in Nordic countries

Yiyu Ding [a,*], Thomas Ohlson Timoudas [b], Qian Wang [c,d], Shuqin Chen [e], Helge Brattebø [a], Natasa Nord [a]

[a] Department of Energy and Process Engineering, Norwegian University of Science and Technology (NTNU), Trondheim 7491, Norway
[b] RISE Research Institutes of Sweden, Sweden
[c] Department of Civil and Architectural Engineering, KTH Royal Institute of Technology, Brinellvägen 23, Stockholm 100 44, Sweden
[d] Uponor AB, Hackstavägen 1, Västerås 721 32, Sweden
[e] College of Civil Engineering and Architecture, Zhejiang University, Hangzhou 310058, China

ARTICLE INFO

Keywords:
Nursing homes
District heating load prediction
Linear regression
Artificial neural network
Low-temperature district heating

ABSTRACT

In the face of green energy initiatives and progressively increasing shares of more energy-efficient buildings, there is a pressing need to transform district heating towards low-temperature district heating. The substantially lowered supply temperature of low-temperature district heating broadens the opportunities and challenges to integrate distributed renewable energy, which requires enhancement on intelligent heating load prediction. Meanwhile, to fulfill the temperature requirements for domestic hot water and space heating, separate energy conversion units on user-side, such as building-sized boosting heat pumps shall be implemented to upgrade the temperature level of the low-temperature district heating network. This study conducted hybrid heating load prediction methods with long-term and short-term prediction, and the main work consisted of four steps: (1) acquisition and processing of district heating data of 20 district heating supplied nursing homes in the Nordic climate (2016–2019); (2) long-term district heating load prediction through linear regression, energy signature curve in hourly resolution, providing an overall view and boundary conditions for the unit sizing; (3) short-term district heating load prediction through two Artificial Neural Network models, f_{72} and g_{120}, with different prediction input parameters; (4) evaluation of the predicted load profiles based on the measured data. Although the three prediction models met the quality criteria, it was found that including the historical hourly heating loads as the input to the forecasting model enhanced the prediction quality, especially for the peak load and low-mild heating season. Furthermore, a possible application of the heating load profiles was proposed by integrating two building-sized heat pumps in low-temperature district heating, which may be a promising heat supply method in low-temperature district heating.

1. Introduction

The background, literature review, and objective of this study are presented in Sections 1.1–1.3, respectively.

1.1. Background

In 2019, the building sector accounted for 35% of the global final energy use and 38% of energy-related CO_2 emissions [1]. Although there was a drop in CO_2 emissions in 2020, mainly due to the COVID-19 pandemic, the building sector's share of the final energy use and CO_2 emissions that year were 36% and 37%, respectively, almost the same as in 2019 [2].

District heating (DH) systems play a vital role in reducing primary energy use and CO_2 emissions in the building sector. In general, the primary energy factor may vary due to variation of the fuel and incentives within national policies. In the European context electricity has a primary energy factor of 2–2.5 [3], while DH of 0.6–1.3 depending on the heating sources varying from renewable-based to fossil-based fuels [4]. For example, in Sweden DH supplies 60% of the total building heating demand [5], while in Norway DH use has doubled over the past

* Corresponding author.
E-mail address: yiyu.ding@ntnu.no (Y. Ding).

https://doi.org/10.1016/j.enconman.2022.116163
Received 9 April 2022; Received in revised form 16 July 2022; Accepted 18 August 2022
Available online 27 August 2022
0196-8904/© 2022 The Authors. Published by Elsevier Ltd. This is an open access article under the CC BY license (http://creativecommons.org/licenses/by/4.0/).

Nomenclature

ANN	artificial neural network
ASHRAE	American Society of Heating, Refrigerating and Air-Conditioning Engineers
CPT	changing point temperature
CV(RMSE)	coefficient of variation of the root mean squared error
DC	datacenter
DHW	domestic hot water
ES curve	energy signature curve
f_{72}	ANN model with 72 input units defined in this study
g_{120}	ANN model with 120 input units defined in this study
HDD	heating degree day
HP	heat pump
LTDH	low-temperature district heating
(s)MAPE	(symmetric) mean absolute percentage error
NMBE	normalized mean bias error
SH	space heating
WD	weekday
WE	weekend
el	electricity
€	EUR (currency)
n	number of observations
R^2	coefficient of determination
t_τ	outdoor ambient temperature at time instance τ
yr	year

decade, and currently 26.7% of DH production is used for the residential heating and 54.5% of DH production for the service heating [6]. Given the rapid electrification process in buildings, and in countries like Norway also in the transportation sector, DH has great potentials to alleviate the pressure on power grid in climates with high heating demands, such as the Nordic countries. However, DH expansion also faces two challenges, the competition from heat pumps (HPs) due to their high flexibility for the end users and consequent reduction in the final energy demand, and the decrease in the building heating demand. For the latter, this is due to the future building stock, with a growing share of renovated existing buildings, low-energy buildings, passive houses, and nearly zero energy/emission buildings (nZEB), are commonly characterized by improved building envelope, space heating (SH) demand will be greatly reduced, as noted in e.g., the Norwegian standards [7] and regulations [8], as well as the European Union's legislative framework [9]. Low-temperature DH (LTDH) enables the exploitation of economical piping options, such as PEX/Aluminum/PE material with low heat loss through distribution networks, and more importantly, provides wider opportunities for integrating distributed renewable energy, such as by use of building-sized HPs or renewables for peak shaving [10]. These advantages of the LTDH were proven in a pilot study of a renewable energy-based Danish municipality, which showed that primary energy demand was reduced by 4.5%, thermal grid loss was reduced by 6%, and costs were reduced by 2.7%, when the current 3rd generation DH system was changed to an LTDH system with the supply and return temperature of 55 and 25 °C, respectively [11].

The desire for circular economy may facilitate LTDH expansion in the Nordic countries as a result of the ban of using oil for heating [10] and increased capacity stress on the power grid due to increased power trading among neighboring countries requiring resource recovery and expansion of renewables [12]. Therefore, decreasing the DH supply temperatures from the current 80–120 °C range to a much lower level is accelerated by both political landscapes and energy efficiency directives [10]. To upgrade either the existing DH system to LTDH or build new LTDH, the change of heating load is the fundamental premise. Therefore, analyzing the potentials and challenges by understanding the key heating loads from planning and operating perspectives is the first necessary step to accelerate the LTDH transition.

A review study investigated the existing low-temperature based 5th generation district heating and cooling (LTDHC) systems in Europe, and reported that the LTDHC requires more advanced control strategies due to bi-directional energy flows and decentralized interactions [13]. Therefore, the information and communication technologies will be required to advance LTDH [13]. For example, heating and electricity load profiles on demand side may change after using power-to-heat (P2H) technologies to couple LTDH with electricity networks [14]. The change on heat and power flow may lead to operational problems and require enhanced communication between the power supply and the DH system. A control algorithm applying fuel shift control was proposed to avoid high peak power load and reduce DH network loss [14]. Another example is the need to address the impacts on DH operation network when utilizing datacenter's (DC) waste heat, e.g. due to the changing DC workload and dynamic heating load distribution, there is a need to improve DC management for automatic dynamic resources allocation, computing workloads for power management, and heating load balancing [15]. From the analysis of the challenges and potentials for LTDH in a Nordic climate, it can be seen that an LTDH system is very sensitive to the indoor set-point temperature, and it is necessary to optimize the outdoor temperature compensation curve prediction to facilitate the indoor temperature and mass flow rate [16]. Moreover, another crucial task in the LTDH system management is peak shaving, as this provides the possibility of expanding the heat network to connect more heat users without enlarging the infrastructure capacity [17]. To conclude, the above explained challenges and findings in achieving the best performance for LTDH and in establishing the feasible interaction among users; LTDH and electricity networks require intelligent prediction of peak heating load and control system, which can be adjusted by measures such as thermal storage implementation [18] and load distribution over the preceding hours [19].

1.2. Previous studies

As introduced above, LTDH and its integrations with renewables still face fundamental challenges to understand the heating load by using smart tools. Accordingly, energy prediction must be improved for effective sizing and operation of LTDH. By utilizing a large amount of measured data, data-driven methods, such as statistical methods and machine learning (ML), have shown strength in predicting heating load [20–22].

Artificial neural network (ANN), one of the ML methods, is found to be the most widely used one for energy planning, followed by support vector machine (SVM) and autoregressive integrated moving average (ARIMA) method, as well as statistical methods like linear regression (LR) [23]. A review of the last 30 years' applications of ANNs in building energy analysis shows that there is a strong growing development of ANN-based building energy analysis towards the exploitation of newer and extended types of ANNs [24]. Due to early implementation of smart meters, ANN and other data-driven methods have been mostly focused on electricity use, but not on heat use. For example, to estimate occupancy-related electricity demand by air-conditioning systems in non-residential buildings, an ANN-based model was developed by using occupancy as the input, which was determined by the blind system identification, showing an improved accuracy of energy prediction [25]. However, the proposed model needed to be validated for at least a one-year period, to account for seasonal variations of occupancy interactions with the electricity profiles [25]. Another ANN-based model compared

two back-propagation learning algorithms (Bayesian regularization and Levenberg-Marquardt), which were carried out respectively for day-ahead and hour-ahead electricity load forecast in a district [26]. Comparing with the total forecasted load for the district, aggregating the forecasts of heterogenous building types in the district may improve the day-ahead load forecasting performance by 7.9–11.9% [26]. The recent broad implementation of smart heat meters collecting (sub-)hourly heat use data has largely accelerated better quality in heating load prediction and clustering research for heating use data analysis [20]. The knowledge and experience gained from studies of building electricity demand data were transferable to heating demand analysis and uncertainties (i.e. weather forecasting), as mentioned in [27]. Two types of models, autoregressive multiple linear regression (MLR) and autoregressive multiple non-linear regression (MNLR), were firstly built to predict the DH load profiles of reference buildings and then aggregated the defined reference profiles into district levels [21]. In the work, it was shown that for predicting buildings with high daily load variation (such as office buildings), the ANN-based MNLR gives better performance than MLR in terms of a 4.2% reduction in mean squared error (MSE) [21]. Three ML methods, SVM, deep neural network (DNN, i.e. ANN with two or more hidden layers), and extreme gradient boosting (XGBoost), were respectively adopted to establish a multi-step ahead forecasting model of DH load with direct strategy and recursive strategy [22]. By feeding day-before influential factors, all three ML methods using these two strategies may accurately forecast the day-ahead DH load. Finally, it is recommended to further explore the potential of these heating load forecasting to optimize operation of the DH system [22]. Gaussian mixture model (GMM) clustering enables defining the four typical DH operation patterns in office buildings in a semi-arid climate (with cold and dry winters) by considering temperature and occupant behavior related sub-patterns [28]. After combining the GMM clustering with the regression and ANN models respectively, the qualities of hourly heating load forecasting are improved by 38.7–75.7% [28]. However, it was still difficult predicting the peak heating loads during night-to-daytime periods due to possible random operation behaviors [28]. A forecasting model based on convolutional neural network long-short term memory (CNN-LSTM) outperforms other ML methods when solving thermal inertia problems in DH system, mainly thanks to its integration of CNN's feature extraction ability and LSTM's two-dimensional space ability as shown in [29]. However, this model requires large numbers of sensors, large data storage, and re-training every day [29]. Two ML methods, SVM and nonlinear autoregressive exogenous recurrent neural network (NARX-RNN), were compared for DHC load prediction [30]. The results present that the NARX-RNN exceeds the SVM regarding the quality indicators and computation time. However, the overfitting tendency of NARX-RNN needs further study [30]. As introduced above, ANN-based prediction methods have enhanced energy prediction, especially greatly improved heating load prediction performance, such as computation time and prediction quality. However, the models' problems such as lack of big data for training, difficulty in peak load prediction, regular re-training, and others, need to be solved.

Additionally, Q-algorithm was used for developing a data-driven model by splitting the data into two parts with a reference load, $Q_{REF,}$ under three-level decision trees [27]. This model is robust for heating load prediction at district scale. Nevertheless, the claimed favorable accuracy results (R^2) in [27] are clearly lower than the common value, ca. 0.75 [31]. Based on 10-year DH production data, operation logics and outdoor temperatures were identified as the fundamental drivers for DH load prediction by analyzing load profile patterns and energy signature curves (ES curves) of the network [32]. The authors pointed out that, in the future, the parameters of a heating system should be studied according to features of each building type [32]. However, the conclusion that hourly time steps are not numerically useful is contrary to the research in [28], which presented ES curve in each cluster. Considering use of data-mining for DH operation, a temperature control method for the secondary network for transforming the existing DH to LTDH was introduced in [33]. Based on operation data and weather data, the optimized supply temperature could be obtained by summing the defined minimum return temperature and optimized temperature difference, which was evaluated by a LR model for hour-ahead return temperature prediction. This optimization strategy may contribute to stable daily operation. Meanwhile, the authors mention that this control strategy was limited within certain areas [33]. So far, only a few researchers have addressed the problems of LTDH's prediction, load analysis, and improved operation by using data-mining methods.

As the IEA DHC Annex TS2 puts forward, future decarbonized heating systems need enhanced DH technologies [10], such as installation of HPs in future's multi-energy systems [34]. This implies that shifting from competition between HPs and DH system to ensuring a collaboration between the two may be a promising approach in LTDH. An investigation of two combinations (central HPs only and central HPs plus booster HPs) for supplying space heating (SH) and domestic hot water (DHW), showed that the latter combination enables the DH system running at significantly lower temperatures and reduces operation costs by 39% over the former combination [35]. With the focus on predictions at district scale, the authors used daily average ambient air temperatures instead of hourly values [35]. This may not accommodate well for predictions at building scale, where in-depth heating response from atmospheric condition is crucial to be accounted for.

1.3. Objective and structure of this study

Previous research that focusses on improving DH system treats the measured energy data as a package, while most energy forecasts have not yet conducted in-depth studies on sizing or energy demand requirements for typical building types. Therefore, a bridge must be built to link the gap between smart meters and DH suppliers. In this study, the main objective was to develop hybrid heating energy prediction methods for typical building types, by combining the advanced ANN-based prediction method and a plant sizing method based on well-measured energy data. To focus the scope of the study, one important public building type, nursing home, was selected for the analysis. The reasons for selecting this building type and its wider applications are discussed in Section 4.1. The novel contribution of this study may be summarized as follows. Three-year measured DH use data in real buildings were utilized for analysis and modelling, which was to predict another year's DH demand in hourly resolution. The heating load profiles predicted by the hybrid methods are of high accuracy and can help plant sizing and daily operation with different inputs. Finally, the predicted load was proposed to be fed as building user's demand input in an LTDH system integrating two building-sized HPs, which may benefit the operation of building energy supply system in LTDH and compare the cost impacts from different load prediction, as discussed in Section 4.2.

The rest of the paper is organized as follows. Section 2 briefs the methods including the data information of the observed buildings and description of the two DH prediction methods. The main results of this study are presented in Section 3. Lastly, the limitations, future work, and conclusions are discussed and summarized in Sections 4 and 5.

2. Methods

The proposed framework consists of four phases. Section 2.1 explains Step 1, how building information is collected. Sections 2.2 and 2.3 explain Step 2 and Step 3, the two heating load prediction methods, dealing with the long-term and short-term prediction, respectively. Step 4 works on the prediction performance evaluation, as introduced in Section 2.4.

2.1. Building and energy data inventory

Statistically, the annual representative specific energy demand of Norwegian nursing homes is 260 kWh/m^2 with deviations between −25

and +6 kWh/m^2 according to different statistics sources, nearly half of which is for heating purpose owing to its high requirements of hygiene and thermal comfort under stable occupancy [36]. The high heating needs in the cold climates may involve considerable saving potential. In this study, 20 DH supplied nursing homes located in Trondheim, Norway, were used for the analysis. These observed buildings have heated floor areas ranging from 1350 to 10,940 m^2. DH delivers the SH and DHW to each building, which were recorded summarily in the meter. The DH use data in hourly resolution of the 20 buildings from 2016 to 2019 were retrieved from the energy monitoring platform of Trondheim Municipality [37]. Weather impacts were considered in the heat energy analysis, and the local historical weather data over the period were obtained from the Norwegian Meteorological Institute [38].

The building information regarding annual DH demand, energy labelling, and construction year, is briefed in Table 1. The building construction year and energy labelling were obtained from the Norwegian Energy Efficiency Agency (Enova) [39]. The labelling scheme goes from A (best building energy performance) to G (weakest performance) by considering the calculated delivered energy to each building. Except one building without information, all the others were built no earlier than 1980s, and most of them are labelled with C or D level [39]. The analysis was performed on the average specific DH load across the 20 buildings (W/m^2), to define the representative heating demand concerning buildings with different characteristics.

2.2. Prediction Method 1 – Prediction of annual district heating profile with energy signature curve models

As addressed above, large proportion of energy is used to heat buildings in cold climates, following the building's heating curve relative to the outdoor temperature.

In nursing homes DHW heat usage accounts for 15–20% to 40–65% of their total annual heat use, depending on the building standard (buildings built in 1980 s, passive house standard, etc.) [40]. Since DHW heat use is less sensitive to climate than SH, it is reasonable to separate DHW from the total DH load, for exploring a more accurate relationship between the outdoor temperature and the SH load. The typical per-room's hourly DHW heat use profiles for Norwegian nursing homes were identified in [41] providing detailed description and giving representative DHW profiles for the given climate and resident type. These typical hourly profiles (kW/room) were transferred into specific load density (W/m^2) and used as reference profiles in this study. As summarized in Fig. 1, there are apparent differences between the weekdays (WD as shortcut) and the weekends (WE) in the same season, especially during the peak load periods, as shown by the solid line and the dashed line of the same color. In Fig. 1, the solid lines represent the WDs, and the dashed lines the WEs. Meanwhile the seasonal differences between the same day type are small. As assumed elsewhere in literature [42], the daily DHW demand can be treated nearly constant throughout the year, and any effect on DHW would be insignificant. Similarly, in this study these four typical daily DHW profiles in Fig. 1 were extrapolated into an annual DHW profile, which was then extracted from the total DH to obtain SH use. The necessity and challenges of separating SH and DHW in the aggregated heating load was also mentioned in a Danish example for demand side management in DH networks [43].

The relationship between the outdoor temperature and SH load was identified by using energy signature curve (ES curve). This method has been widely employed in building energy planning and management by researchers and engineers at all levels. The ES curve generally consists of two parts, the temperature dependent part and temperature independent part, which are divided by the changing point temperature (CPT) or heating effective temperature. The ES curve may be expressed as:

if $t_\tau \le \mathrm{CPT}, P(t_\tau) = p_1 \bullet t_\tau + p_2 + \varepsilon$ (1).

if $t_\tau > \mathrm{CPT}, P(t_\tau) = p_1 \bullet t_\tau + p_2 + \varepsilon; = p_2$ (2).

In Eqs. (1) and (2), $P(t_\tau)$ is the SH load for a given outdoor temperature t, p_1 and p_2 are the coefficients of each ES curve model, and ε is the residual error. The SH load follows the linear growth under the slope of p_1. In addition to the outdoor temperature, the building operation schedules were also considered in the models. The identified ES curve model may be applied to estimate building energy performance in another year by combining the regression coefficients in Eqs. (1) and (2) with the corresponding weather data. Finally, Method 1 was used for the following purpose in this study: (1) for the system sizing, (2) to define boundary conditions of the DH units, and (3) to check boundary for the prediction load by Method 2.

2.3. Prediction Method 2 – Artificial neural network short-term district heating prediction

In this study, day-ahead prediction refers to the problem of, at a given point in time, predicting the DH load for the following 24-hour period. This prediction was done with an hourly resolution. Two separate ANN prediction models were developed to serve as decision-supporting tools for short-term planning and operation purposes in the future LTDH transitions. The first model considered only the historical and forecasted outdoor temperature, which are the measured outdoor temperature for the 48 h preceding the prediction period plus the 24-hour forecast for outdoor temperature. The second model included the historical DH load, the measured DH load for the 48 h preceding the prediction period, in addition to the outdoor temperature used in the first model. The first model might be helpful when there is difficulty to access real-time energy data or when data storage failure occurs with many missing values for planning energy generation.

The two models can be mathematically formulated as follows: Q_τ and t_τ represent the measured DH load and the measured outdoor temperature, at hour τ, respectively; and $\widehat{Q}_{\tau,s}$ and $\widehat{t}_{\tau,s}$ represent the predicted DH load and the forecasted outdoor temperature, respectively, at hour τ for each of the hours $\tau+s$ (defined for $s = 1,\cdots,24$). Historical data from the previous 48 h were used to make the prediction as the following:

$$\widehat{Q}_\tau^{24} = \left(\widehat{Q}_{\tau,1}, \cdots, \widehat{Q}_{\tau,24}\right), \tag{3}$$

$$\widehat{t}_\tau^{24} = \left(\widehat{t}_{\tau,1}, \cdots, \widehat{t}_{\tau,24}\right), \tag{4}$$

$$Q_\tau^{48} = (Q_{\tau-48+1}, \cdots, Q_\tau), \text{ and} \tag{5}$$

$$t_\tau^{48} = (t_{\tau-48+1}, \cdots, t_\tau) \tag{6}$$

where Q_τ^{48} and $\widehat{Q}_\tau^{24}$ represent, at hour τ, the historical measured DH load for the previous 48 h (including τ) and the predicted DH load for the next 24 h, respectively. Similarly, t_τ^{48} and $\widehat{t}_\tau^{24}$ represent, at hour τ, the historical measured outdoor temperature for the previous 48 h (including

Table 1
List of observed buildings' information.

Average measured annual DH demand (kWh/m^2)	≤70	≤90	≤120	≤160	≤190	>190	
No. of buildings	/	7	6	6	1	/	
Energy labelling with maximum	A	B	C	D	E	F, G	No infor.
Delivered annual energy (kWh/m^2)	140	190	240	295	355	440, >440	
No. of buildings	/	4	6	6	3	/	1
Construction year	Before 1950	1950–1979	1980–1999	2000–2010	After 2010		No infor.
No. of buildings	/	/	7	9	3		1

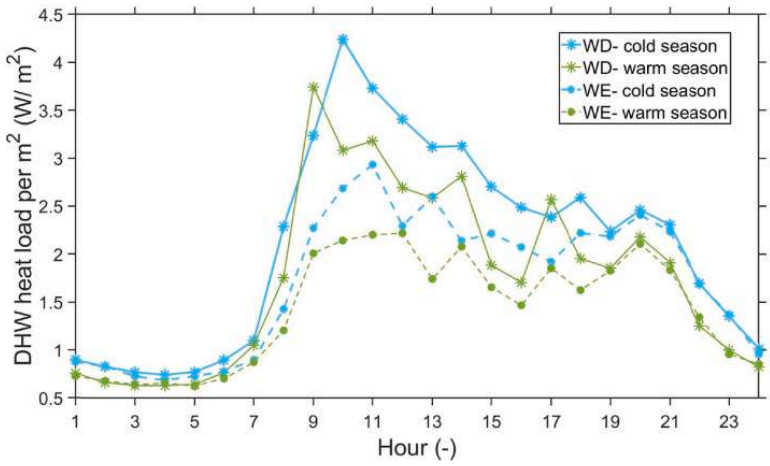

Fig. 1. Daily DHW heat load profiles in the nursing homes, divided by day of week and seasons.

τ) and the predicted outdoor temperature for the next 24 h, respectively. Using these notations, the two models could be expressed mathematically as:

$$\text{if historical heating load is not an input to the model, } \widehat{Q}_{\tau}^{24} = f\left(\widehat{t}_{\tau}^{24}, t_{\tau}^{48}\right), \tag{7}$$

$$\text{if historical heating load is an input to the model, } \widehat{Q}_{\tau}^{24} = g\left(\widehat{t}_{\tau}^{24}, t_{\tau}^{48}, Q_{\tau}^{48}\right) \tag{8}$$

where f and g are the abstract representations of the two ANN prediction models. Eq. (7) presents the first model considering outdoor temperature as the predictor, while Eq. (8) presents the second model considering both outdoor temperature and DH load as the predictors.

Both ANN models were established with one input layer (the first model, f, with 72 input units, and the second model, g, with 120 units), one hidden Rectified Linear Unit (ReLU) layer with 64 nodes and one output layer. 64 nodes were determined through hyperparameter search. For simplicity, notation f_{72} represents model $f\left(\widehat{t}_{\tau}^{24}, t_{\tau}^{48}\right)$ in Eq. (7) and notation g_{120} represents model $g\left(\widehat{t}_{\tau}^{24}, t_{\tau}^{48}, Q_{\tau}^{48}\right)$ in Eq. (8). These two notations are used in the following text. All the layers are densely connected. Mean squared error (MSE) was used as the loss function, and *Adam* was used for the parameter optimization with the maximum number of epochs at 100. The models were originally tested with 24, 48, and 72 h of historical data (weather and/or DH load). It was found that the difference between using 48 and 72 h of historical data was not significant while between using 24 and 48 h was significant, regarding the loss function. 48-hour historical data were therefore chosen due to the faster speed of running the models. The datasets of 2016 and 2017 were used as the training set establishing the ANN model, and the dataset for 2018 were used as the validation dataset for assessing the model performance during building and tuning the model process. To examine whether the model overfits the training set and is capable for future deployment, the resulting models were used to predict the DH load profile for 2019 and the prediction quality was evaluated using the measured data for the entire 2019, which was an unseen dataset during modelling process.

2.4. Evaluation of the prediction performance

Quality of the prediction models was evaluated by the commonly used criteria: mean absolute percentage error (MAPE), normalized mean bias error (NMBE), and the coefficient of variation of the root mean squared error (CV(RMSE)); meanwhile symmetric mean absolute percentage error (sMAPE) was also used as a supplementary criterion of MAPE, with lower and upper bounds. MAPE summarizes the relative error between the actual and predicted use in absolute value with a division by the observation number n. The directionality of the NMBE implies whether there is over-prediction or under-prediction. CV(RMSE) indicates whether the predicted model can reflect the real load shape. The criteria NMBE and CV(RMSE) shall be no more than 10% and 30%, respectively, when analysis is on hourly basis, according to the ASHRAE guidelines [31,44], while the MAPE shall be no more than 20% for a good forecasting model [45].

MAPE was given as:

$$MAPE = \frac{1}{n}\sum_{i=1}^{n}\left|\frac{A_i - F_i}{A_i}\right| \bullet 100\% \tag{9}$$

sMAPE was given as:

$$sMAPE = \frac{1}{n}\sum_{i=1}^{n}\frac{\lceil A_i - F_i \rceil}{(\lceil A_i \rceil + \lceil F_i \rceil)/2} \bullet 100\% \tag{10}$$

NMBE was given as:

$$NMBE = \frac{1}{n}\frac{\sum_{i=1}^{n}(A_i - F_i)}{\overline{A}} \bullet 100\% \tag{11}$$

CV(RMSE) was given as:

$$CV(RMSE) = \frac{\sqrt{\frac{1}{n}\sum_{i=1}^{n}(A_i - F_i)^2}}{\overline{A}} \bullet 100\% \tag{12}$$

where A_i is the measured value, F_i is the predicted value, and n is the number of the observations.

3. Results

The daily SH profiles, analysis results of the ES curve model, and the predicted annual DH profiles are presented in Sections 3.1 and 3.2. The 24-hour period prediction results for the warm and cold seasons are presented in Section 3.3. Lastly, the prediction performance is evaluated in Section 3.4.

3.1. Average daily space heating profiles and heating degree day results

After removing the daily DHW heat use in Fig. 1, the average daily SH load profiles for the nursing homes 2016–2018 were made by using arithmetic mean value of each hour, as shown in Fig. 2. This was to

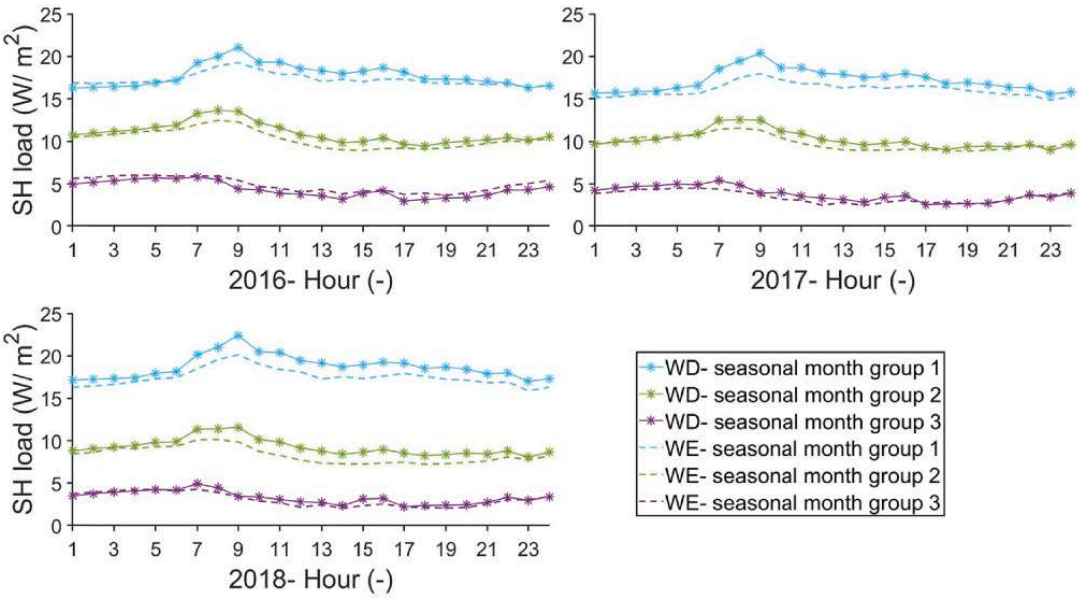

Fig. 2. Average daily SH load profiles 2016–2018, considering three seasonal month groups.

compare the load profiles between seasons and day types in general. In Fig. 2, the solid lines with stars and the dashed lines represent weekdays (WD) and weekends (WE), respectively.

The seasonal month group 1 included November – March, the seasonal month group 2 included April, May, September and October, and the seasonal month group 3 included June, July and August. Among the three seasonal groups, the heating load generally arose between 6 o'clock and 16–17 o'clock with the peak load at around 9 o'clock, which could be noted on weekdays, weekends, and short holidays. This is in line with the survey that most of the nursing homes take their main daily activities such as medical treatment, health training, and reading, between 7 and 16 o'clock, when large SH demand is needed in common areas. Due to stable occupancy of patients and residents, the heating load profiles for nursing homes demonstrate a milder peak load during the working hours and relatively higher level during the non-working hours in nursing homes, comparing with the buildings featured with distinct night setback control operation and different attendance levels between the weekdays and the weekends, such as educational buildings, office buildings, and other administrative buildings [46,47].

Further, to see whether day types might affect SH use, the obtained SH use was segregated into four heating seasons by using the heating degree days (HDDs) [48,49]. HDD was calculated as the daily average difference between heating balance temperature t_{bal} and hourly outdoor temperature: $\frac{1}{24}\sum_{\tau=1}^{24}(t_{bal}-t_{\tau})$, by assuming t_{bal} at 15 °C and setting negative values to zero. Days with HDD lower than $\frac{5}{24}$°C were considered as summer, between $\frac{5}{24}$ and $\frac{100}{24}$°C as the transition season, between $\frac{100}{24}$ and $\frac{510}{24}$°C as the heating season, and with over $\frac{510}{24}$°C as the very cold season. As shown in Fig. 3, it can be concluded that the daily SH operation generally follows the daily HDD closely, without influence of the

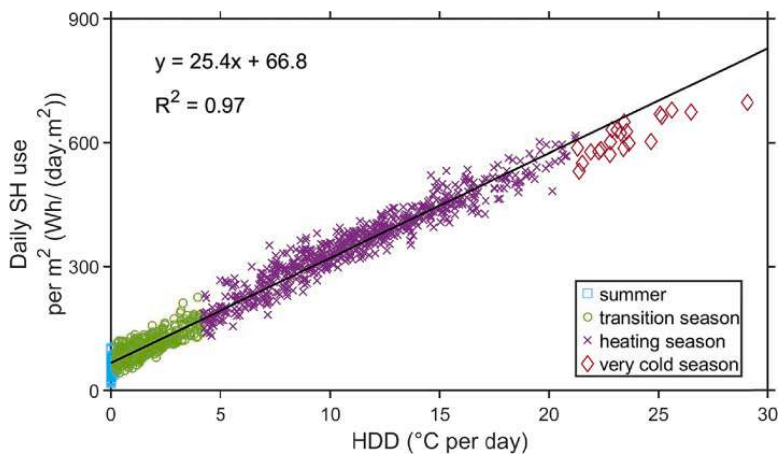

Fig. 3. Daily SH use vs. daily HDD, based on four different heating seasons, summer, transition season, heating season, and very cold season (high-heating season).

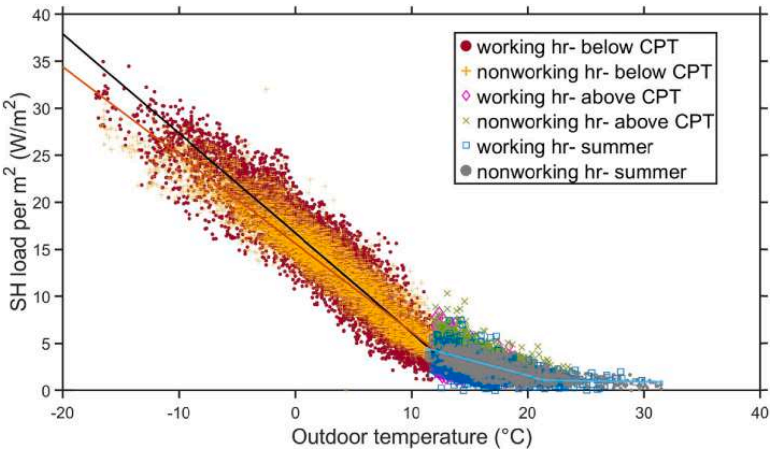

Fig. 4. Energy signature curve models of SH load. The black line below CPT represents working hours and red line non-working hours.

day type (weekday or weekend) nor manual false operation. Therefore, the ES curve models for SH prediction were established based on working hours and non-working hours, respectively, by following Eqs. (1) and (2).

3.2. Energy signature curve model and annual district heating profile

The ES curve models for the SH load are presented in Fig. 4, where the CPT was found at around 12 °C for providing a proper piece-wise approximation. The outdoor temperatures above the CPT covered 22.4% of the entire heating periods, when the SH loads were less temperature dependent as shown under the mild and constant slope. These small loads could be described by one regression line regardless of working hours and non-working hours. The remaining 77.6% of the time, the outdoor temperatures were below the CPT, falling into high-heating season. Along the regression lines below the CPT, there was a small region where non-working hours might need a slightly higher SH load than working hours under the same outdoor temperature (ca. 10–12 °C). This might be explained by residents spending more time outdoor during working hours at higher outdoor temperatures, causing the ventilation heat demand to decrease slightly due to changes in occupancy. The quality of regression models was evaluated with the coefficients of determination R^2, and the results are given in Table 2, together with the coefficients for the ES curves.

In Table 2, for the outdoor temperatures lower than CPT, it might be noted that R^2 were much higher than the required 0.75 for achieving a satisfying regression model [31,44]. However, for the part above the CPT, the SH needs had minor impacts on energy system requiring small load within short duration time. Comparing with those buildings with distinct time clock control operation, there were not pronounced SH differences between the working and the non-working hour periods in nursing homes, it is still worth analyzing them separately.

By using Method 1 introduced in Section 2.2, the reversely predicted annual DH profile of 2016–2018 was compared with each year's measured DH profile in Fig. 5. It can be observed that the DH load had large seasonal variation with the peak load during winter and early spring, and most of the predicted DH loads (green lines) were close to the measured DH loads (red lines). The annual DH demand of the three years were around 111–113 kWh/m^2 with peak SH load 31–35 W/m^2. By using the coefficients and knowledge obtained from the three years, the annual DH profile for 2019 was predicted, as shown in Fig. 6 giving a breakdown of the SH and DHW heat load profile. The peak SH load was 29–31 W/m^2 at outdoor temperature of −11.6 to −9.3 °C and the minimum load was close to 0.9 W/m^2 for the network circulation, while the DHW use was considered process heat with seasonally stable usage patterns. The predicted annual total DH demand for 2019 was 114 kWh/m^2, 15% of which was for DHW heat use. The results follow the statistical data of heat use in nursing home including the share for DHW heat use [40]. From this, a typical nursing home with an average area of 7000 m^2 may need around 800 MWh energy for heating purpose annually with a peak SH load of 203–245 kW under the similar climate. This also provides the boundary conditions that the day-ahead predictions shall be constrained by the operation scenarios, instead of allowing the network temperature drift freely with load variations.

Table 2
Coefficients of Eqs. (1) and (2), and the corresponding R^2.

	Outdoor temperature dependent ≤ 12 °C		Outdoor temperature less dependent	
	Working hour	Non-working hour	13–20 °C	>20 °C
p_1	−1.1	−0.94	−0.3	/
p_2	16.7	15.9	8.0	0.9
R^2	0.89	0.90	0.37 (↓)	

3.3. Results of short-term district heating load prediction

The day-ahead prediction performance of the two models f_{72}, g_{120} are compared in Fig. 7 and Fig. 8, and examples from different heating seasons were selected. To recall, model f_{72} did not consider the historical DH load as input, whereas g_{120} did consider the historical DH load, as stated in Section 2.3. In both models, the next 24-hour heating load prediction for the whole year of 2019 was made from 0 o'clock (τ) on January 1 to 0 o'clock (τ) on December 31 and gave 8737 prediction results in total, respectively.[1]

In Figs. 7 and 8, the top row subplots show the prediction results for f_{72}, and the bottom row subplots the results for g_{120}. Each column subplot shows the prediction for the next 24-hour period following the time instance indicated at the top, e.g., the prediction of the heating load $\widehat{Q}_\tau = (\widehat{Q}_{\tau,1}, \cdots, \widehat{Q}_{\tau,24})$ is plotted for the τ on the given date. By looking at each column subplots, it is therefore easy to compare the performance of

[1] Since weather of 2020 was not included, the prediction finished at 0 o'clock (τ) on December 31 with weather input by 23 o'clock on December 31. Therefore, each model ran 8737 times prediction (excluding 1–23o'clock (τ) on December 31) and produced 8737 prediction results, respectively.

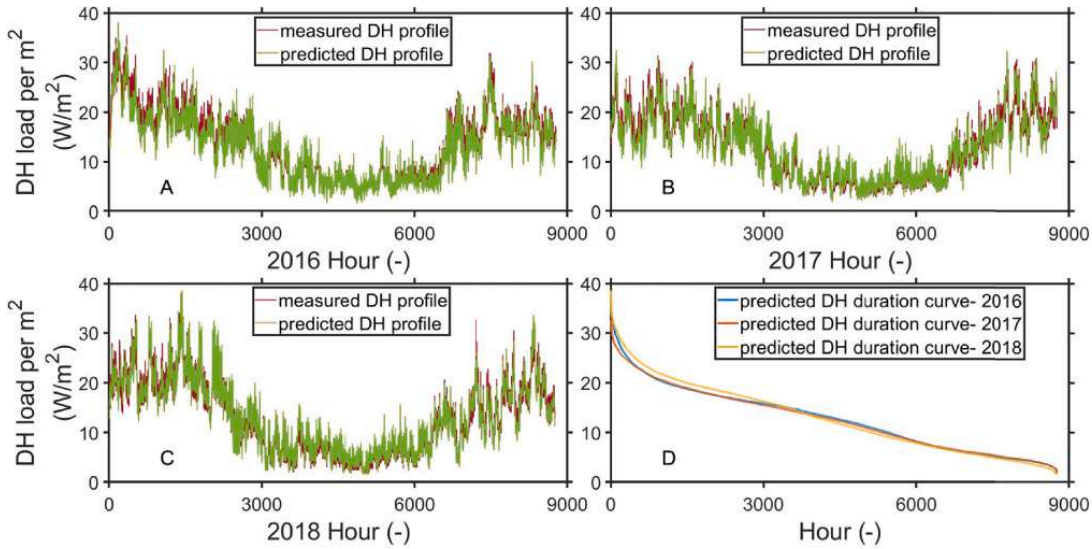

Fig. 5. Measured vs. predicted DH load profile during 2016–2018 (subplot A–C), and predicted DH duration curves during 2016–2018 (subplot D).

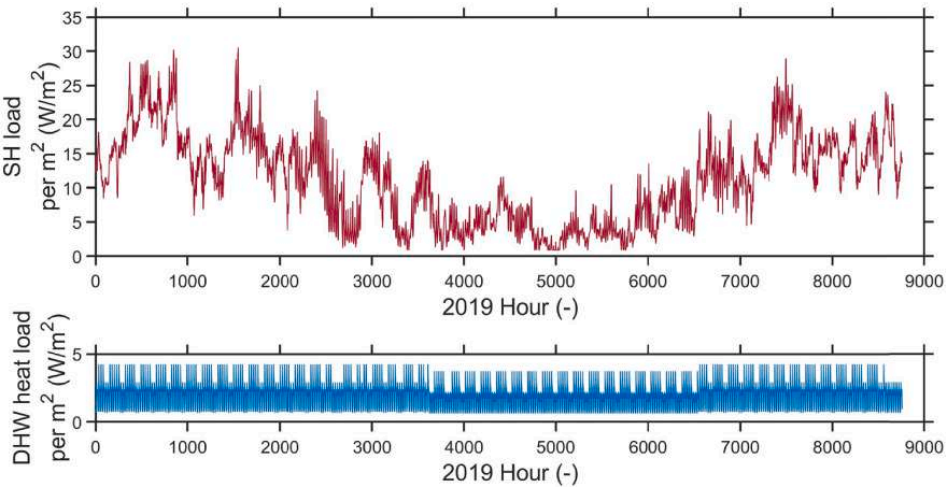

Fig. 6. Predicted DH load profile for 2019 with a breakdown of SH load profile (top row subplot) and DHW heating load profile (bottom row subplot).

model f_{72} and model g_{120} for the same time instance. In Figs. 7 and 8, the dashed black line represents the forecasted outdoor temperature for the corresponding 24-hour period, which are the actual outdoor temperature and used for evaluation in this case. To hold statistical reliability, three prediction results out of the 8737 instance τ were randomly selected from the 2019 testing data using a uniform probability distribution. The sample results are presented in Fig. 7, in which there were two DH load spikes, one was measured at 9 o'clock on September 16 and the other one at 3 o'clock on October 27, see the green squares pointed by the gray arrows. Since the first random samples were not part of the (high-) heating season (cold period with high heating demand), further, the prediction results for three dates during January, February, and December were randomly selected, covering the outdoor temperature from −11 to 2 °C, as shown in Fig. 8. In all the seasons, the load predicted by model g_{120} was apparently closer to the measured load than the one predicted by model f_{72}, both to the curve patterns and load values.

3.4. Results of the prediction performance evaluation

Due to thermal and hydraulic inertia in DH systems, and energy source availability, daily operation is commonly planned and arranged based on energy demand prediction for satisfying end-users' heating need in an economical way. By accumulating the daily prediction from Method 2 introduced in Section 2.3, a summed deviation between the predicted and the measured data throughout a year may be visualized. The deviation accumulated during (high-) heating season is especially important for evaluating peak loads prediction performance. Since the models, f_{72} and g_{120}, respectively produced next 24-hour heating load prediction at (any) hour τ, it is possible to select the same hour τ of each

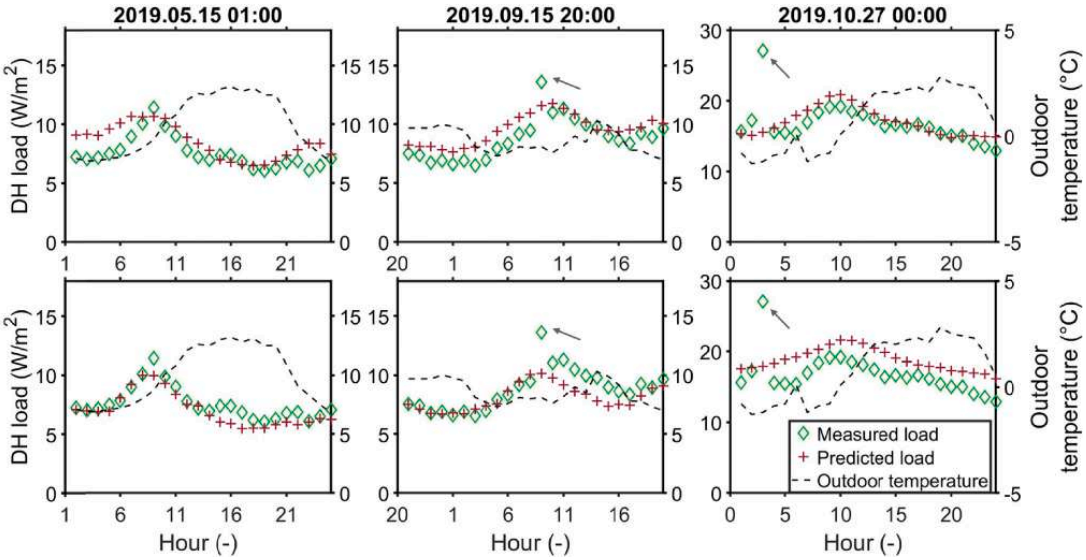

Fig. 7. Predicted DH load for the 24-hour period following the date indicated above each column, showing the randomly selected prediction results by model f_{72} (top row subplots) and by model g_{120} (bottom row subplots).

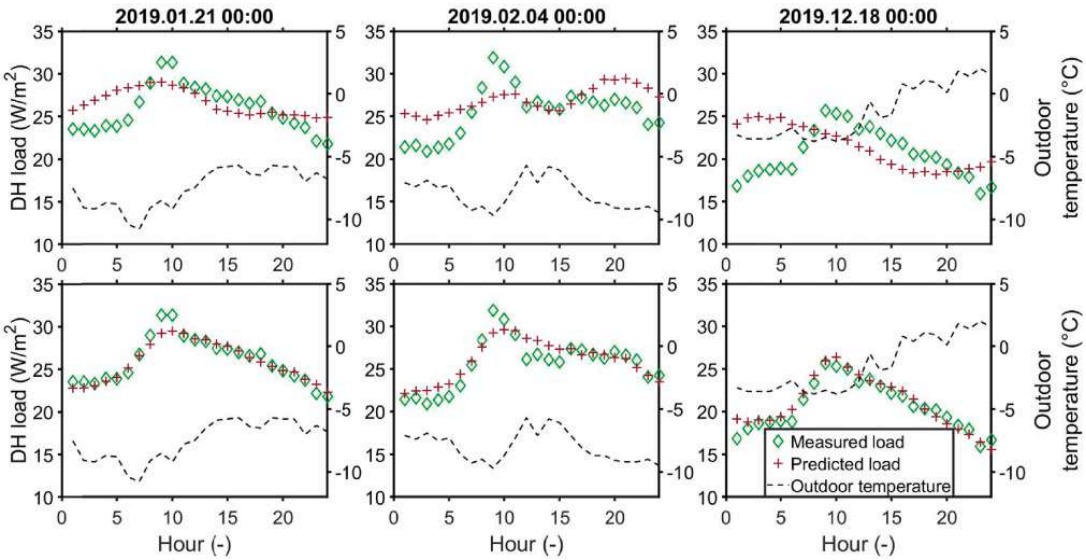

Fig. 8. Predicted DH load for the 24-hour period following the date indicated above each column, showing the selected three dates prediction results by model f_{72} (top row subplots) and by model g_{120} (bottom row subplots).

day for planning the next-day's production. Accordingly, the 24-hour ahead prediction results made at 0 o'clock every day from January 1 to December 31 were accumulated for obtaining the annual predicted load profile for 2019. It shall be noted that these accumulated annual profiles were obtained differently than the one presented in Section 3.2, which was made by Method 1, the ES curve model – directly on a long-term basis.

Fig. 9 compares the predicted load profiles for 2019 made by Method 1- ES curve model (the green line), Method 2, model f_{72} (the dark red line), and model g_{120} (the yellow line), with the measured load profile (the blue line). The deviation between the measured load and the predicted load, $\Delta(\tau) = measured\ \ Q_\tau - predicted\ \ \widehat{Q_\tau}$, by the three models for 2019 are shown in Fig. 10, and the prediction accuracy evaluation of the three models is summarized in Table 3. In Fig. 9 all the three predicted load profiles followed seasonal variations, and the profiles by models f_{72} and g_{120} fell within the sizing boundary set by Method 1. g_{120} demonstrated an advantage in predicting heating load in mild- and low-heating seasons, during which most of the heating needs were DHW use and therefore had a weak linear relationship with the outdoor

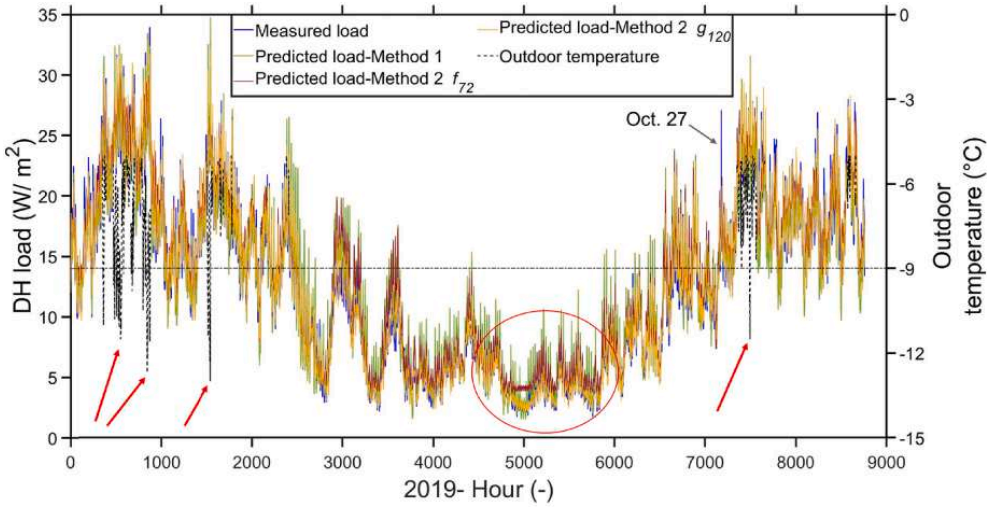

Fig. 9. Measured vs. predicted annual DH load profiles by the three models for 2019.

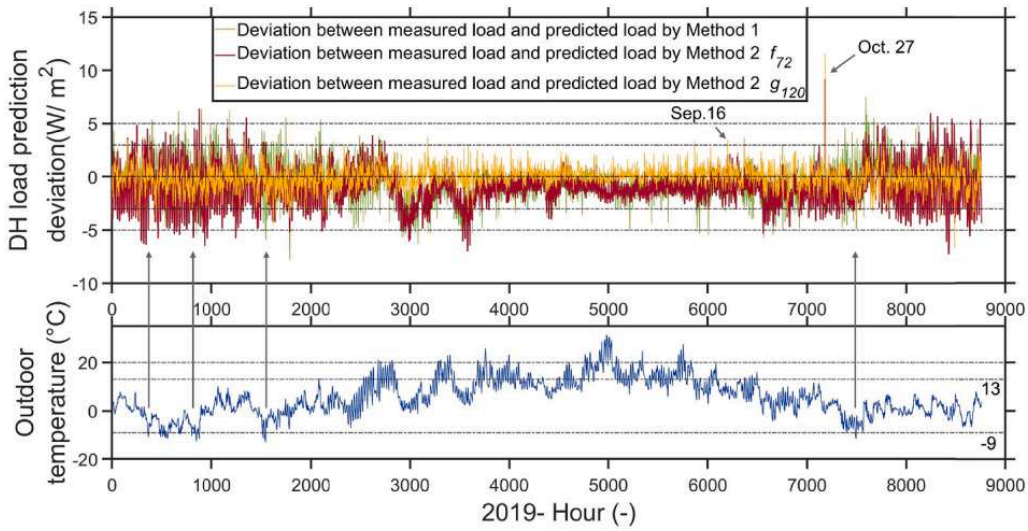

Fig. 10. Deviation plot between measured and predicted DH load by the three models for 2019.

Table 3
Evaluation results of 2019 DH load forecast produced by the three models. The criteria, MAPE, sMAPE, NMBE, and CV(RMSE), are used for quality evaluation.

Prediction method	MAPE (%)	sMAPE (%)	NMBE (%)	CV(RMSE) (%)
Method 1-ES curve model	13.94	12.81	−3.91	13.79
Method 2-model f_{72}	16.77	14.75	−8.13	15.51
Method 2-model g_{120}	7.23	7.28	−0.36	7.90

temperatures, as indicated by the red circle. In Fig. 9, the horizontal dash-dotted line refers to the reference line of the outdoor temperature at −9 °C, and only outdoor temperatures below −5 °C are presented as shown in the black dashed line; the red arrows point to the four examples of the peak heating load periods, as presented in Fig. 11. As compared in Fig. 10, g_{120} held the prediction deviations within ±3 W/ m^2 during most of the time, f_{72} had highest deviations during cold periods either over-predicting DH load or under-predicting DH load, and the ES curve kept the prediction deviation in between. The deviation high spikes on October 27 were mostly caused by measurement failure, see Fig. 7, when a sudden high DH load was measured.

In Fig. 11, Model f_{72} was least sensitive to the outdoor temperature changes by underpredicting the peak load and overpredicting the load during other time, also seen in Fig. 10; the ES curve model and model g_{120} catch most of the peak load periods, whereas the ES curve model might have overpredicted the peak load and caused unnecessary costs comparing to g_{120}. To recall Fig. 3, the regression line generally correlated well between the daily HDDs and the daily SH demand, however it might have overpredicted the SH use in the short and very cold season.

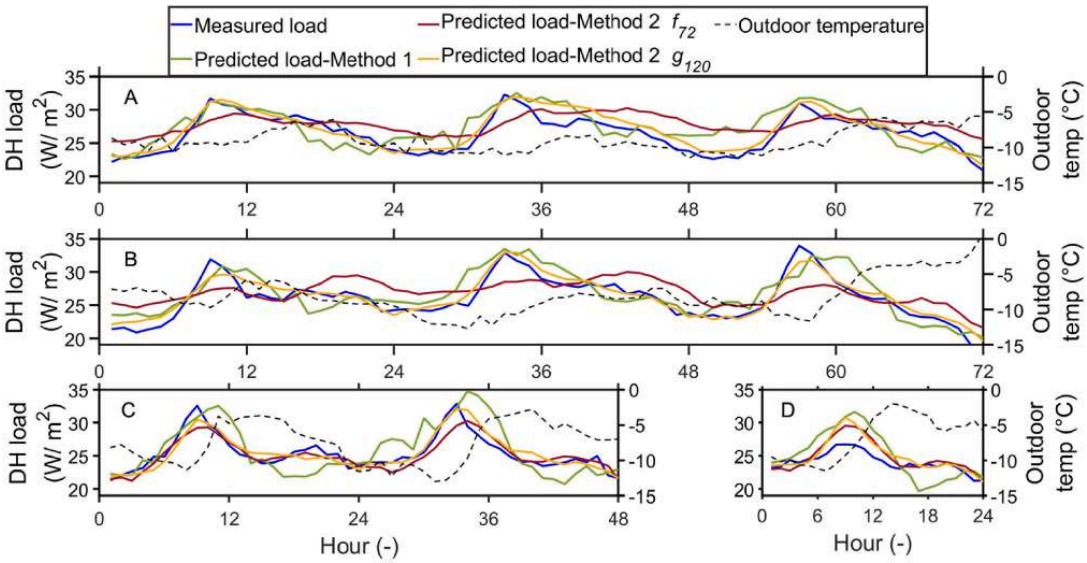

Fig. 11. Four examples of peak load periods in 2019, measured vs. predicted DH profiles by the three prediction models. Subplot A represents the load profiles comparison from 1 o'clock on January 22 to 24 o'clock on January 24. Subplot B represents the load profiles comparison from 1o'clock on February 4 to 24 o'clock on February 6. Subplot C represents the load profiles comparison from 1 o'clock on March 5 to 24o'clock on March 6. Subplot D represents the load profiles comparison from 1 o'clock to 24 o'clock on November 9.

Since the ES curve model below the CPT was determined by considering heating season and very cold season together, this might explain the possible overprediction of the peak SH load by Method 1.

As listed in Table 3, the MAPE and sMAPE results of the three models were less than 20%, NMBE within ±10%, and CV less than 20%, meeting the criteria upper limits [31,44,45]. Despite using the same training set for f_{72} and g_{120}, g_{120} had the best prediction performance on a yearly basis benefitting from using both the nearest historical two-day heating load and the outdoor temperatures as inputs, while f_{72} only considered the ambient condition as the inputs and its prediction accuracy was reflected by the poorest results regarding all the criteria. However, it was still good to notice that the load predicted by f_{72} to some extent was able to catch the pattern from the measured load curves, even without historical DH load as inputs, as reflected by its criterion CV (RMSE) result, much lower than the limit, 30%. Besides setting load boundary, the heating load prediction quality of the ES curve model was in the middle of the three models.

This means the models and their predicted DH load profiles provided high accuracy for use in the following work, regardless of the different input settings and algorithms of the three prediction models.

4. Discussions and future study

Selection of the analyzed building type data is reasoned in Section 4.1. Section 4.2 discusses three points, rationality of the models, limitation, and future work. The value of transferring this work is presented in Section 4.3.

4.1. Rationale of building type data inventory

A selection of nursing homes in the city of Trondheim was selected for the data analysis and modelling. A modern nursing home covers a large floor area and includes residents' private rooms with round-the-clock occupancies, large common area, 24/7 nursing service, and administrative offices. In 2018, the Norwegian long-term care expenditure accounted for 3.5% of GDP, while the average expenditure in OECD countries was 1.5% [50]. The function and characteristics of this building type make it an important public residential building with respect to social welfare progress and residents' care needs in the aging society.

The energy use in special residential building types, such as nursing homes, has more true-needs for users during whole heating seasons, and has not yet been extensively studied compared to residential buildings, especially in the cold climate, as mentioned in [41]. Since most of them are supplied by DH, it is important to study their energy needs in the transition to LTDH and to improve building energy supply, and for this, it is important to develop reliable prediction methods.

4.2. Discussions

4.2.1. Rationality of the models

By making good use of big data, data-driven models were selected over physical models. In Fig. 7, there were two DH load spikes, whereas the load profiles predicted by the two ANN models demonstrated a smoother trend. After checking the outdoor temperature during the two days, no "sudden" weather changes were recorded. Thus, these unusual data values might have been caused by metering failures or false operation. Nonetheless, the established models showed more reasonable heating load prediction. Besides the proper algorithms, the three-year's large data for training/validation also contributed to the appropriate prediction.

4.2.2. Limitation

The models adopted the actual measured outdoor temperature (the predictor) as the forecasted outdoor temperature for prediction. Practically, this weather forecast would however be inaccurate to some extent and may consequently cause a weaker performance than the observed in this study. Therefore, it is important to build the base model as accurately as possible, to reduce the spread and impacts of such weather uncertainties and inaccuracies. Meanwhile, due to this study's limited scope and length, only the hybrid of a linear regression model and an ANN model was considered. Although the prediction results were

satisfactory, a further study shall investigate whether there are other types of prediction methods, and newer types of ANN architectures may achieve better results, even with less training data available.

4.2.3. Future work – integration of building sized heat pumps in low-temperature district heating

In addition to improving DH load prediction quality, the above-described heating load profiles for DHW and SH may be utilized respectively in building energy supply operation when the building is connected into LTDH system. For example, it would be helpful to respond the different minimum allowable supply temperature requirements of DHW and SH by integrating two building-sized boosting HPs in LTDH. This may be regarded as a promising solution towards one of the challenges in LTDH. One possible application may be proposed as shown in Fig. 12, where from left to right side are the emerging heat source from waste heat, the temperature upgrade process, and the building user.

According to the Norwegian regulation, when a water storage tank is included, the DHW temperature should be maintained at not lower than 65 °C to prevent Legionella's growth [51]. One booster HP (HP1) may be accordingly employed for upgrading the heat source temperature e.g., from 55 to 65 °C for DHW heating, which connects to a water storage tank and a heat exchanger at substation.

The second booster HP (HP2) may be employed for upgrading the heat source for satisfying the peak SH load, when the outdoor temperature reaches a critical point that the source temperature is unable to maintain thermal comfort. For example, when using the conventional radiators in Nordic housings, the critical point may be determined as in [52] giving the equation as:

$$t_{in} = -0.75 \bullet t_\tau + 51 \tag{13}$$

where t_τ is the outdoor temperature and t_{in} is the minimum heating supply temperature. Additionally, selection of the critical point shall also consider the energy system's flexibility and use of building thermal inertia as shown elsewhere [53,54].

When the HPs or other boosting units are electric-driven, the annual electricity bill for heat source upgrade process is calculated by summarizing the monthly cost, which may follow Eq. (14):

$$C_{mon} = (1 + 0.25) \bullet \sum_{t=1}^{720or744} v_\tau \bullet \dot{E}_\tau + f \bullet \sum_{t=1}^{720or744} \dot{E}_\tau + \frac{F}{12} \tag{14}$$

where τ is the time instance, 0.25 is the tax rate on spot price, v_τ is the variable power market price, considered with the NordPool spot price of Trondheim in 2019 [55], $\dot{E}_\tau$ is the hourly electricity use, f is the grid rent with a value of 0.023€/kWh, and F is the fixed annual fee with a value of 190€/yr to ensure customers' access to electricity covering the costs associated with power grid operation, retrieved from grid company Elvia [56]. Many European countries adopt a price charging model similar to the one shown in Eq. (14) [57], containing fixed grid rent, tax, and variable market price; in some cases, surcharge of high peak load in winter are also included.

To analyze the impacts from different prediction models on the overall costs of the building heat supply system, a thorough study shall be carried out involving several key factors, e.g., types of HPs compressors driving force, operation optimization strategy, and sizing of the boosting HPs and water storage tank to avoid high peak surcharge. In addition to focusing heating load prediction and supply on building side, it would be interesting to examine the interactive response between DH plant/network and building user side. For example, when integrating renewables and short-to-medium-term thermal storage into LTDH, which is likely to come more in the near future, pricing models for both heat source and boosting costs shall be considered in the overall network cost optimization. Due to the length of the paper, an in-depth analysis and scenario-based projection of system cost shall be the goal of future study.

4.3. Value of transferring the developed models

There is a noticeable difference in heating load prediction performance between the model using historical heating loads and outdoor temperature as prediction inputs (g_{120}) and the models only using the outdoor temperature as inputs (the ES curve model and f_{72}), e.g. during the mild-low heating season. One reason could be the thermal inertia effects of the buildings and suboptimal control of the heating loads, which likely makes the historical heating loads be useful to model. Additionally, during this period, DHW heat use accounted for a higher

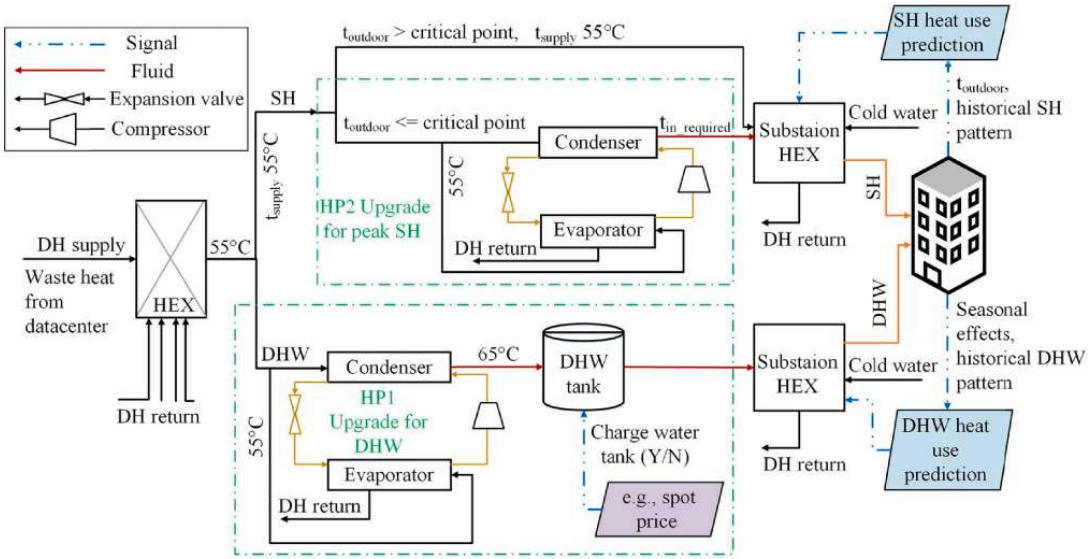

Fig. 12. Schematic diagram of integrating building-sized HPs.

share of heat demand under the weaker relationship between the outdoor temperature and the heating load. This evidence presented a basis for future LTDH transitions under different climates, that more heating loads may fall into mild-heating season and only peak loads into high-heating seasons.

Although it is important to include historical heating load for prediction models as found in the results, historical heating load data are unfortunately either accessible with delays or low data quality, i.e., low time resolution, different from historical weather data, which are usually publicly accessible via meteorological institutions. Accordingly, another potential application of the results is to map load predictions in other relevant buildings, either existing ones without high quality data collection or newly built ones with limited data for training. One of the promising methods is transfer learning (TL), which is a state-of-the-art ML technique showing excellent performance in different fields. Lately, TL has shown advantages for building energy management with adjustment of buildings' identities [58]. The gained knowledge is therefore beneficial for understanding such as newly built nursing homes or existing ones in need of renovation assessment, by transferring the developed energy prediction models of one typical building type to individual buildings.

5. Conclusions

This study proposed hybrid heating load prediction methods and examined the feasibility of integrating two building-sized HPs in an LTDH system. The work was established on the average heating load of 20 nursing homes, involving different building ages, areas, and energy labelling levels in the Nordic climate.

The main findings are as the following:

- From Method 1, the ES curve model provided a long-term heating load prediction in hourly resolution, showing a strong linear relationship between the outdoor temperature and the heating load over half of the heating seasons.
- Under the sizing boundary by Method 1, it was found to be important to include historical heating data as inputs when developing the two ANN models in Method 2, f_{72} and g_{120}. Through the accumulation of every day's day-ahead prediction, models f_{72} and g_{120} were comparable with the ES curve model on a yearly basis.
- The three models were evaluated on the actual measured data from real cases, demonstrating the feasibility of such prediction models. Among them, benefitting from considering both the historical heating load and the outdoor temperature as the inputs, the ANN model g_{120} showed the best results in the quality evaluation, especially in predicting the heating load in the mild-low heating season and peak periods.
- As one of the challenges in LTDH system, the different minimum allowable temperature requirements of DHW and SH, may be handled by integrating two building-sized heat pumps, with the respective load profiles for DHW and SH as demand inputs.

This study demonstrated hybrid building heating load prediction methods and present their possible application in building energy supply operation. The proposed methods and results were established and evaluated on a large amount of measured data and may give a better insight into building energy management and the LTDH system.

CRediT authorship contribution statement

Yiyu Ding: Conceptualization, Methodology, Data curation, Software, Formal analysis, Validation, Writing – original draft. **Thomas Ohlson Timoudas:** Methodology, Software, Validation, Writing – review & editing. **Qian Wang:** Conceptualization, Methodology, Formal analysis, Writing – review & editing. **Shuqin Chen:** Supervision, Writing – review & editing. **Helge Brattebø:** Supervision, Writing – review & editing. **Natasa Nord:** Conceptualization, Funding acquisition, Project administration, Supervision, Writing – review & editing.

Declaration of Competing Interest

The authors declare that they have no known competing financial interests or personal relationships that could have appeared to influence the work reported in this paper.

Acknowledgement

This article has been written within the research project "Methods for Transparent Energy Planning of Urban Building Stocks– ExPOSe". The authors gratefully acknowledge the main support from the Research Council of Norway (ExPOSe programme, grant number: 268248) and aided support from the Swedish Energy Agency (grant number: 51544-1). Special thanks go to the Department of Energy and Process Engineering of NTNU and Trondheim Municipality.

References

[1] U. N. Environment. 2020 global status report for buildings and construction. <https://globalabc.org/news/launched-2020-global-status-report-buildings-and-construction> [accessed Nov. 15, 2021].
[2] U. N. Environment. Global status report for buildings and construction. UNEP – UN Environment Programme, Oct. 19, 2021; 2021. <http://www.unep.org/resources/report/2021-global-status-report-buildings-and-construction> [accessed Nov. 15, 2021].
[3] European Biomass Association, EGEC geothermal, and European Solar Thermal Industry Federation. Primary energy factor for electricity in the energy efficiency directive; 2017. <http://www.estif.org/fileadmin/estif/The-role-of-PEF-in-ecodesign_AEBIOM-EGEC-ESTIF_April-2017-1_1_.pdf> [accessed Dec. 09, 2021].
[4] Latõsov E, Volkova A, Siirde A, Kurnitski J, Thalfeldt M. Primary energy factor for district heating networks in European Union member states. Energy Proc 2017; 116:69–77. https://doi.org/10.1016/j.egypro.2017.05.056.
[5] IEA. Energy policies of IEA countries: Sweden 2019 Review. IEA. <https://www.iea.org/reports/energy-policies-of-iea-countries-sweden-2019-review> [accessed Dec. 09, 2021].
[6] SSB. District heating and district cooling. SSB. <https://www.ssb.no/en/energi-og-industri/energi/statistikk/fjernvarme-og-fjernkjoling> [accessed Dec. 09, 2021].
[7] Standard Norge. NS 3700: Kriterier for passivhus og lavenergibygninger–Boligbygninger; 2013. <https://www.standard.no/no/Nettbutikk/produktkatalogen/Produktpresentasjon/?ProductID=636902> [accessed Dec. 09, 2021].
[8] Directorate of Building Quality. TEK17. Veiledning om tekniske krav til byggverk/Building Technology Regulations, Norway; 2017. <https://www.regjeringen.no/contentassets/20503ddfe0664fac9e2185c1a6c80716/veiledning-til-byggteknisk-forskrift-tek17_01_07_2017_oppdatert_15_09_2017.pdf> [accessed Dec. 09, 2021].
[9] EU Commission. Energy performance of buildings directive. <https://energy.ec.europa.eu/topics/energy-efficiency/energy-efficient-buildings/energy-performance-buildings-directive_en> [accessed Jul. 07, 2022].
[10] Averfalk H, Benakopoulos T, Best I, Dammel F, Engel C, Geyer R, et al. Low-temperature district heating implementation guidebook. IEA DHC Report; 2021. p. 206.
[11] Sorknæs P, Østergaard PA, Thellufsen JZ, Lund H, Nielsen S, Djørup S, et al. The benefits of 4th generation district heating in a 100% renewable energy system. Energy 2020;213:119030.
[12] The Research Council of Norway, "Research for Sustainable Societal and Industrial Development. <https://www.forskningsradet.no/om-forskningsradet/publikasjoner/2017/research-for-sustainable-societal-and-industrial-development/>.
[13] Buffa S, Cozzini M, D'Antoni M, Baratieri M, Fedrizzi R. 5th generation district heating and cooling systems: a review of existing cases in Europe. Renew Sustain Energy Rev 2019;104:504–22. https://doi.org/10.1016/j.rser.2018.12.059.
[14] Wang J, Cai H, You S, Zong Y, Zhang C, Træholt C. A framework for techno-economic assessment of demand-side power-to-heat solutions in low-temperature district heating. Int J Electr Power Energy Syst 2020;122:106096. https://doi.org/10.1016/j.ijepes.2020.106096.
[15] Wahlroos M, Pärssinen M, Rinne S, Syri S, Manner J. Future views on waste heat utilization – case of data centers in Northern Europe. Renew Sustain Energy Rev 2018;82:1749–64. https://doi.org/10.1016/j.rser.2017.10.058.
[16] Nord N, Løve Nielsen EK, Kauko H, Tereshchenko T. Challenges and potentials for low-temperature district heating implementation in Norway. May Energy 2018; 151:889–902. https://doi.org/10.1016/j.energy.2018.03.094.
[17] Guelpa E, Barbero G, Sciacovelli A, Verda V. Peak-shaving in district heating systems through optimal management of the thermal request of buildings. Energy Oct. 2017;137:706–14. https://doi.org/10.1016/j.energy.2017.06.107.
[18] Zhang Y, Johansson P, Kalagasidis AS. Applicability of thermal energy storage in future low-temperature district heating systems – case study using multi-scenario

analysis. Energy Convers Manage 2021;244:114518. https://doi.org/10.1016/j.enconman.2021.114518.
[19] Kauko H, Kvalsvik KH, Rohde D, Hafner A, Nord N. Dynamic modelling of local low-temperature heating grids: a case study for Norway. Energy 2017;139:289–97. https://doi.org/10.1016/j.energy.2017.07.086.
[20] Gianniou P, Liu X, Heller A, Nielsen PS, Rode C. Clustering-based analysis for residential district heating data. Energy Convers Manage 2018;165:840–50. https://doi.org/10.1016/j.enconman.2018.03.015.
[21] Talebi B, Haghighat F, Mirzaei PA. Simplified model to predict the thermal demand profile of districts. Energy Build 2017;145:213–25. https://doi.org/10.1016/j.enbuild.2017.03.062.
[22] Xue P, Jiang Y, Zhou Z, Chen X, Fang X, Liu J. Multi-step ahead forecasting of heat load in district heating systems using machine learning algorithms. Energy 2019;188:116085. https://doi.org/10.1016/j.energy.2019.116085.
[23] Debnath KB, Mourshed M. Forecasting methods in energy planning models. Renew Sustain Energy Rev 2018;88:297–325. https://doi.org/10.1016/j.rser.2018.02.002.
[24] Mohandes SR, Zhang X, Mahdiyar A. A comprehensive review on the application of artificial neural networks in building energy analysis. Neurocomputing 2019;340:55–75. https://doi.org/10.1016/j.neucom.2019.02.040.
[25] Wei Y, Xia L, Pan S, Wu J, Zhang X, Han M, et al. Prediction of occupancy level and energy consumption in office building using blind system identification and neural networks. Appl Energy 2019;240:276–94. https://doi.org/10.1016/j.apenergy.2019.02.056.
[26] Dagdougui H, Bagheri F, Le H, Dessaint L. Neural network model for short-term and very-short-term load forecasting in district buildings. Energy Build 2019;203:109408. https://doi.org/10.1016/j.enbuild.2019.109408.
[27] Lumbreras M, Garay-Martinez R, Arregi B, Martin-Escudero K, Diarce G, Raud M, et al. Data driven model for heat load prediction in buildings connected to district heating by using smart heat meters. Energy 2022;239:122318. https://doi.org/10.1016/j.energy.2021.122318.
[28] Lu Y, Tian Z, Peng P, Niu J, Li W, Zhang H. GMM clustering for heating load patterns in-depth identification and prediction model accuracy improvement of district heating system. Energy Build 2019;190:49–60. https://doi.org/10.1016/j.enbuild.2019.02.014.
[29] Song J, Zhang L, Xue G, Ma Y, Gao S, Jiang Q. Predicting hourly heating load in a district heating system based on a hybrid CNN-LSTM model. Energy Build 2021;243:110998. https://doi.org/10.1016/j.enbuild.2021.110998.
[30] Koschwitz D, Frisch J, van Treeck C. Data-driven heating and cooling load predictions for non-residential buildings based on support vector machine regression and NARX recurrent neural network: a comparative study on district scale. Energy 2018;165:134–42. https://doi.org/10.1016/j.energy.2018.09.068.
[31] Menard S. Coefficients of determination for multiple logistic regression analysis. Am Stat 2000;54(1):17–24. https://doi.org/10.1080/00031305.2000.10474502.
[32] Noussan M, Jarre M, Poggio A. Real operation data analysis on district heating load patterns. Energy 2017;129:70–8. https://doi.org/10.1016/j.energy.2017.04.079.
[33] Bai Y. A temperature control strategy to achieve low-temperature district heating in North China. Int J Sust Energy Plan Manage 2020;25:3–12. https://doi.org/10.5278/ijsepm.3392.
[34] Guelpa E, Marincioni L, Capone M, Deputato S, Verda V. Thermal load prediction in district heating systems. Energy 2019;176:693–703.
[35] Østergaard PA, Andersen AN. Booster heat pumps and central heat pumps in district heating. Appl Energy 2016;184:1374–88. https://doi.org/10.1016/j.apenergy.2016.02.144.
[36] Langseth B. Analyse av energibruk i yrkesbygg (Analysis of energy use in non-residential buildings). NVE, 2016. <https://nve.brage.unit.no/nve-xmlui/handle/11250/2488849> [accessed: Dec. 02, 2021].
[37] iEOS – Planning. <https://www2.esave.no/Esave.nsf/iEOS_Hovedbilde.xsp> [accessed Feb. 24, 2021].
[38] "Norsk Klimaservicesenter." https://seklima.met.no/observations/ (accessed Feb. 24, 2021).
[39] Enova Offentlig søk etter energiattester. <https://attest.energimerking.no/> (accessed May 10, 2021).
[40] Enova. Hensiktsmessige varme- og kjøleløsninger i bygninger (Appropriate heating and cooling solutions in buildings); 2013. [Online]. <https://www.enova.no/upload_images/380D698AC6CC4A0D98695AC29342ECDC.pdf> [accessed: Nov. 15, 2021].
[41] Ivanko D, Walnum HT, Nord N. Development and analysis of hourly DHW heat use profiles in nursing homes in Norway. Energy Build 2020;222:110070. https://doi.org/10.1016/j.enbuild.2020.110070.
[42] Østergaard PA, Andersen AN. Variable taxes promoting district heating heat pump flexibility. Energy 2021;221:119839. https://doi.org/10.1016/j.energy.2021.119839.
[43] Cai H, Ziras C, You S, Li R, Honoré K, Bindner HW. Demand side management in urban district heating networks. Appl Energy 2018;230:506–18. https://doi.org/10.1016/j.apenergy.2018.08.105.
[44] American Society of Heating Refrigerating and Air Conditioning Engineers. 2013 ASHRAE handbook: fundamentals; 2013. <http://app.knovel.com/hotlink/toc/id:kpASHRAEC1/2013-ashrae-handbook> [accessed: Feb. 27, 2021].
[45] Meade N. Industrial and business forecasting methods, Lewis, C.D., Borough Green, Sevenoaks, Kent: Butterworth, 1982. Pages: 144. J Forecast 1983;2(2):194–6. https://doi.org/10.1002/for.3980020210.
[46] Frederiksen S, Werner S. District heating and cooling. Studentlitteratur AB; 2013.
[47] Ding Y, Brattebø H, Nord N. A systematic approach for data analysis and prediction methods for annual energy profiles: an example for school buildings in Norway. Energy Build 2021;247:111160. https://doi.org/10.1016/j.enbuild.2021.111160.
[48] Lundström L, Wallin F. Heat demand profiles of energy conservation measures in buildings and their impact on a district heating system. Appl Energy 2016;161:290–9. https://doi.org/10.1016/j.apenergy.2015.10.024.
[49] Carragher M, De Rosa M, Kathirgamanathan A, Finn DP. Investment analysis of gas-turbine combined heat and power systems for commercial buildings under different climatic and market scenarios. Energy Convers Manage 2019;183:35–49. https://doi.org/10.1016/j.enconman.2018.12.086.
[50] OECD. Spending on long-term care Brief-November-2020.pdf. <https://www.oecd.org/health/health-systems. https://www.oecd.org/health/health-systems/Spending-on-long-term-care-Brief-November-2020.pdf> [accessed Dec. 02, 2021].
[51] TEK. Inneklima og legionella-Temaveiledning. Building technical regulations. <https://dibk.no/globalassets/byggeregler/tidligere_regelverk/eldre_temaveiledere_og_rundskriv/2003ho-1-legionella.pdf> [accessed Jan. 27, 2022].
[52] Ploskić A, Wang Q, Sadrizadeh S. Mapping relevant parameters for efficient operation of low-temperature heating systems in nordic single-family dwellings. Appl Sci 2018;8(10). https://doi.org/10.3390/app8101973.
[53] Li Y, Wang C, Li G, Wang J, Zhao D, Chen C. Improving operational flexibility of integrated energy system with uncertain renewable generations considering thermal inertia of buildings. Energy Convers Manage 2020;207:112526. https://doi.org/10.1016/j.enconman.2020.112526.
[54] Romanchenko D, Kensby J, Odenberger M, Johnsson F. Thermal energy storage in district heating: centralised storage vs. storage in thermal inertia of buildings. Energy Convers Manage 2018;162:26–38. https://doi.org/10.1016/j.enconman.2018.01.068.
[55] See market data for all areas. <https://www.nordpoolgroup.com/Market-data1/> [accessed Feb. 24, 2021].
[56] Elvia AS. Alt om nettleiepriser – Elvia. <https://www.elvia.no/nettleie/alt-om-nettleiepriser/> [accessed Jul. 08, 2022].
[57] Electricity price statistics – statistics explained. <https://ec.europa.eu/eurostat/statistics-explained/index.php/Electricity_price_statistics#Electricity_prices_for_non-household_consumers> [accessed Feb. 27, 2021].
[58] Fan C, Sun Y, Xiao F, Ma J, Lee D, Wang J, et al. Statistical investigations of transfer learning-based methodology for short-term building energy predictions. Appl Energy 2020;262:114499. https://doi.org/10.1016/j.apenergy.2020.114499.